UNIVERSITY OF MINING AND GEOLOGY "ST. IVAN RILSKI"

JOURNAL

OF

MINING AND GEOLOGICAL SCIENCES

Volume 60
Part I: Geology and Geophysics

Publishing House "St. Ivan Rilski"
Sofia, 2017

ISSN 2535-1176

www.mgu.bg

C O N T E N T S

Part 1 – Geology, Mineralogy and Mineral Deposits

Part 2 – Geophysics, Hydrogeology and Engineering Geology, Drilling and Oil and Gas Production

С Ъ Д Ъ Р Ж А Н И Е

Раздел 1 – Геология, минералогия и полезни изкопаеми

Раздел 2 – Геофизика, хидрогеология и инженерна геология, сондиране и добив на нефт и газ

THE URANIUM-POLYMETALLIC DEPOSITS IN THE SLIVEN-TVARDITSA ORE REGION IN THE WEST BALKAN METALLOGENIC ZONE, BULGARIA

Petko Popov[1], Kamen Popov[1]

[1]University of Mining and Geology "St. Ivan Rilski", 1700 Sofia; E-mail: kpopov@mgu.bg

ABSTRACT. Late Cretaceous hydrothermal uranium deposits are found in the West Balkan Metallogenic Zone. Sliven-Tvarditsa Ore Region is outlined in the Central Balkan Mountain, in which the Sliven and Shivachevo Ore Fields and the Yavorovets ore occurrence are distinguished. The ore bodies are bed-like, metasomatic, in Triassic and Upper Cretaceous carbonate rocks or in interbedding breccia. Besides, vein ore bodies are developed along the faults in the Paleozoic basement rocks. The ore mineralization is hydrothermal in type, medium to low temperature. The main ore minerals are pitchblende, galena, sphalerite and chalcopyrite, and the non-ore are quartz and to a lesser extent dolomite, calcite and barite. Pyrite, arsenopyrite, chalcocite, hydro pitchblende, chalcanthite, renardite, anglesite, uranospinite, torbernite, cerussite, malachite, azurite, autunite, uranophane, hematite and limonite are more rarely observed. Bornite, chalcocite, hydro pitchblende, uranium soot, chalcanthite, renardite, anglesite, uranospinite, torbernite, cerussite, malachite, azurite, autunite, uranophane, hematite and limonite are hypergenous. The hydrothermal alterations are represented by sericitization, advanced argillization, pyritization, kaolinization and carbonization. The ore deposits are formed in the frame of a non-volcanic island chain, adjacent to the Srednogorie Zone from the Apuseni-Banat-Timok-Srednogorie Magmatic and Metallogenic Belt.

Keywords: Uranium deposits, Upper Cretaceous West Balkan Metallogenic Zone.

УРАНОВО-ПОЛИМЕТАЛНИТЕ НАХОДИЩА В СЛИВЕН-ТВЪРДИШКИЯ РУДЕН РАЙОН ОТ ЗАПАДНОБАЛКАНСКАТА МЕТАЛОГЕННА ЗОНА, БЪЛГАРИЯ

Петко Попов[1], Камен Попов[1]

[1]Минно-геоложки университет "Св. Иван Рилски", София 1700; kpopov@mgu.bg

РЕЗЮМЕ. В Западнобалканската металогенна зона са установени къснокредни хидротермални уранови находища. В Централния Балкан се оконтурва Сливен-Твърдишки руден район, в който се отделят Сливенското и Шивачевското рудни полета, както и рудопроявление Яворовец. Рудните тела са пластообразни, метасоматични, в триаски и горнокредни карбонатни скали или междупластови брекчи. Освен това са развити жилообразни рудни тела в разломите от палеозойски скали от фундамента. Рудната минерализация е от хидротермален тип, средно- до нискотемпературна. Главните рудни минерали са настуран, галенит, сфалерит и халкопирит, а нерудните – кварц и по-малко доломит, калцит и барит. По-рядко се срещат пирит, арсенопирит, халкозин, тенантит, тетраедрит и борнит. Хипергенни са борнит, халкозин, хидронастуран, настуран, уранови чернилки, халкантит, ренардит, англезит, ураноспинит, торбернит, церусит, малахит, азурит, отонит, уранофан, хематит и лимонит. Хидротермалните промени са представени от серицитизация, окваряване, пиритизация, каолинизация и карбонатизация. Рудните находища са образувани в рамките на невулканска островна верига, прилежаща към Средногорска зона от Апусени-Банат-Тимок-Средногорския магматичен и металогенен пояс.

Ключови думи: уранови находища, горнокредна Западнобалканска металогенна зона.

Introduction

The geological setting in Bulgaria is determined by the Balkan and Carpathian Systems of the Alpine Orogeny and the adjacent Moesian Platform. The sub latitudinal Balkan, Srednogorie and Morava-Rhodope Zones are distinguished from North to South in the Balkan System (Zagorchev et al. (ed.), 2009). The evolution of the Balkan System is a result of consecutive geotectonic events, as intracontinental rifting, ocean spreading, subduction, Austrian collision, Upper Cretaceous rifting, Illyrian collision and post-collisional orogenesis (Popov, 1981; Popov, 1996; 2002). The Balkan Zone covers the outer parts of the orogeny, as it is overthrust on the Moesian Platform and part of the Southern Carpathians to the North, and it borders on the Srednogorie Zone to the South. The Balkan Zone section is represented by Mesozoic and Paleocene – Middle Eocene sediments with numerous hiatuses and compressional deformations (Zagorchev et al. (ed.), 2009).

The ore forming processes are manifested during the Late Cretaceous events in the Balkan Zone, and differentiate the West Balkan Metallogenic Zone. This zone covers the major part of Western and Central Stara Planina Mountain, from the Eastern parts of Serbia in the west, to the town of Sliven in the east (Fig. 1) (Popov, 1985; 1989; Popov, 1995). According to the scheme by Dabovski, Zagorchev (Zagorchev et al. (ed.), 2009) it includes the West Balkan, Central Balkan and part of the Fore Balkan units from the Balkan Zone, as well as parts from the Srednogorie and SW Bulgaria.

The West Balkan Metallogenic Zone position during the Upper Cretaceous is of great significance. To the South it borders to the Srednogorie through which it is part of the Apuseni-Banat-Timok-Srednogorie Magmatic and Metallogenic Belt (Popov et al., 1978; Popov et al., 2002), where intensive sedimentation and volcanic activity are observed. At the same time, a shallow epicontinental sea is formed over the Moesian

Plate to the North. The analyses by different authors (Bonchev, 1955; Nachev, 2003) show that the studied territory is above the sea level during this period and represents a non-volcanic island chain. It includes part of the Austrian fold-overthrust belt, uplifted during the Late Cretaceous rift forming. The noted West Balkan Metallogenic Zone position supposes that the ore forming processes are result of hydrothermal activity, controlled by the Upper Cretaceous magmatism in the Srednogorie area (Popov, 1985; 1989).

The West Balkan Metallogenic Zone is characterized by series of endogenous mineral deposits, compounds of lead, zinc, copper, uranium, barite and rarely iron, antimony and molybdenum ores in different proportions. Stratiform and less vein or vein-like deposits predominate. The Sliven-Tvarditsa Ore Region is marked by the development of uranium-polymetallic ores and it is differentiated in part of the Central Stara Planina Mountain, within the frame of the metallogenic zone.

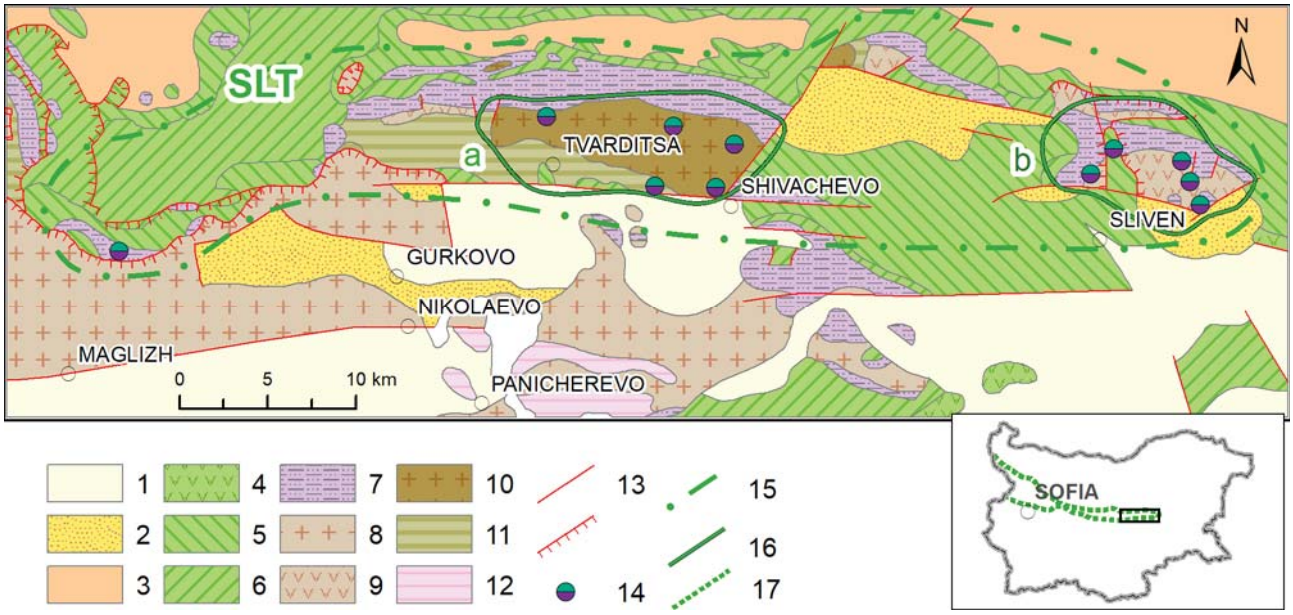

Fig. 1. Geological map of the Sliven-Tvarditsa Ore Region.
1 – Quaternary sediments; 2 – Upper Eocene – Pliocene sediments; 3 – Paleocene – Lutetian sediments; 4 – Upper Cretaceous volcanic rocks; 5 – Coniacian – Maastrichtian sediments; 6 – Cenomanian – Turonian sediments; 7 – Triassic sediments; 8 – Srednogorie Upper Paleozoic granitoid; 9 – Upper Paleozoic volcanic rocks; 10 – Stara Planina granitoid (Devonian – Lower Carboniferous); 11 – Neoproterozoic – Cambrian metamorphic rocks; 12 – Neoproterozoic metamorphites; 13 – fault and overthrust; 14 – uranium-polymetallic deposit; 15 – Sliven-Tvarditsa Ore Region (SLT); 16 – Ore Fields (a - Shivachevo, b - Sliven); 17 – West Balkan Zone (on the overview map).

Geology

The Sliven-Tvarditsa Ore Region covers the southern slopes of the Central Stara Planina Mountain, including parts of Tryavna, Elena-Tvarditsa and Sliven Mountains. It is traced north of the towns of Maglizh, Gurkovo, Tvarditsa, Shivachevo and Sliven, to the village of Sotirya (Fig. 1). Pre-Alpine basement is outcropped in the region, and represented by Neoproterozoic and Cambrian metamorphic rocks, Middle and Late Paleozoic granitoids and Late Paleozoic volcanites. Triassic terrigenous and carbonate sediments are observed at the Alpine section base. They are differently preserved in the separate areas due to the erosion. The Jurassic and Lower Cretaceous sediments are completely eroded. The Upper Cretaceous sediments are represented by terrigenous, coal-bearing, limestone, flysch and other sequences from the Cenomanian to the Maastrichtian. Late Cenomanian to Campanian of age volcanic rocks are also included within the limestone and flysch formations. Hiatuses between the Cenomanian and Turonian as well as between the Turonian and Coniacian sediments are observed at some places. Paleocene – Lutetian sediments are traced north of the area. Upper Eocene – Quaternary terrigenous and terrigenous-carbonate sediments are developed in the southern margins of the region (Zagorchev et al. (ed.), 2009).

The limited presence of Triassic and the complete lack of Jurassic and Lower Cretaceous rocks hinder the determining of the character of the Early Cimmerian and Austrian tectonic structures. The later deformations allow to differentiate from west to wast the Shipka anticline, the Borushtitsa structure, the Tvarditsa anticline, the Kachulka structure and the Predela anticline with Sliven overthrust, which are allochthonous in position (Bonchev, 1986, Kanchev, 1995, Kanchev et al., 1995, Popov 1971, Valchanov, 1974, Popov et al., 1980, Paskalev, 1983). The setting of the region is complicated due to the imposition of different in character and age deformations. The Sub-Hercynian deformations are quite distinct, as they are marked by standing and overturned Cenomanian – Turonian beds, overlaid by Early Senonian carbonate sediments in the town of Tvarditsa area (Kanchev, 1962). This is confirmed by the transgressive position of the Early Senonian sediments over different older rocks in the town of Sliven area (Popov et al., 1980). The Laramian structures manifestations are not clarified. Popov et al.. (1980) assume that the Sliven overthrust is Laramian, while Paskalev (1983) and Tzankov et al. (1991) define it as Illyrian. The presence of numerous olistoliths within

the Upper Cretaceous sediments should be noted (Ivanov, Moskovski, 1974, Nachev, 1977, Paskalev 1989). The presence of the Illyrian structures is demonstrated by the Luda Kamchiya synclinorium, compounded by Senonian – Lutetian sediments. It is overthrust from the south on the rocks from the Sub-Hercynian structures. The Stara Planina overthrust is observed along the southern margins of the region. It is compounded mainly by Neoproterozoic, Paleozoic and Triassic rocks, which partially overlay the above-mentioned rocks (Kanchev, 1962, 1995; Kanchev et al., 1995; Tsankov et al., 1995a). The post-collisional processes form the Stara Planina horst system and the Back Balkan graben system (Gurkovo-Tvarditsa, Belenski, Sotirya and other grabens), filled with Upper Eocene – Quaternary sediments (Kanchev, 1995, Kanchev et al., 1995; Tsankov et al., 1995a,b).

Metallogeny

The metallogenic processes in the Sliven-Tvarditsa Ore Region are marked by the forming of uranium-polymetallic Sinite Kamani and Sborishte deposits and numerous ore occurrences. These ore mineralizations are localized within the Pre-Alpine basement rocks or in the Triassic and partially Upper Cretaceous sediments. The spatial and structural position of the ores outlines the Sliven and Shivachevo ore fields as well as the separate Yavorovets ore occurrence.

Sliven Ore Field

The Sliven Ore Field is located north f the town of Sliven, in the Sliven part of Stara Planina Mountain. The oldest outcropped rocks are Permian volcanites, represented by quartz-porphyry, quartz-porphyry lava breccia, granophyre and granite porphyry (Popov, Tsanova, 1967). They are transgressive, overlaid by Lower Triassic sandstone, siltstone, rarely conglomerate, with thickness from 0 to 30 m. Upwards Middle – Upper Triassic limestone, dolomitic limestone, dolomite and rarely calcareous argillite cover them or the Permian volcanites. Cenomanian coal-bearing sediments, sandstone, marl and Turonian terrigenous flysch are transgressive, deposited with hiatus, as they are outcropped at the western margins of the ore field. Insufficiently studied Senonian (Upper Turonian – Senonian) limestone, clayey limestone and flysch, with volcanic lava and tuff at some places, and with transition to Paleocene-Lutetian flysch to the North (Zagorchev et al. (ed.), 2009), are deposited with new hiatus. The trachiandesite and quartz latite lava and pyroclastic rocks manifestations in the southeastern part of the ore field should be mentioned as well (Pashov et al., 1966f). Upper Eocene molasse sediments are deposited in the southern border of the region (Fig. 2).

The Triassic and Upper Cretaceous sediments set up the Predela (southern) and the Karakyutyuk (northern) anticlines, with cores of Permian volcanic rocks (Popov, 1971). These antiform structures are allochthonous in position, as they are included in the Sliven overthrust (Popov, 1971; Valchanov, 1974; Popov et al.., 1980; Paskalev, 1983). The last one represents the eastern part of Sliven-Shipka overthrust, described by Kockel (1927) (Fig. 2). Field and drill data show that the allochthone, set up by the Predela's anticline overturned northern bed, lie over Campanian – Maastrichtian sediments. Its interrelations with the Paleocene – Lutetian sediments from the upper section levels outcropped to the North have not been determined till now. Accordingly, the overthrust is described as Laramian by Popov et al. (1980), and as Illyrian by Paskalev (1983) and Kanchev (1995). It should be noted that the sediments below the overthrust are assigned by Kanchev (1995) to the Paleocene, and during the later revisions by Sinyovski (Zagorchev et al. (ed.), 2009) these rocks are referred to the Campanian – Maastrichtian.

Intensive faulting is observed in the studied region (Popov, 1970; 1971). Sub-Hercynian normal faulting along the sub latitudinal Daula fault in the ore field's northwestern part and slip faulting along diagonal ruptures are determined. The later deformations are significantly more intensive, while allochthonous Predela and Karakyutyuk anticlines are cut by sub latitudinal (90-100°), NE (40° – Sotira, Tepavitsa, etc.) and NNW (160° – Ablanovo, Rogovets, Golyama Chatalka, etc.) faults and the so called Ablanovo graben is formed. As a result of the tectonic deformations 0.5-10 m thick breccia is formed along the contact between the Paleozoic core and the Triassic or Upper Cretaceous sediments.

The Sinite Kamani deposit and Tyulbeto-West, Tyulbeto-East, Zmeyovi Dupki, Golyama Chatalka, Karakyutyuk and Ablanovo ore occurrences are found within the Sliven Ore Field (Fig. 2).

The Sinite Kamani deposit is located about 3 km northwestern from the town of Sliven. Permian volcanic rocks covered by Lower Triassic terrigenous, Middle Triassic carbonate and Senonian clayey carbonate rocks are observed here. The Lower Triassic rocks are often missing in the section, as the Upper Cretaceous sediments overlay directly the Permian volcanites in some places. The Mesozoic rocks are part of the Predela anticline's southern bed. Series of sub latitudinal, NE and NNW faults are differentiated. Pre-Senonian movements are accomplished along some faults, which is documented by the different thickness in the separate blocks of the Triassic rocks, covered by the Senonian sediments (Fig. 2). The breccia between the Permian volcanic rocks and the covering different Mesozoic rocks is well developed. The Sliven overthrust possesses ore conductive role, as it is probably connected with the latitudinal fault zone delimiting the Srednogorie and Balkan regions. The diagonal faults have ore distributing role, as they connect the overthrust zone with the ore controlling and hosting zone of the breccia between the rock formations (Pashov et al., 1966f). The low permeable Senonian clayey carbonate rocks and the slightly cracked Triassic carbonates are sealed both in structural and in geochemical aspect.

Complex uranium-lead-zinc-copper ores are found in the Sinite Kamani deposit. The uranium content in the ore reaches 3.5%, the lead is up to 6.28%, the zinc is up to 3.7% and the copper is up to 0.86% in some nests. Only the uranium was mined. The ore mineralization set up mainly bed-like ore bodies with highly meandering contours in plane. They are formed predominantly in the brecciated zone between the rock formations, formed along the contact between quartz porphyry and the Triassic carbonate rocks, and dipping 20-30° to the

South. Five main ore bodies are determined in the deposit. The ore body № 1 is more than 400 m in length and has thickness from 0.17 to 2.2 m. The ore bodies № 2, 3 and 4 are analogous in character but much smaller in size. The ore mineralization metasomatically replaces the brecciated dolomitic limestone or cements the tectonic breccia. In the areas, were the Lower Triassic sediments are preserved, the ore is developed in the permeable sandstone beds, usually below clayey layers. The ore is partly formed in the brecciated quartz porphyry, where it is mainly veinlet-disseminated in type.

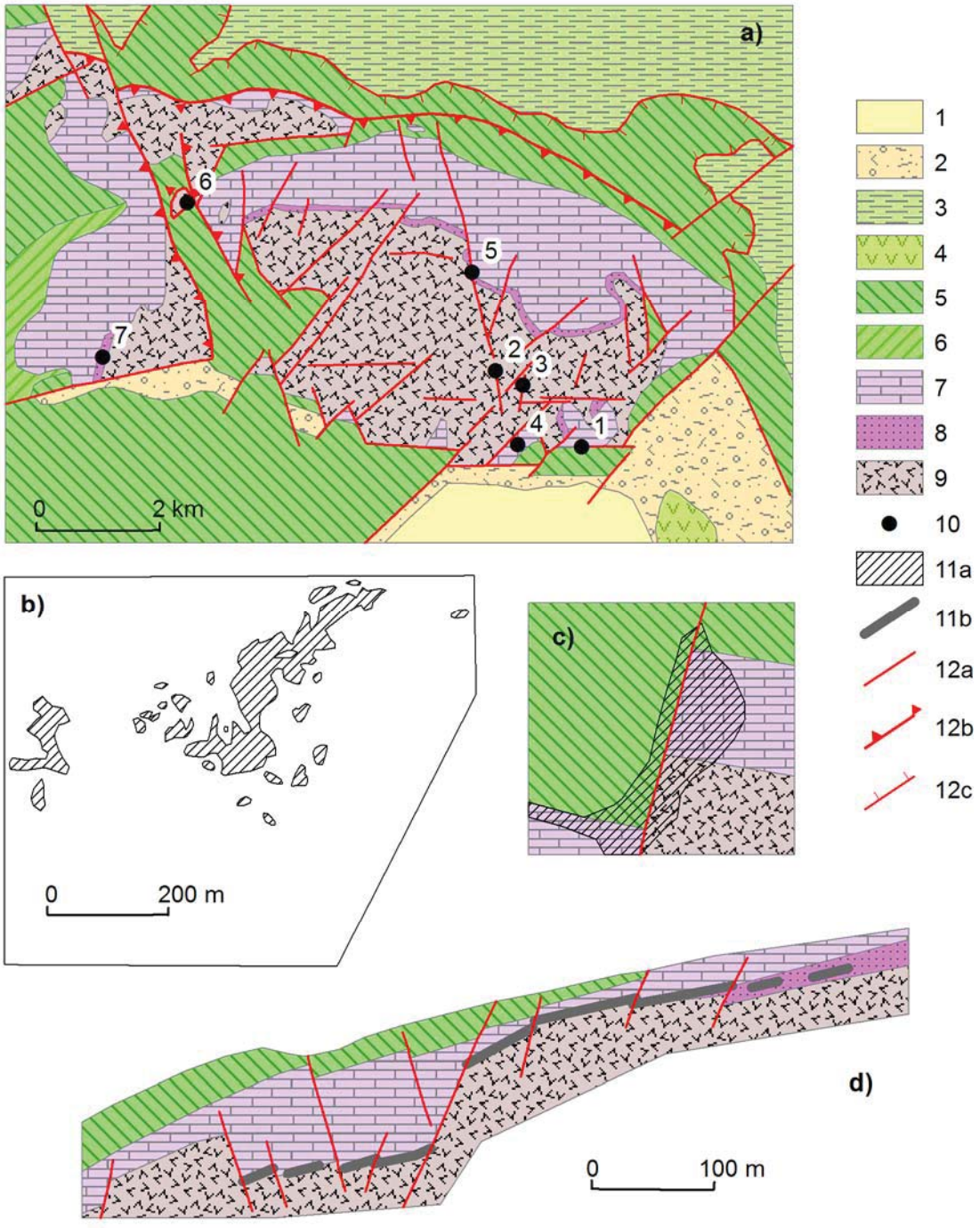

Fig. 2. Geological map of the Sliven Ore Field (a), plane of the ore bodies in Sinite Kamani deposit (b), fragment from the uranium ore body in Adit 7 area (c), geological section across Sinite Kamani deposit (d).
1 – Quaternary sediments; 2 – Upper Eocene sediments; 3 – Campanian – Maastrichtian flysch; 4 – Upper Cretaceous volcanic rocks; 5 – Coniacian – Campanian (?) clayey limestone and volcanites; 6 – Cenomanian – Turonian sediments; 7 – Middle – Upper Triassic carbonate sediments; 8 – Lower Triassic terrigenous sediments; 9 – Upper Paleozoic (Permian) volcanic rocks; 10 – ore deposits and occurrences on (a) (1 – Sinite Kamani, 2 – Tyulbeto-West, 3 – Tyulbeto-East, 4 – Zmeyovi Dupki, 5 – Golyama Chatalka, 6 – Karakyutyuk, 7 – Ablanovo); 11a – ore bodies on (b) and (c); 11b – ore bodies on section (d); 12a – fault; 12b – reverse slip fault; 12c – overthrust.

The ore bodies' position is controlled by the diagonal faults, as the ore is developed along them. Besides, in the intervals where the faults cut the contact between Triassic and Paleozoic rocks, the ore is developed within the faults as well,

forming vein-like bodies (ore shear zone). Usually these vein-like bodies are component of the bed-like ones, as they form kind of root-like apophyses in the volcanic rocks, down to 30-40 m below them, and much less in the overlaying Mesozoic sediments. Thus, the ore bodies are complicated step-like in structure, sometime additionally complicated by the after ore forming faulting. It should be noted that in the places, where the Upper Cretaceous clayey carbonate rocks directly overlay the Permian volcanites, the ore is developed in the breccia between them and insignificantly in the clayey limestone near the feeding diagonal faults, which is observed in the mining works (Pashov et al., 1966f). The ore bodies are nest-like or irregular in shape. Ore mineralization in the Upper Cretaceous rocks is also found in some drills (Pashov, 1965f). No doubt, these facts confirm the Upper Cretaceous age of the deposit.

The position of the small ore body № 5 from the eastern deposit's part is different as it is concordant to the planar parallelism in the Permian volcanic rocks.

The ore forming process starts with the pneumatolytic deposition of magnetite with less specularite, martite and the non-ore quartz and little tourmaline. The hydrothermal mineral forming is most important, as the main minerals are represented by nasturan (pitchblende), galena, sphalerite and chalcopyrite and the subordinate pyrite, arsenopyrite, chalcocite, tennantite, tetrahedrite and bornite. The gangue minerals are quartz mainly and less dolomite, calcite and barite. Bornite, chalcocite, hydro nasturan (hydro pitchblende), uranium soot, chalcanthite, renardite, anglesite, uranospinite, torbernite, cerussite, malachite, azurite, autunite, uranophane, hematite and limonite are formed during the hypergenous stage (Пашов, 1965ф). The hydrothermal rock alterations are expressed by sericitization, advanced argillization, pyritization, kaolinization and carbonization (Pashov et al., 1966f).

The Zmeyovi Dupki, *Ablanovo and Karakyutyuk ore occurrences* are similar to the Sinite Kamani deposit, as they are developed near the contact between the Mesozoic sediments and the Permian volcanic rocks. At the same time *the Tyulbeto-West, Tyulbeto-East and Golyama Chatalka ore occurrences*, located northwestern from the Sinite Kamani deposit (Fig. 2), are formed in fault structures in the Permian volcanites and are ore-bearing fault (shear zone) of type (Pashov et al., 1966f).

Shivachevo Ore Field

The Shivachevo Ore Field covers part of the southern slopes of the Elena-Tvarditsa Stara Planina Mountain, in the towns of Tvarditsa and Shivachevo area (Fig. 3). The Pre Alpine basement is compounded by Neoproterozoic – Cambrian metamorphic rocks and Devonian – Lower Carboniferous granitoid. The metamorphic rocks are described as "Shivachevo Complex" (Ivanov et al., 1974; Statelova, Machev, 2005) compounded by schist, granitic gneiss, etc. The granitoid rocks set up the Tvarditsa pluton (Ivanov et al., 1974). Lower Triassic sandstone, conglomerate, siltstone and argillite cover the granitoid and are overlaid by Lower – Upper Triassic carbonate sediments, as the dolomite predominates. The Upper Cretaceous formations lie transgressive upward in the section (Kanchev et al., 1995; Kanchev, 1995). Turonian and Lower Senonian flysch and flysch-like formations are observed at the ore field's southern and eastern margins, as they are overhtrust in certain degree over the basement rocks. Allochthonous fragments of Late Paleozoic granite, metamorphites and Triassic rocks are found at the southern margin. Neogene and Quaternary sediments are also deposited to the South.

The Triassic and Cenomanian – Turonian sediments from the region set up the Tvarditsa anticline's northern bed. These rocks are with overturned bedding and are in allochthonous position in certain degree, which is marked by the Sub-Hercynian deformations. The Senonian – Lutetian beds of the Luda Kamchia synclinorium overlay them to the North (Kanchev et al., 1995; Kanchev, 1995). The southern bed is almost eroded. To the East, the Tvarditsa structure is limited by the Tvarditsa lineament sheaf (Bonchev, 1986). Faults with 100-120° direction and slant dip to the south, as well as steep faults with sub meridional, NE or NW direction are observed in the Paleozoic granitoid.

The metallogenic aspect of the Shivachevo ore field is defined by the development of Sborishte uranium-polymetallic deposit and several ore occurrences as Osenov Rat, Chakaloto, Krivata Cheshma, Kichesta, Domuz Dere, Kashla Dere and Sap Dere (Fig. 3).

The Sborishte deposit is located about 2 km NNE from the Sborishte village. Here the area is set up by the Devonian – Lower Carboniferous granitoid intruded in the Riphean – Cambrian metamorphic rocks. Partially preserved Turonian flysch and Campanian – Maastrichtian marl-limestone sediments are observed along the southern boundary. All these rocks are covered by Quaternary and Tertiary sediments to the south. Series of close, meridional, steep faults is developed in the deposit's area. They represent zones of intensive cracking, brecciating and cataclasis, which cut the high grade metamorphic rocks and the Tvarditsa pluton.

The ore mineralization is located in the sub meridional faults. The ore bodies are ore-bearing fault (shear zone) of type. Lens-like or nest economic ore bodies are traced within the ore hosting faults. The uranium-polymetallic ore is determined down to 150-200 m in depth. Small ore bodies are rarely found in equatorially oriented faults as well. The ore hosting rocks are consecutively altered by potassium and sodium metasomatism, sericitization, chloritization and hematitization. The ore mineralization is represented mainly by nasturan (pitchblende) and chalcopyrite and less pyrite, marcasite, sphalerite, galena, antimonite, tennantite, rammelsbergite, and the non-ore minerals are quartz and less calcite and dolomite. The secondary mineralization is well developed and represented by uranium soot, autunite, torbernite, etc. (Stoyanov et al., 1989f).

The ore occurrences in the ore field are similar in geological and mineralogical features to the Sborishte deposit. Ore bodies localized in sub meridional faults predominate (Osenov Rat, Chakaloto, Kichesta, Kashla Dere, Sap Dere mineralizations). Besides, northwestern (Krivata Cheshma, Domuz Dere mineralizations) and northeastern (Kichesta and Domuz Dere occurrences) ore hosting faults are also observed. The ores are developed mainly within the granitoid rocks, but the Kashla Dere ore occurrence is in the metamorphites, while in the

northern parts of Krivata Cheshma occurrence the ore mineralization affects the Triassic rocks as well.

Yavorovets ore occurrence

The Yavorovets ore occurrence is located about 2.5 km NE from the Yavorovets railway station, the town of Kazanlak area, at the eastern margin of Shipka anticline. Neoproterozoic and Paleozoic rocks, Lower Triassic terrigenous and Middle Triassic carbonate sediments and sequence of Upper Cretaceous formations are outcropped in this area. The Mesozoic beds are overturned, as a sheaf of North-vergent overthrustings are observed. Ivanov, Moskovski (1974) noted Triassic olistoliths included in the Upper Cretaceous sediments. The Upper Paleozoic Srednogorie granite and the Neoproterozoic metamorphites from the Stara Planina overthrust lie at the top (Kanchev et al., 1995).

Yavorovets ore occurrence is characterized by the uranium-polymetallic mineralization, developed within olistoliths from Triassic rocks. Geological explorations outlined numerous small ore bodies, which are located in several sites: Mostov Dol, Vrabnitsa, Stoykov Most, Yavorovo Dere and Ralevska Reka. These ore bodies are formed near the Lower Triassic sandstone contact with the Middle Triassic carbonate rocks. The ore mineralization is developed most often in the highly cracked limestone and dolomite, rarely in the sandstone. Ore bodies in hard, coarse grained sandstone are also found. Secondary mineralization is rarely observed, along the sandstone bedding surfaces. The ore hosting rocks are sericitized, silificated, and less chloritized, kaolinized and dolomitized. Uranium, lead, zinc and copper are the main ore elements. The determined maximum contents are 0.557% uranium, 3.8% lead, 1.85% zinc and 2.6% copper. Silver, cobalt, nickel, etc. show increased contents. Varied association of primary and secondary ore minerals is formed (Krastev, Dzhelepov, 1974f).

It should be noted that the ore hosting Triassic rocks are included in the flysch-like formation by Kanchev et al. (1995). The same formation is nominated by Sinyovski as “limestone formation” with Coniacian – Campanian age (Zagorchev et al., (ed.), 2009).

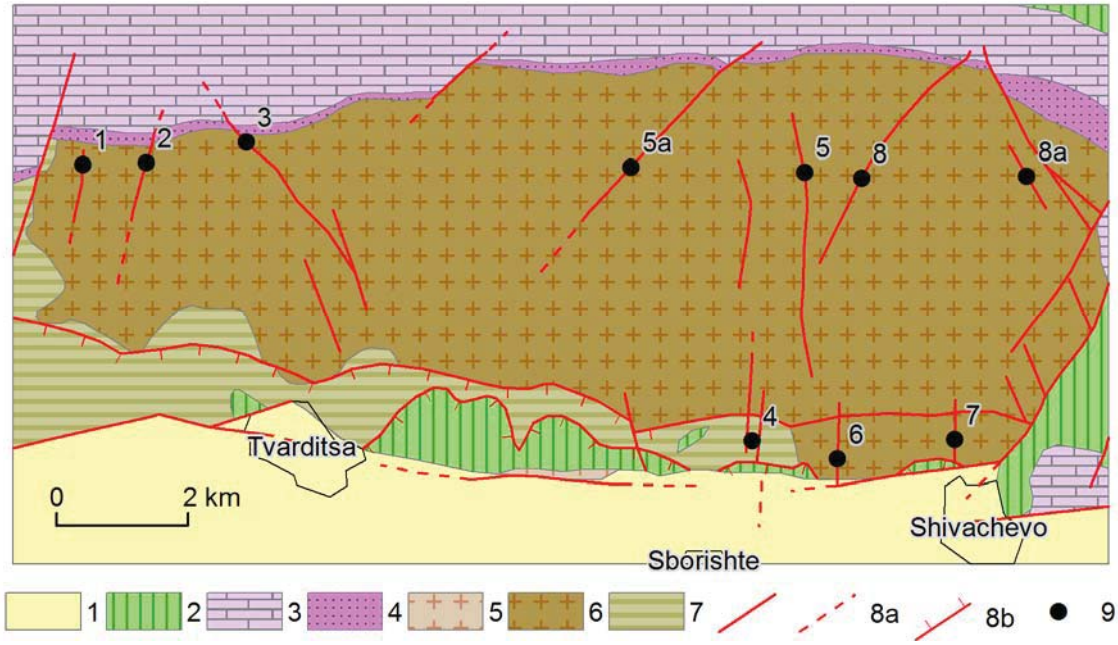

Fig. 3. Geological map of the Shivachevo Ore Field (based on data by Kanchev et al., 1995; Kanchev, 1995; Stoyanov et al., 1989f).
1 – Quaternary sediments; 2 – Upper Cretaceous sediments; 3 – Middle – Upper Triassic carbonate rocks; 4 – Lower Triassic terrigenous sediments; 5 – Upper Paleozoic (Srednogorie) granite; 6 – Devonian – Carboniferous Stara Planina granitoid (Tvarditsa pluton); 7 – Neoproterozoic – Cambrian metamorphic rocks; 8a – fault; 8b – overthrust and upthrust; 9 – uranium deposits and occurrences (1 – Osenov Rat, 2 – Chakaloto, 3 – Krivata Cheshma, 4 – Sborishte, 5 – Kichesta, 6 – Kashla Dere, 7 – Sap Dere, 8 – Domuz Dere).

Conclusions

The Sliven-Tvarditsa Ore Region covers the eastern part from the West Balkan Metallogenic Zone. The region is marked by the development of uranium-polymetallic ores, which are determined in the Sliven and Shivachevo Ore Fields and the Yavorovets ore occurrence. The ore mineralizations are localized in the Triassic and partially in the Upper Cretaceous sediments, as well as in the Pre-Alpine basement rocks such as Permian volcanites, Devonian – Lower Carboniferous granitoids and Neoproterozoic – Cambrian metamorphites.

The ore bodies are formed in the breccia between Mesozoic sediments and Paleozoic basement rocks, as well as in the brecciated Lower Triassic siltstone and argillite or Middle Triassic or Senonian carbonate rocks. Besides, “ore breccia” type ore bodies are found in the NW, sub meridional or NE faults in the basement. Ores in olistoliths from Triassic rocks are also noted.

The ore mineralization is of hydrothermal type. The main ore minerals are pitchblende, galena, sphalerite and chalcopyrite, and the non-ore are quartz and less dolomite, calcite and barite. Pyrite, arsenopyrite, chalcocite, hydro pitchblende,

chalcanthite, renardite, anglesite, uranospinite, torbernite, cerussite, malachite, azurite, autunite, uranophane, hematite and limonite are more rarely observed. The hydrothermal alterations are sericitization, advanced argillization, pyritization, kaolinization and carbonization.

The presented data show that the ore mineralizations are of hydrothermal type, medium to low temperature, as they are not related to concrete magmatic activities. The ore manifestations within the Upper Cretaceous rocks, as well as the development of Upper Cretaceous rocks in the region point that the ore forming is controlled by the Upper Cretaceous magmatism. However, concrete volcanic structures are known at 10-15 km south of the region. This indicates that the examined ore deposits are formed in the frame of the noted non-volcanic island chain, adjacent to the Srednogorie Zone from the Apuseni-Banat-Timok-Srednogorie Magmatic and Metallogenic Belt.

References

Бончев, Е. Геология на България. Част I. С. Наука и изкуство, 1955. - 260 с. (Bonchev, E. Geologia na Bulgaria. S., Nauka i izkustvo, 1, 1955. - 260 p.)

Бончев, Е. Балканидите – геотектонско положение и развитие. С., Изд. БАН, 1986. - 274 с. (Bonchev, E. Balkanidite – geotectonsko polozhenie i razvitie. S., BAN, 1986. - 274 p.)

Вълчанов, А. Съдържание, произход и взаимоотношения на Средногорския алохтон със съседните морфотектонски единици. – Год. Геол. проучв., 20, 1974. - 97-111. (Valchanov, A. Sadarzhanie, proizhod i vzaimootnoshenia na Srednogorskia alohton sas sasednite morfotectonski edinitsi. – God. Geol. Prouchv., 20, 1971. - 97-111.)

Загорчев, И., Х. Дабовски, Т. Николов. (ред.). Геология на България, т. II, ч. 5. Мезозойска геология на България. С. Акад. изд. „Проф. М. Дринов", 2009. - 766 с. (Zagorchev, I., H. Dabovski, T. Nikolov. (ed.). Geologia na Bulgaria. II, 5 Mezozoyska geologia na Bulgaria. S. Akad. Izd. "Prof. Marin Drinov", 2009. - 766 p.)

Иванов, Ж., С. Московски. Горнокредни олистостроми в Централна Стара планина. – Год. Соф. Унив., Геол.-геогр. фак., 68, 1, Геол., 1974. - 101-109. (Ivanov, J., S. Moskovski. Gornokredni olistostromi v Tsentralna Stara Planina. – God. Sof. Uni., Geol-geogr. Fac. 66, 1, 1974. - 101-109)

Иванов, Ж., К. Колчева, С. Московски. Строеж на част от ядката на Твърдишката антиклинала. – Год. Соф. Унив., Геол.-геогр. фак., 66, 1, Геол., 1974. - 245-277. (Ivanov, J., K. Kolcheva, S. Moskovski. Stroezh na chast ot yadkata na Tvardishkata antiklinala. – God. Sof. Univ., Geol.-geogr. Fac., 66, 1, 1974. - 245-277.)

Кънчев, И. Тектоника на Елено-Твърдишка и Тревненска Стара планина. – Приноси геол. Балг., 1, 1962. - 329-408. (Kanchev, I. Tectonica na Eleno-Tvardishka i Trevnenska Stara Planina. – Prinosi geol. Bul., 1, 1962. - 329-408.)

Кънчев, И. Обяснителна записка към геоложката карта на България М 1:100 000, картен лист Сливен. КГМР „Геология и геофизика" АД, 1995. - 139 с. (Kanchev, I. Obyasnitelna zapiska kam geolozhkata karta na Bulgaria M 1:100 000, karten list Sliven. KGMR "Geologiya i geofizika" AD, 1995. - 155 p.)

Кънчев, И., Т. Николов, Н. Рускова, В. Миланова. Обяснителна записка към геоложката карта на България М 1:100 000, картен лист Твърдица. КГМР „Геология и геофизика" АД. 1995. - 139 с. (Kanchev, I., T. Nikolov, N. Ruskova, V. Milanova. Obyasnitelna zapiska kam geolozhkata karta na Bulgaria M 1:100 000, karten list Tvarditsa. KGMR "Geologiya i geofizika" AD, 1995. - 139 p.)

Начев, И. Еминският флиш и олистотромите в Сливенския Балкан. – Палеонт., страт. и литол., 7, 1977. - 45-68. (Nachev, I. Eminskiyat flish i olistostromite v Slivenskia Balkan. – Paleont., Stratig., Lithol., 7, 1977. - 45-58.)

Начев, И., Ч. Начев. Алпийска плейт-тектоника на България. С. Арктик 2001, 2003. - 198 с. (Nachev, I., Ch. Nachev. Alpiyskata pleyt-tectonica na Bulgaria. S., Artik 2001, 2003. - 198 p.)

Паскалев, М. Нови данни за строежа на Сливенския навлак. – Геотект., тектонофиз. и геодин., 15, 1983. - 40-46. (Paskalev, M. Novi danni za stroezha na Slivenskiya navlak. – Geotect., Tectonophys., Geodyn., 15, 1983. - 40-46.)

Паскалев, М. Олистостроми в горнокредните и лютеските седименти от Сливенска Стара планина и взаимоотношенията им с разломно-блоковата тектоника. – Сп. Бълг. геол. д-во, 50, 3, 1989. - 38-49. (Paskalev, M. Olistostromi v gornokrednite i lyuteskite sediment ot Slivenska Stara planina i vzaimootnosheniyata im s razlomno-blokovata tectonica. – Sp. Bulg. Geol., D-vo, 50, 3, 1989. - 38-49.)

Попов, П. Върху структурообразувателните процеси в Сливенската планина. – Год. ВМГИ, 31, 1, 1970. - 1-11. (Popov, P. Varhu strukturoobrazuvatelnite protsesi v Slivenska planina. – God. VMGI, 31, 1, 1970. - 1-11.)

Попов, П. Тектонска характеристика на Сливенската планина. – Год. ВМГИ, 15, 2; 1971. - 5–20. (Popov, P. Tectonska harakteristika na Slivenskata planina. – God. VMGI, 15, 2, 1971. - 5-20.)

Попов, П. Върху тектоно-металогенното развитие на Алпидите на Балканския полуостров и положението на Балканидите в тях. – Год. ВМГИ, 27, 2, 1981. - 27-35. (Popov, P. Varhu tectono-metalogennoto razvitie na Alpidite na Balkanskia poluostrov i polozhenieto na Balkanidite v tyah. – God. VMGI, 27, 2, 1981. - 27-35.)

Попов, П. Геотектонические и структурные условия формирования стратиформных месторождений Западно-Балканскойю металогенной зоны. – Геол. рудн. месторожд., 6, 1985. - 26-34. (Popov, P. Geotectonicheskie i structurnie usloviya formirovaniya stratiformnih mestorozhdeniy Zapadno-Balkanskoyu metalogennoy zoni. – Geol. Rudn. Mestorozhd., 6, 1985. - 26-34.)

Попов, П. Тектонска позиция и структура на горнокредните орудявания в Банат-Средногорската и Западнобалканската металогенни зони в България.

Автореферат, МГУ „Св. И. Рилски“, 1989. - 62 с.(Popov, P. Tectonska pozitsiya i structura na gornokrednite orudyavaniya v Banat-Srednogorskata i Zapadnobalkanskata metalogenni zoni v Bulgaria. Avtoreferat, MGU „Sv. I. Rilski”, 1989. - 62 p.)

Попов, П., Т. Цанова. Петрография и структурни особености на младопалеозойските вулканити от Сливенската планина. - Сп. Бълг. геол. д-во, 28, 3, 1967. - 243-260. (Popov, P., T. Tsanova. Petrografia i structurni osobenosti na mladopaleozoyskite vulkaniti ot Slivenskata planina. – Sp. Bul. Geol. D-vo., 28, 3, 1967. - 243-260.)

Попов, П., М. Антонов, Л. Нафтали, И. Байрактаров, Т. Маринов. Върху структурната характеристика на алпийската Западнобалканска металогенна зона. – В Сб. „25 год. ВМГИ”, 2; 1978. - 141-152. (Popov, P., M. Antonov, L. Naftalli, I. Bairaktarov, T. Marinov. Varhu strukturnata harakteristika na alpiyskata Zapadnobalkanska metalogenna zona. – In Sb. „25 god. VMGI”, 2, 1978. - 141-152.)

Попов, П., Л. Нафтали, М. Антонов, И. Байрактаров. Някои особености в алпийския строеж на Сливенската и източните отдели на Елено-Твърдишка Стара планина. – Год. ВМГИ, 25, 2, 1980. - 91-101. (Popov, P., L. Naftalli, M. Antonov, I. Bairaktarov. Nyakoi osobenosti v alpiyskiya stroezh na Slivenskata i iztochnite otdeli na Eleno-Tvardishka Stara planina. – God. VMGI, 25, 2, 1980. - 91-101.)

Цанков, Ц., Л. Филипов, Н. Кацков. Обяснителна записка към геоложката карта на България М 1:100 000, картен лист Стара Загора. КГМР „Геология и геофизика” АД, 1995а. - 58 с. (Tsankov, Ts., L. Filipov, N. Katskov. Obyasnitelna zapiska kam geolozhkata karta na Bulgaria M 1:100 000, karten list Stara Zagora. KGMR “Geologiya i geofizika” AD, 1995a. - 58 p.)

Цанков, Ц., Р. Наков, Н. Недялков, Д. Ангелова. Обяснителна записка към геоложката карта на България М 1:100 000, картен лист Нова Загора. КГМР „Геология и геофизика” АД. 1995b. - 86 с. (Tsankov, Ts., R. Nakov, N. Nedjalkov, D. Angelova. Obyasnitelna zapiska kam geolozhkata karta na Bulgaria M 1:100 000, karten list Nova Zagora. KGMR “Geologiya i geofizika” AD, 1995b. - 86 p.)

Kockel, C. W. Zur Stratigraphie und Tektonik Bulgariens. – Geol. Rund. XVIII, 5, 1927. - 349-395.

Popov, P. Postsubduction Alpine Metallogenic Zones in the Balkan Peninsula. – Geologica Macedonica, 9, 1995. - 97-101.

Popov, P. On the Tectono-Metallogenic Evolution of the Balkan Peninsula Alpides. In: Popov, P. (ed.). Plate Tectonic Aspects of the Alpine Metallogeny in the Carpatho-Balkan Region IGSP Project No 356 Annual Meet., Sofia, 1, 1996. - 5-17.

Popov, P. Alpine geotectonic evolution and metallogeny of the eastern part of the Balkan Peninsula. – Ann. Univ. Min. geol. „St. I. Rilski”, 45, 1, 2002. - 33-38.

Popov, P., T. Berza, A. Grubić, I. Dimitru. Late Cretaceous Apuseni-Banat-Timok-Srednogorie (ABTS) Magmatic and Metallogenic Belt in the Carpathian-Balkan Orogen. – *Geol. Balc.,* 32, 2-4, 2002. - 145-163.

Statelova, I., P. Machev. Metagranites from Bercovica Group, Central Balkan area – structural and petrographic evidence. – Ann. Univ. Sofia, Fac. geol., geogr., 97, 1, 2005. - 149-160.

Tzankov, Tz., M. Paskalev, R. Nakov. Post-Illyrian major-fold subdivision of the transitional area between the Middle and Eastern Balkan Mountains. – *Geologica Balcanica*, 21, 1, 1991. - 41-58.

National Geofund Reports

Кръстев, К., Т. Джелепов. Уранови орудявания в триаса в условията на рудопроявление Яворовец. – Геофонд, XXIII-3907. 1974ф. (Krastev, K., T. Dzhelepov. Uranovi orudyavaniya v triasa v usloviata na rudoproyavlenie Yavorovets. – National Geofund, XXIII-3907, 1974f.)

Пашов, И. Геология и минералогия на Сливенското ураново месторождение. – Геофонд, XXIII-3714. 1965ф. (Pashov, I. Geologia i mineralogia na Slivenskoto uranovo mestorozhdenie. – National Geofund, XXIII-3714, 1965f.)

Пашов, И., П. Попов, М. Латифян. Основни закономерности на хидротермалните уранови орудявания в Сливенска Стара планина. – Геофонд, XXIII-945, 1966ф. - 946. (Pashov, I., P. Popov, M. Latifyan. Osnovni zakonomernosti na hidrotermalnite uranovi orudyavaniya v Slivenska Stara Planina. – National Geofund, XXIII-945, 946, 1966f.)

Стоянов, С., И. Петров, И. Михнев. Отчет за проведените геологопроучвателни работи през 1989 година на находище Сборище с изчисление на запасите. – Геофонд, XXIII-3161. 1989ф. (Stoyanov, S., I. Petrov, I. Mihnev. Otchet za provedenite geologoprouchvatelni raboti prez 1989 godina na nahodishte Sborishte s izchislenie na zapasite. – National Geofund, XXIII-3161, 1989f.)

The article is reviewed by Assoc. Prof. Slavcho Mankov and Prof. Dr. Strashimir Strashimirov.

"SOPOLIVITE KAMANI" ("RUNNY STONES") GEOSITE IN SASHTINSKA SREDNA GORA MOUNTAIN

Boris Valchev[1], Valentina Nikolova[1]

[1]"St. Ivan Rilski" University of Mining and Geology, 1700 Sofia, e-mail: b_valchev@mgu.bg

ABSTRACT. The present article represents the results from the investigation of the geoconservation value of "Sopolivite Kamani" ("Runny Stones") geosite (its nomination for a geosite is proposed here), located in the central part of Sashtinska Sredna Gora Mountain between the towns of Koprivshtitsa and Strelcha. It has not been described yet as geological phenomenon and it is not included in the "Register and cadastre of the geological phenomena in the Republic of Bulgaria" as well as in the State Register of Natural Sites. The geosite represents a complex of granite blocks of varied sizes and shapes formed mainly in the rocks of Late Carboniferous Smilovene pluton and partly in these of Early Permian Strelcha pluton, both of them referred to Srednogorie granitoids. The outcrops allow examination of the prototectonics of the two plutons as well as different stages of spheroidal weathering in the granites. According to the classification of the geological phenomena "Sopolivite Kamani" geotope is referred to the geosites of aesthetic value (geomorphologic class), and according to the original Bulgarian methodology for estimation of geological phenomena it is of local importance. The further popularization of the geosite will increase its total expert value by adding investigational and educational value to its present characteristics.

Keywords: geological heritage, geoconservation, "Sopolivite Kamani" ("Runny Stones") geosite, Sashtinska Sredna Gora Mountain.

ГЕОТОП „СОПОЛИВИТЕ КАМЪНИ" В СЪЩИНСКА СРЕДНА ГОРА

Борис Вълчев[1], Валентина Николова[1]

[1]Минно-геоложки университет "Св. Иван Рилски", София 1700

РЕЗЮМЕ.Настоящата статия представя резултатите от изследването на геоконсервационното значение на геотопа „Сополивите камъни" (номинирането му за геотоп се предлага тук), намиращ се в централната част на Същинска Средна гора между градовете Копривщица и Стрелча. Той не е описван като геоложки феномен и не фигурира в „Регистър и кадастър на геоложките феномени в Република България", както и в Държавния регистър на природните забележителности. Представлява комплекс от гранитни блокове с различна форма и размери, оформен главно в скалите на къснокарбонския Смиловенски плутон и отчасти в тези на раннопермския Стрелчански плутон, които се отнасят към Средногорските гранитоиди. Разкритията позволяват изучаването на прототектониката на двата плутона, както и различни етапи от сферичното изветряне на гранитите. Съгласно класификацията на геоложките феномени геотопът „Сополивите камъни" попада в групата на обектите с естетическа стойност (клас геоморфоложки), а според оригиналната българска методика за оценяване на геоложки феномени, той е с локално значение. Популяризирането на геотопа ще повиши общата му експертна оценка, добавяйки към досегашната му характеристика изследователска и образователна стойност.

Ключови думи: геоложко наследство, геоконсервация, геотоп„ Сополивите камъни", Същинска Средна гора.

Introduction

The central part of Sashtinska Sredna Gora Mountain, between the towns of Koprivshtitsa and Strelcha, reveals a great diversity of natural sites, as most of the mare included in the State Register of Natural Sites. Seven of these sites, representing geological phenomena (Zhelev, Petrov, 2017a, b), were nominated for natural sites in 1972 on the basis of an order of the Ministry of Forest and Environment Protection. They are exposed in the south slopes of the mountain, north and northeast of the town of Strelcha (Fig. 1): Arbushki Rocks, Goranitsa, Kiselitsata, Gabrovitsa, Gerekinski Gyol, Garvanov Kamak, Turchanov Kamak. Later on Petrov (in Zhelev, Sinyovski, 2003[1]) compiled files for them within the project "Register and cadastre of the geological phenomena in the Republic of Bulgaria"(1999-2003) financed by the Ministry of Environment and Water in the Republic of Bulgaria. During the compilation of the Register the experts did not describe and estimate the outcrops of granite blocks of varied size and shape in the highest central parts of Sashtinska Sredna Gora Mountain west of Koprivshtitsa-Strelcha road in the Sopolivite Kamani locality. Бакалова (2014) noted the presence of "*bizarre rock forms on the crest of Sashtinska Sredna Gora Mountain*", but she did not give any data for their spatial distribution. The present article aims (i) to represent in brief the geological setting, (ii) to give a description of "Sopolivite Kamani" ("Runny Stones") geosite, and (iii) to estimate its geoconservation value.

Geological Setting

The area of "Sopolivite Kamani" ("Runny Stones") geosite is composed of Neoproterozoic-Lower Paleozoic high-graded metamorphic rocks, Paleozoic intrusive bodies, Upper Cretaceous subvolcanic rocks, and Quaternary deposits (Fig. 2).

[1]Jelev, V., D. Sinnyovsky (Eds.). 2003. Register and cadastre of the geological phenomena of Republic of Bulgaria. 188 files in 5 volumes. – National Geofund, XV-1232 (In Bulgarian, Russian and English).

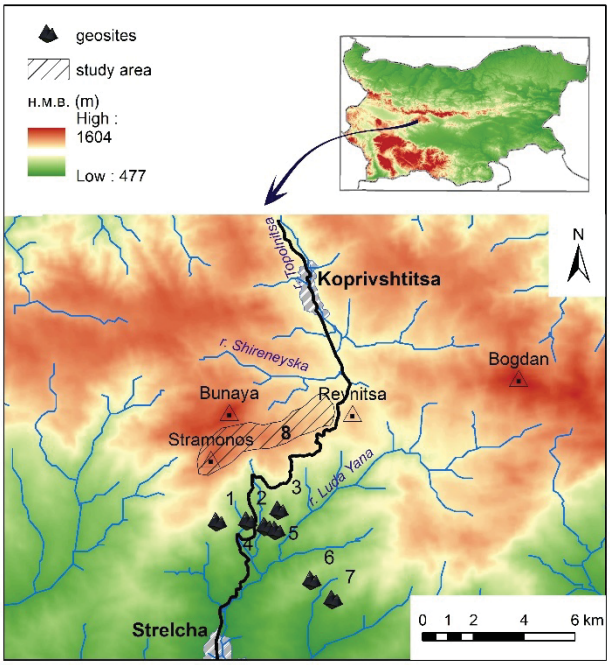

Fig. 1. Geological phenomena in the central part of Sashtinska Sredna Gora Mountain
1 – Arbushki Rocks, 2 - Goranitsa, 3- Kiselitsata, 4 - Gabrovitsa, 5 – Gerekinski Gyol, 6 – Garvanov Kamak, 7 – Turchanov Kamak, 8 – "Sopolivite Kamani" ("Runny Stones") geosite

The oldest rocks are referred to *Koprivshtitsa amphibolitic complex* and *Pirdop gneissic complex*. The first one forms a narrow strip in the southeastern outskirts of the town of Koprivshtitsa, and the second one crops out as west-east oriented broad strip south, southeast and east of the town of Koprivshtitsa, as well as in two isolated areas southwest of the same town. The two complexes were named respectively "lower amphibolitic formation" and "upper gneissic formation" (Dabovski et al., 1972), "Koprivschtitsa Group" and "Pirdop Group" (Dabovski, 1988). Later on (Iliev, Katskov, 1990; Katskov, Iliev, 1993) they were characterized as "Unsubdivided Boturče Group" and "Unsubdivided Arda Group"of the "Prarhodopes Supergroup" (introduced in the Rhodopes by Kozhuharov, 1987), and Zagorchev (2008) nominated them as "Koprivschtitsa amphibolitic complex" and "Pirdop gneiss-migmatic complex" according to the recommendations of Hrischev et al. (2005) on the terminology of the non-layered lithostratigraphic units. The *Koprivshtitsa amphibolitic complex* is composed of amphibolites and migmatised amphibole-biotitic gneisses, while the *Pirdop gneissic complex* comprises mainly migmatised two-mica gneisses and minor amount of muscovitic, biotitic and amphibole-biotitic gneisses. On the base of U-Pb analyses conducted by Arnaudov et al. (1989) and Peycheva et al. (2004), as well as these for the lateral relationships of the two complexes, Antonov (in Antonov et al., 2011) determined for them Neoproterozoic-Lower Paleozoic age.

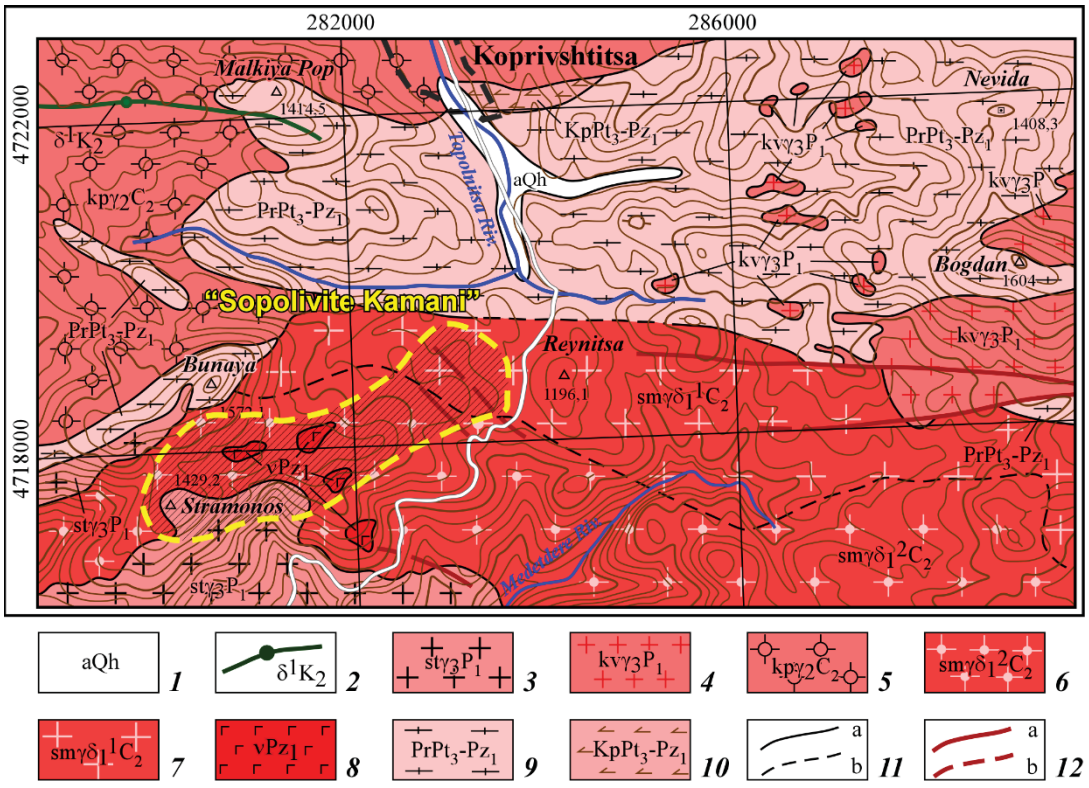

Fig. 2. Geological map of the area of "Sopolivite Kamani" ("Runny Stones") geosite (amended after Iliev, Katskov, 1990)
1, Quaternary: alluvium (Holocene gravels and sands); *2*, Upper Cretaceous: quartz-diorite porphyritic dykes; *3-7*, Upper Paleozoic (Srednogorie granitoids): *3*, Strelcha pluton (coarse-grained felsic wo-micagranites; Lower Permian), *4*, Karavelovo pluton (even-grained felsic biotite granites; Lower Permian), *5*, Koprivshtitsa pluton (porphyroid biotite to two-micagranites; Upper Carboniferous), *6*, *7*, Smilovene pluton (*6*, porphyroid granites and granodiorites, *7*, granodiorites – contaminated facies; Upper Carboniferous); *8-10*, Neoproterozoic and Lower Paleozoic: *8*, gabbrodiorites and peridotites (Lower Paleozoic), *9*, Pirdop gneiss complex (Neoproterozoic-Lower Paleozoic), *10*, Koprivshtitsa amphibolitic complex (Neoproterozoic-Lower Paleozoic); *11*, geological boundary (*a*, proven, *b*, supposed); *12*, fault (*a*, proven, *b*, supposed).

Amongst the high-graded metamorphic *Paleozoic intrusive bodies* of ultramafics and granitoides are intruded. The first ones are small-sized bodies of gabbrodiorites to peridotites of Early Paleozoic age (Katskov, Iliev, 1993), cropping out as 4 small areas east of Stramonos Peak. The granitoid intrusions, referred by Dabovski (1968) to Srednogorie granitoids, were divided into four intrusive complexes (Dabovski et al., 1972), represented of totally 9 plutons. Four of them crop out in the studied area: *Smilovene pluton* (first intrusive complex; Upper Carboniferous), *Koprivshtitsa pluton* (second intrusive complex; Upper Carboniferous), *Karavelovo and Strelcha plutons* (third intrusive complex; Lower Permian). The first three are intruded entirely amongst the high-graded metamorphic complexes, while the last one crosses the rocks of Smilovene pluton. The plutons are composed of porphyroid granites and granodiorites (Smilovene pluton), porphyroid biotitic and two-micagranites (Koprivshtitsa pluton), even-grained biotitic (Karavelovo pluton) and coarse-grained two-micafelsic granites (Strelcha pluton).

Upper Cretaceous dykes were established (Iliev, Katskov, 1990) amongst the high-graded metamorphics and the granites of Koprivshtitsa pluton. They are composed of quartz-diorite porphyrite and crop out west of the town of Koprivshtitsa.

*The Quaternary deposits*are developed on a small area in Topolnitsa River valley south of the town of Koprivshtitsa. They include alluvial gravels and sands of Holocene age.

The area of "Sopolivite Kamani" geosite is formed in the frames of a tectonic unit named Srednogorie anticlinorium (Bonchev, Karagyuleva, 1961), Topolnitsa-Tundzha unit (Ivanov, 1998), or Central Srednogorie unit (Dabovski, Zagorchev, 2009), which is a part of the Srednogorie tectonic zone (Cvijić, 1904; Bonchev, 1946, 1971).

Characteristics of the geosite

The complex of rock outcrops, nominated here for a geosite after Sopolivite Kamani locality, forms a southwest-northeast oriented strip, 6 km long and 1-1.5 km wide, including separate groups of granite blocks with a great variety of shapes and sizes. It is located between the massive of Stramonos Peak and Koprivshtitsa-Strelcha road, as its northeastern end is located 3.5 km south of the town Koprivshtitsa (Figs. 1, 3). The formation of the geosite is a result of a spheroidal weathering characteristic for jointed intrusive rocks, under the combined impact of temperature, surface water and wind, as well as the further removal by surface waters of the disintegrated debris. The weathering is also predetermined by the prototectonics of the intrusives – three systems of joints are observed in granites (two subvertical and one subhorizontal - PlateI, *1, 2*). The influence of the exogenic processes could be investigated clearly along the subvertical joints (Plate I, *3, 4*), as the geosite gives an opportunity for observation of different stages of the spheroidal weathering.

The area of "Sopolivite Kamani" geosite is characterized by middle-mountain relief and as a whole it has low values of horizontal relief disintegration, mainly to 0.5 km/km^2 (Fig. 3). These values and small slopes angles determine a reminder of flat (denudation) surface, which is laid down in the range of 1200 to 1400 m above sea level. According to Kanev (1989) and Bakalova (2014) this surface is of Early Miocene age. Our field observations confirmed the relationship between the weathering stage and the horizontal relief disintegration. The areas with lowest values (eastern part of the geosite and the area around Stramonos Peak – Fig. 3) reveal groups consisting of well-rounded and clearly separated granite blocks (Plate I, *5-8*), i.e. these are the areas with advanced stage of spheroidal weathering and the disintegrated debris has been removed by surface streams. The highest values of horizontal relief disintegration are characteristic for the central area of the geosite, where the prototectonics of Strelcha pluton, as well as the initial stages of spheroidal weathering could be observed (Plate II, *1-4*).

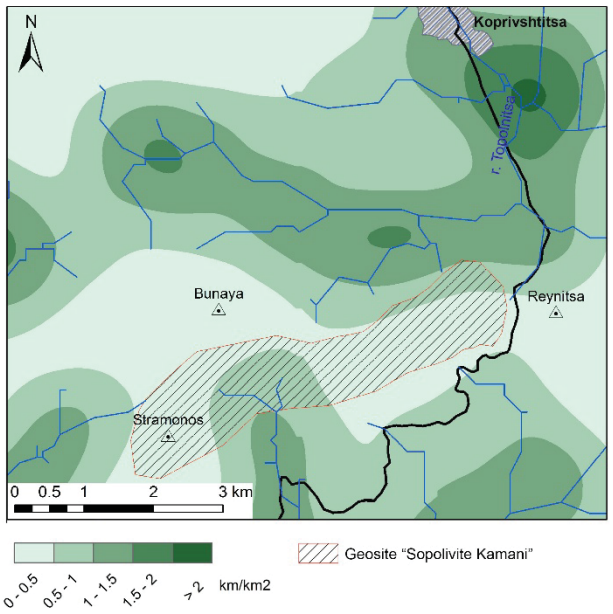

Fig. 3. Horizontal relief disintegration in the area of "Sopolivite Kamani" ("Runny Stones") geosite

Sopolivite Kamani locality is included by Koprivshtitsa Municipality in tourist's routes (Map of Koprivshtitsa). For this purpose at several places sign boards with general information were placed (Plate II, *5*), and at 600 m west of Koprivshtitsa-Strelcha road, next to the pathway to Stramonos Peak, a bower was built (Plate II, *6*). It gives a good opportunity to view a panorama to north (Plate II, *7*) and east, revealing the highest peak of Sredna Gora Mountain - Bogdan Peak (Plate II, *8*).

The geosite, described in the present article, is referred to the geosites of aesthetic value (geomorphological class). After the conducted expert estimation, according to the original Bulgarian methodology for estimation of geological phenomena (Sinyovski et al., 2002), we concluded that it is of local importance, and it could be estimated as a geosite of high degree of preservation, exposure, resistance and accessibility.

Conclusion

The central part of Sashtinska Sredna Gora Mountain reveals a great diversity of natural sites, as considerable group of them are geological phenomena. The intrusive rocks, forming "Sopolivite Kamani" ("Runny Stones") geosite, on one hand are resistant to the influence of exogenic processes, and

on the other hand, they are located away from regions with well developed road infrastructure and intensive antropogenic influence, which suggests a long period of existing for the geosite. Its further popularization requires placing of signboards with geological information (data concerning the mineral composition, genesis, and age of the rocks), which will increase its total expert value by adding investigational and educational value to its present characteristics.

References

Арнаудов, В., Б. Амов, Е. Бартницкий, М. Павлова. Изотопная геохронология магматических и метаморфических пород в Балканидах и Родопском массиве. – Тезисыдокл., XIVконгресс КБГА, 1989. – 1154-1157. (Arnaudov, V., B. Amov, E. Bartnitskij, M. Pavlova. Izotopnaya geohronologiya magmaticheskih I metamorficheskih porod Balkanidah i Rodopskom masive. – Tezis idokl..XIV Kongres CBGA, 1989. - 1154-1157).

Бакалова, Г. Причудливи скални образувания по високите билни части на Същинска Средна гора. – Геол.и мин. рес., 7-8, 2014. - 21-23. (Bakalova, G. Prichudlivi skalni obrazuvaniya po visokite bilni chasti na Sashtinska Sredna Gora. – Geol. i Min. Res., 7-8, 2014. - 21-23).

Бончев, Е. Основи на тектониката на България. – Год. Дир. геол. и минни проучв., А, 4,1946. - 336–379. (Bonchev, E. Osnovi na tektonikata na Bulgaria. – Godishnik Dir. Geol. i Min. prouchvaniya, A, 4,1946. - 336–379).

Бончев, Е. Проблеми на българската геотектоника. С.,Техника, 1971. - 204 с. (Bonchev, E. Problemi na balgarskata geotektonika. Sofia, Tehnika, 1971. – 204 p.).

Бончев, Е., Ю. Карагюлева. Средногорският антиклинорий и Старопланинският гранитен навлак. – Тр. геол. Б-я, сер. стратигр. и тект., 2, 1961. –31-42. (Bonchev, E., Y. Karagyuleva. Srednogorskiyat antiklinorij i Staroplaninskiyat graniten navlak. - Trudove Geol. Bulg., ser. stratigr. i tect., 2, 1961. –31-42).

Дабовски, Х. Палеозойски магматизъм. – В: Цанков, В., Х. Спасов (ред.), Стратиграфия на България. С., „Наука и изкуство“, 1968. - 121-166. (Dabovski, H. Paleozojski magmatizam. – In: Tsankov, V., H. Spasov (Ed.), Stratigrafiya na Bulgaria. Sofia, Nauka I Izkustvo, 1968. - 121-166).

Дабовски, Х., И. Загорчев. Алпийска тектонска подялба на България. – В: Загорчев, И., Х. Дабовски, Т. Николов (ред.), Геология на България. Том II, Мезозойска геология. С., Акад. изд. „Проф. Марин Дринов“, 2009. - 30-37. (Dabovski, H., I, Zagorchev. Alpijska tektonska podyalba na Balgaria. – In: Zagorchev, I., H. Dabovski, T. Nikolov (Ed.). Geologiya na Bulgaria. Volume II. Part 5. Mesozojska geologiya. Sofia, Akad. Izdatelstvo Prof. Marin Drinov, 2009. - 30-37).

Дабовски, Х., И. Загорчев, М. Русева, Д. Чунев. Палеозойските гранитоиди в Същинска Средна гора. – Год. Гл. упр. геол., 16, 1972. – 57-95. (Dabovski, H., I. Zagorchev, M. Ruseva, D, Chunev. Paleozojskite granitoidi v Sashtinska Sredna Gora. – Godishnik na glavnoto upravlenie po geologiya, 16, 1972. – 57-95).

Желев, В., П. Петров. Стрелчанските природни феномени. Част 1. – Геол. и мин. рес., 1-2, 2017.а. – 42-46. (Jelev, V., P. Petrov. Strelchanskite prirodni fenomeni. – Geol. Min. Res., 1-2, 2017.a. – 42-46).

Желев, В., П. Петров. Стрелчанските природни феномени. Част 2. – Геол. и мин. рес., 3-4, 2017. б. – 24-29. (Jelev, V., P. Petrov. Strelchanskite prirodni fenomeni. – Geol. Min. Res., 3-4, 2017. b. – 24-29).

Иванов, Ж. Тектоника на България. Непубл. хабилит. труд, Соф. унив., 1998. - 545 с. (Ivanov, Zh. Tectonica na Bulgaria. Nepublikuvan habilitatsionen trud, Sofia Univ., 1998. - 545 p.).

Илиев, К., Н. Кацков. Геоложка карта на НР България в М 1:100 000. Картен лист Панагюрище. С., Комитет по геология, Предприятие за геофизични проучвания и геоложко картиране. 1990. (Iliev, K., N. Katzkov. Geolozhka karta na Bulgaria v mashtab 1:100 000. Karten list Panagjuriste. Sofia, Komitet po Geologiya, Predpriyatie za geofizichni prouchvaniya i geol. kartirane. 1990).

Канев, Д. Геоморфология на България. София, Изд. СУ "Св. Климент Охридски", 1989. - 323 с. (Kanev. D. Geomorphologiya na Bulgaria. Sofia, Universitetsko izdatelstvo “Sv. Kliment Ohridski”. 1989. - 323 p.).

Кацков, Н., К. Илиев. Геоложка карта на България в М 1:100 000, картен лист Панагюрище. Обяснителна записка. С., „Болид“, 1993. - 53 с. (Katzkov, N., K. Iliev. Geolozhka karta na Bulgaria v mashtab 1:100 000, karten list Panagyurishte. Obyasnitelna zapiska. Sofia, Bolid Publ. House, 1993. - 53 p.).

Кожухаров, Д. Литостратиграфия и строение докембрия в ядре Белоречкого поднятия в Восточных Родопах. – Geologica Balc., 17, 2, 1987. – 15-38. (Kozhoukharov, D. Litostratigrafiya i stroenie dokembriya v yadre Belorechkogo podnyatiya v Vostochnih Rodopah. – Geologica Balc., 17, 2, 1987. – 15-38).

Карта Копривщица. Забележителности. Туристически маршрути. Стара Загора, Домино ЕООД, печат „Жанет-45“. (Karta Koprivshtitsa. Zabelezhitelnosti. Turisticheski marshruti. Stara Zagora, Domino Ltd., pechat Zhanet-45).

Синьовски, Д., В. Желев, М. Антонов, С. Джуранов, З. Илиев, Д. Вангелов, Г. Айданлийски, П. Петров, Х. Василев. Метод за оценка на геоложки феномени. –В:II Международна конференция SGEM, Варна, 2002. - 25-33.(Sinnyovsky, D., V. Jelev, M. Antonov, S. Juranov, Z. Iliev, D. Vangelov, G. Ajdanlijsky, P. Petrov, Ch. Vasilev.2002. Method za otsenka na geolozhki fenomeni.– In: II Mezhdunarodna Konf. SGEM. Varna, 2002. - 25-33).

Христев, Х., В. Ангелов, М. Антонов. Терминология и номенклатура на неслоестите литостратиграфски единици при геоложкото картиране в М 1:50 000 на Западния Балкан. – Сп. Бълг. геол. д-во, 66, 1-3, 2005. –171-175. (Khrischev, Kh., V. Angelov, M. Antonov. Terminologiya i nomenklatura na nesloestite litostratigrafski edinitsi pri geolozhkoto kartirane v mashtab 1:50 000 na Zapadniya Balkan. – Spisanie Bulg. Geol. Druzhestvo., 66, 1-3, 2005. - 171-175).

Antonov, M. Pirdop gneissic complex. – In: Antonov, M., S. Gerdzhikov, L. Metodiev, H. Kiselinov, V. Sirakov, V. Valev, Explanatory note to the Geological Map of the Republic of Bulgaria in scale 1:50 000, K-35-37-B map sheet (Pirdop). Sofia, Ministry of Environment and Water, Bulg. Nat. Geol. Surv., 2011. - 10-11.

Cvijić, J. Die Tektonik der Balkan halbinsel mit besonderer Berüksichtigung der neueren Fortschrittein der Kentniss der Geologie von Bulgarien, Serbien und Makedonien. – C. R. IXCongr. Geol. Intern., Vienne, I, 1904. - 347–370.

Dabovski, H. Precambrian in the Srednogorie Zone (Bulgaria). – In: Zoubek, V., J. Conge, D. Kozhoukharov, H. Krautner (eds.), Precambrian in Younger Fold Belts. Wiley-Intersciens Publication, Wiley&Sons, Chichester, 1988. - 841-847.

Peycheva, I., A. von Quadt, M. Frank, B. Kamenov, C. Heinrich. The subcontinental lithosphere beneath Central Srednogorie (Bulgaria): U-Pb and Hf-zircon, Nd and Sr whole rock constrains. – Goldschmidt Conf., Conf. Abstracts Suppl., Geochim. Cosmochim. Acta, Copenhagen, Denmark, Vol A, 2004. - 624.

Zagorchev, I. Amphibolite facies metamorphic complexes in Bulgaria and Precambrian geodynamics: controversies and "state of art". – Geologica Balc., 37, 1-2, 2008. - 33-46.

This article was reviewed by Prof. Dr. Venelin Jelev and Assoc. Prof. Dr. Ivan Dimitrov.

PLATE I

1, 2, clear formed subvertical fractures in the eastern part of "Sopolivite Kamani" ("Runny Stones") geosite; *3, 4*, examples for gradual broadening of the subvertical fractures (*3*,advancedstage, *4*,initial stage); *5-8*, clearly separated well rounded granite blocks (*5, 6*,eastern part of the geosite, *7, 8*,western part of the geosite between Stramonos and Boev Shamak Peaks).

PLATE II

1, 2, primary fractures of Strelcha pluton in the initial stage of spherical weathering southwest of Boev Shamak Peak; *3, 4*, granite blocks with tapered edges southwest of Boev Shamak Peak; *5*, signboard, placed by Koprivshtitsa Municipality at the eastern part of the geosite; *6*, a bower built by Koprivshtitsa Municipality next to the pathway to Stramonos Peak 600 m west of Koprivshtitsa-Strelcha road; *7*, view north of the bower; *8*, Bogdan Peak(at the background) seen from the bower.

ON THE DISTRIBUTION OF IRON IN MINERALS FROM JASPERS FROM THE EASTERN RHODOPES ACCORDING TO SPECTROSCOPIC DATA

Ruslan I. Kostov[1], Radostin Pazderov[1], Lyubomir Michaylov[1]

[1]University of Mining and Geology "St. Ivan Rilski", 1700 Sofia; rikostov@yahoo.com; rpazderov@abv.bg; lyubomihaylov@abv.bg

ABSTRACT. The Eastern Rhodopes are the main area of distribution of various in color and genesis jaspers in Bulgaria. With the help of Mössbauer spectroscopy and Electron Paramagnetic Resonance (EPR) spectroscopy, the iron status and distribution of different valence states of iron were studied in the three most important impurity phases of jasper – hematite, goethite and celadonite, which are associated with red, yellow to yellowish-brown and green coloration, respectively. In the Mössbauer spectrum of red jasper, Fe^{3+} sextes characteristic of hematite and goethite are detected, in the spectrum of yellow jasper – Fe^{3+} sextets characteristic only of goethite, and in the green jasper spectrum – dominant Fe^{3+} and Fe^{2+} doublets associated with celadonite. The EPR spectra of jasper samples reveal information about the concentration of iron-bearing phases and iron ions in tetrahedral coordination.

Key words: jasper, hematite, goethite, celadonite, Eastern Rhodopes

ВЪРХУ РАЗПРЕДЕЛЕНИЕТО НА ЖЕЛЯЗОТО В МИНЕРАЛИ ОТ ЯСПИСИ ОТ ИЗТОЧНИТЕ РОДОПИ ПО СПЕКТРОСКОПСКИ ДАННИ

Руслан И. Костов[1], Радостин Паздеров[1], Любомир Михайлов[1]

[1]Минно-геоложки университет "Св. Иван Рилски", 1700 София; rikostov@yahoo.com; rpazderov@abv.bg; lyubomihaylov@abv.bg

РЕЗЮМЕ. Източните Родопи са главния район на разпространение на разнообразни по цвят и генезис ясписи в България. Чрез помощта на Мьосбауерова спектроскопия и чрез Електронен парамагнитен резонанс (ЕПР) са изследвани статута и разпределението на разновалентни железни йони в трите най-важни примесни фази на ясписите − хематит, гьотит и селадонит, които са свързани съответно с червено, жълто до жълтокафяво и зелено оцветяване. В Мьосбауеровия спектър на червен яспис се отбелязват Fe^{3+} секстети, характерни за хематит и гьотит, в този на жълт яспис − Fe^{3+} секстети, характерни само за гьотит, а в този на зелен яспис − доминиращи дублети от Fe^{3+} и Fe^{2+}, свързани със селадонит. ЕПР спектрите на пробите от ясписи разкриват информация за концентрацията на желязо-съдържащи фази и тетраедрично координирани железни йони.

Ключови думи: яспис, хематит, гьотит, селадонит, Източни Родопи

Introduction

The Eastern Rhodopes are the main region of localization of various in color and genesis jaspers in Bulgaria (Atanasov and Yordanov, 1986). In recent years their widespread distribution has been established both in the host rocks and in deluvial and alluvial manifestations along the main river valleys of the Eastern Rhodopes (Kostov et al., 2016a). At the same time, differently colored jaspers in the form of artifacts are found both in random finds and as a result of detailed archaeological studies of prehistoric settlements in the region (Kostov et al., 2016b). The mineralogy of jasper is poorly studied on an international scale and the existing systems are based on mineralogical or genetic traits without being universally accepted (Kostov, 2006; 2010). To clarify the role and distribution of iron in the composition of the most common and frequently occurring iron-containing phases in jasper, spectroscopic studies were performed using Mössbauer spectroscopy and Electronic Paramagnetic Resonance (EPR) spectroscopy. Both methods are complementary to the possibility of interpretations of valence, position and type of iron in the respective mineral phases or in the SiO_2 matrix itself, represented most commonly by fine grained quartz, chalcedony and various opals.

Samples and methods

Five samples of single coloured jasper of three different colours (two with red, one with yellow to yellowish-brown and two with green colour) were studied from artefacts from regions of their maximum concentration around the town of Momchilgrad (Chukovo − aCh, Varhari − aVu) and the village of Nanovitsa in the Krumovgrad region. Similar in colour jaspers found in the host rocks (Piyavets, Neophyt Bozvelievo and Pazartsi, marked correspondently Pi, Ne and Pa) were used for comparison. On the geological map of Bulgaria at a scale of 1:50000, in the region are revealed predominantly materials from the Lower and Upper Tuff epiclastic batch, as well as basic to medium-acid volcanic rocks of the upper effusion, all of them with an Oligocene age (Yordanov et al., 2008). The samples were analyzed by X-ray in order to determine the mineral phases contained in them and the distribution of dominant microcrystalline quartz or chalcedony (Kostov et al., 2017b). The data from the X-ray diffraction

analyses show a similar and relatively homogeneous phase composition: in the green varieties − quartz (±chalcedony, opal) with celadonite $K(MgFe^{3+})[Si_4O_{10}](OH)_2$, in the yellow ones – quartz (±chalcedony) with goethite α-FeOOH, and in red ones – quartz (±chalcedony, opal) with hematite α-Fe_2O_3.

The Mössbauer spectra were measured on an electromechanical spectrometer (Wissenschaftliche Elektronik GMBN, Germany), operating in steady-state mode at room temperature. The source is ^{57}Co/Rh (activity ≅25 mCi) and an α-Fe standard has been used (Institute of Catalysis of the Bulgarian Academy of Sciences). Experimentally obtained spectra were processed with the program CONFIT2000 (Žák and Jirásková, 2006). The parameters of the hyperfine interactions – isomer shift (δ), quadrupole splitting (Δ), effective internal magnetic field (B) as well as line width (Γ_{exp}) and relative influence of the partial components (G) are determined.

The samples, that were pre-ground (60 mg) in an agate mortar, were examined for impurity and electrone-hole defects, mostly at room temperature (294 K) on a Bruker EMXplus-10/12/P/L Spectrometer System in different mode (modulation amplitude of 2 G; microwave power 2 mW and 0.6 mW) (IGIC BAS) and on a JEOL JES-FA100 spectrometer both operating in the X-band (IC BAS). Electron Paramagnetic Resonance (EPR) spectra were recorded at a magnetic field width of 4000 G (in the range ~4100-8000 G for the diagnosis of broad lines associated with iron ions and iron impurities; 150 s) and at 200 G (in the range ~3200-3400 G for diagnostics of electrone-hole centers in the range of g~2; 60 s).

Results and Discussion

The experimental Mössbauer spectrum of a red jasper specimen (hematite-containing; sample aCh2) is a combination of a sextet and a doublet (Figure 1). Mathematical processing was performed using a model of two sextets and one doublet. As a result of the treatment, parameters of the sextet components corresponding to hematite α-Fe2O3 and goethite α-FeOH were obtained (Table 1). The dublet component has Fe^{3+} ions parameters in a compound with paramagnetic or superparamagnetic behavior. A distinction between the two alternatives (paramagnetic phase/superparamagnetic particles) can be made after measuring spectra at a liquid nitrogen temperature.

The experimental Mössbauer spectrum of a yellow jasper (goethite-bearing; sample aYu3) is composed of broad sextet lines with distribution of the magnetic field (Figure 2). The spectrum processing uses a combination of two sextets, one of which has a magnetic field distribution (Sx2). The sextet parameters are typical for the mineral goethite (Fe^{3+} ions in octahedral environment), and the decreasing internal magnetic field (Sx2) is probably due to an isomorphic substitution of iron with an element, for example Al. The lower internal magnetic field value is indicative of a reduction in the magnitude of magnetic interactions due to the magnetic discharging of the chemical system with diamagnetic Al^{3+} ions. With such a substitution in the structure of goethite, there is a presence of iron ions with different number of iron and aluminum closest neighbours, whose iron nuclei are located in a different internal magnetic field, respectively. The function of the internal magnetic field distribution for Sx2 is presented (Figure 3). Similar spectra have been reported for solid solutions in the system of compositions α-FeOH - α-AlOH (Fysh and Clark, 1982).

Another possibility for explanation of the broad spectral lines is the manifestation of the dimensional effect of the goethite particles, i.e. presence of particle size distribution, in size from fine dispersed to ultra-dispersed, for example from ~70 nm to ~10 nm). This is the so-called collective magnetic excitation effect. Measuring spectra at low temperatures can confirm or reject its presence.

In the case of Mössbauer spectroscopy of goethite in the form of yellow ocher from the supergenic area of the Sakhalin nickel deposit, it is found that the spectrum (sextet, sextet with doublet or doublet) is not constant and changes in the samples from one point to another at the same horizon, as well as in the transition at different horizons (Bobkovskii and Yalovoi, 1987). It is noted that two factors can influence the goethite spectrum: the degree of substitution of iron by a non-magnetic element (in this case, aluminum up to 16%) and the degree of dispersion (crystallinity) of the goethite. To elucidate the two main factors, experimental studies were conducted simultaneously using Mössbauer spectroscopy and X-ray diffraction analysis, as there are a number of contradictory and ambiguous data regarding alumina-containing and fine disperse goethite and hematite (Tkacheva and Umnova, 1982). Upon increase in the aluminum content at 8 mol%, a B parameter narrowing from 37.5 T to 24.2 T is noted and a change in the geometry of the peaks of the sextet in the spectrum is observed (the second and fifth lines have a higher intensity compared to the first and sixth lines), and at >18 mol% of aluminum appears a doublet. The X-ray diffraction analysis of the specimens showed that with the Fe-Al increased isomorphic substitution, a reducing of the parameters of the elementary cell is observed, associated with the interplanar distances of the reflections 110 and 111 (they decreased and widened, the substitution was also influenced by the higher dispersion of the sample). The doublet in the goethite spectra with a high degree of isomorphic impurity is explained by the disruption of the spines of antiferromagnetic subcells. It should be noted that the Mössbauer spectra of goethite α-FeOOH and lepidocrockite γ-FeOOH differ significantly – for the first mineral is typical a sextet, and for the secondone – a quadruple doublet. More recent studies on both hematite and goethite indicate that the parameters of the Mössbauer spectra depend to a higher degree on structural factors than on the aluminum content and the degree of crystallinity (Vandenberghe et al., 2000).

The experimental Mössbauer spectrum of green jasper (celadonite-bearing; sample aNa8) is a combination of sextets and doublets (Figure 4). Mathematical processing was performed using a model with two sextets and two doublets. As a result of the processing, parameters of sextet components corresponding to α-Fe_2O_3 (hematite) and α-FeOOH (goethite) were obtained. The parameters of the two doublets correspond to Fe^{3+} and Fe^{2+} ions in octahedral coordination, probably

introduced into the structure of celadonite. The ratio of the relative values of the two-component components is Fe^{3+}/Fe^{2+}=2.35. The low iron content of the specimen, as well as the presence of other iron-containing phases (hematite and goethite) in the sample, impedes the correct use of more sophisticated processing patterns (such as those in Daynyak and Drits, 1987). The possible positions of Fe^{3+} in the structure of the celadonite are described in detail (Drits et al., 1997).

Earlier published Mössbauer spectra of jasper samples from the Eastern Rhodopes show some close-up data but are with no relevant parameters, and were used mainly for diagnosis of the admixed mineral phase in the quartz matrix (Atanasov and Yordanov, 1986).

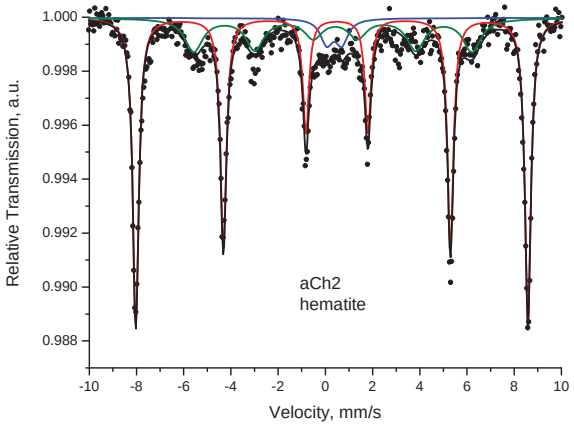

Fig. 1. Mössbauer spectrum of sample aCh2 (red jasper; hematite-bearing)

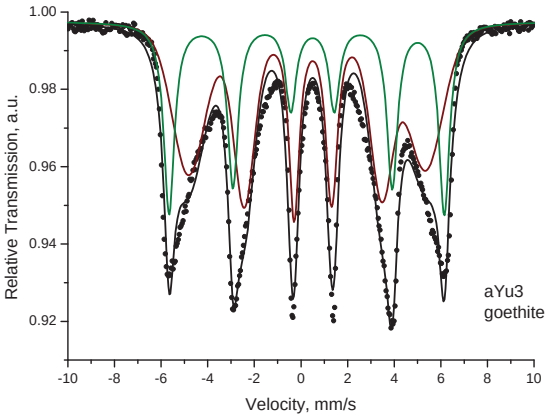

Fig. 2. Mössbauer spectrum of sample aYu3 (yellow jasper; goethite-bearing)

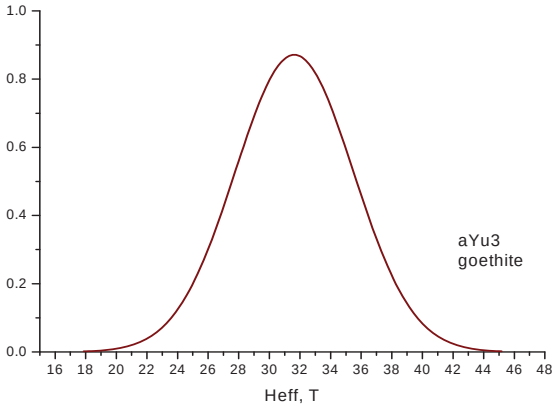

Fig. 3. Function of internal magnetic field distribution of Sx2 in the sample aYu3 spectrum (yellow jasper, goethite-bearing)

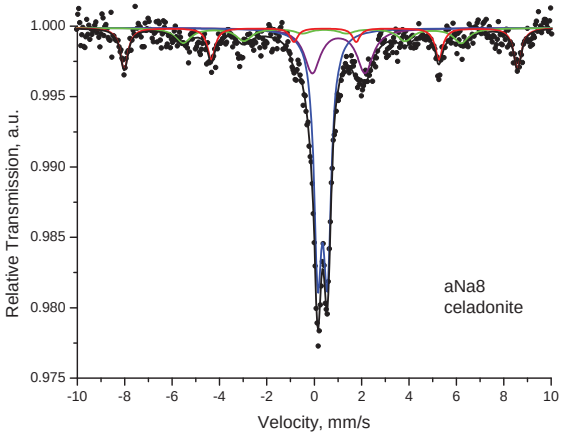

Fig. 4. Mössbauer spectrum of sample aNa8 (green jasper, celadonite-bearing)

Table 1.
Values of the specified Mössbauer parameters

Sample, colour	Components	δ, mm/s	Δ, mm/s	B, T	Γ, mm/s	$Γ_{exp}$, mm/s	G, %
aCh2 red	Sx1 – Fe^{3+}, hematite	0.38	-0.22	51.6	-	0.31	69
	Sx2 – Fe^{3+}, goethite	0.37	-0.11	36.6	-	0.92	26
	Db1 – Fe^{3+}	0.38	0.65	-	-	0.64	5
aVu3 yellow	Sx1 – Fe^{3+}, goethite	0.37	-0.25	36.7	-	0.55	36
	Sx2 – Fe^{3+}, goethite	0.39	-0.25	31.6	1.1	0.47	64
aNa8 green	Sx1 – Fe^{3+}, hematite	0.37	-0.18	51.6	-	0.40	19
	Sx2 – Fe^{3+}, goethite	0.39	-0.10	36.5	-	0.80	14
	Db1 – Fe^{3+}, celadonite	0.35	0.40	-	-	0.39	47
	Db2 – Fe^{2+}, celadonite	1.03	2.22	-	-	0.82	20

In the Mössbauer spectrum of the red jasper sample dominates the presence of hematite, in the yellow jasper sample – of goethite, and in the green jasper sample – of celadonite with doublets of iron of varying valency, predominantly Fe^{3+} and subordinate Fe^{2+} in structural position. Apparently, in the so-called brocade jaspers with yellowish and reddish spots, the ratio of hematite to goethite can be different. The presence in the Mössbauer spectra of green jasper of Fe^{3+} sextets associated with hematite and goethite indicates the presence of these minerals in the SiO_2 matrix, even when they are not visually (initiation of heliotrope) observed. Increasing their content leads to the formation of a visually distinct heliotrope.

In the EPR spectra of the jaspers (Figs. 5-9), the following main types of signals are distinguished: N1 – signal, sometimes with large width and intensity at g~10; N2 – signal at g=4.3 attributed to structural Fe^{3+}; N3 – a wide signal ~1000 G at g ~2.3-2.1 attributed to Fe impurity; N4 – signal at g~2.1-2.0; N5 – signal at g=2 attributed to the presence of hole centers in the SiO_2 matrix (in each figure is given at a smaller scale a detailed spectrum within this range, with the corresponding electron-hole centers, characteristic of SiO_2 and not being discussed here).

The results are reported in Table 2, with data from earlier EPR studies of chalcedony (Plyusnina and Kostov, 1988) and jasper (Hemantha Kumar et al., 2010). The interpretation of the EPR spectra is made according to the existing system and methodology of description of electron-hole centers in polycrystalline quartz samples (Kostov and Bershov, 1987; Lyutoev, 2004). The obtained ESR spectra of jasper can be compared with other ones – for example, of jaspers with the same three colours from occurrences in the same region in Momchilgrad in the Eastern Rhodopes (Kostov and Pazderov, 2016).

The wide signal N1 is recorded in samples of any colour and therefore can not be used as a typomorphic spectroscopic sign. The signal N2 at g=4.3 is associated with structural iron in tetrahedral coordination in the quartz matrix and apparently is not associated with any of the admixing mineral phases. The wide signal N3 in the range of g~2.3-2.1 is not noted in red hematite-bearing jaspers, but it may be associated with a goethite impurity. The signal N4 at g~2.1-2.0 is present in all jasper samples (with maximum intensity in red hematite-bearing samples) and its intensity may possibly correlate with the N5 signal intensity, which is interpreted as a total amount of defect hole centers in SiO_2 matrix. According to EPR data for synthetic hematite and goethite specimens, both minerals have only one signal of varying width, centered at g~2, while magnetite gives broad lines in different magnetic field ranges (Guskos et al., 2002). The latter phase may be the cause of EPR signals N1 and/or N3. Visually magnetite is found in samples of red jasper from the area of Zvezdel.

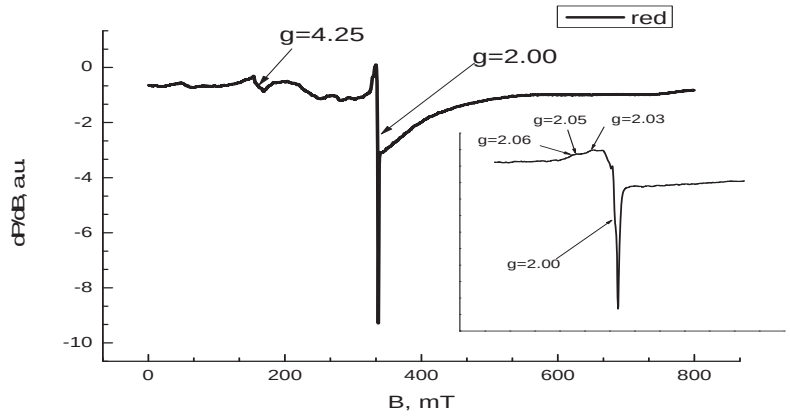

Fig. 5. EPR spectrum of green jasper (aVu1); second smaller spectrum – detail in the g=2 range

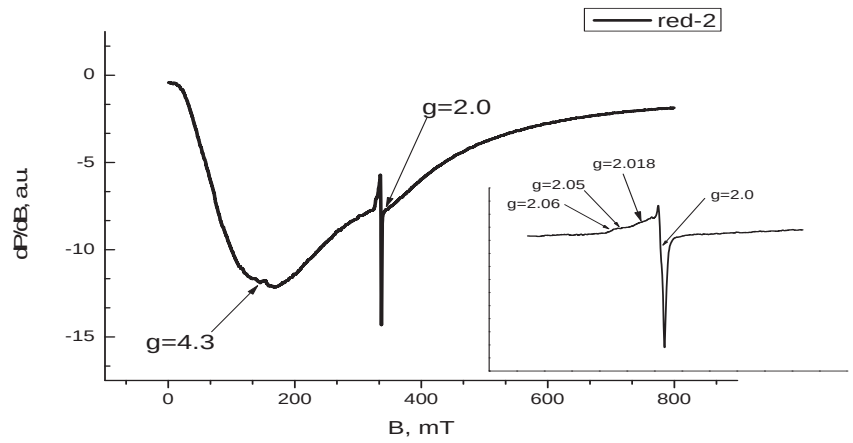

Fig. 6. EPR spectrum of red jasper (aCh2); second smaller spectrum – detail in the g=2 range

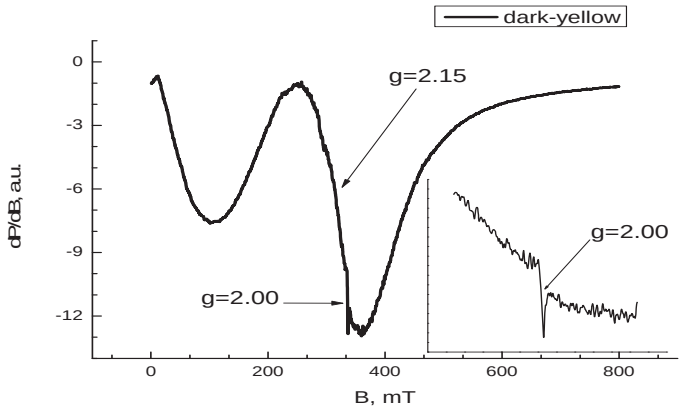

Fig. 7. EPR spectrum of yellow jasper (aVu3); second smaller spectrum – detail in the g=2 range

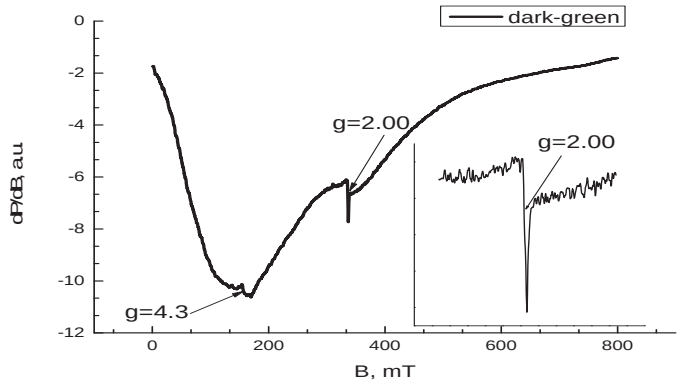

Fig. 8. EPR spectrum of dark green jasper (aNa8); second smaller spectrum – detail in the g=2 range

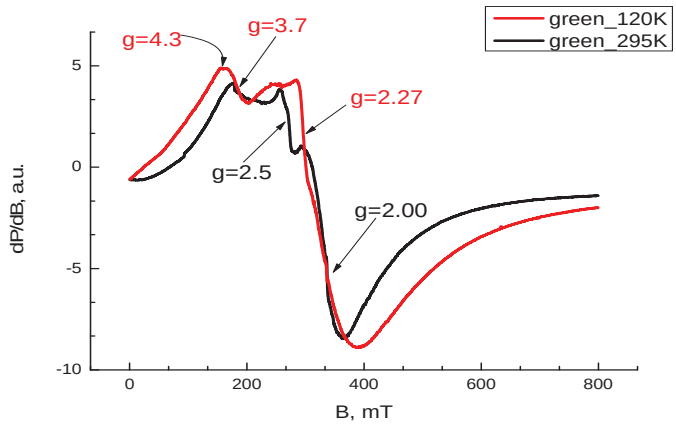

Fig. 9. EPR spectrum of green jasper (aVu4); upper line – at temperature 120 K

Table 2.
EPR data (g factor) and intensity (in arbitrary units) of signals in the EPR spectra (g_q – g=2 of importance for the silica phase)

Sample, colour	g~10	g=4.3	g~2.3-2.1	g~2.1-2.0	g_q=2
aVu1 red	-	0.6	-	9.4	2.7
aCh2 red	+	0.3	-	8.5	1.1
aVu3 yellow	+	-	+	3.0	0.8
aNa8 dark green	+	0.5	-	1.6	0.4
aVu4 green	-	+	+	0.8	+
Pi1 red	+	++	-	+	+
Ne1 green	-	+	-	+	+
Ne2 yellow	-	+	+	+	+
Ne3 red	-	+	-	++	++
Pa1 green	-	-	-	+	-
X* colourless	n.a.	n.a.	+	-	+
XX** red	+	+	-	+	+

*Colourless chalcedony from the Momchilgrad area (Plyusnina and Kostov, 1988; n.a. – not analyzed); **Red jasper from Taiwan (Hemantha Kumar et al., 2010).

Conclusion

Through Mössbauer spectroscopy and through Electronic Paramagnetic Resonance (EPR), the iron status and distribution of different in valence iron ions in the three most important impurity phases of jasper from the Eastern Rhodopes – hematite, goethite and celadonite are studied, which are related to red, yellow to yellowishbrown and green colouration, respectively. In the Mössbauer spectrum of red jasper, Fe^{3+} sextes characteristic of hematite and goethite are detected, in the spectrum of yellow jasper – Fe^{3+} sextets characteristic only of goethite, and in the green jasper spectrum – Fe^{3+} and Fe^{2+} doublets associated with celadonite, as well as at a lower degree Fe^{3+} sextets characteristic of hematite and goethite.

The EPR spectra data helps to establish the role of iron in the SiO_2 matrix or in the impurity mineral phases responsible for one or another coloration of the jasper. The distribution and intensity of the EPR signals in the respective spectra can be used in the correlation of geological and archaeological samples, as well as a guide in the search for the source of raw material or local geochemical anomalies.

Acknowledgements. The authors express their gratitude for access to spectroscopic facilities, assistance with analyses and useful discussions on the topic to Prof. DSc. I. Mitov, Assoc. Prof. Dr. N. Velinov and Assoc. Prof. Dr. Y. Karakirova (Institute of Catalysis of the Bulgarian Academy of Sciences), as well as to Prof. Dr. R. Stoyanova and Dr. R. Kukeva (Institute of General and Inorganic Chemistry of the Bulgarian Academy of Sciences). Acknowledgments are also for the colleagues - archaeologists Assoc. Prof. Dr. Y. Boyadzhiev and Dr. S. Taneva (National Archaeological Institute and Museum of the Bulgarian Academy of Sciences) for providing information and access to samples of jasper from the Varhari prehistoric site in the Eastern Rhodopes.

References

Atanasov, V. A., Y. A. Yordanov. Deposits of jasper in Bulgaria. – In: Morphology and Phase Equilibria of Minerals. Bulgarian Academy of Sciences, Sofia, 1986. - 379-386.

Bobkovskii, A. G., A. A. Yalovoi. Estimation of the replacement of natural goethites according Mossbauer spectra. – Geochemistry, 12, 1987. - 1802-1805.

Daynyak, L. G., V. A. Drits. Interpretation of Mössbauer spectra of nontronite, celadonite, and glauconite. − Clays and Clay Minerals, 35, 5, 1987. - 363-372.

Drits, V. A., G. Dainyak, F. Muller, G. Besson, A. Manceau. Isomorphous cation distribution in celadonites, glauconites and Fe-illites determined by infrared, Mössbauer and EXAFS spectroscopies. − Clay Minerals, 32, 1997. - 153-179.

Fysh, S., P. Clark. Aluminous goethite: A Mössbauer study. − Physics and Chemistry of Minerals, 8, 1982. - 180-187.

Guskos, N., G. J. Papadopoulos, V. Likodimos, S. Patapis, D. Yarmis, A. Przepiera, K. Przepiera, J. Majszczyk, J. Typek, M. Wabia, K. Aidinis, Z. Drazek. Photoacoustic, EPR and electrical conductivity investigations of three synthetic mineral pigments: hematite, goethite and magnetite. – Materials Research Bulletin, 37, 6, 2002. - 1051-1061.

Hemantha Kumar, G. N., G. Parthasarathy, R. P. S. Chakradhar, J. Lakshmana Rao, Y. C. Ratnakaram. Temperature dependence on the electron paramagnetic resonance spectra of natural jasper from Taroko Gorge (Taiwan). – Physics and Chemistry of Minerals, 37, 4, 2010. - 201-208.

Kostov, R. I. Review on the mineralogical systematics of jasper and related rocks. – Geology and Mineral Resources, 13, 9, 2006. - 8-12.

Kostov, R. I. Review on the mineralogical systematics of jasper and related rocks. – Archaeometry Workshop, 7, 3, 2010. - 209-213.

Kostov, R. I., L. V. Bershov. Systematics of the electron and hole paramagnetic centers in natural quartz. – Izvestiya AN SSSR, Ser. Geol., 7, 1987. - 80-87.

Kostov, R. I., R. Pazderov. Mineralogical and geochemical peculiarities of jaspers from the area of Momchilgrad, Eastern Rhodopes. – In: 50 Years Museum Activity in the Eastern Rhodopes – Investigations, Studies and Perspectives. USB, Kurdzhali, 2016.

Kostov, R. I., R. Pazderov, L. Michaylov. Mineral composition of jasper from the Eastern Rhodopes. – Annual of the University of Mining and Geology "St. Ivan Rilski", 59, Part I, 2016a. - 47-54.

Kostov, R. I., R. Pazderov, L. Michaylov. Mineralogy and distribution of jasper artifacts from the Eastern Rhodopes. – National Conference 'Geosciences 2016'. BGS, Sofia, 2016b. - 175-176.

Lyutoev, V. P. Structure and Spectroscopy of Chalcedony. UrB RAS, Ekaterinburg, 2004. - 116 p.

Plyusnina, I. I., R. I. Kostov. 1988. On the disorder of chalcedony according to electron spin resonance (ESR) data. – Geochemistry, Mineralogy and Petrology, 25, 1988. - 20-27.

Tkacheva. T. V., E. G. Umnova. On the peculiarities of synthetic and natural aluminum-bearing goethites and hematites. – New Data on Minerals, 30, 1982. - 200-205.

Vandenberghe, R. E., C. A. Barrero, G. M. da Costa, E. Van San, E. De Grave. Mössbauer characterization of iron oxides and (oxy)hydroxides: the present state of the art. – Hyperfine Interactions, 126, 1-4, 2000. - 247-259.

Yordanov, B., S. Sarov V. Valkov, S. Georgiev, I. Kalinova, D. Kamburov, E. Raeva, E. Voinova, M. Ovcharova, B. Kuncheva. Explanatory Note to the Geological Map of Bulgaria. 1:50,000. Card Sheet Dzhebel and Kirkovo (in Bulgarian). Sofia, 2008. - 132 p.

Žák, T., Y. Jirásková. CONFIT: Mössbauer spectra fitting program. − Surface and Interface Analysis, 38, 4, 2006. - 710-714.

The article is reviewed and recommended for publication by Prof. DSc. D. Stavrakeva and Assoc. Prof. Dr. S. Stoikov.

"KOBILINI STENI" ("MARE'S WALLS") GEOSITE IN WESTERN BALKAN MOUNTAIN

Boris Valchev

"St. Ivan Rilski "University of Mining and Geology, 1700 Sofia, e-mail: b_valchev@mgu.bg

ABSTRACT. The present article represents the results from investigation of "Kobilini Steni" ("Mare's Walls") geosite (the nomination for a geosite is proposed here) located in the Beglichki Part of Vratsa Mountain, 1.3 to 4 km north of the village of Opletnya (Western Balkan) in the frames of "Vratsa Balkan" Natural Park. The geosite consists of three parts. The most impressive of them represents series of WNW-ESE exposed stepped rock cliffs and steep rock walls located between 900 and 1400 m altitude at the southwestern slope beneath Parshevitsa and Beglichka Mogila Peaks. They are formed mainly in the limestones of the Opletnya and Lakatnik Members of the Mogila Fm (Olenekian – Anisian) and partly in these of Babino Fm (Anisian). The combined activity of the paleorivers, modern streams, and karst processes has led to the formation of a cirque-like view of the slope. In addition, rock crest and rock pinnacles formed in the Opletnya Member beneath the cliffs and impressive recent proluvial deposit along the valley north of the village of Opleynya could be observed. The rocks have not been described yet as geological phenomena and they are not included in the "Register and cadastre of the geological phenomena of the Republic of Bulgaria" as well as in the State Register of Natural Sites. According to the classification of the geological phenomena, "Kobilini Steni" geosite is referred to the geosites of aesthetic value (geomorphologic class), and according to the original Bulgarian methodology for estimation of geological phenomena, it is of local importance.

Keywords: geological heritage, "Kobilini Steni" ("Mare's Walls") geosite, Western Balkan mountain.

ГЕОТОП „КОБИЛИНИ СТЕНИ" В ЗАПАДНА СТАРА ПЛАНИНА

Борис Вълчев

Минно-геоложки университет "Св. Иван Рилски", София 1700

РЕЗЮМЕ. Настоящата статия представя резултатите от изучаването на геотопа „Кобилини стени" (номиниран тук), намиращ се в Бегличкия дял на Врачанска планина между 1,3 и 4km северно от с. Оплетня (Западна Стара планина) в рамките на природния парк „Врачански Балкан". Геотипът се състои от три части. Най-впечатляващата от тях представлява поредица от стъпаловидно разположени скални венци и стръмни скални стени, разположени между 900 и 1400 m надморска височина в склона югозападно под върховете Пършевица и Бегличка могила. Те са с посока ЗСЗ-ИЮИ и са оформени главно във варовиците на Оплетненския и Лакатнишкия член на Могилската свита (Оленек–Аниз) и отчасти в Бабинската свита (Аниз). Образувани са под комбинираното действие на палеореките, временните потоци и карстовите процеси, което е придало амфитеатрален изглед на склона. Непосредствено под скалните венци могат да се наблюдават скален гребен и скални пирамиди, оформени в скалите на Оплетненския член, а по дола северно от с. Оплетня се разкриват впечатляващи съвременни пролувиални наслаги.Скалните образувания не са описвани като геоложки феномени и не фигурират в „Регистър и кадастър на геоложките феномени в Република България", както и в Държавния регистър на природните забележителности. Съгласно класификацията на геоложките феномени, геотопът „Кобилини стени" попада в групата на обектите с естетическа стойност (клас геоморфоложки), а според оригиналната българска методика за оценяване на геоложки феномени, той е с локално значение.

Ключови думи: геоложко наследство, геотоп „Кобилини стени", Западна Стара планина.

Introduction

The Triassic carbonate successions are broadly distributed in the Western Balkan Mountain and they form impressive rock cliffs and rock walls especially along the Iskar Gorge between the villages of Tserovo and Opletnya. The most famous amongst them are developed in "Lakatnik Rocks" geosite (Ajdanlijsky, 2004), as well as these near the villages of Tserovo, Bov (Valchev, Nachev, 2015) and Zasele (Sinyovski, Sinyovska, 2009). The area north of the villages of Opletnya and Ochindol reveals a picturesque view in a Triassic carbonate terrain with long rock cliffs and steep rock walls, combined with rock pinnacles and crests that are not so popular because of the lack of direct view from the road Sofia – Mezdra in the Iskar Gorge.

The present article aims to represent the results from the field investigation of "Kobilini Steni" ("Mare's Walls") geosite located in the Beglichki Part of Vratsa Mountain, 1.3 to 4 km north of the village of Opletnya (Western Balkan) in the frames of "Vratsa Balkan" Natural Park (Fig. 1). The rocks have not been described yet as geological phenomena and they are not included in the "Register and cadastre of the geological phenomena of the Republic of Bulgaria" as well as in the State Register of Natural Sites. Short notes on the geological setting are also given.

Geological Setting

Stratigraphy

The area of "Kobilini Steni" ("Mare's Walls") geosite is composed predominantly of Triassic terrigenous, carbonate, and terrigenous-carbonate rocks (Fig. 2), which are well exposed. Upper Paleozoic volcanic and terrigenous sedimentary deposits, as well as Jurassic terrigenous and carbonate-terrigenous successions also crop out here.

The oldest rocks are represented by *Upper Carboniferous volcanics* (effusive and explosive facies - Angelov et al., 2008) and they crop out in the south part of the studied area along the Iskar valley south of the villages of Opletnya and Ochindol. This complex is covered by *Upper Carboniferous* (the Stephanian Ochindol Formation (Fm) – Tenchov, 1973) and *Lower Permian terrigenous succession* (Zverino, Buk and Vranska Formations – Yanev, Tenchov, 1972, 1978) cropping out in the outskirts of the village of Ochindol. *Lower Permian volcanics* (subvolcanic facies - see Angelov et al., 2008) are also represented here.

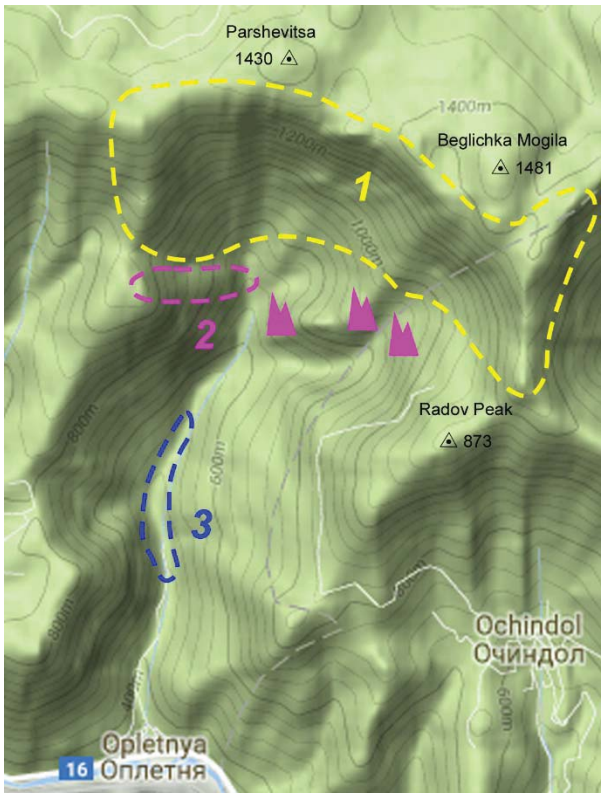

Fig. 1. Location of "Kobilini Steni" ("Mare's Walls") geosite
1, rock cliffs and walls in Kobilini Steni locality, *2*, rock crest and rock pinnacles, *3*, proluvium

The *Triassic* includes Petrohan, Iskar and Miziya Groups that are wide spread in the Western Balkanides.

The *Petrohan terrigenous Group* (Tronkov, 1981; Lower Triassic) covers transgressively varied levels of the Paleozoic section and it crops out as three northwest-southeast oriented strips.

The *Iskar carbonate Group* (Tronkov, 1981; Olenekian – Carnian) covers the terrigenous succession with gradual transition and it could be observed in almost the whole investigated area. It includes five units: *Svidol Formation* (Чаталов, 1974; Olenekian), *Mogila Formation* (Ассерето et al., 1983; Olenekian-Anisian) subdivided into two members (*Opletnya* and *Lakatnik* introduced as Formations by Tronkov, 1968), *Babino* (Anisian), *Milanovo* (Ladinian), and *Rusinov del* (Ladinian-Carnian) Formations, all of them introduced by Tronkov (1968). The boundaries between all carbonate units are distinct - sharp or gradual.

The *Miziya Group* (Chemberski et al., 1974) is represented here only by the *Komshtitsa Formation* (Tronkov, 1969; Carnian-Norian), covering with sharp boundary the Rusinov del Formation. It crops out in three separate localities in the western and eastern part of the area.

The *Jurassic* forms a narrow strip north of Beglichka Mogila Peak and includes *Kostina* (Hettangian-Sinemurian)and *Ozirovo* (Sinemurian-Aalenian) Formations introduced by Sapunov (in Sapunov et al., 1967).

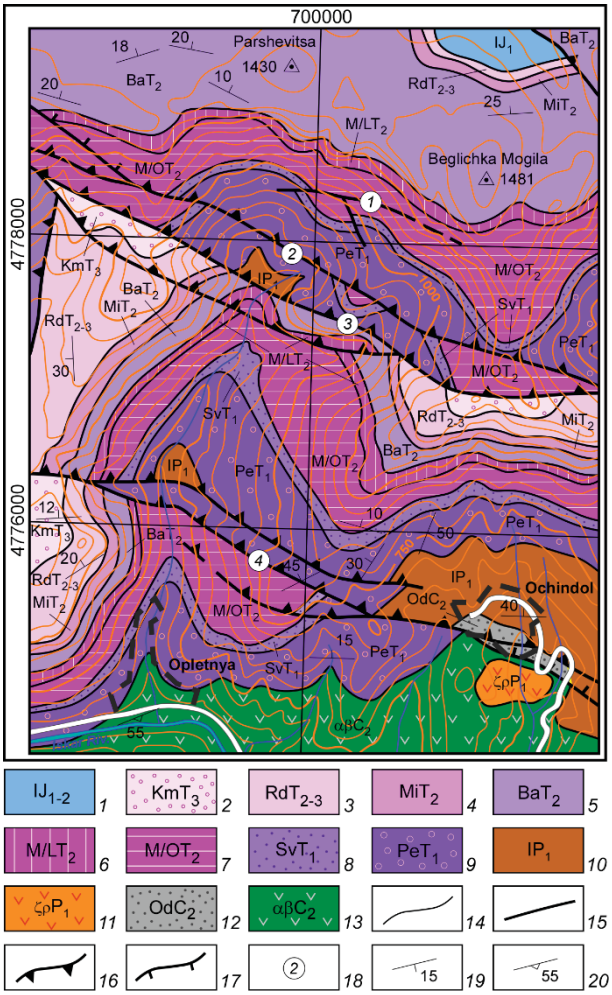

Fig. 2. Geological map of the area of "Kobilini Steni" ("Mare's Walls") geosite (emended after Angelov et al., 2009)
Lower Jurassic: *1*, Ozirovo and Kostina Fms (Hettangian-Aalenian); Triassic (*2-9*): *2*, Komshtitsa Fm (Carnian-Norian); *3*, Rusinov Del Fm (Ladinian-Carnian); *4*, Milanovo Fm (Ladinian); *5*, Babino Fm (Anisian); *6,7*, Mogila Fm (*6*, Lakakatnik Member, Anisian, *7*, Opletnya member, Olenekian-Anisian); *8*, Svidol Fm (Olenekian); *9*, Petrohan terrigenous group (Lower Triassic); Upper Paleozoic: *10*, Vranska, Buk, and Zverino Fms (Lower Permian); *11*, Permian vocanics (Lower Permian); *12*, Ochindol Fm (Stephanian); *13*, Upper Carboniferous vovlasnics; *14*, lithostratigraphic boundary; *15*, normal fault; *16*, reverse fault; *17*, thrust; *18*, faults: *1*, South Beglich normal fault; *2*, Ostra Mogila reverse fault; *3*, Pop Sokolets reverse fault; *4*, Arzhishta reverse fault;*19*,bedding; *20*, planar parallelism

Tectonics

The area of "Kobilini Steni" ("Mare's Walls") geosite belongs to the Berkovitsa Tectonic Unit of the Western Balkan Zone (according to Ivanov, 1998) or the Western Balkan Unit (according to Dabovski, Zagorchev, 2009). It is tectonically

complicated by four steep and south deepening faults that have been previously established and described in details by Tronkov (1963, 1965). From north to south they are: South Beglich normal fault, Ostra Mogila, Pop-Sokolets, and Arzhishta reverse faults.

Characteristics of the geosite

"Kobilini Steni" ("Mare's Walls") geosite comprises three main parts (Fig. 1): (i) the rock cliffs and rock walls at Kobilini Steni locality, (ii) rock crest and rock pinnacles beneath the cliffs, and (iii) proluvial deposit along the valley north of the village of Opletnya.

Rock cliffs and rock walls at Kobilini Steni locality

This geological phenomenon represents series of stepped rock cliffs and steep rock walls (Plate I, *1-4*, Plate II, *1-3*) located between 900 and 1400 m altitude at the south-western slope of Beglichki Part of Vratsa Mountain beneath Parshevitsa and Beglichka Mogila Peaks (Plate I, *5*). The cliffs and walls are exposed in west-northwest to east-southeast direction and their total length is 2.6 km (measured at the uppermost edge). They are formed mainly in the limestones of the Opletnya and Lakatnik Members of the Mogila Formation (Plate I, *6-8*), and the uppermost levels of the uppermost cliff are formed in the rocks of Babino Formation (Plate I, *9*). The height of the cliffs in the central part of the locality is over 100 m (Plate I, *10,11*). The exposure of these forms was predetermined by the presence of a vertical primary fractures in the rocks. The combined activity of the paleorivers, modern streams and karst processes has led to the formation of a cirque-like view of the slope (Fig. 3; Plate I, *12*). This locality is named by local people Zlite Ratove (The Evil Hills) (Topografska karta na zemlishteto na selo Milanovo (Osikovo).

Fig. 3. Satellite image of Kobilini Steni locality, view to the north (Google Earth)

Rock crest and rock pinnacles

On the right riverside of the valley below Kobilini Steni locality, amongst the rocks of the Babino Formation, a rock crest is formed (Fig.1; Plate II, *4*). It is exposed across the slope in west-southwest to east-northeast direction, and comprises several rock pinnacles (Plate II, *5, 6*) with height over 10 m. On the left riverside of the same valley there are three single pinnacles (Fig.1; Plate II, *7-9*) formed in the rocks of the Opletnya member. All the pinnacles are due to the effect of karst processes, as well as the vertical primary fractures in the rocks.

Proluvial deposit

In the valley north of the village of Opletnya a fan of impressive recent proluvial sediments is deposited (Figs. 1, 4; Plate II, *10-12*). It could be seen between 1,3 to 2,9 km north of the village. It consists of poorly sorted and angular boulders to cobbles predominantly of limestones from the Iskar carbonate group. Single boulders from red sandstones of the Petrohan terrigenous group could be seen. The widest south part of this deposit is 65 m wide and the narrowest north one is about 10 m wide.

Fig. 4. Satellite image of the proluvial deposit north of the village of Opletnya, view to the north (Google Earth)

Expert estimation

The geological phenomena, described in the present article, are referred to the geosites of aesthetic value (geomorphological class). After the conducted expert estimation, according to the original Bulgarian methodology for estimation of geological phenomena (Sinyovski et al., 2002), we concluded that they are of local importance, and they could be estimated as geosites of high degree of preservation, exposure, resistance and accessibility.

Conclusion

The high degree of exposure of the Triassic carbonate rocks in the Iskar Gorge give a good opportunity for observation of geomorphological geosites of high aesthetic value. "Kobilini Steni" ("Mare's Walls" or The Evil Hills) geosite reveals impressive views of rock cliffs, rock walls and pinnacles and thus it could be included in the Lakatnik Rocks massive as its northeastern segment. For this purpose a further popularization by placing of signboards with geological information (data concerning the lithology, genesis, age of the rocks, and the mechanism of forming of the geosite) is required.This activity will increase the total expert value of the geosite by adding investigational and educational value to its present characteristics.

References

Айданлийски, Г. Лакатнишки скали, с. Миланово, Софийска област. – Геол. и мин. рес., 5, 2004. - 20-25. (Ajdanlijsky, G. Lakatnshki skali, selo Milanovo, Sofijska oblast. – Geol. Min. Res.,5, 2004. - 20-25).

Ассерето, Р., Г. Чаталов, Д. Тронков. Могильская свита (нижний-средний триас) в Западной Болгарии. – Geologica Balc.,13, 6, 1983. - 25-27.(Asseretto, P., G. Chatalov, D. Tronkov. Mogilskaya svita (nizhnij-srednij trias) v Zapadna Bulgaria. - Geologica.Balc.,13, 6, 1983. - 25-27).

Вълчев, Б., Г. Начев. Геоложки феномени в Понор планина (Западна България). - Год. МГУ, 58, св. I – Геол. и геофиз., 2015. - 45-54.(Valchev, B., G. Nachev. Geolozhki fenomeni v Ponor planina (Zapadna Bulgaria). – Godishnik MGU, 58, 1, 2015. - 45-54).

Дабовски, Х., И. Загорчев. Алпийска тектонска подялба на България. – В: Загорчев, И., Х. Дабовски, Т. Николов (ред.), Геология на България. Том II, Мезозойска геология. С., Акад. изд. „Проф. Марин Дринов“, 2009. - 30-37. (Dabovski, H., I, Zagorchev. Alpijska tektonska podyalba na Bulgaria. –In: Zagorchev, I., H. Dabovski, T. Nikolov(Eds.). Geologiya na Bulgaria. Tom II. Chast 5. Mesozojska geologiya. Sofia, Akad. Izdatelstvo Prof. Marin Drinov, 30-37).

Иванов, Ж. Тектоника на България. Непубл. хабилит. труд, Соф. унив., 1998. - 545 с. (Ivanov, Zh. Tektonika na Bulgaria. Nepublikuvan habilitatsionen trud, Sofia Univ., 1998. - 545 p.).

Сапунов, И., П. Чумаченко, В. Шопов. Биостратиграфия на долноюрските скали при с. Комщица, Софийско (Западни Балканиди). - Изв. геол. инст., сер. стратигр. и литол., 16, 1967. - 125-143. (Sapunov, I., P. Tschoumachenko, V. Shopov. Biostratigrafiya na dolnoyurskite skali pri selo Komshtitsa, Sofijsko (Zapadni Balkanidi).–Izvestiya Geol. inst., ser. stratigr. ilithol., 16, 1967. - 125-143).

Синьовски, Д., В. Желев, М. Антонов, С. Джуранов, З. Илиев, Д. Вангелов, Г. Айданлийски, П. Петров, Х. Василев. Метод за оценка на геоложки феномени. – II Международна конференция SGEM, Варна, 2002. - 25-33. (Sinnyovsky, D., V. Jelev, M. Antonov, S. Juranov, Z. Iliev, D. Vangelov, G. Ajdanlijsky, P. Petrov, Ch. Vasilev.2002. Metod za otsenka na geolozhki fenomeni.– In: II Mezhdunarodna. Konf. SGEM. Varna, 2002. - 25-33).

Синьовски, Д., Д. Синьовска. Скален венец Скакля. - http://mgu.bg/geosites/skaklya.html. 2009. (Sinnyovsky, D., D. Sinnyovska. Skalen venets Skaklya. - http://mgu.bg/geosites/skaklya.html. 2009).

Топографска карта на землището на село Миланово (Осиково).-http://milanovo-sf.bashtina.org/?page_id=180. (Topografska karta na zemlishteto na selo Milanovo (Osikovo).- http://milanovo-sf.bashtina.org/?page_id=180).

Тронков, Д. Характер на старокимерския структурен етаж, тип и време на старокимерските тектонски движения в Северозападна България. – Тр. Геол. Б-я, сер. стратигр. и тект., 5, 1963. – 171-196. (Tronkov, D. Harakter na starokimerskiya strukturen etazh, tip i vreme na starokomerskite tektonski dvizheniya v Severozapadna Bulgaria. - Trudove. geol. Bulgaria, ser. stratigr. itect.,5, 1963. – 171-196).

Тронков, Д. Тектонски строеж и анализ на структурите на Врачанския блок от Западна Стара планина. Пластична деформация в съседство с разломните равнини. - Тр. геол. Б-я, сер. стратигр. и тект., 6, 1965. - 217-250. (Tronkov, D. Tektonski stroezh i analiz na strukturite na Vrachanskiya blok ot Zapadna Stara Planina. Plastichna deformatsiya v sasedstvo s razlomnite ravnini. - Trudove. geol. Bulgaria, ser. stratigr. itect., 6, 1965. - 217-250).

Тронков, Д. Границата долен триас – среден триас в България. – Изв. Геол. инст., сер. палеонт., 17; 1968. - 113-131. (Tronkov, D. Granitsata dolen trias-sreden trias v Bulgaria. – Izvestiya Geol. inst., ser. paleontol., 1968. - 113-131).

Тронков, Д. Стратиграфия триасовой системы в части Западного Средногорья (Западная Болгария). – Geol. Balc., 11, 1; 1981. - 3-20. (Tronkov, D. Stratigrafiya triasovoj sistemi v chasti Zapanogo Srednogoriya (Zapadnaya Bolgaria). - Geologica Balc.,11, 1; 1981. - 3-20).

Чаталов, Г. Фации в Свидольской свите (нижний триас) Тетевенского антиклинория. – Докл. БАН, 27, 2, 1974. - 239-242. (Chatalov, G. Facii v Svidolskoj svite (nizhnij trias) Tetevensogo antiklinoriya. – Dokladi BAN, 27, 2, 1974. - 239-242).

Чемберски, Г., Я. Вапцарова, И. Монахов. Литостратиграфия на пъстроцветните теригенно-карбонатни и карбонатни седименти, свързани с триаса, разкрити при дълбокото сондиране в СЗ и ЦС България. – Год. ДСО “Геол. проучв“., 20, 1974. - 327-341. (Chemberski, Ch., Y. Vaptsarova, I. Monahov. Lithostratigrafiya na Tsentralna Severna Bulgaria. – Godishnik DSO Geolozhki prouchvaniya, 20, 1974. - 327-341).

Янев, С., Я. Тенчов. Стратиграфия, литология и строеж на стефан-пермските скали при с. Стакевци, Видинско. – Изв. Геол. инст., сер. стратигр и тект., 21, 1972. – 19-40. (Yanev, S., Y. Tenchov. Stratigrafiya, litologiya i stroezh na stefan-permskite skali pri selo Stakevtsi, Vidinsko. – Izvestiya Geol. inst., ser. stratigr. i tect., 21, 1972. – 19-40).

Янев, С., Я. Тенчов. Стефан-пермските скали при селата Згориград, Зверино и Игнатица, Северозападна България. – Палеонтол., стратигр. и литол., 9, 1978. - 3-26. (Yanev, S., Y. Tenchov. Stefan-permskite skali pri selata Zgorigrad, Zverino i Ignatitsa, Severozapadna Bulgaria. – Paleontol., stratigr. ilithol., 9, 1978. - 3-26).

Angelov, V., M. Antonov, S. Gerjikov, P. Petrov, H. Kiselinov, G. Ajdanlijsky, V. Valev. Explanatory Note to the Geological Map of Bulgaria in scale1:50 000 Map Sheet K-34-35-Г (Lakatnik). Ministry of Environment and Water, Bulgarian National Geologic Survey, Sofia, Uniskorp Ltd., 2008. - 92 p.

Angelov, V., M. Antonov, S. Gerjikov, P. Petrov, H. Kiselinov, G. Ajdanlijsky, V. Valev. Geological Map of Bulgaria in scale 1:50 000 Map Sheet K-34-35-Г (Lakatnik). Ministry of Environment and Water, Bulgarian National Geologic Survey, Sofia, Apis 50 Ltd., 2009.

Tronkov, D. NeueAngaben über das Alter derbunten Gesteinedes “Räts” (obere Trias) in Bulgarien. – C. R. Acad. Bulg. Sci., 21, 4, 1969. - 363-366.

This article was reviewed by Prof. DSc. Dimitar Sinnyovsky and Assoc. Prof. Dr. Valeri Sachansky.

PLATE I

1, general view of the uppermost rock cliff with Beglichka Mogila Peak at the background (view to southeast);*2*, a detail from the eastern part of the uppermost rock cliff beneath Beglichka Mogila Peak (view to southeast); 3, steep rock wall, formed in the Opletnya Member south of Beglichka Mogila Peak (view to north);*4*, rock cliff (Lakatnik Member) and rock wall (Opletnya Member) east of Beglichka Mogila Peak (view to north);*5*, general view of Kobilini Steni locality (view from the village of Milanovo); *6-8*, the Opletnya and Lakatnik Members of the Mogila Formation south of Beglichka Mogila Peak; *9*, the edge of the uppermost rock cliff at the central part of Kobilini Steni locality formed in the Babino Formation (view to northwest); *10, 11*, the highest rock cliffs at the central part of Kobilini Steni locality formed in the Opletnya and Lakatnik Members; *12*, cirque-like view of the slope southwest of Beglichka Mogila and Parshevitsa Peaks (view to northwest) due to the combined activity of the paleorivers, modern streams and karst processes

PLATE II

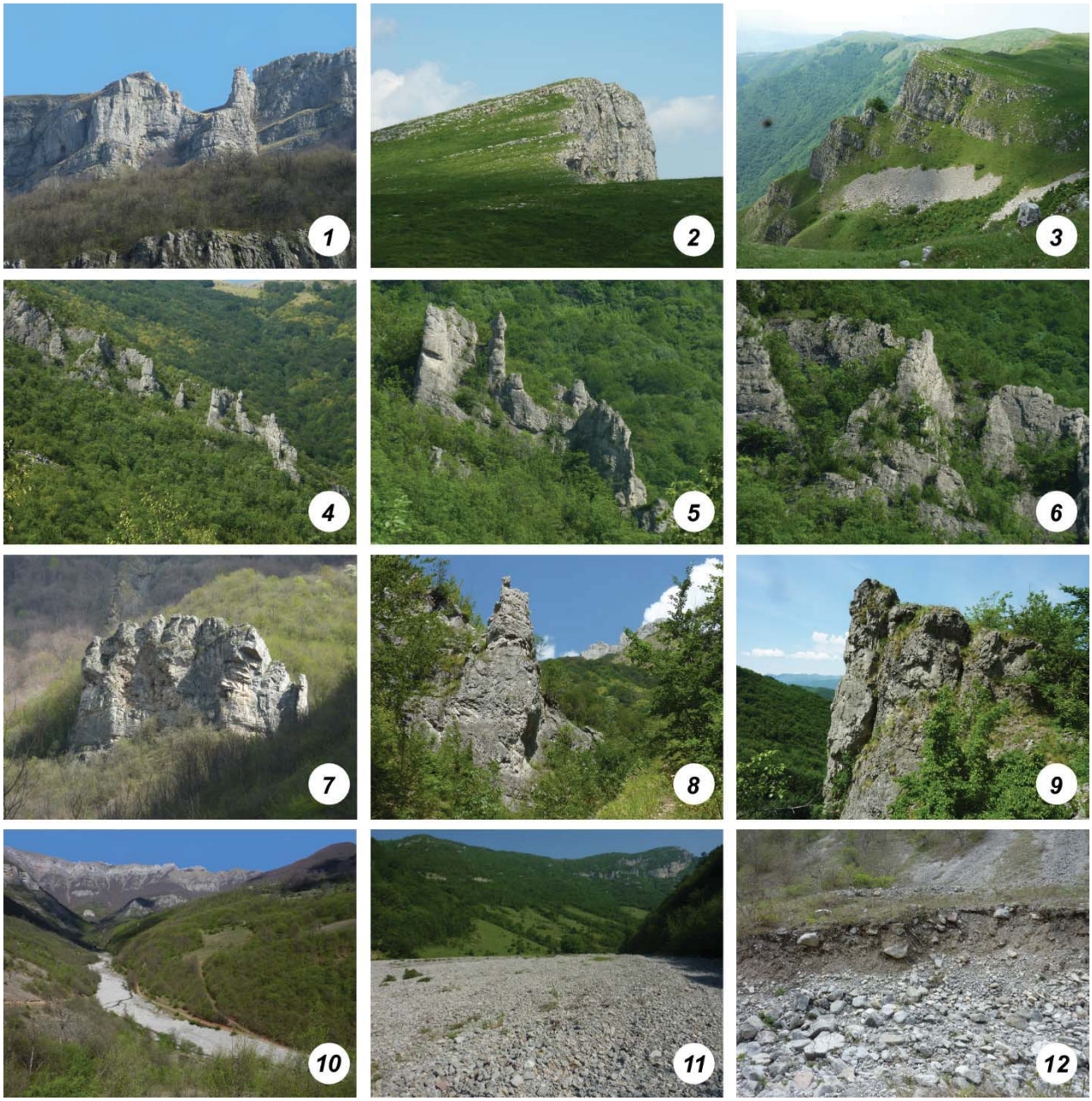

1, initial stage of rock pinnacles forming in the uppermost rock cliff south of Beglichka Mogila Peak (view to north); *2*, the sharp edge of the uppermost rock cliff south of Beglichka Mogila Peak (view to east);*3*, steeped rock cliffs and a small colluvium deposit south of Parshevitsa Peak (view to west); *4-6*, rock crest across the right riverside south of Parshevitsa Peak (*4*, general view to northwest, *5, 6*, details showing rock pinnacles);*7-9*, single rock pinnacles on the left riverside south of Kobilini Steni locality; *10-12*, recent proluvial deposit along the valley north of the village of Opletnya (*10*, general view to northeast with Kobilini Steni locality at the background, *11*, the 60-meter wide south part of deposit, *12*, the 10-meter wide north part of deposit)

SEISMIC SEQUENCE STRATIGRAPHIC ANALYSIS OF THE TERRESTRIAL PART OF DOLNA KAMCHIYA SEDIMENTARY BASIN

Tsvetelina Toleva[1], Hristo Dimitrov[1]

[1]University of Mining and Geology "St. Ivan Rilski", Sofia 1700, Bulgaria, E-mail: tsvetelina.toleva@abv.bg; hristo_dimitrov@mgu.bg

ABSTRACT. Dolna Kamchiya sedimentary basin is the longest studied petroleum zone in Bulgaria. It has been the focus of petroleum geologists for 67 years. Despite the numerous studies mainly on the terrestrial part of Dolna Kamchiya sedimentary basin, there are still unresolved tasks related to its lithofacial and stratigraphic variability. Dolna Kamchiya sedimentary basin is longitudinally oriented (subparallel), filled predominantly by terrigenous Paleocene-Neogene sediments with considerable thickness, and an asymmetrical transverse and longitudinal profile. More than 2/3 of the territorial scope of the basin is located in the Black Sea area, only its westernmost periphery is developed on a relatively small terrestrial territory. Northern, western and southern borders are well-defined and traceable to this part of the sedimentary basin. The main goal of this study is to carry out a seismic-sequence stratigraphic analysis of the terrestrial part of Dolna Kamchiya sedimentary basin.The main tasks in this study are summarized as follows: identifying sedimentary sequences by seismic data as well as recognition and delineation of their systems tracts. Solving the assigned tasks is based on data from 48 (prospecting and exploratory) wells and 15 migrated 2D seismic profiles in the basin, and is achieved by the application of seismostratigraphic analysis supplemented by paleotectonic and paleogeographic analysis. The application of the seismostratigraphic methods contributes to obtaining qualitatively new information about the deep geological structure and the geological development as well as increasing the efficiency of oil and gas prospecting. The identification of sedimentary sequences by seismic data allows more accurate prediction of sedimentary environments and lithofacies. This in turn, improves the forecasting of reservoirs, seals, source rocks and hydrocarbon migration pathways. The seismostratigraphic analysis of the sedimentary complex in Dolna Kamchiya sedimentary basin shows the development the I-type sequences formed within the stratigraphic cycles of the 2nd and 3rd order. The sequences have terrigenous, predominantly clayey-sandy composition.

Keywords: accumulations seismic-sequence stratigraphic analysis, Dolna Kamchiya sedimentary basin.

СЕИЗМИЧЕН СЕКВЕТНО-СТРАТИГРАФСКИ АНАЛИЗ НА СУХОЗЕМНАТА ЧАСТ ОТ ДОЛНОКАМЧИЙСКИЯ СЕДИМЕНТЕН БАСЕЙН

Цветелина Толева[1], Христо Димитров[1]

[1]Минно-геоложки университет "Св. Иван Рилски", София 1700, България, tsvetelina.toleva@abv.bg; hristo_dimitrov@mgu.bg

РЕЗЮМЕ. Долнокамчийският седиментен басейн е най-дълго проучваната нефтогазоносна зона в България. Вече 67 години той е във фокуса на петролните геолози. Независимо от многобройните изследвания, основно в участъка на сушата от Долнокамчийския басейн, остават все още не малко нерешени задачи, свързани с неговите литофациална и стратиграфска изменчивост. Долнокамчийският седиментен басейн е надлъжно (субпаралелно) ориентиран, запълнен с палеоцен-неогенски, предимно теригенни седименти със значителна дебелина, и има асиметричен напречен и надлъжен профил. Повече от 2/3 от териториалния обхват на басейна са разположени в Черноморската акватория, като само най-западната му периферия е развита на сушата върху сравнително малка територия. На този участък от басейна дълбочинните му северна, западна и южна граници са проследени и изяснени най-добре. Главната цел на изследването е провеждането на сеизмичен секвентно-стратиграфски анализ на сухоземната част от разреза на басейна. Основните задачи в настоящата работа се свеждат до: идентифициране на седиментните секвенции по сеизмични данни и разпознаване и очертаване на изграждащите ги трактови единици. Решаването на поставените задачи се базира на данни от 48 търсещо-проучвателни сондажи и 15 мигрирани 2D сеизмични профили в басейна и се постига с прилагането на сеизмостратиграфския анализ, допълнен с палеотектонски и палеогеографски анализ. Прилагането на методите на сеизмостратиграфията допринася за получаването на качествено нова информация за дълбочинния геоложки строеж и геоложкото развитие, както и за повишаване на ефективността на търсещите проучвания за нефт и газ. Идентифицирането на седиментните секвенции по сеизмични данни дава възможност за по-точно предсказване на седиментните обстановки и литофациеси. Това от своя страна позволява да се подобри прогнозирането на резервоари, покривки, нефтомайчини скали, капани и пътищата за въглеводородна миграция. Сеизмостратиграфският анализ на седиментния комплекс в Долнокамчийския седиментен басейн показва развитието на секвенции от I тип, формирани в рамките на стратиграфски цикли от II и III порядък. Секвенциите се отличават с теригенен, доминиращо глинесто-песъчлив състав.

***Ключови думи**: сеизмичен, секвентно-стратиграфски анализ, Долнокамчийски седиментен басейн*

Introduction

Dolna Kamchiya sedimentary basin is the longest studied petroleum zone in Bulgaria (Fig. 1). It has been the focus of petroleum geologists for 67 years. Despite the numerous studies mainly on the terrestrial part of Dolna Kamchiya sedimentary basin, there are still unresolved tasks related to its lithofacial and stratigraphic variability. Until now, seismostratigraphic analysis has only been applied to the offshore part of the basin, the results of which are presented in several publications (Georgiev et al., 2004; Dimitrov and Georgiev, 2005; Dimitrov, 2007; Dimitrov , 2008; Dimitrov and Georgiev, 2011). The main goal of this study is to carry out a seismic-sequence stratigraphic analysis of the terrestrial part of Dolna Kamchiya sedimentary basin. The main tasks in this study are summarized as follows: identifying sedimentary sequences by seismic data as well as recognizing and delineating of their systems tracts. The application of the seismostratigraphic methods contributes to obtaining

qualitatively new information about the deep geological structure and the geological development as well as increasing the efficiency of oil and gas prospecting. The identification of sedimentary sequences by seismic data allows more accurate prediction of sedimentary environments and lithofacies. This in turn, improves the forecasting of reservoirs, seals, source rocks and hydrocarbon migration pathways in the section of Dolna Kamchiya sedimentary basin.

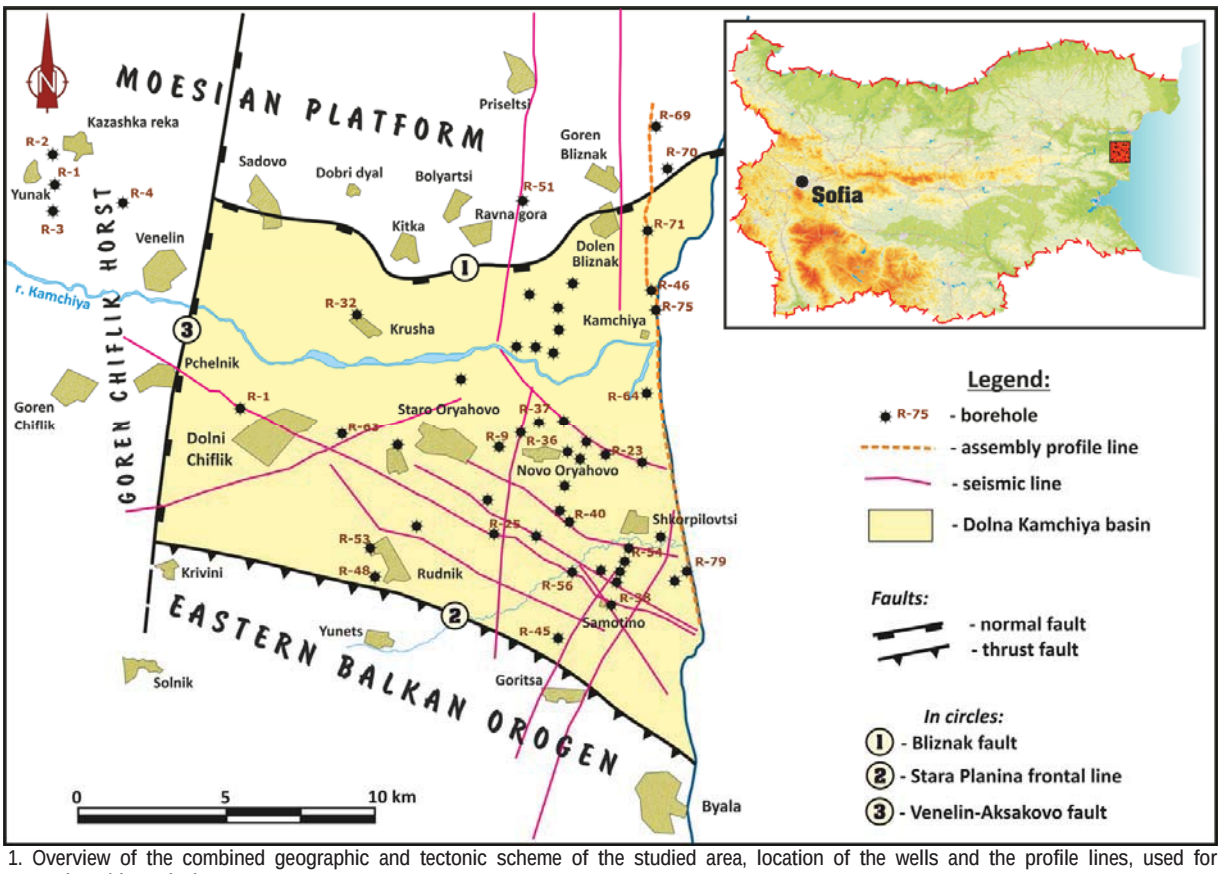

Fig. 1. Overview of the combined geographic and tectonic scheme of the studied area, location of the wells and the profile lines, used for the seismostratigraphic analysis

Materials and methods

For identifying, within Dolna Kamchiya sedimentary basin, seismic-sequence boundaries, maximum flooding surfaces and analyzing sequences with their systems tracts are used data from 48 wells (prospecting and exploratory) and 15 migrated 2D seismic profiles (Fig. 1). Interpretation and correlation of the seismic boundaries with lithostratigraphic units, separated during drilling, are made by the detailed analysis of the sections composite well logs. The quality of some profiles is not the best, but still available material allowed to be made sufficiently good interpretation. The approach used for the purpose of the study is entirely based on the concept of sedimentary sequences (Sloss, 1963; Vail et al., 1977; Van Wagoner and Posamentier, 1988; Van Wagoner et. all., 1990) and seismostratigraphic analysis (Vail et al. 1977, 1991; Bally-ed., 1987; Miall, 1996).

Geological Framework

Tectonics

Dolna Kamchiya sedimentary basin is longitudinally oriented (subparallel), filled predominantly by terrigenous Paleocene-Neogene sediments with considerable thickness, and an asymmetrical transverse and longitudinal profile. More than 2/3 of the territorial scope of the basin is located in the Black Sea area, only its westernmost periphery is developed on a relatively small terrestrial territory. Northern, western and southern borders are well-defined and traceable to this part of the sedimentary basin. (Fig. 1). The northern border with Moesian platform is marked by Bliznak fault, while to the south by Stara Planina frontal line. Sub-meridional Gornochiflishki narrow horst restricts the development of Dolna Kamchiya sedimentary basin to the west along Venelin – Aksakovo fault. The spatial lithofacies distribution in Dolna Kamchiya sedimentary basin and its geometry decisively confirm its development as a foreland basin (Dimitrov, 2012), superimposed on the structures of the Fore Balkan zone and the southern flank of the Moesian platform as a result of intensive folding and thrusting of the Balkanides system throughout the Illyrian tectogenesis. Dolna Kamchyia sedimentary basin opens to the east and extends its width from 10-15 km to the west to 80 km and more in the eastern part. The total thickness of the sedimentary complex, filling Dolna Kamchiya basin, exceeds 5 km (Georgiev, 1996).

Lithostratigraphy

Figure 2 shows the spatial-temporal relationships of lithostratigraphic units involved in the substrate and the filling of Dolna Kamchiya basin. The sedimentary section at the base of the basin is presented by Middle Eocene conglomerates and sandstones of Dvoinitsa formation (Dzhuranov, Pimpirev,

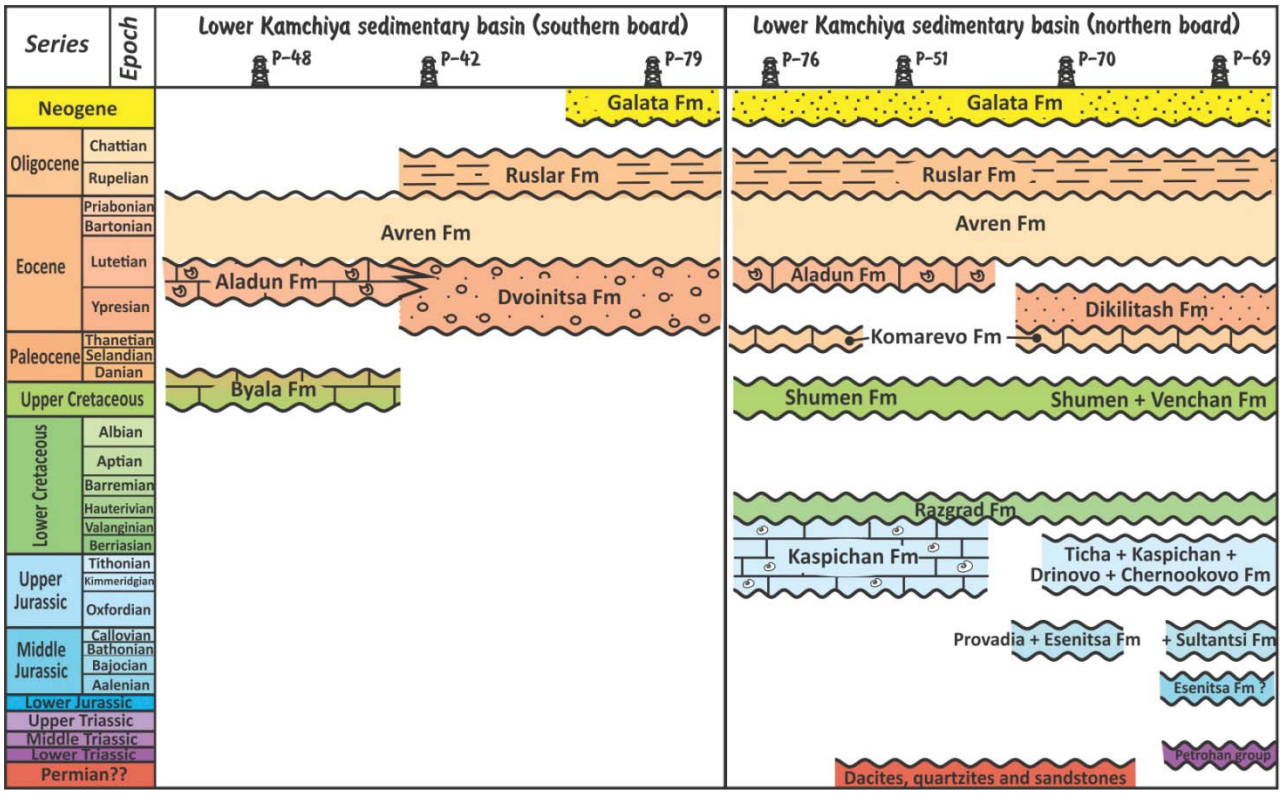

Fig. 2. Lithostratigraphic scheme of the filling and the basement substructure of Dolna Kamchiya sedimentary basin by drilling data

1989), which have been penetrated both onshore and offshore by several wells. The upper-Eocene sediments of Avren formation (Gochev, 1933) are typified by sandstones at the base and alternation of marls, sandstones, siltstones and sandstones with detritus at the top. Ruslar formation (Aladzhova-Hrischeva, 1991) starts with transgressive sandstones at the base, passing up into marine clays. The middle Miocene (Chokrakian) sediments of Galata formation (Koyumdzhieva, Popov, 1986) unconformably overlie the Oligocene sediments and together form a common sedimentary complex.

The basement substructure on the northern and southern board of the basin differs from its typical formations. In the northern part, it is represented by Paleozoic (Permian?) rocks (dacites, quartzites and sandstones), which are penetrated by R-51 Ravna Gora and R-70 Bliznatsi wells. Unfortunately, these deposits are not stratified because of the absence of fossils and lack of their basement substructure. The lack of fauna does not give a chance to determine the exact age of rocks. Mesozoic section in the northern board of Dolna Kamchiya basin is presented by Lower Triassic sandstones.

Seismic-Sequence Stratigraphic Analysis

Seismic Sequences

Firstly, in order to be identified and spatially traced seismic sequences, the seismic sequence boundaries were traced, which are substantially unconformities. The significance of the unconformities is expressed in the fact that they indicate a fundamental change in the environment of the basin – from sedimentation to lack of replenishment or erosion, related to significant tectonic or eustatic changes.

Two types of unconformities are traced (angular and parallel) in the analysis of the 15 migrated 2D seismic profiles from the terrestrial part of the Dolna Kamchiya sedimentary basin (Fig. 3). The angular unconformities are traced in the southern board of the basin and they are related to the occurrence of folding and thrusting during the Illyrian (Middle Eocene), the Pyrenean (Late Eocene) and the Savian (Late Oligocene) alpine folding phases. They are marked by the presence of erosional truncation of older sediments, which are covered by younger ones with a different angle of onlap and downlap. To the northern direction (to the depocenter of the basin) the surfaces gradually pass to the parallel unconformities. As a result of the analysis, three sequence boundaries are marked and traced, which are proved by the type of discontinuity of the reflections under and over them. The sequence boundaries outline three seismic sequences, which are essentially sedimentary complexes, marked on the seismic sections (Fig. 3). These three sequences are involved in filling the terrestrial part of the basin and are conditionally numbered from 1 to 3 as follows: 1 - Miocene; 2 - Oligocene; And 3 – Upper Eocene. Spatial development, geometry, and sequence relationships are shown on a combined seismic cross-section (Fig. 3).

The Upper Eocene sequence (indicated by the number 3) is restricted by type 1 unconformity boundaries, which define it as a type 1 sequence boundary. Its lower boundary is the Illyrian unconformity marking the beginning of the development of the Dolna Kamchiya sedimentary basin, and the upper boundary is the unconformity surface related to the occurrence

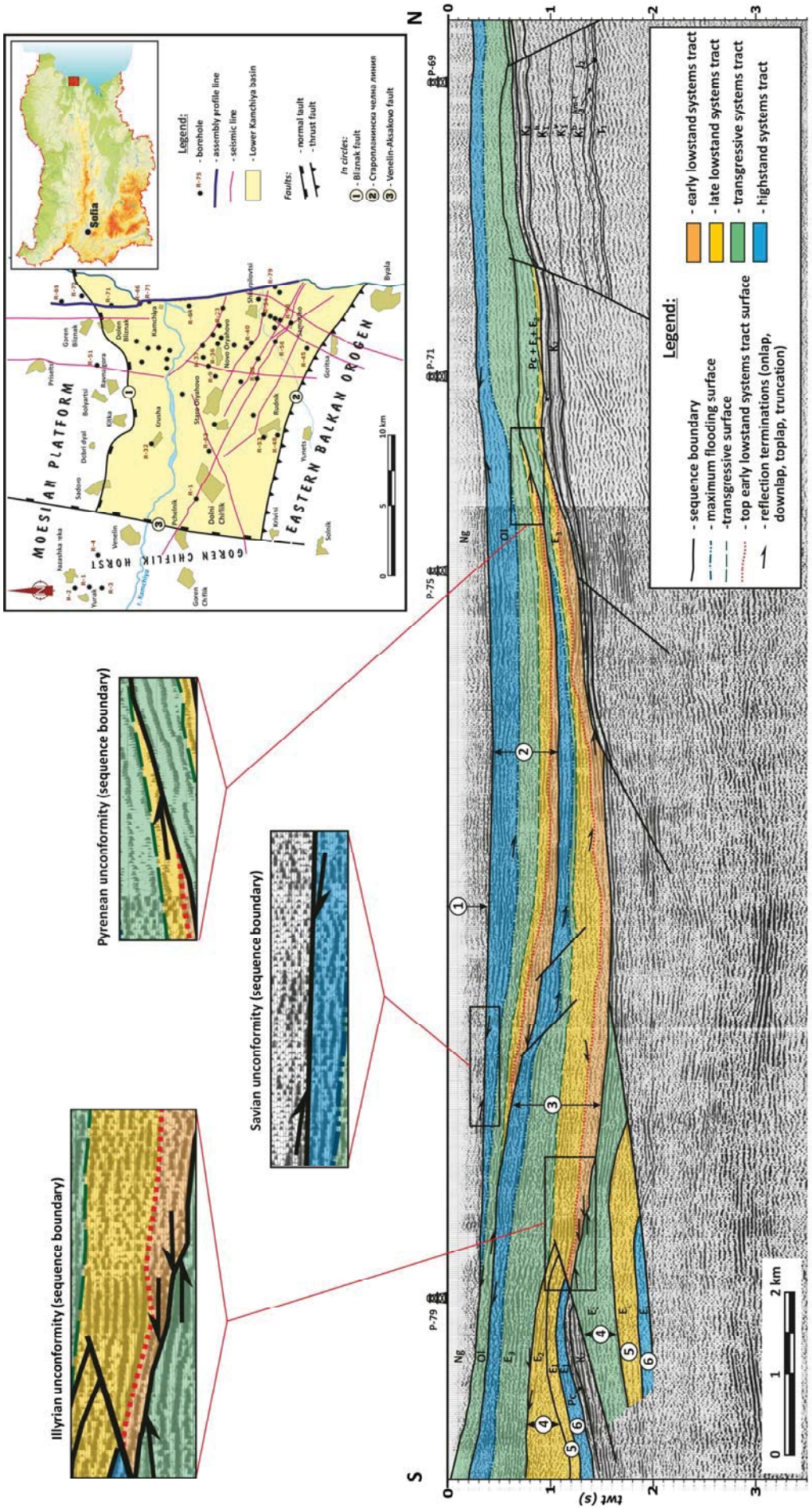

Fig. 3. A combined seismic profile line with south-north direction showing separated and outlined seismic sequences and systems tracts. The identified sequence boundaries are unconformity surfaces, and the internal seismic systems tracts are maximum flooding surfaces. In the circles with numbers from 1 to 3, the sequences of the section of the Dolna Kamchiya sedimentary basin are marked, and the numbers from 4 to 6 - those that construct the basement substructure in the southern part of the basin.

of the Pyrenean folding phase. The sedimentation of the sequence is within a sedimentary cycle of about 3.3 million years, which determines it as a stratigraphic unit of the third order.

The Oligocene sequence (indicated by the number 2) is traced by type 1 unconformity boundaries and because of that it is added to type 1 sequence boundaries. The role of its lower boundary performs the Pyrenean unconformity, and the upper boundary is the unconformity surface associated with the occurrence of the Savian folding phase. The sediments involved in the construction of the sequence are formed in the interval of a sedimentary cycle of about 10.8 million years, which determines it as a stratigraphic unit of the second order.

The Miocene sequence (indicated by the number 1) is with the smallest thickness in the scope of the studied part of the terrestrial part of the Dolna Kamchiya sedimentary basin. It is extremely difficult to analyze and interpret its internal construction and this is the reason to indicate confidently only its lower boundary, which is the result of the Savian folding phase. It is divided in detail in the offshore part of the basin (Georgiev et al., 2004, Dimitrov and Georgiev, 2005, Dimitrov , 2007, Dimitrov , 2008, Dimitrov and Georgiev, 2011). It is identified as a type 1 sequence, restricted between the Savian unconformity and the Messinian unconformity. Its formation lasted about 14 million years in a stratigraphic cycle of the second order.

In the southern part of the basin substrate, three additional sequences are separated and are conditionally numbered from 4 to 6 (Fig. 3). These are: the Middle Eocene sequence (indicated by the number 4) and two sequences with Lower Eocene age (indicated by the numbers 5 and 6). The location of the traced sequence boundaries is fully compliant with the R-79 well in which, on the basis of SP log, there is convincing data for their marking. Unfortunately, on the interpreted seismic profiles, data of their separation and tracing has not been seen. This is explained by the complex situation resulting from the active tectonics during the Illyrian folding phase. The sedimentary complexes are removed from their initial formation position, as they have undergone folding and thrusting and it is extremely difficult to comment what part from the paleobasin they represent.

Seismic Systems Tracts

In interpreting the seismic sections from the studied area, the development of three systems tracts is well established in the Upper Eocene and the Oligocene sequences, described in the classic model of Vail et al. (1977).

The Upper Eocene sequence starts with the early lowstand systems tract, which is developed in the central part of the basin. Its lower boundary is the unconformity surface, and the upper boundary is the first flooding surface (Fig. 3). It is characterized on the seismic sections with wavy and hummocky configurations, which are interpreted as basin floor fans and slope fan complexes. Over the early lowstand systems tract is formed the late lowstand systems tract. Its upper boundary is the next significant maximum flooding surface – transgressive. The seismic sections reveal the characteristic wedge geometry and seismic reflections ending with downlap to the top of the basin and slope fans, which gives a reason to interpret that this tract is associated with the formation of a wedge-prograding complex. The transgressive systems tract lies between two significant flooding surfaces - the transgressive surface at the bottom and the maximum flooding surface at the top. The maximum flooding surface is marked by a downlap seismic configuration. The transgressive systems tract is widespread as the smallest thicknesses are recorded in the central part of the basin. The highstand systems tract is marked at the top of the section, whose upper boundary is the Pyrenean unconformity. The characteristic seismic reflections (truncation type) are clearly noted below it.

In the Oligocene sequence, the lowstand systems tract is also represented by its two distinct parts - the early lowstand systems tract and the late lowstand systems tract (Fig. 3). The early lowstand systems tract is restricted by the unconformity surface at the bottom (the Pyrenean unconformity) and the first significant flooding surface at the top. The floor fan fans and the slope fan complexes are clearly identified on the basis of the seismic sections. The late lowstand systems tract covers the early one, its upper boundary is the transgressive surface and, according to the seismic reflections, it can be interpreted as the wedge-prograding complex. After that, it follows the development of the transgressive systems tract, whose lower boundary, in the majority of the basin, is transgressive, and the smaller one is the sequence boundary. The upper boundary of the transgressive systems tract is the maximum flooding surface. The highstand systems tract is marked at the top of the section, whose upper boundary is the Savian unconformity. The characteristic seismic reflections (truncation type) are clearly noted below it.

Well Log Sequence

The separated well log sequences with their system tracts in the terrestrial part of the section of the Dolna Kamchiya sedimentary basin are shown in Figures 4, 5 and 6. The well diagram of P-79, which is located in the southern part of the basin, is applied to fragments of the combined seismic section (Figs. 1 and 3). The geometry of spontaneous potential and resistivity logs is analyzed along the well section. Each of the situations is adapted to the theoretical model of Mitchum, et al. (1993).

The trends in the geometric shape of the spontaneous potential log from 50 m to 318 m, for the Miocene sequence (indicated by 1), indicate the development of the highstand systems tract (Fig. 4). The medium-grained sandstones, siltstones and clayey sediments are located at the bottom of the tract, and upward the sediments are found in more coarse-grained facies. The model of PS log has a funnel shape, which is interpreted as a sedimentary section formed under conditions of progradation in the basin.

The Oligocene sequence (indicated by 2) in the well section of R-79 is represented only by the transgressive systems tract (Fig. 5). At a depth of 319 m to 407 m, the spontaneous potential log has a pronounced bell–shaped curve that is interpreted by a lithological change from the bottom to the top. The coarse-grained terrigenous sediments are located at the bottom of the section, and upward they pass into more clayey

sediments, suggesting the formation of a typical retrograde model in this part of the basin.

Two systems tracts are separated by the spontaneous potential log of P-79, involved in the construction of the Upper Eocene sequence (indicated by 3) – the transgressive systems tract (from 458 m to 1038 m) and the high stand systems tract (from 407 m to 458 m) (Fig. 5). The boundary between two systems tracts is very clearly marked because it reflects the presence of a maximum flooding surface. Above it, the model of a logging curve is with the funnel shape indicating of progradating architecture, while the bell–shaped curve below it shows a retrograde model of the sedimentary section. The R-79 well also reveals the substrate section of the Dolna Kamchiya basin (Fig. 6). Firstly, for the Middle Eocene sequence (indicated by 4), in the depth interval 1039 m - 1365 m, according to the geometry of the spontaneous potential log, which is the bell-shaped, the lowstand systems tract (the wedge–progradating complex) is interpreted. Two sequences are separated by the logging curve in the Lower Eocene section (indicated by 5 and 6). The first, according to the logging curve, is interpreted as the wedge–progradating complex from the late lowstand systems tract (from 1365 m to 1955 m). The breccia–conglomerates are found at the bottom, which gradually begin upward to alternate with more coarse-grained sand-

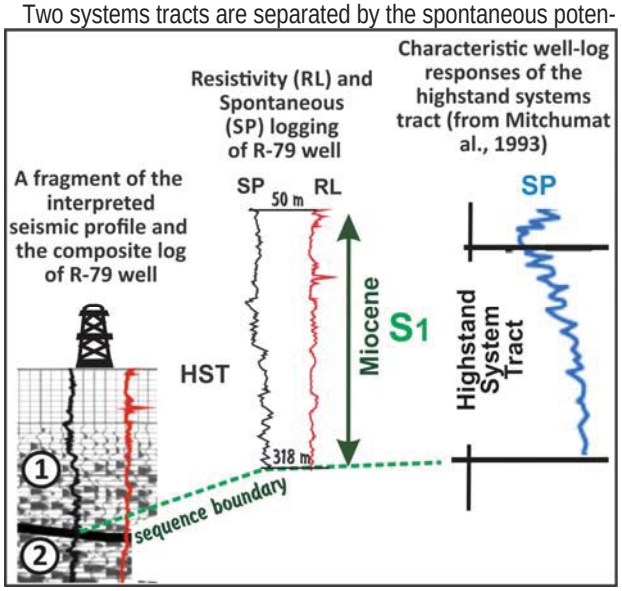

Fig. 4. The Miocene sequence (indicated by 1), separated on basis of the spontaneous potential log of R-79 well

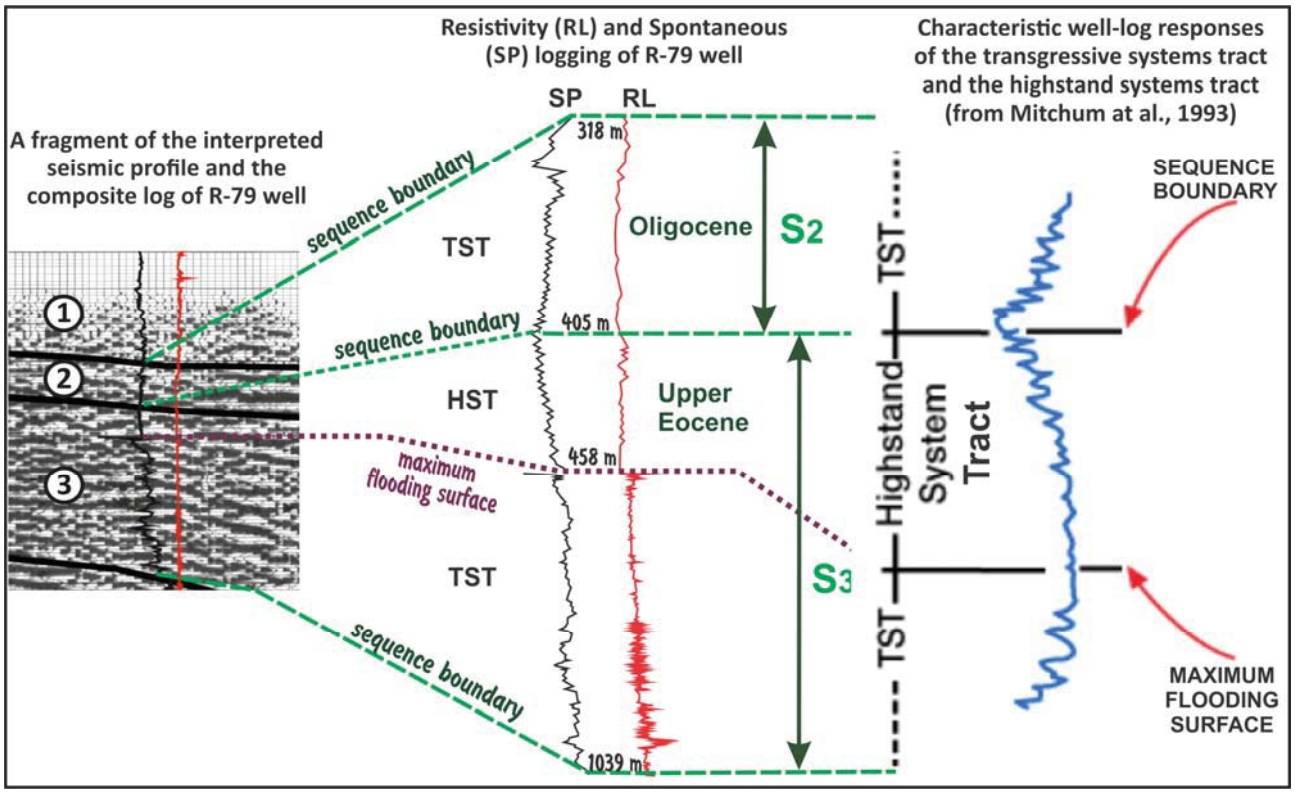

Fig. 5. The Oligocene (indicated by 2) and the Upper Eocene (indicated by 3) well log sequences, separated on basis of the spontaneous potential log of R-79 well

stones in the beginning of the tract, and more fine-grained sandstones at the top. The second, the lower Eocene sequence (indicated by 6), which is the depth interval from 1955 m to 2367 m, according to the model of the spontaneous potential log, is interpreted as the high stand systems tract. According to the well table of R-79, the sedimentary section is defined in the interval from 2367 m to the bottom hole of the well (3490 m) with the lower Eocene-Paleocene age, which is questionable. In our view, there is really a Paleocene section at the top, as evidenced by the carbonate sediments, but from 2407 m to the bottom hole of the well, the logging curve does not repeat any elements separated by two lower Eocene sequences. The typical breccia – conglomerates are absent in the sequence 5, and the characteristic argillites in the

sequence 6. This fact, as well as the interpretation of the combined seismic section, gives us the reason to believe that this part of the section is with the Middle Eocene age, which is revealed under the thrust sheet, including the sediments with the lower Eocene, Paleocene and Upper Cretaceous age. Due to the lack of serious and accurate dating data, this part of the section is not added to any of separated sequences of the basin substrate.

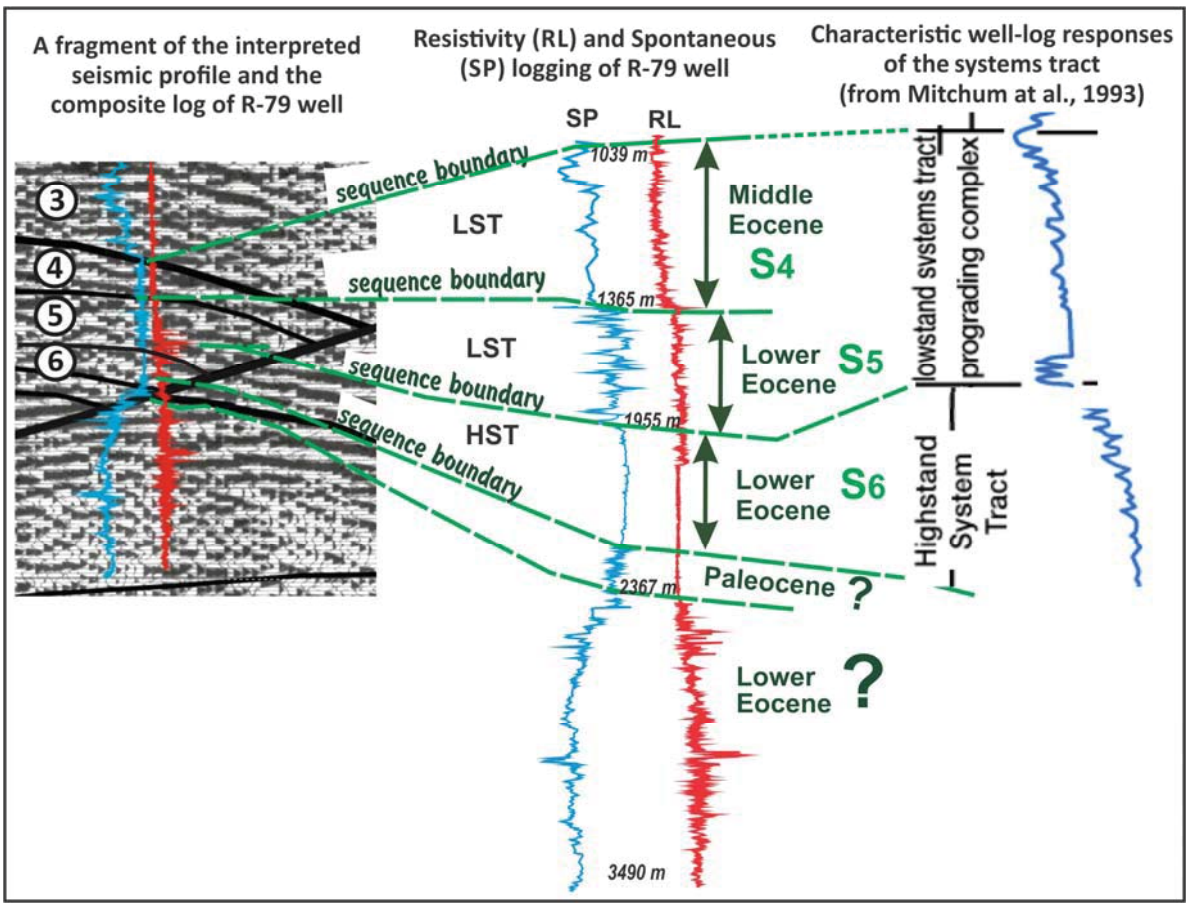

Fig. 6. The Middle Eocene (indicated by 4) and two Lower Eocene (indicated by 5 and 6) well log sequences, separated on the basis of the spontaneous potential log of R-79 well

Conclusion

The conducted seismostratigraphic study for the terrestrial part of the Dolna Kamchiya sedimentary basin gives the reason to make several important conclusions and put some tasks for future research.

Three unconformity surfaces are separated and traced by seismic wave fields in the basin section and they are accepted as basic seismic reflecting boundaries. The geometry of discontinuity of the seismic reflections under and over them, gives the reason for their identification as sequence boundaries. They outline three seismic sequences – the Upper Eocene, Oligocene and Miocene.

The Miocene and Oligocene sequences are separated on the seismic sections as well as correlating of logging diagrams, and they are defined as sequences of type 1, formed within a second-order stratigraphic cycle (10-100 million years), while the upper Eocene sequence is defined as a sequence of type 1, formed in the interval of a third order stratigraphic cycle (1-10 million years).

The seismic systems tracts, constructing sequences, are identified on the basis of recognizing and tracing secondary reflection surfaces (flooding surfaces between the early and the late low stand systems tract, transgressive surfaces and maximum flooding surfaces).

Another three sequences are separated by the methodology of well log sequence in the basin substrate – the Middle Eocene and two lower Eocene sequences, which are very difficult to analyze on the seismic sections due to the complicated geological environment in which they are located.

After conducting the study, a lot of unresolved issues remain that may be the subject of future exploration in the terrestrial part of the basin. The work should be continued with seismic facies analysis and tracing eustatic sea-level change, which will give the opportunity to perform forecast evaluation of the natural reservoirs and traps in connection with hydrocarbon prospect in this part of the basin.

References

Аладжова-Хрисчева, К. Стратиграфское расчленение и коррелация палеогеновых отложений Северо-Восточной Болгарии. – Geologica Balc., 21, 2, 1991. - 12-88. (Aladzhova-Hrischeva, K. Stratigrafckoe raschlenenie i korelatsiya paleogenovuih otlojeniya Severo-Vostochnoi Bolgarii. Geologica Balc., 21, 2, 1991. - 12-88.)

Георгиев, Г., Х. Димитров, Ф. Рейд, Дж. Прингъл, Н. Ботушаров. Сеизмостратиграфия и 3-Д модел на Долно-Камчийския седиментен басейн (морска част). - "Проблеми на нефта и газа", Варна, 2004, - 142-147. (Georgiev, G., H. Dimitrov, F. Reid, G. Pringal, N. Botushrov. Seismostratigrafiya i 3-D model na Dolno-Kamchiiskya sedimenten basein (morska chast).- "Problemi na nefta i gaza", Varna, 2004, - 142-147.)

Гочев, П. Палеонтологични и стратиграфски изучавания върху еоцена във Варненско. – Сп. Бълг. геол. д-во, 5, 1, 1933. - 1-82. (Gochev, P. Paleontologichni i stratigrafski izuchavaniya varhu eotsena vav Varnensko. - Sp. Balg. geol. d-vo, 5, 1, 1933. - 1-82.)

Джуранов, С., Хр. Пимпирев. Литостратиграфия на горната креда и палеогена в приморската част на Източна Стара планина. – Сп. Бълг. геол. д-во, 2, 1989. - 1-18. (Dzhuranov, S., H. Pimpirev. Litostratigrafiya na gornata kreda I paleogena v primorskata chast the Iztochna Stara planina. - Sp. Balg. geol. d-vo, 2, 1989. - 1-18)

Димитров, Х. Анализ на относителните изменения на морското ниво в Долнокамчийския седиментен басейн (морската част) през средно-късноеоценската и олигоценската епоха. – Год. МГУ "Св. Иван Рилски", 50, св. I, Геология и геофизика, 2007. - 43-48. (Dimitrov, H. Analiz na otnositelnite izmeneniya na morskoto nivo v Dolnokamchiyskiya sedimenten basein (morska chast) prez sredno-kasnoeotsenskata i oligotsenskata epoha. - God. MGU, 50, sv. I, Geol. i geofiz., 2007. - 43-48)

Димитров, Х. Палеогеографска реконструкция на Долнокамчийския седиментен басейн (морската част) през средно-късноеоценската и олигоценската епоха. – Год. МГУ "Св. Иван Рилски", 51, св. I, Геология и геофизика, 2008. - 28-33. (Dimitrov, H. Paleogeografska rekonstruktsiya na Dolnokamchiyskiya sedimenten basein (morska chast) prez sredno-kasnoeotsenskata i oligotsenskata epoha. - God. MGU, 51, sv. I, Geol. i geofiz., 2008. - 28-33)

Димитров, Х. Идентифициране на депозони в Долнокамчийския седиментен басейн по геофизични данни. - Journal Science & Tehnologies, Natural & Mathematical science, Vol. II, 3, 2012. - 54-58. (Dimitrov, H. Identifitsirane na depozoni v Dolnokamchiyskiya sedimenten basein po geofizichni danni. - Journal Science & Tehnologies, Natural & Mathematical science, Vol. II, 3, 2012. - 54-58)

Димитров, Х., Г. Георгиев. Литофациален анализ на седиментните секвенции в Долнокамчийския седиментен басейн (акваториална част). Год. МГУ, 48, св. I, Геология и геофизика, 2005. - 47-52. (Dimitrov, H., G. Georgiev. Litofatsialen analiz na sedimentnite sekventsii v Dolnokamchiyskiya sedimenten basein (akvatorialna chast). God. MGU, 48, sv. I, Geol. i geofiz., 2005. - 47-52.)

Коюмджиева, Е., Н. Попов. Стратиграфия и корелация на неогена от Средиземноморската област – решения и дискусии. – Сп. Бълг. геол. д-во, 47, 3, 1986. - 124-126. (Koyumdzhieva, E., N. Popov. Stratigrafiya i korelatsiya na neogena ot Sredizemnomorskata oblast - resheniya i diskusii. - Sp. Balg. geol. d-vo, 47, 3, 1986. - 124-126)

Bally A. W. (ed.). Atlas of seismic stratigraphy. – AAPG Studies in Geology, Tulsa, No 27, 1987. - 125 p.

Dimitrov, H., Georgiev, G. Correlation between main seismic sequence boundaries in Kamchia basin (offshore Bulgaria) and Western Black Sea basin. In: 73rd EAGE Conference & Exhibition incorporating SPE EUROPEC, Vienna, Austria, Extended Abstracts (CD-ROM), 2011.

Georgiev, G. Hydrocarbon generation in the Tertiary filling (above the Illyrian unconformity) of the Kamchya Depression – offshore. – IVth Intern. Conf. "Gas in marine sediments". Varna, Bulgaria, 1996.

Miall, A. D. The Geology of Stratigraphic Sequences. Springer, Berlin, 1996. - 433 p.

Mitchum, R., J. Sangree, P. Vail, W. Wornardt. Recognizing Sequences and Systems Tracts from Well Logs, Seismic Data, and Biostratigraphy: Examples from the Late Cenozoic of the Gulf of Mexico: Chapter 7: Recent Applications of Siliciclastic Sequence Stratigraphy. AAPG Memoir, 58, 1993. - 163-197.

Sloss, L. L. Sequence in the cratonic interior of North America. – Geological Society of America Bulletin, 74, 1963. - 93-114.

Vail, P. R., Audemard, F., Bowman, S.A., Eisner, P.N., Perez-Cruz, C. The stratigraphic signatures of tectonics, eustasy and sedimentology an overview. In Einsele, G., Ricken, W., and Seilacher, A. (Eds.), Cycles and Events in Stratigraphy. Berlin, Springer-Verlag, 1991.

Vail, P. R., R. M. Mitchum, S. III Thompson. Relative Changes of Sea Level from Coastal Onlap. – In: Seismic stratigraphy – application to hydrocarbon exploration (Ed. C.E. Payton). AAPG Memoir, 26, 1977. - 63-81.

Van Wagoner, J.C., Mitchum, R.M., Campion, K.M., Rahmanian, V.D., Siliciclastic sequence stratigraphy in well logs, cores, and outcrops: concepts for high-resolution correlation of time and facies. – AAPG, Methods in Exploration Series, 7, 1990.

Van Wagoner J. C., H. W. Posamentier. An overview of the fundamentals of sequence stratigraphy and key definitions. – SEPM, 42, Sea-level Changes: an Integrated Approach, Tusla, Oklahoma, USA, 1988. - 39-46.

The article is reviewed by Prof. Vasiv Balinov, DSc. and Assoc. Prof. Dr. Nikola Botusharov.

NATIVE GOLD FROM SEDEFCHE DEPOSIT, EASTERN RHODOPES, BULGARIA

Georgi Lyutov

University of Mining and Geology "St. Ivan Rilski", 1700 Sofia; georgi_lutov@yahoo.com

ABSTRACT: The epithermal Sedefche deposit is located in the Eastern Rhodopes (Bulgaria). It is part of the Zvezdel-Pcheloyad ore field. The ore mineralization is hosted in intermediate volcanic tuffs, affected by intensive hydrothermal alteration. The primary ore minerals are sulfides and sulfosalts, including silver-bearing minerals (mostly sulphides and sulphosalts such as acanthite, pyrargyrite, freibergite and others). The upper parts of the deposit are near the ground surface and are subjected to supergene changes. The presence of gold in the deposit is proven by geologic surveys and chemical analyses. Still until now, gold from the deposit has not been observed as a standalone macroscopic phase or under optical or electron microscope. As part of this study, 8.63 kg ore-bearing host rock from the deposit is crushed, milled, sifted and processed by Knelson's concentrator and pan in order to extract heavy minerals. Subsequently the heavy mineral fraction was bonded in polymer resin and polished in order to expose the surface of the minerals and facilitate their observation under optical and electron microscopes. In one of these specimens native gold was discovered. The discovered native gold is of sub-microscopic size. Despite its small size, it is a physical proof of the presence of gold in Sedefche deposit. This discovery may improve and refine techniques for gold extraction from the deposit. At least some of the gold from the deposit could be recovered by using conventional physical-mechanical techniques.

Keywords: native, gold, epithermal, Sedefche deposit

САМОРОДНО ЗЛАТО ОТ НАХОДИЩЕ СЕДЕФЧЕ, ИЗТОЧНИ РОДОПИ, БЪЛГАРИЯ

Георги Лютов

Минно-геоложки университет „Св. Иван Рилски", 1700 София; georgi_lutov@yahoo.com

РЕЗЮМЕ: Епитермалното находище Седефче се намира в Източните Родопи (България). То е част от Звездел-Пчелоядското рудно поле. Рудната минерализация е вместена в среднокисели вулкански туфи, засегнати от интензивна хидротермална промяна. Първичните рудни минерали са сулфиди и сулфосоли, включително среброносни минерали (предимно сулфиди и сулфосоли като акантит, пираргирит, фрайбергит и др.). Горните части на находището са близо до земната повърхност и са подложени на хипергенни промени. Присъствието на злато в находището е доказано от геоложките проучвания и химични анализи. Въпреки това, досега злато от находището не е наблюдавано като самостоятелна макроскопска фаза или под оптичен или електронен микроскоп. Като част от това изследване, 8.63 kg рудоносна вместваща скала от находището е натрошена, смляна, пресята и обработена с Нелсънов концентратор и промивна купа, за извличане на тежки минерали. В последствие тежката минерална фракция е споена с полимерна смола и полирана за разкриване на минералите и улесняване на наблюдението им с оптичен и електронен микроскоп. В един от изработените образци е открито самородно злато. Откритото самородно злато е със субмикроскопични размери. Въпреки малките си размери, то е физическо доказателство за присъствието на злато в находище Седефче. Това откритие би могло да подобри и усъвършенства техниките за извличане на златото от находището. Част от златото от находището би могла да се извлече с използване на конвенционални физико-механични техники.

Ключови думи: самородно, злато, епитермално, находище, Седефче

Introduction

The Sedefche deposit is located in the Eastern Rhodopes, South Bulgaria, roughly between the towns of Momchilgrad and Krumovgrad (Fig. 1). Sedefche has been known as ore occurrence at least since 1963, when modern prospecting and surveying in the area were initiated (Atanasov and Breskovska, 1964; Atanasov, 1965). These early geologic surveys have discovered traces of ancient mining works in the deposit (Tsekova, 1965; Dragiev and Dragieva, 2006).

Geological setting

The deposit is part of the Zvezdel-Pcheloyad ore field in the area of Zvezdel paleo-volcano (Georgiev, 2012).

The ore field belongs to Momchilgrad ore sub-region, which coincides spatially with Momchilgrad depression (Fig. 2). The area of the deposit consists of two tectonic complexes (Georgiev, 2012):

Fig. 1. Location of the Sedefche deposit in the Republic of Bulgaria.

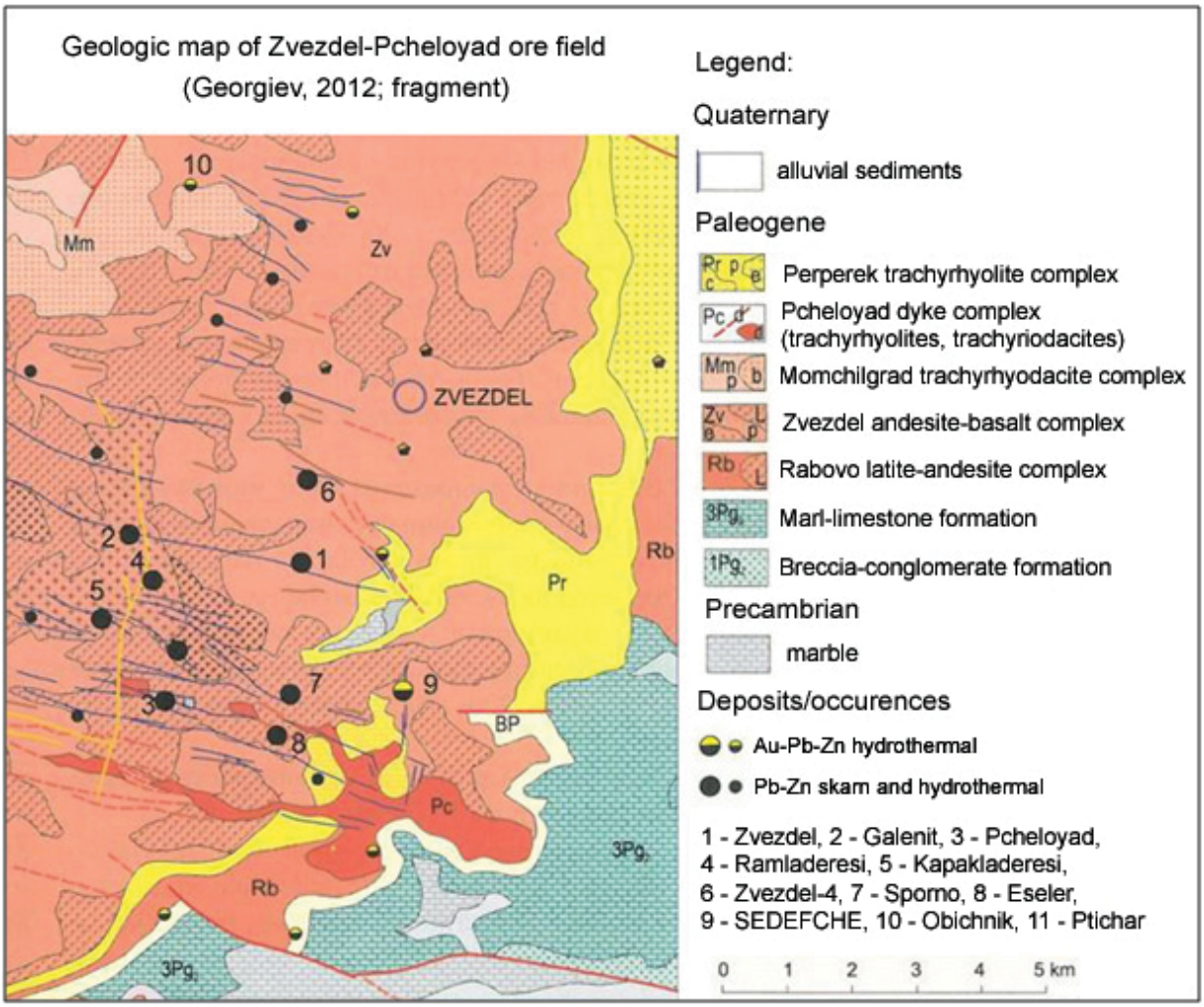

Fig. 2. Momchilgrad depression and Zvezdel-Pcheloyad ore field (Georgiev, 2012). On this map, the Sedefche deposit is marked with #9.

Pre-tertiary metamorphic complex – it consists of metamorphic rocks, represented by biotite and dual-mica gneiss, amphibolite-biotite gneiss, marble and kyanite-garnet-biotite schists. Their age is considered to be Precambrian.

Tertiary volcanogenic-sedimentary cover – it is represented by sedimentary, volcanogenic-sedimentary and volcanic rocks. Limestones and sandy-loam rocks lie above the metamorphic rocks. In some areas, limestones are partially silificated. Volcanic manifestations in Oligocene (Pg_3) formed acid to intermediate lava plains and dykes of rhyolite, dacite and andesite.

Geologic surveys outlined three ore bodies in the deposit - Northern (central) ore body, Southern ore body and Ralitza Dere. The Northern (central) ore body is the most promising one for finding Au and Ag according to the results of geological surveys. The ore minerals are hosted within intermediate volcanic tuffs, subjected to heavy hydrothermal alteration, such as silification, sericitization, propylytization (Atanasov 1965; Radonova 1973). The ore bodies in the Sedefche deposit have layer-like, pseudo-conform shape (Georgiev, 2012).

Ore minerals

The Sedefche deposit exhibits diverse mineral composition. More than 20 ore minerals have been reported by various studies and authors (Mladenova, 1998; 1999), (Strashimirov et al. 2005), (Milev et al., 2007). The primary ore minerals are sulphides and sulphosalts (pyrite, marcasite, arsenopyrite, sphalerite, galena, chalcopyrite, acanthite, tennantite-tetrahedrite-freibergite, pyrargyrite, miargyrite and others). Earlier studies suggest the presence of "invisible gold" as sub-microscopic particles/inclusions within primary ore minerals such as pyrite, marcasite and arsenopyrite (Mladenova, 1998). Supergene ore minerals are represented by oxides, hydroxides, sulfates, carbonates and arsenates. The most widespread supergene ore minerals in the deposit are goethite, scorodite and jarosite.

Methods of study

For more profound investigation of the ore minerals (and particularly searching for native gold), heavy mineral fraction was extracted. A total of 8.63 kg rock samples from the trial quarry in the Northern (central) ore body were subjected to the following operations: crushing with jaw crusher, milling with hammer-mill, sifting, extraction of heavy minerals by Knelson's concentrator, thereby obtaining fraction K1. Afterwards part of fraction K1 was bonded with polymer resin (butyl-2-cyanoacrilate) and polished to expose fresh surfaces of the heavy minerals in the form of briquette-like specimens (K1-1 and K1-2). The remainder of heavy fraction K1 was washed

with pan to extract heavy fraction K2. In the same way as above, two more briquette-like specimens were made from it (K2-1 and K2-2) (Fig. 3).

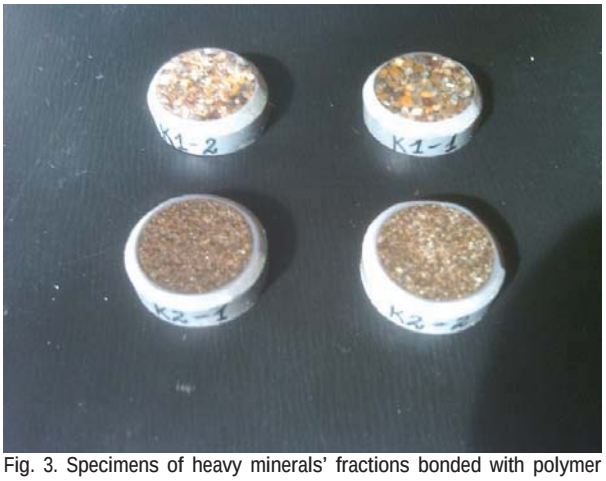

Fig. 3. Specimens of heavy minerals' fractions bonded with polymer resin and polished ("briquettes").

The crushing, milling and panning were carried out in the laboratories of UMG "St. Ivan Rilski" with the support of eng. V. Nojarov and eng. I. Raikov.

The processing with Knelson's concentrator was done in "Eurotest Control" with the help of eng. St. Stamenov and eng. N. Nestorov.

The 4 specimens were investigated with optical reflected-light microscopes and subjected to semi-quantitative electron microscope EDS analyses in order to determine their mineral composition. The diameter of the electron beam was about 4 μm.

The optical microscope observations were carried out in UMG "St. Ivan Rilski" and Montanuniversitæt Leoben with microscopes Meiji 9430 and Olympus BX60 respectively.

Electron microscope investigations of the samples were completed in Montanuniversitæt Leoben with device Zeiss EVO|MA10, EDS detector Bruker, with the help and guidance of Prof, PhD Frank Melcher.

Results of the study

The microscope observations revealed only the most common ore minerals present in the deposit (such as pyrite, marcasite and arsenopyrite). Many of the smaller mineral grains in the "briquettes" could not be identified by this method due to their small size. For this reason the specimens were carefully examined with electron microscope in order to determine and identify the small-sized mineral grains. A total of 34 analyses were made and they discovered the following primary ore minerals – acanthite, barite, pyrite, marcasite, arsenopyrite, sphalerite, galena, gersdorffite, gold and secondary (supergene) minerals – jarosite, scorodite and Fe-hydroxides. One of these semi-quantitative EDS analyses discovered a small grain of native gold (Fig. 4), within a matrix of jarosite.

The result of the semi-quantitative analysis, corresponding to the gold grain and surrounding area is shown in Table 1.

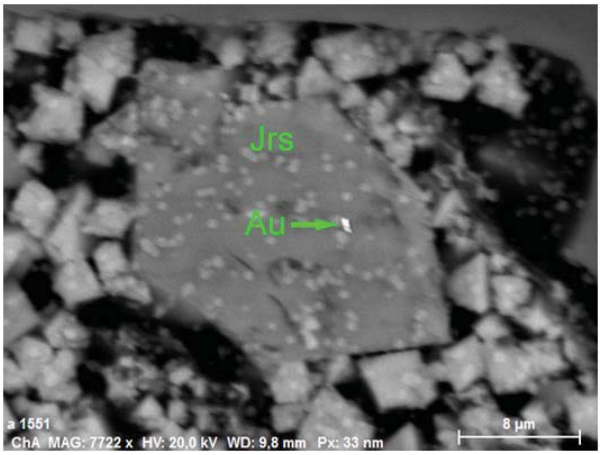

Fig. 4. Miniature grain of native gold within a matrix of jarosite.

Table 1.
Results from semi-quantitative analyses of jarosite hosting a grain of native gold

Element	*mass %*	*normalized mass %*	*atom.%*	*Error (3σ) [mass %]*
O	*35.06*	*34.72*	*63.77*	*4.51*
S	*12.96*	*12.84*	*11.76*	*0.50*
K	*6.72*	*6.66*	*5.01*	*0.24*
Fe	*31.70*	*31.40*	*16.52*	*0.89*
As	*1.39*	*1.37*	*0.54*	*0.11*
Ag	*1.34*	*1.33*	*0.36*	*0.08*
Au	*11.47*	*11.36*	*1.69*	*0.44*
Sum:	*100.97*	*100.00*	*100.00*	*-*

The discovered grain of native gold is slightly elongated, with size not larger than 0.5 × 1 μm. Due to its small size the analysis contains data from the matrix's composition as well. The sharp boundaries and brightness of the gold grain, which is typical for elements with greater atomic mass, are well defined and visible on the image from the electron microscope. The image is taken at magnification of 7722 times. The results from the semi-quantitative analyses, of the jarosite matrix are shown in Table 2.

Table 2.
Results from semi-quantitative analyses of jarosite matrix

Element	*mass %*	*norm. mass %*	*atom. %*	*Error (3σ) [mass %]*
O	*31.99*	*36.50*	*62.10*	*3.91*
S	*13.72*	*15.66*	*13.29*	*0.52*
K	*5.49*	*6.26*	*4.36*	*0.20*
Fe	*34.86*	*39.78*	*19.39*	*0.97*
As	*1.29*	*1.47*	*0.54*	*0.11*
Sum:	*87.64*	*100.00*	*100.00*	*-*

As a typical endogenous mineral, gold has formed in association with some of the primary minerals in the deposit. Most likely, during the supergene processes, gold was liberated from its matrix of primary minerals as they were transformed and later enveloped by a matrix of secondary jarosite. The origin of this gold grain cannot be linked directly with some of the primary minerals as these relationships were erased by the supergene processes.

Conclusions

The current study confirmed the assumed presence of native gold in the Sedefche deposit, although it most likely appears as grains of very small, sub-microscopic size (0.5 – 1 μm or smaller), originally as inclusions ("invisible gold") in primary minerals. In the oxidation zone of the deposit original primary minerals hosting gold have been transformed to secondary minerals, such as jarosite, which in turn may contain native gold. The current study suggests that at least some of the gold from the deposit could possibly be recovered by using conventional physical-mechanical techniques. For extraction of gold particles with smaller sizes, other technologies may need to be applied.

Acknowledgements

I would like to express my gratitude and highest esteem towards my advisor Prof. PhD Strashimir Strashimirov for the guidance he provided during preparation of my studies.

I would like to thank Prof. PhD Frank Melcher for his help and support for X-ray spectral semi-quantitative microanalyses completed in Montanuniversitæt Leoben.

References

Атанасов А., В. Бресковска. Сулфосоли от Звезделски руден район и тяхната минерална парагенеза; - Год. СУ, 57, 1, 1964. - 197-203. (Atanasov A., V. Breskovska. Sulfosoli ot Zvezdelski ruden rayon i tyahnata mineralna parageneza. – God. SU, 57, 1. 1964. - 197-203.)

Атанасов А. Изследвания върху минералната парагенеза и структурата на Звезделското оловно-цинково рудно поле в Източните Родопи; - Год. СУ, 58, 1, 1965. - 285-323. (Atanasov A. Izsledvaniya varhu mineralnata parageneza i strukturata na Zvezdelskoto olovno-tsinkovo pole of Iztochnite Rodopi . – God. SU, 58, 1, 1965. - 285-323.)

Георгиев В., „Металогения на Източните Родопи", академично издателство „проф. Марин Дринов", 2012, 262 с. (Georgiev, V. Metalogeniya na Iztochnite Rodopi. Akademichno izdatelstvo "Prof. Marin Drinov", Sofia. 2012, 262 p)

Милев В., Обретенов Н., Георгиев В., Аризанов А., Желев Д., Бонев И., Балтов И., Иванов В.; „Златните находища в България", изд. „Земя 93", 2007, 208 с (Milev, V., Obretenov, N., Georgiev, V., Arizanov, A., Zhelev, D., Bonev, I., Baltov, I., Ivanov, V. Zlatnite nahodishta v Bulgaria. Izdatelska kashta "Zemya 93", Sofia, 2007, 208 p)

Младенова В.; „Минералогия и проблемът на златото в находище Седефче, Източни Родопи"; Год. СУ, Книга 1, Том 90, 1998, 101-130 (Mladenova V. Mineralogiya I problemat na zlatoto v nahodishte Sedefche, Iztochni Rodopi; God. SU, 90, 1, 1998. 101-130)

Младенова В.; „Благородните метали в находище Седефче, Източни Родопи"; Минно дело и геология, 1-2, 1999, 36-40 (Mladenova V. Blagorodnite metali v nahodishte Sedefche, Iztochni Rodopi; Minno delo I geologiya, 1-2, 1999. 36-40)

Радонова Т. Г.; „Метасоматични изменения на скалите в Звезделския руден район"; Изв. Геол. Инст. Св. Геохим. Минер. и Петр., 22, 1973, 123-140 (Radonova R. G., Metasomatichni izmenenia na skalite v Zvezdelskiya ruden rayon. Izv. Geol.Inst. Sv. Geohim., Miner. i Petr., 22, 1973. 123-140)

Strashimirov St., S. Dobrev, St. Stamenov, H. Dragiev. Silver-bearing minerals from the ore body "North" in Sedefche epithermal Au-Ag deposit (Eastern Rhodopes); Annual MGU "St. Ivan Rilski", Vol. 48, Part I, Geology and geophysics. 2005. 143-148.

Reports of geological surveys; National Geofund:

Драгиев Х., Б. Драгиева; 2006, „Звездел-Пчелоядско рудно поле, проучвателни площи „Момчилград" и „Асара" – геоложки доклад с преизчисляване на запасите и ресурсите от златно-сребърни руди по състояние към 01.01.2006 г. на находище Седефче (Dragiev H., B. Dragieva; "Zvezdel-Pcheloyadsko rudno pole, prouchvatelni ploshti "Momchilgrad" and "Asara" – geolozhki doklad s preizchislyavane na zapasite i resursite ot zlatno-sreburni rudi po sastoyanie kam 01.01.2006 g. na nahodishte Sedefche. Geofund MEW. 2006)

Цекова В., 1965. Доклад за проведеното геоложко картиране на обект Звездел-Галенит-Пчелояд в М = 1:5000 през 1962-1964 година (Tzekova V. Doklad za provedenoto kartirane na obekt Zvezdel-Galenit-Pcheloyad v M=1:5000 prez 1962-1964. Geofund MEW. 1965)

The article is reviewed by Assoc. Prof. Dr. Vassilka Mladenova and Prof Dr. Strashimir Strashimirov.

THE STRUCTURAL GEOLOGICAL APPROACH IN THE EVALUATION OF THE GEOLOGICAL LOSSES IN THE DEPOSITS OF CARBONATE ROCKS – LIMESTONES, DOLOMITES AND MARBLES

Ivan Dimitrov[1], Dimitar Sachkov[1]

[1]University of Mining and Geology "St. Ivan Rilski", 1700 Sofia, e-mail: idim68@abv.bg

ABSTRACT. The losses represent this part of the geological reserves, which cannot be extracted, or for one or another reason, cannot be sold for a profit. The amounts of the losses in all deposits are different, because of differences in the geological situation and in the technology of extraction and processing. The errors in the evaluation of the losses can result in shortening the life of the deposits. Via the concession contracts, the concessioners are obliged to make payments to the state, which they may not afford to do if the losses are too significant. This paper presents a short review on the problem with the evaluation of the losses in the carbonate deposits. An evaluation approach is described, which is based on structural geological mapping of the karst-controlling fractures and faults. An example is shown of computer modeling of the karst in a real deposit.

Keywords*:* economic geology, limestone, karst, solution cavity, structure, reserves

СТРУКТУРНОГЕОЛОЖКИЯТ ПОДХОД ПРИ ОЦЕНКАТА НА ГЕОЛОЖКИТЕ ЗАГУБИ В НАХОДИЩАТА НА КАРБОНАТНИ СКАЛИ – ВАРОВИЦИ, ДОЛОМИТИ И МРАМОРИ

Иван Димитров[1], Димитър Съчков[1]

[1]Минно-геоложки университет „Св. Иван Рилски", София 1700, e-mail: idim68@abv.bg

РЕЗЮМЕ. Загубите представят тази част от геоложките запаси, която не може да бъде иззета или поради една или друга причина, не може да бъде икономически реализирана. Загубите във всички находища се различават количествено, поради различията в геоложките особености и технологичната схема на извличане и преработване. Погрешното оценяване на загубите може да съкрати значително живота на находищата. Чрез концесионния договор концесионерът се задължава да направи плащания на държавата, които могат да се окажат непосилни, ако загубите са твърде големи. В тази работа е направено кратко ревю на проблема с оценката на геоложките загуби в находищата на карбонатни скали. Описан е подходът за оценяване на загубите чрез структурногеоложко картиране на контролиращите карста пукнатини и разломи. Показан е пример на компютърна моделиране на карста в реално находище.

Ключови думи: икономическа геология, варовици, карст, структури, запаси

Introduction

The reserves of pure carbonate rocks in Bulgaria are fast declining, because of the increased demand caused by the desulfurization installations in the coal TPP. In spite of the demand, there is a tendency for the investors to face financial losses, because of poor evaluation of the projected losses of the geological reserves. In case of underestimated losses of the geological reserves, via the concession contract the investor is obliged to pay royalty fees, which he may not afford to pay simply because he is not making enough profit. The geological losses of the reserves are usually caused by the tectonics and karstification. In this paper, the current state of affairs in Bulgaria is exposed and an approach is presented for tackling the problem with the proper evaluation of these losses based on structural geological mapping and modeling of volumetric bodies of karst domains using modern software.

Short economic and geological evaluation of the carbonate deposits

The limestones and marbles comprise of the mineral calcite ($CaCO_3$) and less commonly the minerals dolomite ($CaMg(CO_3)_2$), magnesium calcite and aragonite. The limestones are biogenic sedimentary rocks, which are formed in various environments that is why they contain undesired components. The chemically pure limestone contains more than 98% $CaCO_3$ and almost always was deposited in reefs (Walker and James, 1992). The reefal bodies are massive and without primary bedding or with slightly detectable bedding. The pollutants in otherwise chemically pure carbonate deposits are found in solution cavities or karst. The karst caverns are partially filled with the residual material from the karstification and represent a mixture of SiO_2, Al_2O_3, Fe_2O_3(SAF), as well as negligible amounts of CaO, MgO,TiO_2 and other oxides and hydroxides.

The residual products accumulate is the form of yellowish or reddish clays with varying consistency. Some clay is oily in palpation and water saturated. It can be easily detached from the cavern walls. Other has a bauxite like appearance and is firmly attached to the cavern walls. During blasting the latter tends to stick to the rock fragments and pollutes the product with clay, sometimes making it completely unusable.

The solutional cavities form in stages depending on the level of the nearby rivers' erosional bases. Following the geological epochs of warming and cooling the karst cavern climb up section or down section in relation with the change in the sea level, which changes the river bases and the ground water level. Stage formation may occur also because of tectonic reasons. In the geological evolution of the rock massif, karst caverns of different age are superimposed one upon another. This results in redeposition of the residual material that fills them.

Apart from the stage formation the karst caverns do not follow some pronounced spatial regularity in its distribution and for this reason are difficult to be prospected. In spite of this, some slight regularity still exists, which is expressed in the fact that the movement of ground waters is facilitated by weak zones in the rock massif, predestinated by fractures, joints and faults (Fig.1). The joints and faults of course have systematic and more or less predictable position.

Fig. 1. Tectonized limestone from the Slivnitsa formation in West Bulgaria. Angular rock fragments are visible on the photograph, included in grinded mass with predominantly clay composition. In the absence of industrial washing installation this rock represent 100% loss from the reserves for production of products of higher technological grade.

During the exploitation, the preferred distribution of caverns along fractures is evidenced by the fact, that the karstificaton visible in a blasting front, which is developed perpendicular to the fractures looks very different than the karstification visible is a front developed parallel to the predominant joints and faults.

In the deposits of marbles the problem of karstification is usually more aggravated than in the limestone deposits, because the marbles are usually older and reflect longer periods of karst superposition. The marble deposits have been elevated to surface level and depressed under sediments more times and longer in the geological history, so the residual material in the caves is more mature, denser and firmer. In the marbles even the slightest traces of primary bedding have been obliterated by the foliation formation so the observed fabric of the rock is not related to the primary sedimentary fabric and with the spatial distribution of the carbonate body.

Another problem related to the assessment of marble and limestone deposits is the significant difference in the physical properties, structure and texture of the rocks from different deposits. Some finer grained (micritic) limestones have uniaxial compression strength in the range of 1200 kg/sm^2, while other barely reaches 400 kg/sm^2. In relation to this, gas permeability during roasting and chemical reactivity with sulfuric gasses substantially vary not only between deposits but between the various parts of one deposit. These variations of course can also result in geological losses.

As a whole, the following specifics are valid for the Bulgarian deposits:

The Paleogenic (litotamnium algal type) deposits are very cavernous and porous. They have low density but very high specific reactivity with acids even in rocks with relatively low content of $CaCO_3$. Unfortunately the pollutants are evenly distributed in the entire rock volume on meso and microstructural level, so selective extraction is difficult and the total mined mass rarely exceeds 98% of $CaCO_3$. It is beneficial for this rock to be stored in open piles for longer periods, so the rains partially wash them and allow usage in drier periods of the year. The Paleogenic limestone is frequently intercalated with marl layers and volcanic tuffs, which may not be described in the primary prospecting reports and may result is serious economic losses.

Cretaceous limestone the type of Mezdra formation. This limestone has good chemical composition and mechanical properties but it is located far from the large industrial consumers and this hinders its usage.

Jurassic micritic limestone the type of Slivnitsa formation. It is pure, very strong mechanically and moderately cavernous limestone, however it is located in west Bulgaria and so far it is inaccessible in southeast Bulgaria where the large TPP are located. Its reserves are still substantial but declining because of exclusion of some deposits for environmental and other social reasons.

The Triassic limestones are nearly universally dolomitized, which results in decline of the quality for chemical application. In East Bulgaria these limestones were also metamorphosed and turned into various types of marbles or slightly marbalized limestones, which affect negatively their chemical reactivity although it improves their usage as a construction stone.

Precambrian limestone of the Dobrostan formation was deposited in two sedimentary facies – reefal facies and lagoonal facies (Dimitrov, 2009). In the lagoonal facies dolomitic zones and intercalations are common, which leads to decline of the chemical reactivity and other industrial qualities.

Problems of the geological prospecting of the Bulgarian deposits of carbonate rocks

Most of the significant carbonate deposits in Bulgaria were prospected prior to the 10th of November 1989 (the official date of overthrow of the centralized communist system) by state owned specialized companies, such as Zavodproekt, as the geological reserves were accepted after examination in the state commission for the geological reserves (DKZ), which still exists in a modified form named SEC – Specialized Expert's Commission. During the privatization concession contracts were made with new private owners. These concession contracts were based on rather superficial evaluation of the residual reserves. During the prospecting of these deposits frequently but not always *the coefficient of cavernosity* was found. This coefficient represents the ratio between the intersected lengths of the caverns and the total drilled length of the drill hole multiplied by 100 to achieve percentage. Obviously, if the number of the drills is small or insufficient, the evaluation is far from realistic. This coefficient can give reliable evaluation of the caverns only in perfect drilling with 100% of retrieved core. However, nearly universally the drilling was made by a single tube technology, using the simplest and cheapest materials so the percentage of the retrieved core varied significantly. It is then, highly doubtful that 3% or 5% of caverns, as stated in the reports, are a proper estimate. In addition, the fault zones in the limestone are heavily brecciated and saturated with clay, so practically limestone core cannot be extracted from the fault zones (Fig. 2).

The new prospecting after "10th of November" is rarely reliable. The protracted bureaucratic procedure, overburdened with environmental assessment and social compliance assessment activities lead to nearly unavoidable financial losses and the investors become impatient in the process. The environmental assessment and social compliance procedures offset the emphasis of the prospecting away from the assessment of the reserves. In general they cost more than the actual geological prospecting. At the end, the investor acquires legally a deposit, which only in his mind is ready for development.

Although, to some degree the examination of the geological reports by the specialized state commission SEC improves the quality of the prospecting it cannot protect the investor from false or poor geological evaluation of the deposit.

Fig. 2. Core of tectonically reworked limestone nearly completely converted to a clay.

As a result of the abovementioned practices in Bulgaria concession contracts were made, and are presently made, based on prospecting, which does not offer enough information about the quantity of the losses from the geological reserves in the deposits. The author of the paper has observations that for some of the largest deposits in these contracts at average 5% losses were envisaged, while in reality they appear to be 3 to 4 times larger.

Comment on the meaning of the terms reserve, loss, dilution

Reserves

In the text below, a brief review is made on the meaning of the conceptual terms of the economic geology, following Petrinsky (1960).The source dates back to the centralized economy as these concepts were integral part of the practical deposit evaluation at that time. They are still used in defining the terms of the concession contracts in Bulgaria in the absence of better substitutes. Although there is well-specified international terminology in this aspect, and in sense these terms correspond to this terminology, they are listed here as being relevant to the discussion on the losses in the carbonate deposits in the Bulgarian context.

Geological reserves. These are all reserves of valuable material at the stage of the geological report, which were found to exist in a given volume of geological space. The geological reserves are divided into *in balance* and *out of balance*.

The *in balance reserves* are these reserves, which correspond to the industry requirements and the demand of the market.

The out of balance reserves are these reserves, which cannot be mined at a profit given the present state of technology and market.

The in balance reserves are the industrial reserves minus the projected losses. These are the industrial reserves that are taken into account when the extraction process is planned. The industrial reserves are divided into: *Uncovered (exhumed) reserves* – the reserves, for which expenses for removing the barren cover were made and *Prepared reserves,* which represent this part of the uncovered reserves ready for immediate mining.

The temporary inactive or blocked reserves are the reserves, which for some reason cannot be mined immediately.

The extinguished reserves are all mined reserves in a given part of the deposit (block, horizon, etc.) after the exploitation stage have passed. These are the exploited and sold for a profit reserves as well as the part of the reserves that went for the losses.

Losses

To mine out completely all known reserves in a deposit is impossible and such a task is never undertaken. What is

generally desired is to mine the deposit with minimal losses of the geological reserves and with minimal total cost of the extraction. The losses at the end represent the difference between the extinguished and the properly utilized reserves.

Fig. 3. Dilution. Mixing of pure limestone blocks with lamps of clay after the blasting so the clay cannot be separated from the limestone.

Three types of losses are recognized. These are *the project losses*, *the planned losses* and *the factual losses*.

The project losses are these parts of the reserves, which are envisaged in the overall long term mine project to be left in the earth with regard to mine safety and minimization of the cost of extraction.

The planned losses are envisaged in the annual mining plan and they depend on the accepted mine exploitation system and various technical decisions taken daily after the acceptance of the overall mine project.

The factual losses are the summed amounts of valuable resource left in the earth notwithstanding the reasons. The factual losses never coincide with the project losses and the planned losses. There are several categories of factual losses. Losses because of the geological and hydrogeological reasons; losses in protecting benches and rock blocks left to support the underground integrity; losses depending on the exploitation system; losses resulting in erroneous management of the mine works etch.

The error in the evaluation of the losses can result in the depletion of a mine in 10 or 15 years instead of the originally projected 20 years, which will distribute unevenly or even prevent the repaying of the main investment or lead to total bankruptcy.

In the case of quarries for limestone, marble and dolomite two main types of losses are common: *geological losses from karstification,* and *technological losses during the blasting and crushing,* usually because of the overgrinding of the rocks.

The losses caused by the karstification are formed in various in size caverns and brecciated zones filled entirely or partially with clay and other karst filler.

All carbonate deposits in the world have such losses, which may comprise between 20 and 30% of the total rock volume. In principle, the losses depend on the technology of processing and on the application of the material. For example, if the limestone is not suitable for production of quicklime it may still be usable for construction stone or cheap filler, of course at lower market price, so this limestone will be considered as a loss for the quicklime production but as an asset for the cheaper construction applications.

Dilution

The dilution is a process of mixing of a valuable material with waste or poor quality material, which is below the application standards. Because of the mixing, the overall quality of the mined mass declines. In the environment of the limestone deposits, the dilution results from mixing of high-grade limestone with clay from the solution cavities (Fig. 3).

In the fault zones, because of the tectonic grinding, the limestone is brecciated and clay was introduced between the fragments by the ground waters. The tectonically reworked rocks are naturally impoverished in valuable components and are usually not suitable for better priced applications, unless the blasted rock is washed or otherwise purified.

Methodology for assessment of the geological losses

There is no universal, widely accepted approach for evaluation of the losses in the carbonate deposits and in fact in any deposit. The article proposes an approach, which is based on geological mapping and structural geological investigation of the fault zones and joint sets; drilling and evaluation of the core; visual expert evaluation of the degree of overall tectonic fragmentation and the amount of residual clay with the aid of CAD and GIS software such as Autodesk Civil 3D, ArcGIS or other, which allows modeling of volumetric rock bodies.

As already mentioned above, the karst caverns do not follow some geometric laws in their development other than the predefined orientation of the fractures and to some extent the path of more soluble rocks as the latter may not be valid in lithological homogeneous massif. Here is the opportunity to geometrically characterize the karst network. For the purpose astructural geological mapping of the deposit is needed for gathering of detailed information for the statistical distribution of the fractures and faults. It is of particular importance to determine the number of the joint sets, the density of the joints in each set and the relative age of the joint sets with relation to the age of the solution cavities. During the mapping it will become evident that some joint sets are particularly prone to facilitate karst formation. While other joint sets are less likely to be affected by solution and deposition of karst products.

The mapping of the faults has the same purpose that is to find which individual faults and fault sets contain karst and to what degree they are affected by it. The orientation of the large faults with relation to bedding, the width of the deformation zones and the intensity of brecciation have to be classified. There is a general rule that faults intersecting the bedding at higher angles have wider deformation zones with abundant brecciation and clay deposition, while faults that are nearly parallel to bedding accommodate shear without much deformation and may not contain substantial amount of clay. Because both joints and faults are predetermined by the tectonic stress directions in the massif their formation is characterized by symmetry and regularity.

The quality of the structural geological mapping must satisfy the following requirements: The deposit should be subdivided into large enough domains that allow sufficient number of structural geological measurements. The structural data should be processed with stereographic software using all geometric techniques that the stereographic method allows, including kinematic analysis. The measurements have to be positioned on the field with GPS receiver or geodetic stations and the data have to be transferred on up to date surveying plan of the mine. The mapping has to be extensive in time, in order to follow the uncovering of various faults and karst zones in a series of several consecutive blasting activities. Data for the chemical composition of the products of the karst caverns have to be integrated with the lithological and structural data to form spatial database of the deposit. Some fault zones have to be drilled in order to finds the percentage of clay in them. The purpose of the drilling is not to delineate the tectonic or karst zones, because the delineation is better done by mapping. Its purpose is to clarify the content of the clay in the tectonic zones and karst cavities, so they can be classified according to their degree of pollution. The intersections between the fault zones have to be geometrically delineated, because they are a preferred location of karstification. An overall classification scheme has to be built for the deposit, in which the domains have to be classified according to their degree of pollution with SAF. Because the process of pollutant's assessment includes combination of precise methods and subjective judgments it cannot be considered accurate. It is desirable that the final results of the calculations are checked with the data for the amount of waste deposited on the depots or sold.

The calculation stage of the assessment includes the following activities: delineation of zones of brecciating, fracturing and pollution using digital surfaces, which confine the volumes of these zones (Sachkov and Dimitrov, 2012; Sachkov, 2015). Examples of such digital surfaces are as follows: the terrain of the quarry (benches) at present, the surface separating the cover rocks from the resource at present, the lower confining surface of the resource at present, the surface of the projected situation of cover rocks and resources in the quarry at a given date in future according to the overall mine project, confining surfaces of the mapped fault zones and karst domains. The delineated larger domains are subdivided into smaller domains, which are also delineated as zones of certain category of resource, according to the degree of pollution and expected application. These may be individual fault zones, intersections of fault zones, fracture zones with moderate, less moderate or intense karstification, etc. The goal is a volumetric model of the deposit, using structural data and data from the sampling coeval with the exploitation, which subdivided the deposit into volumes of rocks with different industrial application. A question may be asked why this was not done at the stage of the original prospecting. And the answer is, because it cannot be done at that stage for many reasons. Visualization of such model for a limestone deposit polluted along fault zones is shown on Figures 4 and 5.

Conclusion

It is obvious that in deposits, which have not been developed yet, the mapping of the structure in such a detail that allows delineation of the karst caverns is not possible, because the exposed surfaces of the benches are missing and the overall accumulation of data is still low. It implies that the evaluation of the losses must be done continuously after the concession contract is made. If this is to have sense, it has to be envisaged in the concession contract so that further evaluations of the losses are easily effected in the contract. At present this is not the case in Bulgaria. After the contract is made, the state will demand payment of royalties based on the amount of losses written in the original contract. Changes of

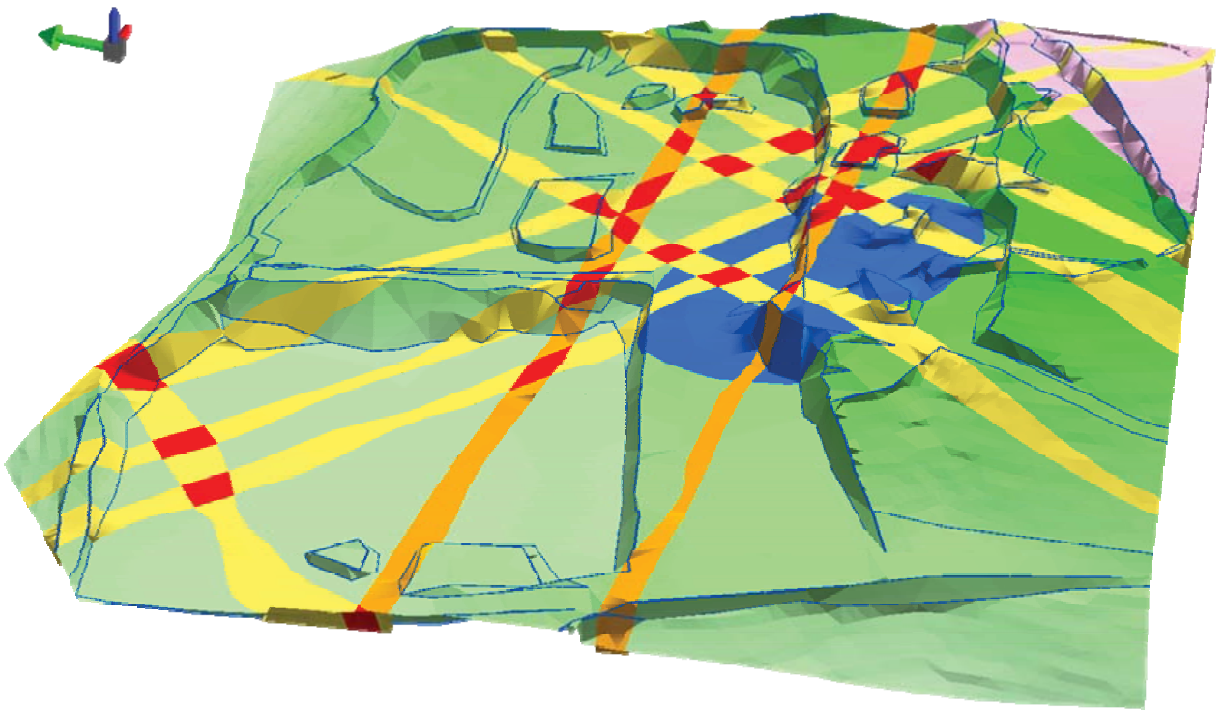

Fig. 4. Geological model of a deposit – map of the karst polluted zones. The traces of the fault zones are shown on the digital modelof the deposit's surface.

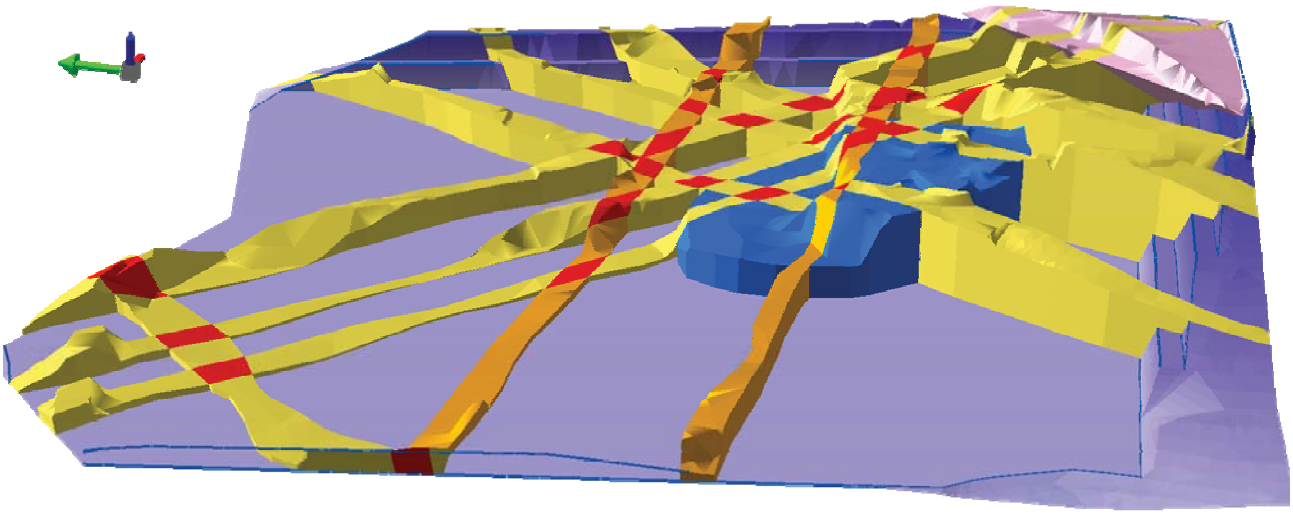

Fig 5. Geological model of a limestone deposit, which is lithologically homogeneous but transected by faults. View from west.

this are possible only after prolonged, expensive and tedious administrative procedure that involves signing of a new contract with all related to it legal requirements. No procedure for adjustment of the amounts of the losses based on data from the exploitation prospecting is envisaged in the regulatory framework or at least not clearly envisaged. The investors are discouraged to file complaints and to attempt readjustment of the contracts based on the flow of data that arrived after the deposit was developed. However, the problem with the losses is serous and if a flexible procedure to address this issue is not designed, the investors will rather abandon mining in some quarries, as it actually happens, instead of continuously investing in geology and production. It is also clear that the re-evaluation of the losses invokes nearly complete recalculation of the amount of the reserves.

References

Димитров, Ив. Съображение за позицията на мраморите в Огняновското стъпало, Пазарджишко. – Год. МГУ „Св. Ив. Рилски, 52, 1, 2009. - 49-54. (Dimitrov, I. Saobrazhenia za pozitsiyata na mramorite v Ognyanovskoto stapalo, Pazardzhishko. – Ann. UMG, “St. Iv. Rilski”, 52, 1, 2009. - 49-54.)

Петрински, С. Загуби и обедняване в рудодобивната промишленост и борбата за намаляването им. – Профиздат – София, 1960. - 1-55. (Petrinski, S. Zagubi i obednyavane v rudodobivnata promishlenost i borbata za namalyavaneto im. – Profizdat – Sofia, 1960, 1-50.)

Съчков, Д., И. Димитров. „Метод на ограничителните повърхнини“– възможности за компютърно моделиране при изчисляването на запаси от индустриални минерали и скали. - Годишник на МГУ, Том 55, Св. I, 2012. - 69-74. (Sachkov, D., I. Dimitrov. “Metod na ogranichitelnite povarhnini” – vazmodzhnosti za kompyutarno modelirane pri izchislyavaneto na zapasi ot industrialni minerali i skali. – Godishnik na MGU, 55, 1, 2012. - 69-74.)

Съчков, Д. Геометрично моделиране на тектонски нарушения в ГИС среда по данни от теренни геоложки изследвания, като възможност за оптимизация на проучването. – Сп. Бълг. геол. д-во, 76, 2015, с. 65-77. (Sachkov D. Geometrichno modelirane na tektonski narushenia v GIS sreda po danni ot terenni geolozhki izsledvaniya, kato vazmodzhnost za optimizirane na prouchvaneto. – Spisanie na Balgarskoto geologichesko drudzhestvo, 2015. - 65-77.)

Walker, R.G. James, N.P. (editors) 1992. Facies models. Response to sea level change, part III. Carbonate and evaporate facies models. GEOtext1, Geological association of Canada, pp. 265-375.

The article is reviewed by Assoc. Prof. Dr. Boris Valchev and Assoc. Prof Dr. Valeri Sachanski.

GEOCONSERVATION VALUE OF THE PERIGLACIAL LANDFORMS IN RILA

Dimitar Sinnyovsky[1], Natalia Kalutskova[2], Nikolai Dronin[2], Valentina Nikolova[1], Nadezhda Atanasova[1], Iliyana Tsvetkova[1]

[1] University of Mining and Geology "St. Ivan Rilski", 1700 Sofia, sinsky@mgu.bg
[2] Moscow State University "M. V. Lomonosov", Moscow, nat_nnk@mail.ru

ABSTRACT. The effects of freezing and thawing drastically modify the ground surface in a periglacial environment. The types of modification include the displacement of huge amounts of soil materials, rock boulders, and the formation of unique landforms. Along with the typical glacial formations like cirques, glacier valleys and carlings, periglacial landforms also have their place in the concept for development of Geopark Rila. Despite the low geodiversity of the mountain, the glacial forms give an alpine appearance to its relief and a high aesthetic value of the high mountain landscapes. The main challenge in presenting geological information to the general public is the interpretation of glacial and periglacial processes. The choice of representative geosites implies a balance between their scientific rationale and the opportunity to be presented in an interesting and attractive way to the visitors to the geopark. That is why the aesthetic, ecological and historical aspects of the geosites are added to the high scientific value. The highly expressed fossil glacial relief of Rila, inherited from the last Würm ice age, continues to be the subject of modern geocryogenic processes and undergoes an active periglacial processing, which can be demonstrated in the most visited high parts of the mountain. Along with the well-known horns, cirques and glacier valleys, which are typical glacial landforms, many geocryogenic formations due to desquamation and solifluction processes, are encountered: periglacial moraines (scree slopes), cryonival cirques, avalanche channels with erosional scree cones, as well as the rounded regolith covered peaks, which have their own specific name in Rila – chals. The periglacial landforms and the fossil glacial relief are an integral part of the modern high mountain landscape of Rila, which attracts thousands of admirers of the alpine nature. The implementation of a holistic concept of conservation, education and sustainable development of Geopark Rila in combination with all other aspects of the natural and cultural heritage can bring the desired economic benefits and prosperity to the whole region.

Keywords: Geopark Rila, periglacial landforms

ГЕОКОНСЕРВАЦИОННА СТОЙНОСТ НА ПЕРИГЛАЦИАЛНИТЕ РЕЛЕФНИ ФОРМИ В РИЛА

Димитър Синьовски[1], Наталия Калуцкова[2], Николай Дронин[2], Валентина Николова[1], Надежда Атанасова[1], Илияна Цветкова[1]

[1] Минно-геоложки университет "Св. Иван Рилски", 1700 София, sinsky@mgu.bg
[2] Московски държавен университет „М. В. Ломоносов", Москва, nat_nnk@mail.ru

РЕЗЮМЕ. Въздействието на замръзването и размръзването променя драстично земната повърхност в условията на периглациална среда. Промените включват преместване на големи количества почвен материал, скални късове и оформяне на уникални релефни форми. Заедно с типичните глациални форми като циркуси, ледникови долини и карлинги, периглациалните релефни форми също имат своето място в концепцията за разработването на Геопарк Рила. Независимо от ниското георазнообразие на планината, ледниковите форми придават алпийски облик на нейния релеф и висока естетическа стойност на високопланинските ландшафти. Основното предизвикателство при поднасянето на геоложката информация на широката публика е интерпретацията на ледниковите процеси. Изборът на представителни геотопи предполага баланс между тяхната научна обосновка и възможността да бъдат поднесени по интересен и атрактивен начин за посетителите на геопарка. Затова към високата научна стойност се добавят естетическите, екологичните и историческите аспекти на геотопите. Силно изразеният фосилен глациален релеф на Рила, наследен от последния Вюрмски ледников период, продължава да е обект на съвременните геокриогенни процеси и е подложен на активна периглациална преработка, която може да бъде демонстрирана в най-посещаваните високи части на планината. Наред с добре изразените хорни, циркуси и ледникови долини, които са типични ледникови форми, тук се срещат и много геокриогенни форми, образувани вследствие на процесите на десквамация и солифлюкция: периглациални морени (сипейни венци), крионивални циркуси, лавинни улеи със сипейни ерозионни конуси, както и заобленитe покрити с реголит върхове, които в Рила имат специфично наименование - чалове. Периглациалните форми и фосилният ледников релеф са неразделна част от съвременния високопланински ландшафт на Рила, който привлича хиляди почитатели на алпийската природа. Осъществяването на една цялостна концепция за опазване, образование и устойчиво развитие на Геопарк Рила, в комбинация с всички други аспекти на природното и културно наследство, може да донесе желаните икономически ползи и просперитет на целия регион.

Ключови думи: Геопарк Рила, перигрaциален релеф

Introduction

The glacier formations are at the base of the concept for the development of Geopark Rila. Despite the low geodiversity of the mountain, the glacial landforms give an alpine shape to its relief and high aesthetic value to the high mountain landscapes. The well expressed fossil glacial relief of Rila (Glovnya, 1969), inherited from the Würm Ice Age, provides unlimited possibilities for interpretation of the varied glacial processes for the general public. The development of promotional materials and their presentation in an attractive and accessible way for the tourists will increase the public awareness of Rila's geological history and the opportunitiy to develop sustainable all-season tourism. Simultaneously with the remarkable glacial landforms - horns (carlings), cirques and glacier valleys, the higher parts of the mountain are affected by

the modern geocryogenic processes, which further shape the fossil glacial landforms. Viewing the most characteristic supraglacial forms - the cryogenic cirques and supraglacial moraines, it is difficult to set the boundary between glacial and post-glacial activity. For this reason, the periglacial landscapes are a wide field for demonstrating the results of the typical glacial activity during the Würm Ice Age and recent frost weathering modifying the high mountain relief. In this article, a retrospection of the most frequent landforms of frost weathering is made, with an emphasis on accessible and demonstrable sites with well-developed periglacial processes and phenomena in the most visited higher parts of Rila Mountain.

Geodiversity

Rila Mountain is built mainly of granitoids and partially by Neoproterozoic metamorphic rocks cropping out in its northern, western and southern parts. For this reason, the fossil glacial landscape, formed during the Würm Ice Age, was mainly developed in granitoid rocks belonging to the Rila-West Rhodopean Batholith characterized by Valkov et al., (1989) as a complicated igneous massive, with four phases of magmatic activity. The first phase includes rocks of granodiorite to quartz-diorite composition, forming several separate bodies: Belmeken, Kapatnitsa and Grancharitsa. During the second phase, medium and coarse-grained biotite granites are introduced, which are most widely represented within the batholith forming four bodies: West Rhodopes, Musala, Mechivrah and Shpanyovitsa, situated around the bodies of the first phase. Three bodies are outside of the batolith: Kalin pluton, Badin and Banya bodies. The third phase includes fine-grained granites to plagiogranites, forming several small bodies - Monastery, Semkovo, Gargalak and Chavcha. Their contacts with the host metamorphic rocks and granitoids of the earlier phases are intrusive. The fourth phase is represented by aplitoid and pegmatoid granites forming small stock-like bodies or veins.

Kamenov et al. (1997) and Peicheva et al. (1998) subdivided the granitoids into three petrographic types: I. Coarse-grained, and occasionally porphyric amphibole-biotite and biotite granodiorites; II. Equigranular, medium-grained biotite and rarely two-mica granites; III. Fine-grained, biotite-muscovite aplitoid granites occurring as lenses, veins and stocks. The boundaries of these types coincide generally with previously distinguished by дрValkov et al. (1989) phases as the third and fourth phases are united into a single petrographic type.

According to Kamenov et al. (1999) Rila-West Rhodopean Batholith consists of two differing in age and tectonic position plutons. Granodiorites of the first type are part of the older (~80 Ma) sinmetamorphic pluton with calcium-alkaline character and mantle magma with crust substance. Granites of the second and third type in age 35-40 Ma are genetically connected phases of postmetamorphic pluton with high potassium-calcium-alkaline character.

The metamorphic rocks in the northwest part of the mountain belong to the Rupchos Group (Kozhuharov, 1984) or Malyovitsa Lithotectonic Unit (Sarov et al., 2011a). Recently they are reviewed in the light of the approach for characterization of the metamorphic rocks developed for the purpose of Geological mapping of the Republic of Bulgaria at a scale 1:50 000 (Hrischev et al., 2005) – Chepelare motley metamorphites of the Rupchos metamorphic complex (Sinnyovsky, 2014, 2015; Sinnyovsky, 2014; Atanasova, Sinnyovsky, 2015; Tsvetkova, Sinnyovsky, 2015). They crop out between Sapareva Banya and Blagoevgradska Bistritsa River. In the southwest part of Rila metamorphic rocks are represented by the Maleshevtsi Group of Zagorchev (1984) (Ograzhden Lithotectonic Unit after Sarov et al., 2011b) and Troskovo Group of Zagorchev (1989), respectively Maleshevtsi and Troskovo metamorphic complexes after Milovanov et al. (2009). Here crop out also the motley metamorphites of the Predela metamorphic complex (Milovanov et al., 2009). Among the metamorphic complexes are located Urdina, Malyovitsa, Dzhendema, Monastery and Pearl Lakes, as well as part of the Seven Rila Lakes. The rest of the Rila's tarns are among the granitoides of the Rila-West Rhodopean Batholith.

Geocryogenic landforms

Geocryogenic (periglacial) processes and phenomena are a collective term to denote the various cryogenic processes occurring during the freezing and thawing of soils and rocks: frost weathering, cryoclasticism, geocryogenic denudation, gelifluction, cryosolifluction. Matthes (1900) introduced the term "nivation" to designate all aspects of frost weathering by the late-lying snow patches in summer. The geocryogenic landforms created as a result of these processes are the consequence of the periglacial weathering associated with the repeated daily and seasonal freezing/thawing in the high-altitude belt at 2200-2800 m above sea level. The most common geocryogenic landforms in Rila are the talus or scree slopes/fields and cryonival cirques formed mainly in the granitoids of the Rila-West Rhodopean Batholith.

The scree slopes or supraglacial moraines are formed as a consequence of the frost weathering which attacks the rock massive through the joints and leads to the separation of blocks. The process whereby glaciers excavate to best effect in hard rock is by „plucking", or „quarrying" entire blocks, called "joint blocks". The manner in which the glacial quarrying process operates is described by Matthes (1930) as follows: "Any joint block in the bed of a glacier, such as that marked A, which is for any reason unsupported or weakly supported on its downstream side, is particularly susceptible of being dislodged, for the force of the glacier is exerted upon it at a small angle forward from the vertical, as indicated by the arrows. The block A and its side companions having been removed, the block B and those flanking it will next be unsupported and ready for removal, and so the process will continue farther and farther up the valley" (Fig. 1).

This weathering model is observed on the slopes of almost all cirques and glacial valleys in Rila carved by the Würm glaciers in the granitoids of the Rila-West Rhodopean Batholith (Fig. 2). The main role for the loosening of the joint blocks plays the repetitive freezing/thawing of the water which fills and extends the joints. Due to the temperature changes the blocks are moving away from each other, separating from the rock massive and falling gravitationally on the slope.

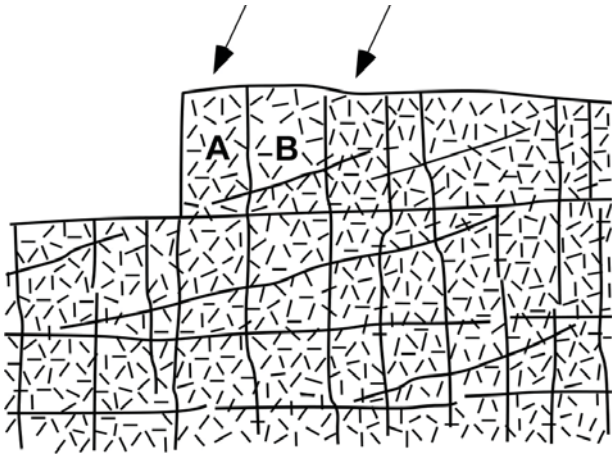

Fig. 1. Glacial excavation of hard rock by „plucking", or „quarrying" of joint blocks (after Matthes, 1930), responsible for the formation of the through valleys and lateral periglacial moraines (scree slopes)

Fig. 2. Dislodging of joint blocks according to Matthes (1930) from the headwall of the Icy Lake cirque along the joints in the granite of the Musala Body of the Rila-West Rhodopean Batholith

Fig. 3. "The Saws" between Musala and Malka Musala Peaks is an arête formed by the Icy Lake cirque and unnamed cirque in Maritsa River valley cropping out and sharpening by the modern desqumation process

The highest part of the wall from which the blocks are detached is formed by the power of the glacier and the structure of the bedrock. For cirquses this is the headwall, which is extremely steep. Desquamation of the bedrock between neighboring cirques results in sharp mountain ridges - arêtes. A typical example in Rila Mountain are "The Saws", formed in the granite of the Musala Body of the second phase of the Rila-West Rhodopean Battolith between Musala and Malka Musala Peaks (Fig. 3). It was formed during the Würm glaciation by the Ice Lake cirque and the opposite unnamed cirque in the Maritsa River valley. Here the bedrock continues to be exposed and sharpened by the modern desquamation process.

Fig. 4. Scree slope on the southern wall of the Grunchar cirque with well expressed sorting of angular phaneritic granodiorite boulders of the Belmeken Body of the first phase of the Rila-West Rhodopean Batholith

Fig. 5. Scree (talus) cones ("stone horseshoes") at the beginning of Malyovitsa Glacier Valley below the „Cocks" arête

The scree (talus) slopes in the cirque began to form during the glacial phase when the glacier filled the back of the cirque bowl with angular boulders, some of which were scraped off the rock when the cirque bowl was carved, and remained at the bottom. The other boulders were poured on the ice and after melting they fell on the other pieces at the base of the headwall. The contemporary cryogenic processes continue to shape the scree slopes, adding new angular boulders and fine material from the cirques walls. Due to their huge mass, the largest blocks reach farthest at the foot of the slope, while the smaller blocks are "captured" on the slope between the other scree boulders (Fig. 4). This predetermines the gravitational sorting of the particles in the scree slopes. Because of their poor transport, they are angular and often form scree cones called the "stone horseshoes" (Glovnya, 1969) at the base of the avalanche troughs (Fig. 5).

The lateral supraglacial moraines on the slopes of the glacier valleys are of the same genesis. Usually in the lower parts of the slope lateral glacier moraines with well-rounded boulders are situated. Above them supraglacial moraines composed of angular boulders are located. However, they are sometimes mixed with the bottom and the lateral moraines, so the angular boulders are usually scattered across the valley, as is the case with the Malyovitsa Glacier valley (Fig. 6).

Fig. 6. The bottom of the Malyovitsa Glacier is dotted with angular boulders of pegmatoid-aplitoid granite of the Monastery Body of the fourth phase of the Rila-West Rhodopean Batholith and amphibole-biotite gneises of the Chepelare metamorphites

Fig. 7. Among the bottom moraine deposits in Malyovitsa Glacier valley huge erratic boulders are encountered with dimensions more than 10 m

Here the typical U-shaped glacier valley is dotted with edged blocks of pegmatoid-aplitoid granites of the Monastery's Body of the fourth phase of the Rila-West Rhodopean Batholith and amphibol-biotype gneisses of the Chepelare metamorphic complexe of the Rupchos Metamorphic Complex (Malyovitsa lithotectonic unit). There are also huge erratics with dimensions up to 8-10 m (Fig. 7). Together with the large angular boulders, frost weathering delivers fine material that fills the interboulder spaces. As Kanev (1988) noted, "temperature weathering continues even before our eyes". Every year after the melting of the snow on the steep cirques walls fine weathered rock particles descend from the rocks and move downslope. They remain unnoticeable among the large boulders or at the bottom of the ice lakes, but can easily be seen on the white background of the snow patches (Fig. 8).

According to most authors, the formation of the supraglacial moraines began in the ice age and continued with geocryogenic denudation in the interglacial period. That is the case with the cryonival cirquses. They are also the product of frost weathering, but some of them arose in the ice age, especially those of southern exposure.

Fig. 8. The fine scree particles descending from the rock due to the frost weathering are clearly visible on the white background of the snow patches

The snow erosion is related to the processes of gelifluction, gelifraction, rock falls, frost landslides, eluvial weathering and rock abrasion known under the general term nivation. The erosion effect of this process results in the sloping of oblique planar negative nivation cavities by constant wetting of the rock pad around and under the melting seasonal snow patches, which facilitates the gelifraction of the bedrock. As a result of the ablation, the nivation hollows are gradually expanded and recessed into the slope as they gradually become circular in shape and turn into nivation (cryonival) cirques. Over time, the volume of the circular bowl is increasing and it begins to accumulate more and more snow, and the headwall becomes steeper and provides shade for a longer period of time, resulting in longer melting snow. According to Derbyshire et al. (1979), at a slanting slope, the material obtained from the gelifraction is deposited at the base of the snowbank and finally it is exported from the subnival gelifluction in front of the cirque by forming gelifluction terraces (Fig. 9), which can easily be confused with glacier moraines.

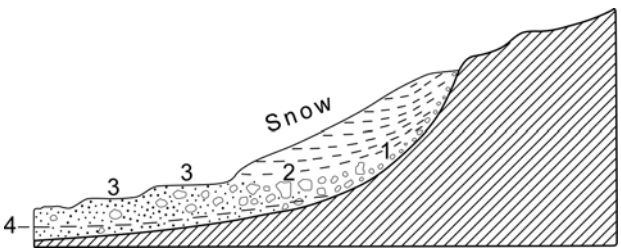

Fig. 9. Section across the snowbank deposits of a cryonival cirque (after Botch, 1946 in Derbyshire et al., 1979): 1 – destroyed particles by the frost weathering; 2 – stone pavement; 3 – solifluction terraces; 4 – upper boundary of the frozen soil

Cryonival cirques occur mainly on the southern slopes of the mountain. They have slanting slopes on which scree slopes are rarely encountered (Fig. 10). As a rule, there are no tarns

in these cirques. According to Glovnya (1969), the cryonival cirques are "a transitional form between the glacial and periglacial relief, both in age and in geomorphological features, but their geocryogenic origin always appears". This means that the strict boundary between the glacial and the supraglacial origin of the cirques can hardly be established. Following the logic of glacial cirque formation, the bottom of which is carved under the influence of the ice weight, it can be easily concluded that the main reason for the lack of tarns in the cryonival cirques is the low density and the small mass of snowbanks.

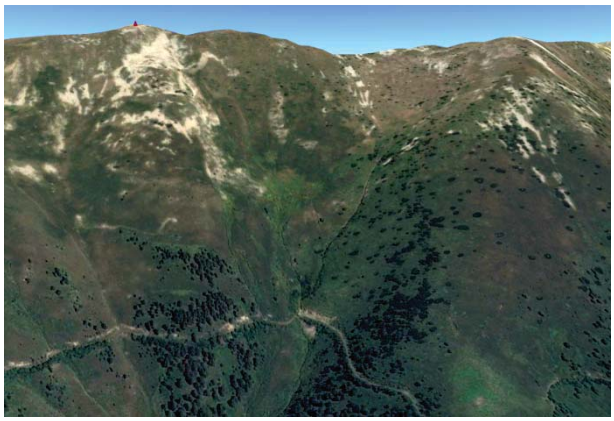

Fig. 10. Cryonival cirques on the northern slope of the glacier valley of Ilijna River in SW Rila, below the summit of Teodosiev Karaul (2666.7 m)

In fact, not all cirques with slanting slopes without tarns are of cryonival origin. Appropriate examples are the cirques in the feeding area of the Ropalitsa Glacier (Musala part of Rila). Regardless of its southeast exposure on the southern slope of Maritsa Chal (2765.2 m), the Ropalitsa cirque is definitely of glacial origin. The rest of the cirques east of Beli Iskar River valley - Grunchar cirque, Yakoruda Lakes cirques and Banenska Lakes cirques are of the same origin. These are the feeding zones of the short glacier valleys, where end moraines are found (Kuhlemann et al., 2013). In spite of its large area, the Ropalitsa cirque remains suspended from the small cirque south of elevation 2531.4 m, with a displacement of about 150 m, proved by the Ropalitsa waterfall (Fig. 11). Therefore, not Ropalitsa cirque but namely this cirque gives rise to over 400 m deep and 4 km long glacial valley of the Ropalitsa Glacier.

Fig. 11. Satellite image of the Ropalitsa glacier feeding zone including Ropalitsa cirque and two unnamed cirques south of elevation 2531.4 m and Yanchov Chal (2480.6 m)

The glacier valley was further fed by another small cirque, located SW from Yanchov Chal (2480.6 m). These cirques, considered by Glovnya (1969) to be cryonival, are smaller than the Ropalitsa cirque and do not differ from the other cryonival cirques on the southern slopes of Rila. However, the fact that they are deeper than the Ropalitsa cirque confirms their glacial origin. In order to incise deeper than the Ropalitsa cirque, they obviously contained larger ice volumes despite their southern exposure. This can be explained by the faster movement of the ice sheets due to the greater slope of their bottoms, which has delayed the “inflowing” of the ice sheet of the Ropalitsa cirque. It was only possible thanks to the intensive firn feeding.

Conclusions

The periglacial morphostructural landforms are an integral part of the modern high mountain landscape of Rila. They are gradually superimposed on the fossil glacial relief of the mountain modeling it by fragmentation of the bedrock and formation of cryonival cirques, scree slopes and cones. Each of the described forms can be presented to the visitors of Geopark Rila in an attractive way through information boards with schematic interpretations, graphics and photos in an accessible for the wide public language. An important stage in the interpretation of geocryogenic processes for the purpose of geotourism is their differentiation from the fossil glacial landforms and the demonstration of the results of their influence on the Wurm glacial relief. Places where modern geocryogenic processes now operate are at an altitude higher than 2000 m. For this purpose, representative outcrops should be selected, located in widely accessible and popular places. Such are the Nehtenitsa area with direct access to the Yakoruda Lakes, Mecha Polyana with access to Malyovitsa, Kirilova Polyana along the Monastery River with access to the Fish Lakes, the Seven Rila Lakes and the Musala Lakes, accessible by lift, Semkovo with access to the Redzhep and Vapski Lakes, the Macedonia hut with access to the Chernahtitsa Lakes, the Mermera and Rilets Peaks. Information boards and pointers for the high mountain glacial landscapes should be located at the starting points like Borovets, Beli Iskar, Mala Tsarkva, Govedartsi, Sapareva Banya, Dupnitsa, Blagoevgrad, Rila, Razlog, Belitsa, Yakoruda, Kostenets, Raduil.

References

Атанасова, Н., Д. Синьовски. Ледникови форми и отложения в района на Рибните езера в природен парк „Рилски манастир“. – Год. МГУ „Св. Иван Рилски”, 58, I-Геол. и геофиз., 2015. – 32-37. (Atanasova, N., D. Sinnyovsky. Lednikovi formi i otlozheniya v priroden park “Rilski Manastir”. – God. MGU “Sv. Ivan Rilski”, 58, I-Geol. i geofiz., 2015. – 32-37.)

Вылков, В., Н. Антова, К. Дончева. Гранитоиды Рило-Западно-Родопского батолита. – Geologica Balc., 19, 2, 1989. - 21-54. (Valkov, V., N. Antova, K. Doncheva. Granitoidi Rilo-Rodopskogo batolita. - Geologica Balc., 19, 2, 1989. - 21-54.)

Гловня, М. Сравнителни геоморфоложки проучвания на периглациалната морфоструктура на Южните Карпати и Рила планина. – Год. СУ „Св. Кл. Охридски",Геол.-геогр. фак., 64, 2-Геогр., 1969. – 27-46. (Glovnya, M. Sravnitelni geomorfolozhki prouchvaniya na periglacialnata morfostruktura na Yuzhnite Karpati i Rila planina. – God. SU "Sv. Kliment Ohridski", Geol.-geogr. fac., 64, 2-Geogr., 1969. – 27-46.)

Загорчев, И. Доалпийски строеж на Югозападна България. – В: Проблеми на геологията на Югозападна България. С. Техника, 1984. - 7-20. (Zagorchev, I. Doalpijski stroezh na Yugozapadna Bulgaria. – V: Problemi na geologiqta na Yugozapadna Bulgaria. S., Tehnika, 1984. – 7-20.)

Загорчев, И. Тросковская амфиболитовая группа (Огражденская надгрупа, докембрий) во Влахина планине, ЮЗ Болгария. – Докл. БАН 42, 11, 1989. - 67-70. (Zagorchev, I. Troskovskaya amfibolitovaya gruppa (Ograzhdenskaya nadgrupa, Dokembrij) vo Vlahina planine, YZ Bolgaria. – Dokl. BAN 42, 11, 1989. – 67-70.)

Каменов, Б., И Пейчева, Л. Клайн, Ю. Костицын, К. Арсова. Нови минералого-петрографски, изотопногеохимични и структурни данни за Западнородопския батолит. – В: Юбилеен сборник „50 год. специалност Геология". С., Унив. изд.; 1997. - 95-98. (Kamenov, B., I. Peycheva, L. Klajn, Y. Kosticin, K. Arsova. Novi mineralogo-petrografski, izotopnogeohimichni i strukturni danni za Zapadnorodopskiya batolit. – "50 god. Specialnost Geologia". S., Univ. izd.,1997. – 95-98.)

Кожухаров, Д. Литостратиграфия докембрийских метаморфических пород Родопской супергруппы в Центральных Родопах. – Geologica Balc., 14, 1. 1984. - 43-92. (Kozhuharov, D. Litostratigrafiya dokembrijskih porod Rodopskoj Supergruppi v Centralnih Rodopah. - Geologica Balc., 14, 1. 1984. - 43-92.

Милованов, П., И. Петров, В. Вълев, А. Маринова, И. Климов, Д. Синьовски, М. Ичев, С. Приставова, Е. Илиева, Б. Банушев. Геоложка карта и обяснителна записка към Геоложка карта на Република България в М 1:50 000. Картен лист К-34-82-Б (Делчево) и К-34-83-А (Симитли). С., МОСВ, Българска национална геоложка служба, 2009. - 108 с. (Milovanov, P., I. Petrov, V. Valev, A. Marinova, I. Klimov, D. Sinnyovsky, M. Ichev, S. Pristavova, E. Ilieva, B. Banushev. Geolozhka karta na Republika Bulgaria v M 1:50 000. Karten list К-34-82-Б (Delchevo) и К-34-83-А (Simitli). S., MOSV, Bulgarska nacionalna geolozhka sluzhba, 2009. – 108 s.)

Пейчева, И., Ю. Костицин, Е. Салникова, Б. Каменов, Л. Клайн. Rb-Sr и U-Pb изотопни данни за Рило-Родопския батолит. – Геохим., минерал., петрол., 35, 1998. - 93-105. (Peycheva, I., Y. Kosticin, E. Salnikova, L. Klajn. Rb-Sr i U-Pb izotopni danni za Rilo-Rodopskiq batolit. – Geohim., mineral., petrol., 35, 1988. – 93-105.)

Саров, С., С. Московски, Т. Железарски, Е. Войнова, Д. Николов, И. Георгиева, В. Вълев, Н. Марков. Обяснителна записка към Геоложката карта на Република България М 1:50 000. Картен лист К-34-71-Б (Сапарева Баня). С., МОСВ, Българска национална геоложка служба, 2011а. - 52 с. (Sarov, S., S. Moskovski, T. Zhelezarski, E. Vojnova, D. Nikolov, I. Georgieva, V. Valev, N. Markov. Obyasnitelna zapiska kam Geolozhkata karta na Republika Bulgaria v M 1:50 000. Karten list К-34-71-Б (Sapareva Banya). S., MOSV, Bulgarska nacionalna geolozhka sluzhba, 2011a. – 52 s.)

Саров, С., С. Московски, Т. Железарски, Е. Войнова, Д. Николов, И. Георгиева, В. Вълев, Н. Марков. Обяснителна записка към Геоложкта карта на Република България М 1:50 000. Картен лист К-34-71-В (Благоевград). С., МОСВ, Българска национална геоложка служба, 2011б. - 52 с. (Sarov, S., S. Moskovski, T. Zhelezarski, E. Vojnova, D. Nikolov, I. Georgieva, V. Valev, N. Markov. Obyasnitelna zapiska kam Geolozhkata karta na Republika Bulgaria v M 1:50 000. Karten list К-34-71-В (Blagoevgrad). S., MOSV, Bulgarska nacionalna geolozhka sluzhba, 2011b. – 52 s.)

Синьовски, Д., Потенциалът на Северна Рила като геопарк. – Год. МГУ „Св. Иван Рилски", 57, I – Геол. и геофиз., 2014. – 13-18. (Sinnyovsky, D., Potentsialat na Severna Rila kato geopark. – God. MGU "Sv. Ivan Rilski" 57, I – Geol. i geofiz., 2014. – 13-18.)

Хрисчев, Х., В. Ангелов, М. Антонов. Терминология и номенклатура на неслоестите литостратиграфски единици при геоложкото картиране в М 1:50 000 на Западния Предбалкан. – Сп. Бълг. геол. д-во, 66, 1-3, 2005. - 171-175. (Hrischev, H., V. Angelov, M. Antonov. Terminologiya i nomenklatura na nesloestite litostratigrafski edinici pri geolovkoto kartirane v M 1:50 000 na Zapadniya Predbalkan. – Sp. Bulg. geol. d-vo, 66, 1-3, 2005. – 171-175.)

Цветкова, И., Д. Синьовски. Скално разнообразие и ледникови форми в района на геотоп Седемте рилски езера. – Год. МГУ „Св. Иван Рилски", 58, I: Геол. и геофиз., 2015. - 26-31. (Tsvetkova, I., D. Sinnyovsky. Skalno raznoobrazie i lednikovi formi v rajona na geotop Sedemte Rilski ezera. - God. MGU "Sv. Ivan Rilski" 58, I – Geol. i geofiz., 2015. – 26-31.)

Derbyshire, E., K. J. Gregory, J. R. Hails. Geomorphological processes. Butterworths, 1979. - 311 pp.

Kuhlemann, J., E. Gachev, A. Gikov, S. Nedkov, I. Krumrei, P. Kubik. Glaciation in the Rila mountains (Bulgaria) during the Last Glacial Maximum. – Quaternary International, 293, 2013. – 51-62.

Kamenov, B., I. Peycheva, L Klain, K. Arsova, Y Kostitsin, E. Salnikova. Rila-West Rhodopes batholith: Petrological and geochemical constraints for its composite character. – Geochem., mineral., petrol., 36, 1999. - 3-27.

Matthes, F.E. Glacial sculpture of the Bighorn Mountains, Wyoming. – 21st Annual Report of the U. S. Geol. Survey 1899-1900 (Part II), 1900. -167-190.

Matthes, F.E. Geologic History of the Yosemite Valley. U. S. Dept. of the Interior Geol. Survey, Prof. Paper 160, 1930. – 130 pp.

Sinnyovsky, D. Geodiversity of Rila Mountain, Bulgaria. - XX Congress of the Carpathian Balkan Geological Association, Tirana, Albania, 24-26 September 2014, 2014. - p. 307.

Sinnyovsky, D. Wurm glacier formations and mountain landscapes in Rila Mountain, Bulgaria. 15th International Multidisciplinary Scientific Geoconference SGEM, Albena, Bulgaria, 18-24 June, 2015. - 529-536.

The article is reviewed by Prof. Dr. Venelin Jelev and Assoc. Prof Dr. Milorad Vatsev.

THE GEOPARK POTENTIAL OF THE BURGAS LAKES COMPLEX

Dimitar Sinnyovsky[1], Natalia Kalutskova[2], Nikolai Dronin[2], Dimka Sinnyovska[1]

[1] University of Mining and Geology "St. Ivan Rilski", 1700 Sofia, sinsky@mgu.bg
[2] Moscow State University "M. V. Lomonosov", Moscow, nat_nnk@mail.ru

ABSTRACT. Burgas Lake Complex comprising Bourgas, Atanasovsko, Mandra and Pomorie Lakes, is situated on the territory of Burgas and Pomorie municipalities. These ramsar sites are of international importance as habitats of water-living birds. Their interesting geological history, rich biodiversity and balneological importance make them reliable basis for development of a Geopark "Burgas Lakes". Important part of the region's geodiversity are also the old marine terraces outlining the ancient shores of the Black Sea basin: the Nymphean, the Neoeuxinian, the Karangatian, the Early Euxinian and the Chaudinian. They are represented by flattened surfaces or sediments dated on the basis of rich bivalvian fauna. Ramsar sites and dune habitats are subject of intensive research due to the rare and protected inhabiting species. These biotopes are the link between geodiversity and biodiversity within the lake complex and have a high potential for geomorphosites and geo-ecotrails to be developed for geotourism purposes. The area comprises several geosites included in the Register and Cadastre of the Bulgarian geological phenomena like the iridium layer at the Cretaceous-Tertiary boundary near Kozichino village, the pillow-lavas of Bulgarovo (bulgarites), dune sands Alepu, Gradina and Kavatsite as well as several geosites of erosional and abrasional origin like the Dobrovan mushrooms near Sini Rid village, Priest's rock near Fazanovo village, Kolokita Peninsula south of Sozopol, Agalina Cape, and others. An important part of the geological heritage of the area are the residual volcanic craters and calderas, remnants of the Upper Cretaceous volcanic structures and outcrops of Mesozoic and Paleozoic rocks in Strandzha Mountain on the territory of Sredets municipality. The remarkable geodiversity of the area is complemented by the ruins around the ancient towns Anhialo (Pomorie) and Apolonia (Sozopol) testifying to the long history of life on the Black Sea coast. The preview of the geological and cultural arguments for geopark establishment reveals that the Burgas region has a great potential for development of geosites of scientific, aesthetic, ecological and cultural value. The establishment of a Geopark on the Black Sea coast will add this unique sea to the European Geoparks Network's theme and will expand its geography to the lullaby of the ancient European civilization – Pontus Euxinus.

Keywords: Burgas Lakes Geopark, geological and non-geological arguments

ПОТЕНЦИАЛЪТ НА БУРГАСКИЯ ЕЗЕРЕН КОМПЛЕКС КАТО ГЕОПАРК

Димитър Синьовски[1], Наталия Калуцкова[2], Николай Дронин[2], Димка Синьовска[1]
[1] Минно-геоложки университет "Св. Иван Рилски", 1700 София, sinsky@mgu.bg
[2] Московски държавен университет „М. В. Ломоносов", Москва, nat_nnk@mail.ru

РЕЗЮМЕ. Бургаският езерен комплекс, включващ Бургаското, Атанасовското, Мандренското и Поморийското езеро, е разположен на територията на общините Бургас и Поморие. Тези рамсарски места са с международно значение като местообитания на водолюбиви птици. Тяхната интересна геоложка история, богато биоразнообразие и балнеоложко значение ги правят подходяща основа за разработване на геопарк „Бургаски езера". Важна част от георазнообразието в района са и старите морски тераси, очертаващи древните брегови линии на Черноморския басейн: нимфейската, новочерноморската, карангатската, староевксинската и чаудинската. Те са представени от заравнени повърхнини или отложения, датирани с богата бивалвийна фауна. Рамсарските места и дюнните местообитания са обект на интензивни изследвания заради редките и защитени видове, които ги населяват. Тези биотопи са свързващото звено между георазнообразието и биоразнообразието на територията на езерния комплекс и имат висок потенциал за разработване на геоморфосайтове и гео-екопътеки за целите на геотуризма. В площта попадат и някои геотопи, включени в Регистъра и кадастъра на геоложките феномени в България, като иридиевият слой на границата Креда-Терциер при с. Козичино, пилоу лавите при с. Българово (българитите), дюнните пясъци Алепу, Градина и Каваците, както и няколко геотопа с ерозионен и абразионен произход като Доброванските гъби при с. Сини рид, Поповата скала при с. Фазаново, п-в Колокита южно от Созопол, нос Агалина и др. Важна част от георазнообразието на площта са остатъчните кратери и калдери от горнокредните вулкански структури и разкритията на мезозойски и палеозойски скали в Странджа планина на територията на община Средец. Забележителното георазнообразие на територията се допълва от останките на античните градове Анхиало (Поморие) и Аполония (Созопол), свидетелстващи за дългата история на живота по Черноморското крайбрежие. Предварителният преглед на геоложките и културни аргументи за установяване на геопарк показва, че Бургаският регион има голям потенциал за разработване на геотопи с научна, естетическа, екологична и културна стойност. Установяването на геопарк на брега на Черно море ще добави този уникален с геоложката си история морски басейн към тематиката на Европейската мрежа от геопаркове и ще разшири нейната география към люлката на древната европейска цивилизация – Евксински Понт.

Ключови думи: Геопарк „Бургаски езера", геоложки и негеоложки аргументи

Introduction

The Burgas Lakes Complex located in the coastline of the Burgas valley, is a natural extension of the Burgas Bay on land (Fig. 1). It includes the largest Bulgarian lagoon called Pomorie Lake and s.str. Burgas Lakes – Burgas, Atanasovsko and Mandra limans, formed as drowned river valleys in historical time as a result of the subsidence of the Black Sea coast.

The Burgas Lakes Complex is the largest complex of near shore lakes in Bulgaria with an exceptionally rich biodiversity. It is disposed on an area of 95 km^2, 33,3 km^2 of which is declared or proposed for protected territory. Atanasovsko, Pomorie and Burgas Lakes are Ramsar places according to the Ramsar Convention and have an international importance as waterfowl habitats. They are formed after the Würm Ice Age due to the glacier thawing and the sea level rise.

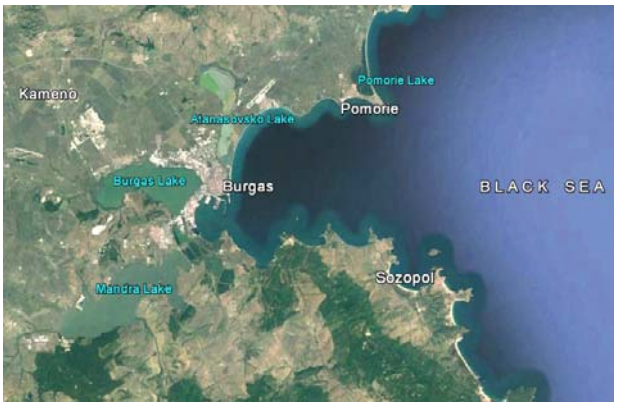

Fig. 1. Satellite image of the Burgas Lakes Complex

Pomorie and Atanasovsko Lakes are unique in the Balkans with the balneo-healing properties of their salty water and anaerobic mud deposits as well as with their endemic plants and animals. On the other side, the various geological structure, remarkable landscapes, rich cultural and historical heritage and well developed coastal tourism are good prerequisites for development of geotourism and other sustainable forms of tourism – ecotourism, rural tourism and mountain tourism that will be a successful complementation to the traditional coastal, spa and balneo-tourism and will provide conditions for all-season engagement of the hotels. Simultaneously geosites and geotrails development inland from the coast will provide a good possibility for the promoting of the geological and cultural-historical heritage of the area through new tourist packets.

Possibility for geopark development

Tourism is a major pillar in the economies of the countries of the Danube Region, part of which is our country. According to the UNESCO Global Geoparks initiative landscapes and geological formations are key witnesses to the evolution of our planet and determinants for our future sustainable development. In the light of the global strategy for better awareness for the Earth's history UNESCO Geoscience and Geoparks Programme encourages the member countries to conserve and enhance the value of areas of geological significance in Earth history and to promote their geological heritage on a global scale. In this aspect development of geosites and their inclusion in the Register and cadastre of the Bulgarian geological phenomena looks ineffective if they are not managed under a holistic concept for protection, education and sustainable development within a modern functioning geopark with the active involvement of the local communities and indigenous people. Burgas region is geologically rather diverse and can provide to the visitors unique geological and geomorphological interpretations. Due to their international prominence and interesting geological history the Burgas Lakes should be in the focus of the future geopark concept. This idea should be discussed in advance with responsible representatives of the local community and disseminated among the local people who can accept or reject it. The preliminary conversations with the mayors of Bourgas and Pomorie municipalities led to a general agreement for geopark development and thematic participation of the two municipalities in the European programmes for funding.

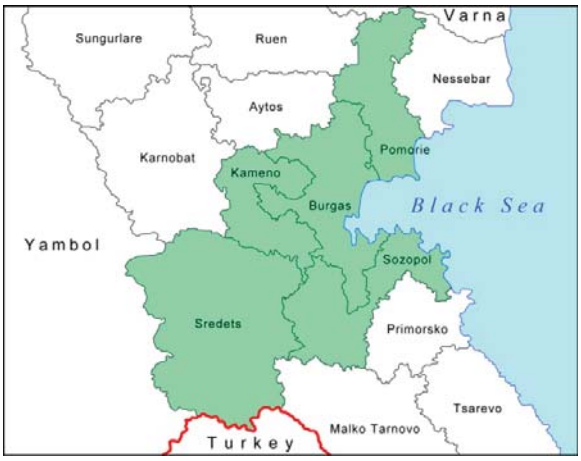

Fig. 2. Burgas District with the composite municipalities of the Burgas Lakes Geopark

However, despite their unique landscapes, Bourgas and Pomorie municipalities do not have the necessary geodiversity to develop a successful geopark. According to the requirements, it must have a sufficiently large territory, which, apart from the sites of the geological heritage of international significance, must also include sites of historical and spiritual value and serve the local economic and cultural development. For this reason the geopark format must include at least two or three adjacent municipalities that can contribute with their geodiversity for the overall geopark concept. From this point of view, the inclusion of the municipalities of Kameno, Sozopol and Sredets will satisfy the requirements for the provision of the necessary geosites of international importance and allow the start of the geopark establishment procedure (Fig. 2).

Geodiversity

In connection with the main theme of the Geopark, the most important geosites must be developed in the context of the coastline proximity and its impact on land. In addition to a clear and accessible concept of the origin of the lakes, the geological and geomorphological interpretations should include data on the development of the ancient sea terraces (paleobeaches) reflecting the high sea levels during the interglacial epochs preserved on the slopes of the Burgas valley. Another important line of geosites should include the localities of the Late Cretaceous volcanic formations - craters, calderas and copper deposits in the Eastern Srednogorie Zone, as well as geological events such as the Cretaceous-Tertiary boundary in the East Balkan Zone, related to the extinction of the dinosaurs and many other Mesozoic animals. Geosites related to the earlier geological history of the area, e. g. Paleozoic, Triassic and Jurassic should be developed in Strandzha Mountain, known for its remarkable geodiversity. The professional identification and description of the geosites associated with the listed geological preconditions combined with the remarkable biodiversity of the protected Ramsar sites and the cultural and historical heritage of the area will be quite enough to develop a modern working geopark with a diverse and attractive themes for the general public.

Historical data for the origin of the lakes

The interpretation of the paleogeographic development during the Late Pliocene and the Quaternary is in direct connection with the modern geomorphological appearance of the region. As early as the beginning of the last century, the first geomorphologists, working on our lands, noted the presence of submerged river valleys along the Bulgarian Black Sea Coast (Cvijić, 1904; Penck, 1925). An interesting interpretation of the origin of the three Bourgas lakes offers Cvijić (1906), according to which they are the result of the dipping of the three sleeves on the so-called "Sub-Balkan River" - the continuation of the modern Tundzha River which at the end of the Pliocene flowed into the Black Sea (Fig. 3). According to this author, the riverbed of the modern Tundzha River has separated from the old riverbed of the Sub-Balkan River (called here Paleo-Tundzha) near the village of Binkos, Sliven district. Now it flows south of it and just before Straldzha Field at the village of Zavoy sharply turns south to Edirne, where it flows into Maritsa River. During the Pliocene Paleo-Tundzha's riverbed was passing through the Sliven field, probably along the 40 km long irrigation channel between Binkos and Gorno Aleksandrovo.

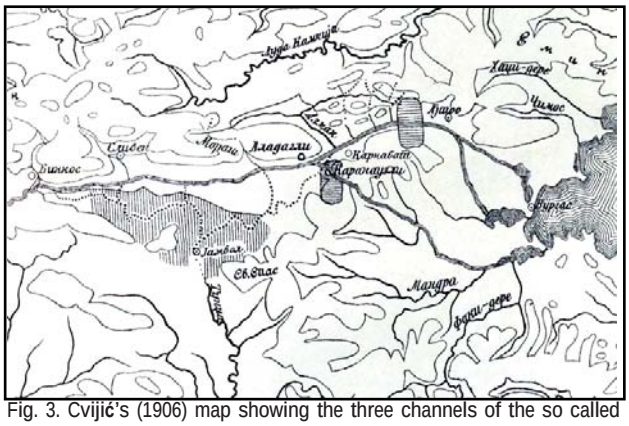

Fig. 3. Cvijić's (1906) map showing the three channels of the so called „Sub-Balkan River" (continuation of Tundzha River to the Black Sea), flowing into the Atanasovsko, Burgas and Mandra Lakes

After another 25 km just before Krumovo gradishte, southwest of the town of Karnobat, the Paleo-Tundzha River was divided into two channels. The right (southern) channel flowed to the southeast where, along the riverbeds of Karaorman, Papazlaka and Rusokastro Rivers, flowed into the Mandra Lake. The left (northern) channel passed through the gorge of the Mochuritsa River through the Hissar Hill, the irrigation channel Azmaka (the old river name of Mochuritsa) between Karnobat and Sigmen, the Topalaka River between Chernograd and Topolitsa villages and the drainage channel south of the town of Aitos along Aitos river. Here it was divided into two more channels, the southern one flowing into the Burgas lake along the Aitos River, and the northern one between the villages of Sadievo and Bulgarovo, through Kandzhikdere and Vetren, flowing into the Atanasovsko Lake.

Burgas Lakes Complex

Pomorie Lake is a super-saline lagoon about 6 km long, with a maximum width up to 1.6 km and an area of about 8.5 km^2. Its depth does not exceed 1.4 m. It is situated NW of Pomorie in the northern part of the Burgas Plain. The mechanism of lagoon formation has been known since the mid-19th century. Lagoons are isolated from the sea basin by sandy bars formed by the waves in the underwater sandy beach as a sandy shaft, which is gradually pushed from the surf to the shoreline as it rises above the water and completely isolates the lagoon from the sea (Fig. 4). The Pomorie lagoon is formed as a double tombolo (Popov, Mishev, 1974) by two sandy bars connecting the island of Pomorie with the land. It was formed in historical times and is associated with the Nymphean transgression that submerged the Black Sea coastline 1000-1500 years ago. The recent researches confirm the tendency for continuing subsidence of the coast. Citing a study of the last century Kanev (1988) concluded that the old road between Anhialo (Pomorie) and Mesemvria (Nessebar) is situated below the Pomorie Lake where a stone pavement was discovered 50 m away from the coastline and 1 m below the lake's surface.

Fig. 4. The sandy bar between the Black Sea and the Pomorie lagoon

Burgas Lake is the largest natural lake in Bulgaria with a length of 9.6 km, a width of 5 km and an area of about 28 km^2, with a depth up to 1.3 m. It represents a liman, separated from the Black Sea by the sandy bar "Kumluka" and connected to it by a narrow channel.

Fig. 5. The Nymphean terrace east of the Atanasovsko Lake

Atanasovsko Lake is a super-salty liman, situated within Burgas between the districts of Izgrev and Sarafovo. To the east it borders the Black Sea with Atanasovska sandy strip, which is about 1 km long sandy bar. Its total area is about 7.2 km^2 with a length of 9 km and a width of 4.3 km with a maximum depth of 0.9 m. It is divided into two halves from the Burgas-Pomorie road. Around the lake the Nymphean marine terrace is well exposed (Fig. 5). The northern half has the status of a protected reserve, and the southern is a protected area. The whole lake falls into the European Network Natura 2000.

Pleistocene-Holocene marine terraces

The marine terraces and their accumulation cover outline the ancient shores of the Black Sea basin. High sea levels during the interglacial epochs are fixed along the coast from ancient

marine terraces. Petrbok (1952) first in Bulgaria proved stratigraphically and paleontologically Pleistocene marine terrace with a length of 1 km and a width of 20 m at Tuzlata near Balchik, which is considered to be probably Karangatian. In the sixties and seventies they were characterized in the works of Fedorov et al. (1962), Lilienberg et al. . (1965), Lilienberg (1966), Boshev et al. (1967), Hristov (1967), Mishev et al. (1969) and summarized later in the monograph of Popov, Mishev (1974). For these terraces were adopted the established Russian names of the Black Sea stratigraphic divisions, which are well correlated with the corresponding terraces of the Crimean and Caucasian coast: Lower Pleistocene – Early Chaudinian at 110-120 m and Late Chaudinian at 85-100 m; Middle Pleistocene – Early Euxinian at 50-60 m and Euxinian-Uzunlarian at 35-40 m; Upper Pleistocene – Early Karangatian at 20-25 m and Lale Karangatian at 8-15 m and Holocene - Neoeuxinian at 4-5 m and Nymphean at 1,5-2 m (Fig. 3). In many places along the Black Sea coast the terraces are paleontologically dated with mollusc (mainly bivalvian) fauna. The scientific development of ancient erosional and accumulation terraces should be made on accessible and representative outcrops appropriate for meditation places, where not only the outcome of the geological activity of the sea but also the paleontological evidence of their age with the characteristic species can be demonstrated.

Erosional and abrasional landforms

Attractive geosites can also be developed in places where current processes of sand-beach formation occur. Most suitable for this purpose are the dunes, which have been developed in many places along the southern Black Sea coast but a small part of them are preserved in a form suitable for demonstration. Geosites with sand dunes "Alepu", "Gradina" and "Kavatsite", included in the Register and Cadastre of the geological phenomena in Bulgaria, fall within the project area of the Geopark. It also includes other erosional and abrasional landforms such as the "Dobrovian mushrooms" near the village of Sini Rid, Priest's Rock at the village of Fazanovo, the Kolokita peninsula south of Sozopol, Cape Agalina and others.

Geosites of scientific and educational value

Two geosites of extraordinary scientific value of the area are described and included in the Register and Cadastre of the Bulgarian geological phenomena. The Iridium layer at the Cretaceous-Terciery boundary, formed as a result of the global catastrophe caused by the asteroide impact 65 million-years ago, known as "the asteroide that killed the dinosaurs" is fixed in a turbidite sequence near Kozichino village. The pillow-lavas near Bulgarovo village is the type locality of the rock "bulgarite" defined as a separate rock type by Stanisheva-Vassileva, Yanev and Harkovska (in Dabovski et al., 1991) (Fig. 6).

Geosites of research and educational value can be selected among the numerous outcrops of the rocks of the Upper Cretaceous Srednogorie Volcanic Complex, such as the preserved crater of the Zidarovo Volcano, which is petrographically well-studied, morphologically well expressed and extremely suitable for demonstration (Fig. 7). On the other hand, the rock formations in Strandzha are crucial for meeting the criteria of the International Union of Geological Sciences in terms of the geodiversity of the proposed territory. Mesozoic rocks with Triassic, Jurassic and Cretaceous age, as well as Paleozoic and Precambrian rocks crop out in Strandzha Mountain on the territory of Sredets Municipality.

Fig. 6. The type locality of Upper Cretaceous pillow lavas defined as a separate rock type "bulgarite" near Bulgarovo village

The oldest rocks in the area are the high-grade metamorphic rocks of the so called "Undivided Precambrian". According to Kozhoukharov and Kozhoukharova (1978) they are formed as a result of progressive metamorphism manifested in amphibolite facies in places revealed as ultrametamorphism. The Paleozoic is represented by metasedimentary and igneous rocks. The oldest Paleozoic rocks are associated with the formation of the phyllitoid argillites, metasandstones and marbleized limestones which are considered as Early Paleozoic. The overlying formation of the marbleized limestones and marbles, which follows with a gradual transition, is also of Early Paleozoic age. These formations are composed of grauwacke-like and arkose-like metasandstones in several places with conglomerate appearance, thin-bedded marbleized limestones and marbles. They are exposed north of Fakia village and between Slivovo and Golyamo Bukovo villages. These rocks are intersected by Late Paleozoic granites and their contacts with the other rock formations in the area are tectonized. Very interesting outcrops of Paleozoic metagabbroids are described in the surroundings of Zhelyazkovo village. These are metamorphosed ultrabasic and basic rocks first described by Yanishevski (1946) as "old gabbro". The ultrabasic rocks are determined as antigorite-tremolite-talk schists and the basic rocks form a large body of gabbro-amphibolites (Kamenov, 1976). The Upper Paleozoic (Hercynian) granitoids of the so called "Central Strandzha Batholith" (Yanishevski, 1946) form a large body between Fakia and Zvezdets villages. The granite body intersects and alters the older Precambrian and Paleozoic rocks and possess xenoliths of them. In turn the granite is intersected by subvolcanic quartz-porphyry and felsite bodies. The Permian is represented by metabreccia-conglomerates, metasandstones and quartz schists of the Sveti Iliya Formation (Chatalov, 1985c) and acid metavolcanics.

Triassic is represented by Sub-Balkan and Strandzha facial types. The former is composed of several formations characreristic for the platform carbonate environment. The underlying unit – the Pitovo Formation of the Tundzha Group, is composed of white arkose sandstones. The rest of the units belonging to the Iskar Carbonate Group, are composed of carbonates – limestones and dolomites with shales and sandstones. The Strandzha facial type united in Veleka Group presents greater diversity of rocks, belonging to several

formations within Bosna and Grahilovo Sub Groups (Chatalov, 19856, 1990).

Jurassic is represented by several formations of the East Thracian Group (Chatalov, 1985a, 1995). The underlying sediments of the Kubarelov Formation (Hettangian-Sinemurian) are represented of quartzitized sandstones and quartzites cropping out as a long strip between Golyamo Bukovo and Zvezdets villages. The younger Kraynovo Formation (Pliensbachian) is composed of different types of marbles and recrystallized limestones cropping out south of Zvezdets village. The Varovnik Formation (Pliensbachian-Bajocian) represents an alternation of biodetritic limestones and fine-grained ferritized sandstones. It crops out only between the villages of Varovnik and Golyamo Bukovo. The Bliznak Formation (Sinemurian-Toarsian) is composed of quartz sandstones. It crops out as a long strip between the villages of Zvezdets and Bliznak. The Zvezdets Formation (Bajocian) cropping out between Zvezdets and Golyamo Bukovo villages is represented by black shales quartzitized sandstones and rare limestone beds.

Fig. 7. The caldera of the Zidarovo volcano with bottom covered by deposits of the Nymphean marine terrace

Cretaceous is represented by widely exposed various sedimentary, volcanic-sedimentary and volcanic rocks grouped into four lithostratigraphic units: Varshilo, Grudovo, Michurin and Burgass Groups (Coniacian-Lower Campanian) as well as intrusive bodies intruded into the older rocks. They are in the core of East Srednogorie structural zone. Fossil volcanic structures like calderas, necks, lava flows, sills, dikes, and volcanic rocks of various composition can be demonstrated in many places in the area, including the Black Sea coast (Fig. 6).

Cenozoic sediments are also well represented in the area. The Burgas Lakes are surrounded by outcrops of Paleogene terrigenous sediments. Well studied deposits of Crimean-Caucasian type Miocene (Tarkhanian-Konkian) are widely exposed on the Black Sea coast with abundant mollusc fauna.

Geosites of cultural-historical value

Geosites of cultural-historical value are related to the many-thousand-year history of the ancient towns Anhialo (Pomorie) and Apolonia (Sozopol). The ancient Thracian tomb in Pomorie, which is the largest antic tomb in Bulgaria built in 1st - 2nd century AD, has recently been open to public access (Fig. 8). The old fortress city wall of Anhialo called by the local people “Rehata”, situated below the present sea level, is an attractive ancient testimony for the subsidence rate from antiquity to recent days. This is an excellent example about the relation between human history and geology that can be demonstrated to the visitors. Another cultural landmark of Pomorie is the Museum of salt which is the only museum in Bulgaria and Eastern Europe specialized in the production of salt through the natural evaporation of sea water by the sun’s heat. It is an original complex of water basins, channels, and other attributes of the ancient Anhialo’s technology for the extraction of sea salt, representing an intangible heritage for the area (Fig. 9).

Fig. 8. The ancient Thracian tomb in Pomorie built in 1st -2nd century AD

Fig. 9. The Museum of salt in Pomorie is a complex of water basins, channels, and other attributes of the ancient Anhialo’s technology for the extraction of sea salt

Apolonia is the most ancient town in Bulgaria founded in 610 BC. The surrounding shallows keep the secrets of the thriving civilization on the western Black Sea coast submerged under sea level. Ancient Greek vases from VII-II century BC, Roman amphorae, coins, ceramic and glassware from I-VI century AD and many artifacts of the many-thousand-year history of the town are saved in the municipal Archaeological museum.

Conclusions

The preliminary analysis of the potentially valuable geosites in the area of the Burgas Lakes Complex reveals a remarkable geodiversity which is a reliable basis for geopark establishment. Obviously, in the focus of the geopark concept will be the development of geomorphosites related to the origin of the lakes and their Quaternary history. Further topics should be related to Black Sea level fluctuations and their relationship to the Quaternary glacial and interglacial epochs, resulting in the formation of marine terraces correlated with the “standard” Black Sea terraces. Another type of Quaternary geological phenomena are the dunes along the sandy beach. Geological phenomena s. str. related to the geological history of the area will be developed on the basis of the rock variety and geological events in the area. The Upper Cretaceous volcanic complex offers various volcanic structures and rocks in perfect condition for demonstration of the volcanic processes. Among the pillow lavas of this complex is situated the type locality of the rock type “bulgarite”. An important outcrop related to one of the most dramatic events in geological history of the planet is the Cretaceous-Tertiary boundary layer preserved in the East

Balkan. With the remarkable geodiversity of Strandzha Mountain, including rocks of different types and ages from Precambrian to Cenozoic, the future geopark has a chance to meet all the requirements of the European Geoparks Network.

References

Бошев, С., Б. Страшимиров, С. Зафиров, Р. Христов, М. Моев. Геология на приморската част на Източна Стара планина. – *Год. ВМГИ, 12,* Св. 2, 1967. – 7-62. (Boshev, S., B. Strashimirov, S. Zafirov, R. Hristov, M. Moev. Geologiya na primorskata chast na Iztochna Stara Planina. – God. VMGI, 12, Sv. 2, 1967. – 7-62.

Каменов, Б. Петрология на Желязковския плутон. – Год. Соф. Унив., Геол.-геогр. фак., 67, 1 – геол., 1976. - 179-212. (Kamenov, B. Petrologiya na Jelyazkovskiya pluton. – God. Sof. Univ., Geol.-geogr. fac., 67, 1 – geol., 1976. – 179-212.

Канев, Д. Към тайните на релефа в България. С., Народна просвета, 1988. - 150 с. (Kanev, D. Kam taynite na relefa v Bulgaria. S., Narodna prosveta, 1988. – 150 s.)

Лилиенберг, Д. А. Опит за морфоложко райониране на Българското Черноморско крайбрежие. – Изв. Бълг. геогр. д-во, 6, 1966. – 23-45. (Lilienberg, D. A. Opit za morfolozhko rayonirane na Bulgarskoto Chernomorsko krajbrezhie. – Izv. Bulg. geogr. d-vo, 6, 1966. – 23-45.)

Лилиенберг, Д. А., В. Попов, К. Мишев. Морфология на терасите по Странджанското Черноморско крайбрежие между Созополския залив и устието на река Велека. – Изв. Геогр. инст. на БАН, 9, 1965. -25-43. (Lilienberg, D. A., V. Popov, K. Mishev. Morfologiya na terasite po Strandzhanskoto Chernomorsko krajbrezhie mezhdu Sozopolskiya zaliv i ustieto na reka Veleka. – Izv. Geogr. Inst. Na BAN, 9, 1965. -25-43.)

Мишев, К., В. Попов, Д. Лилиенберг. Досегашни резултати от геоморфоложките изследвания на Българското Черноморско крайбрежие. - Изв. Бълг. геогр. д-во, 9, 1969. – 37-55. (Mishev, K., V. Popov, D. A. Lilienberg. Dosegashni rezultati ot geomorfolozhkite izsledvaniya na Bulgarskoto Chernomorsko krajbrezhie. – Izv. Bulg. geogr. d-vo, 9, 1969. – 37-55.)

Попов, В., К. Мишев. Геоморфология на Българското Черноморско крайбрежие и шелф. С., Изд. БАН, 1974. – 267 с. (Popov, V., K. Mishev. Geomorfologiya na Bulgarskoto Chernomorsko krajbrezhie i shelf. S., Izd. BAN, 1974. – 267 s.)

Федоров, П. В., Д. А. Лилиенберг, В. И. Попов. Новые данные о террасах черноморского побережья Болгарии. – Докл. Акад. Наук СССР, 144, 2, 1962. – 431-434. (Fedorov, P. V., D. A. Lilienberg, V. I. Popov. Novie dannie o terrasah chernomorskogo poberezhiya Bulgarii. – Dokl. Akad. Nauk SSSR, 144, 2, 1962. - 431-434.)

Христов, Р. Морски тераси по крайбрежието на Черно море в района Бургас-Несебър. – Год. ВМГИ, 12, Св. 2, 1967. – 75-88. (Hristov, R. Morski terasi po krajbrezhieto na Cherno more v rayona Burgas-Nesebar. – God. VMGI, 12, Sv. 2, 1967. – 75-88.

Цвијић, Ј. Основе за географију и геологију Македоније и Старе Србије с проматрањима у Јужној Бугарској, Тракији, суседним деловима Мале Азије,Тесалији, Епиру и Северној Арбанији. – Београд, Српска Краљевска Академија, Књига друга, 1906. - 548-630. (Cvijich, J. Osnove za geogrfiyu i geologiyu Makedonije i Stare Srbije s promatranjima u Yuzhnoj Bugarskoj, Trakii, Epiru I Severnoj Arbaniji. – Reograd, Srpska Kraljevska Akademia, knjiga Druga, 1906. - 548-630.)

Чаталов, Г. Стратиграфия юрской системы в Странджанской области в Болгарии. - Geologica Balc., 15, 4, 1985а. - 3-39. (Chatalov, G. Stratigrafiya jurskoy sistemi v Strandzhanskoj oblasti v Bulgarii. - Geologica Balc., 15, 4, 1985a. - 3-39.)

Чаталов, Г. Стратиграфия триасовых отложении Странджанского типа (Странджанские горы, Юго-Восточная Болгария). - Geologica Balc., 15, 6, 1985б. - 3-38. (Chatalov, G. Stratigrafiya triasovih otlozhenii Strandzhanskogo tipa (Strandzhanskie gori, Yugozapadnoj Bolgarii. - Geologica Balc., 15, 6, 1985b. - 3-38.)

Чаталов, Г. Принос към стратиграфията и литологията на палеозойските и триаски скали в Светиилийските височини. – Сп. Бълг. геол. д-во, 46, 1, 1985в. - 53-70. (Chatalov, G. Prinos kam stratigrafiyata i litologiyata na paleozojskite i triaski skali v Svetiilijskite visochini. – Sp. Bulg. geol. d-vo, 46, 1, 1985v. - 53-70.)

Чаталов, Г. Геология на Странджанската зона в България. Изд. БАН, 1990. – 263 с. (Chatalov, G. Geologiya na Strandzhanskata zona v Bulgaria. Izd. BAN, 1990. – 263 s.)

Чаталов, Г. Триас. Юра. - В: Дабовски (Ред.) Обяснителна записка към Геоложка карта на България М 1:100 000. Картни листове Желязково и Кърклареli. С., КГМР, „Геология и геофизика" - АД, 1995. -15-30. (Chatalov, G. Trias. Jura. V: Dabovski, H. (Red.) Obyasnitelna zapiska kam Geolozhka karta na Bulgaria M 1:100 000. Kartni listove Zhelyazkovo i Karklareli. S., KGMR, "Geologiy ai geofizika" AD, 1995. – 15-30.

Янишевски, А. Кратко изложение върху геологията на Странджа. В: Основи на геологията на България. – Год. Дир. геол. и минни проучв., А, 4, 1946. – 380-388. (Yanishevski, A. Kratko izlozhenie varhu geologiyata na Strandzha. V: Osnovi na geologiyata na Bulgaria. – God. Dir. geol. i minni prouchv., A, 4, 1946. - 380-388.)

Cvijić, J. Die Tektonik der Balkanhalbinsel mit besonderer Berücksichtigung der neueren Fortschritte in der Kenntnis der Geologie von Bulgarien, Serbien und Makedonien. – Compt. Rend. IX Session Congr. Geol. Intern., Vienne 1903, Premier Fasc., Sixième Partie, 1904. -347-370.

Dabovski, Ch., D. Harkovska, B. Kamenov, B. Mavrudchiev, G. Stanisheva-Vassileva, Y. Yanev. 1991. A geodynamic model of the Alpine magmatism in Bulgaria. – Geologica Balc., 21; 3-15.

Kozhoukharov, D., E. Kozhoukharova. Precambrian metamorphic rocks in the Sakar-Strandža Zone. – In: The Precambrian in Bulgaria. - Precambrian in younger fold belts, Materials to the IGCP Project 22, Geogr. Inst. ČAS, Brno. 1978. - 41-47.

Penck, A. Geologische und Geomorphologische Probleme in Bulgarien. – *Der Geologe, 38,* 1925. – 849-873.

Petrbok, J. Měkkýši plistocenní a holocenní marinní terasy Černého moře u Balčíku v Bulharsku a marinní měkkýši bulharského plistocenu. – Acta Musei Nationalis Pragae, series B 8B(2), 1952. –1-21.

The article is reviewed by Assoc. prof. Dr. Boris Valchev and Assoc. prof. Dr. Ivan Dimitrov.

GEOLOGICAL, PETROLOGICAL AND GEOCHEMICAL CHARACTERISTICS OF THE PERLITES FROM THE "SCHUPENATA PLANINA'' DEPOSIT, EASTERN RHODOPES AND HOSTING VOLCANITES

Stanislav Stoykov[1], Anita Metodieva[1], Miloslav Katzarov[1], Milko Harizanov[1]

[1]University of Miningand Geology "St. Ivan Rilski", 1700 Sofia; ststst@abv.bg; mharizanov@mgu.bg;

ABSTRACT. Schupenata planina is the only perlite deposit in operation in Bulgaria. It is located in Kurdjali region, in the area of Djebel town and Vodenicharsko village. They are part of the Eastern Rhodope Paleogene depression. The perlite is hosted in the rhyolites of the Ustren volcanic region. They are part of the Oligocene III-th acid volcanism in the Eastern Rhodopes. The perlites are grey to white – grey, they show sub vertical prismatic joints 7 to 10 m long. The rocks are build up by quartz, sanidine, acid plagioclase and biotite. The rhyolites contain between 74.05 and 76.25 wt. % SiO_2 and the analyzed perlite products - between 73.85 and 74.79. The rhyolites are of high – K type. The volcanic glass content in the perlite is up to 90 %.

Keywords: perlite, rhyolites, Eastern Rhodopes, Schupenata planina deposit, implementation of perlite

ГЕОЛОЖКА, ПЕТРОЛОЖКА И ГЕОХИМИЧНА ХАРАКТЕРИСТИКА НА ПЕРЛИТНАТА СУРОВИНА ОТ НАХОДИЩЕ „СЧУПЕНАТА ПЛАНИНА", ДЖЕБЕЛСКО И ВМЕСТВАЩИТЕ Я ВУЛКАНИТИ

Станислав Стойков[1], Анита Методиева[1], Милослав Кацаров[1], Милко Харизанов[1]

[1]Минно-геоложки университет "Св. Иван Рилски", 1700София; ststst@abv.bg; mharizanov@mgu.bg;

РЕЗЮМЕ. Счупената планина е единственото находище на перлит в България, което се разработва. То се намира в Кърджалийска област, в близост до град Джебел и село Воденичерско. Районът на находището попада в Източнородопското Палеогенско понижение. Перлитната суровина се намира сред риолитите на Устренския вулкански район. Те са част от третия кисел вулканизъм на Олигоцена в пределите на Източните Родопи. Перлитите са сиви до сивобели, наблюдават се сред риолити, показващи субвертикална призматична напуканост с дължина на призмите от 7 до 10 метра. Вулканитите са изградени от кварц, санидин, кисел плагиоклаз, биотит и вулканско стъкло. Риолитите съдържат между 74,05 и 76,25 wt. % SiO_2, а изследваните перлитни продукти - между 73,85 и 74,79 wt. % SiO_2. Вулканитите са високо калиеви. Вулканското стъкло в перлитите достига до 90 %.

Ключови думи: перлит, риолити, Източни Родопи, находище Счупената планина, приложение на перлита

Introduction

Schupenata planina (The Broken Mountain) is the only perlite deposit in operation in Bulgaria. It is located in Kurdjali region, in the area of Djebel town and Vodenicharsko village. They are part of the Eastern Rhodope Paleogene Depression.

The perlite is hosted in the rhyolites of the Ustren volcanic region. They are part of the Oligocene III-th acid volcanism in the Eastern Rhodopes. The rhyolites are build up by quartz, sanidine, acid plagioclase and biotite. They contain between 74.05 and 76.25 wt. % SiO_2 and the analyzed perlite product - between 73.85 and 74.79. The water content of the volcanic rocks is between 2.26 and 3.11 wt. % and in the fractionated perlite between 5.55 and 4.70 (Table 1). The rhyolites are of high – K type. The volcanic glass content in the perlite is up to 90 %. The perlites are grey to white – grey, they show sub vertical prismatic joints 7 to 10 m long.

The perlites were described as petrographical variety at the end of XVIII century. Their mining and industrial application started in 1940 with the production of expanded perlite in USA.

The name perlstein was given in XIXth century by a German petrologist naming certain rhyolotic glassy rock with concentric cracks, which looks similar to pearls. The most modern name perlite is now in use universally (Evans, 1993). The perlite is hydrated volcanic glass, composed mainly of amorphous silica with 12-18 wt. % Al_2O_3. Minor chemical components of the perlite are Na_2O, K_2O, Fe_2O_3, MgO, CaO, etc. This hydrated rocks carry between 2 and 5 wt. % water. Heating the perlite close to their melting temperature results, the contained water is converted into steam and the grains transform into light cellular particles. As a result, the weight of the material decreases 10 – 20 times. The product is with low thermal conductivity, high thermal, fire resistant, and high sound absorption.

The Schupenata planina deposit was in operation by Bentonite, S&B Industrial Minerals and now by Imerys minerals Bulgaria.

The Schupenata planina deposit is located in the Eastern Rhodopes, next to the Vodenicharsko village. It was discovered in 1955 and has been in operation since 1962. The perlite bodies outcrop on the area about 2 km^2.

The processing technology is crashing and fractionation. The fraction 0.5-2 mm is used for expansion and those below 0.5 mm for glass production. The average volume weight of the

expanded perlite from the Schupenata planina deposit is 100 - 150 kg/m3.

Production and use of perlite

The general technology of reworking of the perlite starts with crashing and fractioning of the material. The fraction from 0.5 to 2 mm is expanded. The fraction below 0.5 mm is used for glass production. The expanded perlite has the following properties:

- Specific gravity from 100 to 180 kg/m^3;
- One kg expanded perlite is produced from 135 kg fractionated perlite.

Over half of the world's production goes into the construction industry as aggregate for insulation boards, plasters and concrete in which weight reduction and special acoustic or thermal insulation properties are required (Evans, 1993). It is used for loose – fill insulation of cavity walls and for the thermal insulation of storage tanks for liquefied gases. The agricultural application of perlite includes use as a soil conditioner and as a carrier for herbicides and chemical fertilizers. The perlite is used for filtering water, other liquids, in food processing and as a filler in paints, plastics, etc.

The total world production of crude perlite in 2015 was 4.38 Mt, a slight increase from the revised value of 2014 (USGS, 2015). The world's leading producers of crude perlite in 2015 were, in descending order of production, China, Greece, Turkey, and the United States, accounting for 41%, 23%, 21% and 11%, respectively, of world production. Greece and Turkey remained the leading exporters of perlite. Although China was the leading producer, most crude perlite was believed to be consumed internally. S&B Industrial Minerals S.A. (Greece) was the primary supplier of processed crude perlite imports to the United States. Imerys completed its purchase of S&B Industrial Minerals in early 2015. The acquisition was one of the largest in the perlite industry since Imerys purchased World Minerals, a producer of perlite products with mines in Arizona and New Mexico, in 2010. Including the acquired S&B Industrial Minerals facilities, Imerys owns 6 perlite mines and 11 perlite plants located in 6 countries (O'Driscoll, 2015).

The expanded perlite consumed for construction-related uses, which accounted for about 53% of the market for expanded material, was about 260,000 t, a 6% increase compared to that of 2014. Construction uses of expanded perlite consisted of concrete aggregate, formed products, masonry- and cavity-fill insulation, and plaster aggregate. Expanded perlite consumption increased for fillers, filter aid, formed products, high-temperature insulation, masonry- and cavity-fill insulation, and plaster aggregate.

The main usage of perlite (about 50%) in 2015 is for formed products (including acoustic ceiling panels, pipe insulation, roof insulation board, and unspecified formed products). The second most important usage of perlite is as horticultural aggregate followed by filler and filter aids. Minor quantity of perlite is used as low-temperature insulation, plaster aggregate, etc. (USGS, 2015).

Bulgaria is in the first 15 world largest perlite producers with about 5 000 metric tons production for 2015 (USGS, 2015).

One of the important usages of expanded perlite is for extender design for well cement slurry. Neat cement slurries, when prepared from API Class A, C, G, or H cements using the amount of water recommended in API Spec. 10A (Bulgarian state standard (BDS) , EN ISO 10426-1:2010) will have slurry weights in excess of 15 lb/gal (1800 kg/m^3).

The expanded perlite from Schupenata planina deposit was studied as a component of lightweight well cement slurry based on perlite extender and its parameters in accordance with BDS EN ISO 10426-2:2006 and BDS EN ISO 10426-1:2010 requirements as well as improvement of its formulation by neat and additives treatment cement slurries. Analysis of perlite - containing mixture providing the lowest density while maintaining other required parameters was conducted. As a cement base, cement API Class G HRS, cement CEM I 42,5 N SR 5 and perlite M100 and M150 were used. Perlite typical content varied from 1 ft^3 Perlite additive/1 ft^3 cement to 2 ft^3. Perlite additive/1 ft^3 cement; and water-to-cement-ratio ranged from 0.8 to 1.2. To sum up, despite the fact that lightweight cement slurry based on perlite satisfies BDS EN ISO 10426-2:2006 and BDS EN ISO 10426-1:2010 requirements under laboratory conditions, field studies are necessary in order to make a conclusion about applicability of this slurry for well cementing in field conditions.

There are several different types of materials that can be used as extenders by reducing the average specific gravity of the dry mix and cement slurry. These include:

- Physical extenders (clays and organics);
- Pozzolanic extenders;
- Chemical extenders;
- Gases.

These are particulate materials that function as cement extenders by increasing the water requirements or by reducing the average specific gravity of the dry mix. The most common low-specific-gravity solids used to reduce cement slurry specific weight are bentonite, diatomaceous earth, solid hydrocarbons, expanded perlite and pozzolan.

Perlite cement additive is a physical extender and light, granular material made from crushed volcanic rock. Expanded perlite is a siliceous volcanic glass that is heat-processed to form a porous particle that contains entrained air. The dry weight of perlite is only 8 lb/ft^3 (128 kg/m^3) as opposed to 25–100 lb/ft^3 (400–1600 kg/m^3) the dry weight of the other materials (William, 2010, Nelson, 1990).

Its primary use is to lower the density of cement slurries as low as 1.44 g/cm^3. It can be used at bottom hole temperatures (BHTs) between 4°C and 204°C. Typical concentrations are 1 ft^3 (28.32 Litr.) perlite additive/1 ft^3 (28.32 Litr.) cement or 2 ft^3 (56.64 Litr.) perlite additive/1 ft^3 (28.32 Litr.) cement (William, 2010, Nelson, 1990).

Geology of the perlite deposits

Perlite, like other glasses, devitrifies with time so that commercial deposits are mainly restricted to areas of Tertiary and Quaternary volcanism. Perlite occurs as lava flows, dykes, sills and circular or elongate volcanic domes. The domes are the largest and most commercially important bodies and they can be as much as 8 km across and 270 m in vertical extent. Many of these lava domes cooled quickly in their outer parts to obsidian but the interiors remained hot and formed fine-grained, crystalline rock. In certain instances, the obsidian has been hydrated as a result of penetration by ground water forming perlite. Remnants of unaltered obsidian may remain in the perlite, which may also contain phenocrysts of quartz, feldspar and other minerals (Evans, 1993).

Geology of the region of the Schupenata planina deposit

In the area of the deposit outcrop there are the following rock formations: Djhebel formation (DOl_1) overlies with erosional boundary various Paleogene sedimentary and volcanogenic-sedimentary units: Podrumche formation, terrigenous limestone formation from the volume of the carbonate-terrigenous complex, pyroclastic-limestone formation and Podkova formation from the volume of the Kardzhali Volcano-Sedimentary Group, limestone-pyroclastic formation from the volume of the Chiflik Volcanic Subcomplex (Nanovitsa Volcanic Complex), tuffite-tuffaceous formation (fig. 2). In eastern direction, near Sekirka village, the formation pinches out under rocks of the lower tuffaceous-tuffite epiclastic package of the Zvezdel Volcanic Complex. It is also intersected and covered concordantly by epiclastites, pyroclastites and lavas of the Zvezdel Volcanic Complex, Ustren and Pcheloyad Volcanic complexes, as well as by sediments of the limestone formation (Yordanov et al., 2008).

The sandstones are yellow-beige, loose, displaying coarsely horizontal and characteristic cross bedding. Their structure is massive. Their texture is inequigranular, predominantly psephitic-psammitic to aleuro-psammitic. The rocks are poorly sorted.

The clastic component reaches 75%. The sandstones are polymict, dominated by quartz and feldspar. Subordinately represented are coarse flakes of muscovite, biotite and chlorite, single grains of amphibole and tourmaline. The rock fragments were derived from acid and intermediate volcanics, massive rocks with granitoid composition, schists, etc. The matrix is monomineralic being composed of clay minerals or carbonate. Its type is contact-pore-filling, with limited occurrence of basal type. The matrix is pigmented by iron oxides.

Ustren Volcanic subcomplex - (Ustren Rhyolitic Complex). It includes the acid pyroclastics exposed in the vicinity of Stomantsi village and the rhyolite dome near Zlivrah summit. The complex is exposed in the vicinity of Vodenicharsko village as well as over vast areas between Zlivrah summit and the villages Stomantsi, Rastnik, and Muglene. In structural aspect the rocks belong to the Ustren subzone of the Galenit Tensional Zone. Rock fall blocks are commonly encountered along the periphery of the acid domes (Yordanov et al., 2008).

The rocks intersect or overlie concordantly the Chiflik Volcanic Subcomplex and the Dzhebel Formation. They are respectively intersected by subvolcanic bodies from the volume of the Zvezdel Volcanic Subcomplex. Mainly acid volcanics (rhyolites and dacites) and associated perlites and acid pyroclastics comprise the volume of the complex. “Multiple reopening of fractures and filling with new portions of the same lava and its pyroclastics” was observed in some of the larger rhyolitic bodies. They build relatively uniform sectors with specific features, the Ustren Volcanic complex is subdivided into the following units:

- rhyolites and pyroclastics – Stomantsi volcano;
- and rhyolites – Ustren volcano.

Analytical technics

Volcanic rocks from the quarry and from Ustren volcanic complex west from the deposit were sampled. The major element of 5 samples rhyolites and 2 of fractionated perlite were analyzed by OES – ICP in the laboratories of the University of Mining and Geology ‘St. Ivan Rilski’. Chemical analyses were performed on samples from rhyolites, contact zone of inclusion in rhyolite and fractionated perlite.

Petrological and geochemical characteristics of rhyolites and perlite

The perlite deposits in the Eastern Rhodopes are related to the Oligocene acid volcanism. The Schupenata planina deposit is located in the Ustra volcanic region, part of the volcanism developed in the eastern Rhodope Paleogene Depression. The Ustra volcanic region is located west of town of Djebel and is around the top of Ustra between the villages of Lebed, Ustren and Vodenicharsko.

The volcanics are rhyolitic extrusions, necks, dykes and flows, they contain numerous perlitic bodies. They cut the Djebel sandstone formation of Oligocene age. The Schupenata planina deposit is built up by rhyolitic dome and flows which cover Oligocene sandstones and clays (Yanev, 1985). This results into rock falls and landslides forming the present relief. The base of the rhyolitic dome and flows (sandstone and clay sediments) and the earthquake result in subsiding of the Schupenata planina perlite deposit at the beginning of XIXth century. The perlite deposits are of effusive, extrusive and dyke type. The magmatic rocks are presented by extrusions, necks and lava flows. They are high - K rhyolites. The porphyry generation is represented by quartz, sanidine, acid plagioclase and biotite. The ground mass is glassy.

Rhyolites contain between 74.05 and 76.25 SiO_2, Na_2O from 2.14 to 2.67, K_2O from 4.99 to 5.91 wt. %, the water content of the volcanic rocks is between 2.26 and 3.11 wt. %. The chemical properties of the fractionated perlite are between 73.85 and 74.79 SiO_2, Na_2O from 2.32 to 2.39, K_2O from 4.52

to 5.99 wt. %, the water content is between 5.55 and 4.70 wt. % (Table 1). The rhyolites have higher SiO_2, K_2O, Fe_2O_3 and TiO_2 content and lower water content compared to fractionated perlite.

Fig. 1. Panorama to the Schupenata planina perlite deposit

Table 1.
Chemical composition (wt. %) of rhyolite from the Ustren volcanic region and fractionated perlite from the Schupenata planina deposit

Sample	Description	SiO_2	TiO_2	Al_2O_3	Fe_2O_3	MnO	MgO	CaO	Na_2O	K_2O	LOI	Water
Y1	White volcanic rock	75.16	0.13	12.65	0.68	0.03	0.10	0.29	2.14	5.41	2.94	0.35
Y2	Grey volcanic rock	75.05	0.10	12.36	0.62	0.05	0.07	0.42	2.66	5.12	3.11	0.29
Y3	Pinkish volcanic rock	75.10	0.11	12.68	0.64	0.04	0.07	0.35	2.58	5.00	3.00	0.21
Y4	Dark pink volcanic rock	75.80	0.11	12.61	0.68	0.05	0.07	0.36	2.67	4.93	2.26	0.27
Y5	Contact zone in the volcanics	76.25	0.10	11.66	0.60	0.03	0.07	0.44	2.71	5.32	2.32	2.26
Y6	Darkpink – to black volcanic rock – contact zone	82.99	0.05	9.03	0.37	0.06	0.05	0.29	2.09	3.45	1.13	1.18
E	Fractionated perlite	73.85	0.06	12.50	0.55	0.11	0.06	0.39	2.39	4.99	4.70	0.30
P2	Fractionated perlite	74.79	0.06	11.65	0.48	0.10	0.06	0.38	2.33	4.52	4.55	0.28

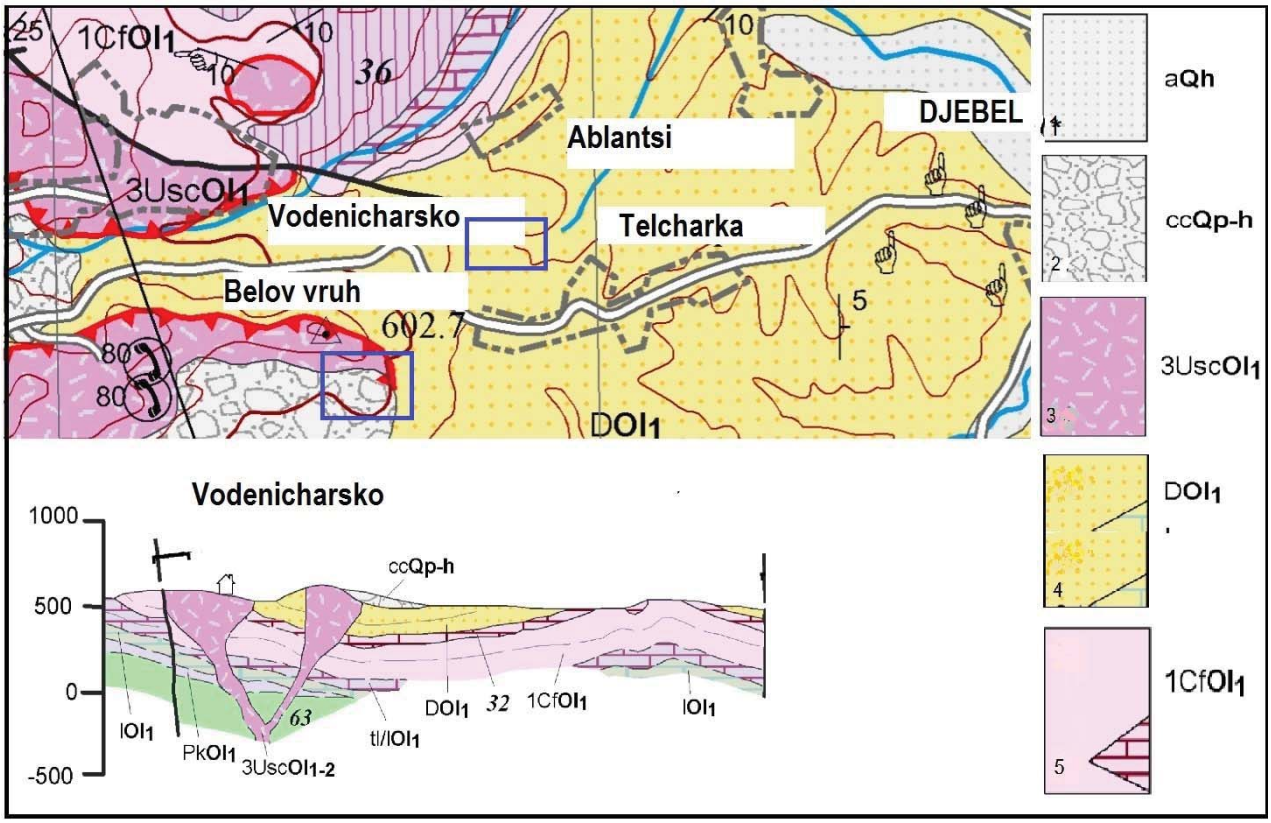

Fig. 2. Geological map of the region of the Schupenata planina perlite deposit (after the Geological map of Bulgaria 1:50 000 scale Map Sheet Djebel and Kirkovo (Yordanov et al., 2008) with addition. Blue squares – schematic location of the perlite bodies. 1 - Quaternary alluvial sediments; 2 - Quaternary proluvial sediments, rock falls and landslides; 3 – Rhyolites of Ustren volcanic complex; 4 – Sediments of Djebel Formation; 5 – Limestone and tuff formation

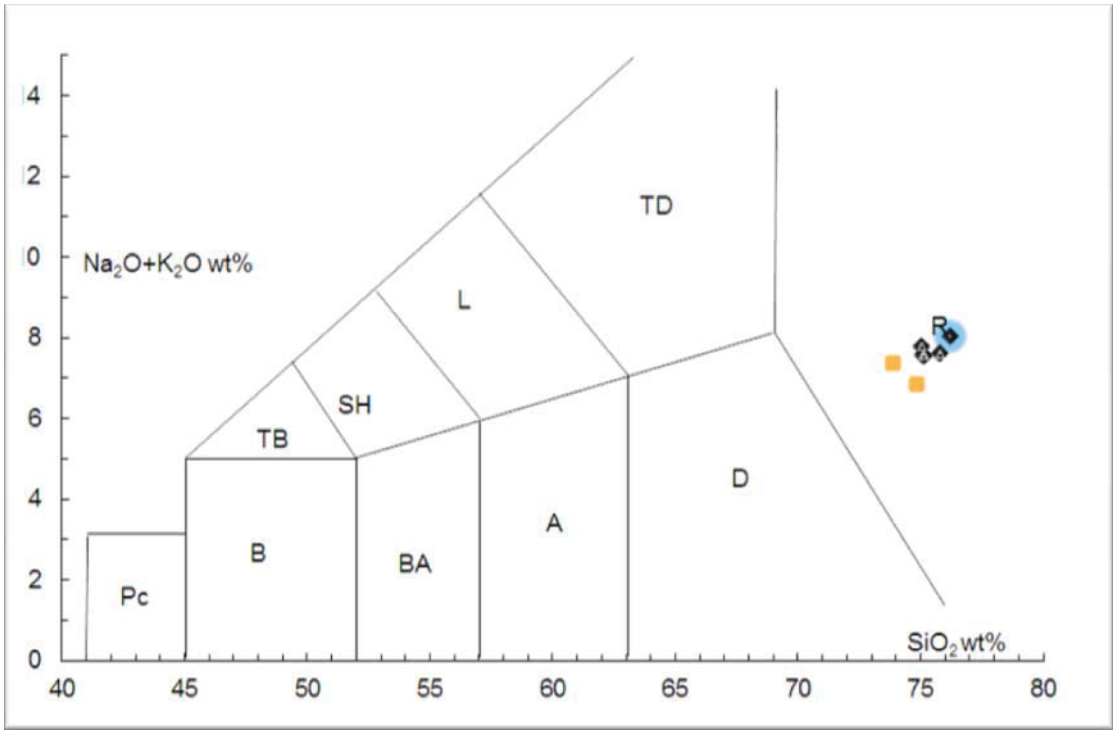

Fig. 3. TAS diagram Le Maitre (1989) for representative magmatic rocks from the studied region (B—basalt; BA—basaltic andesite; A—andesite; D—dacite; SH—shoshonite; L—latite; TD—trachydacite). Diamonds – rhyolites; squares – fractionated perlite from the Schupenata planina perlite deposit

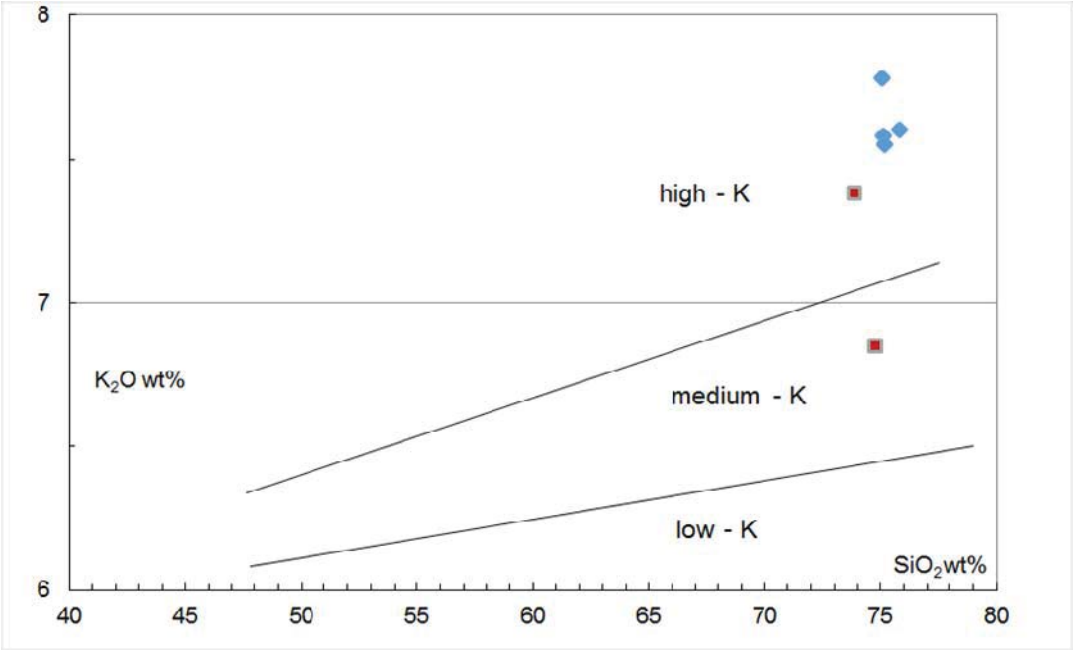

Fig. 4. SiO_2 – K_2O diagram Le Maitre (1989) for representative magmatic rocks from the studied region. Diamonds – rhyolites; squares – fractionated perlite from the Schupenata planina perlite deposit

Conclusions

The Schupenata planina is the only perlite deposit in operation in Bulgaria. It is located in Kurdjali region, in the area of Djebel town and Vodenicharsko village. They are part of the Eastern Rhodope Paleogene depression. The perlite is hosted in the rhyolites of the Ustren volcanic complex. They are part of the Oligocene III-th acid volcanism in the Eastern Rhodopes. The perlites are grey to white – grey, they show sub vertical prismatic joints 7 to 10 m long. The rocks are built up by quartz, sanidine, acid plagioclase and biotite.

Fig. 5. Columnar jointing in rhyolite and perlite bodies in the deposit.

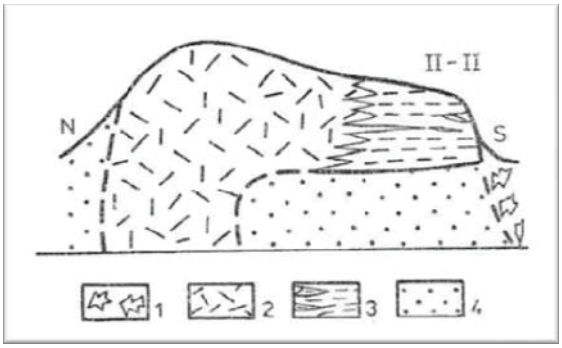

Fig. 6. Geological section of the Schupenata planina deposit after Yanev, (1985). 1. Landslide body; 2. Rhyolite; 3. Perlite and rhyolite lenses; 4. Sands and clays

They are classified as high – K rhyolites and contain between 74.05 and 76.25 SiO_2, Na_2O from 2.14 to 2.67, K_2O from 4.99 to 5.91 wt. %, the water content of the volcanic rocks is between 2.26 and 3.11 wt. %. The chemical properties of the fractionated perlite are between 73.85 and 74.79 SiO_2, Na_2O from 2.32 to 2.39, K_2O from 4.52 to 5.99 wt. %, the water content is between 5.55 and 4.70 wt. %. The rhyolites have higher SiO_2, K_2O, Fe_2O_3 and TiO_2 content and lower water content compared to fractionated perlite.

Acknowledgements. This work was supported by research grant 192/GPF/2015 of the University of Mining and Geology 'St. Ivan Rilski. The thin sections, different analyses and tests have been performed in the laboratories of the University of Mining and Geology 'St. Ivan Rilski, Sofia.

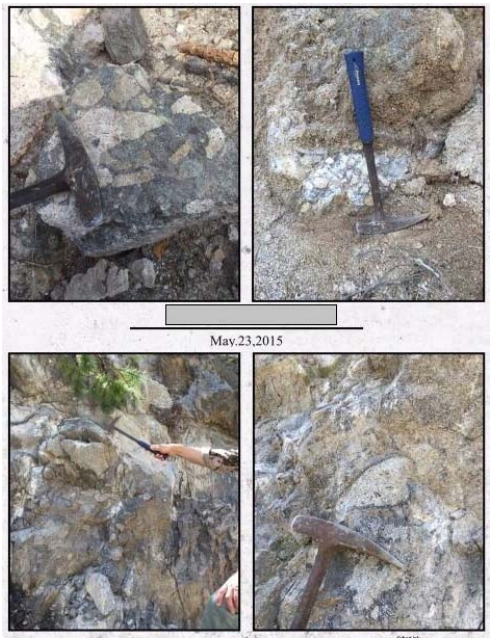

Fig. 7. Brecciation in the volcnanics from the volcanic complex

References

Evans, A. Ore Geology and industrial minerals. An Introduction. 1993. Blackwell Science. P. 387.

Le Maitre, R.W. A classification of igneous rocks and glossary of terms. 1989 Oxford, Blackwell Sci. Publ., 193 pp.

Nelson E. B. Well Cementing, Published by Schlumberger Educational Services., First edition 1990, ISBN: 978-0080868868

O'Driscoll, Mike. Imerys seals S&B acquisition—So what does it mean? Industrial Mineral Forums & Research, March 6. (Accessed June 3, 2015, at http://imformed.com/imerys-seals-sb-acquisition-so-what-does-it-mean/.)

William L. Working Guide to Drilling Equipment and Operations, Published by Elsevier Inc., First edition 2010, ISBN: 978-1-85617-843-3

Yanev Y.1985. Perlites in the East Rhodopes, Bulgaria. World congress on non-metallic minerals, Belgrade, Yugoslavia.

Yordanov, B., S. Sarov, S. Georgiev, V. Vulkov, E. Balkanska, V. Grozdev, V. Marinova, N. Markov. Geological map of Bulgaria 1:50 000 scale Map Sheet Djebel and Kirkovo 2008

https://minerals.usgs.gov/minerals/pubs/commodity/perlite/myb1-2015-perli.pdf

The article is reviewed by Assoc. Prof. Slavcho Mankov and Prof. Dr. Strashimir Strashimirov.

SEQUENCE-STRATIGRAPHIC ANALYSIS BASED ON WELL LOGS IN TERMS OF STUDYING THE TRANSGRESSIVE-REGRESSIVE CYCLES IN PART OF CENTRAL NORTH BULGARIA

Hristomir Stanev

University of Mining and Geology "St. Ivan Rilski", Faculty of Geology, Sofia 1700, Bulgaria, E-mail: hristomir.stanev@abv.bg

ABSTRACT. The area of this study is located within the Central North Bulgaria (CNB). It is relatively well-studied in geological aspect, but to obtain a better understanding and to clarify some issues concerning the sedimentary environments and the evolution of sedimentary fill it is necessary to apply modern approaches, such as sequence-stratigraphic analysis. Thus formulates the main purpose of the study, which is based on well log data that provides valuable information through which one can study the transgressive-regressive cycles and the resulting sedimentary sequences, controlled by eustasy, tectonic movements and sediment supply. As a result, 5 sedimentary sequences from different order (Campanian-Maastrichtian second-order sequence, Valanginian-Aptian second-order sequence, Callovian-Valanginian first-order sequence, Bajocian-Bathonian third-order sequence, Hettangian-Lower Bajocian second-order sequence) were recognized along with their elements (system tracts) formed within transgressive-regressive cycles. Based on the analysis of the participating official lithostratigraphic units and well-log interpretation, the paleoenvironment of sedimentation is predicted for each individual sedimentary sequence. The sedimentary sequences are predominantly with carbonate composition, with interbeds of terrigenous material, typical for the late stages of the highstand system tract at a reached eustatic minimum, increasing the influence of the source of the clastics from south. The paleoenvironments of deposition mainly represent the shelf area of the basin, with individual sequences falling either in the shallow or deep zone. During the Lower Cretaceous period, the depositional environment was represented by a pelagic setting.The most significant differences in the facies appearance and sedimentation settings are found within the scope of the Callovian-Valanginian first-order sequence as a direct response to the complex geodynamic evolution of the basin during that period.The impulsive nature of importing a clastic material in the Lovech Urgonian group (Lower Cretaceous) would produce some collectors with potential for storing natural gas or CO_2 sequestration.

Key words: Sequence stratigraphic interpretation, South Moesian periplatform, Well logs

СЕКВЕНТНО-СТРАТИГРАФСКИ АНАЛИЗ ЗА ИЗУЧАВАНЕ НА ТРАНСГРЕСИВНО-РЕГРЕСИВНИТЕ ЦИКЛИ ПО СОНДАЖНО-ГЕОФИЗИЧНИ ДАННИ ЗА РАЙОН ОТ ЦЕНТРАЛНА СЕВЕРНА БЪЛГАРИЯ

Христомир Станев

Минно-геоложки университет "Св. Иван Рилски", 1700 София, E-mail: hristomir.stanev@abv.bg

РЕЗЮМЕ. Районът на настоящето изследване е локализиран в пределите на Централна Северна България (ЦСБ). Той е относително добре изучен в геоложки аспект, но за постигане на по-добро разбиране и изясняване на някои въпроси, касаещи седиментните обстановки и запълването на част от Южномизийската периплатформена област, е необходимо прилагането на съвременни методи, какъвто е секвентно-стратиграфския анализ. Това формулира и основната цел на изследването, проведено по сондажно-геофизични данни (СГИ), които предоставят ценна информация, благодарение на която могат да се изучат трансгресивно-регресивните цикли и свързаните с тях седиментни секвенции, контролирани от еустатичните колебания, тектонските движения и седиментния приток. В резултат на проведения анализ, бяха отделени 5 седиментни секвенции от различен порядък (Кампан-Мастрихтска, Валанжин-Аптска, Калов-Валанжинска, Байос-Батска и Хетанж-Долно Байоска) и изграждащи ги системни трактове образувани в рамките на трангресивно-регресивни цикли. На база анализ на участващите официални литостратиграфски единици и интерпретация на сондажно-геофизичните изследвания е прогнозирана предполагаемата палеообстановка на седиментиране за всяка отделна седиментна секвенция. Седиментните секвенции са преимуществено с карбонатен състав с прослойки от теригенен материал, характерен за късните стадии на тракта на високо морско ниво при достигнат еустатичен минимум, засилвайки се влиянието на подхранващата суша от юг. Палеообстановките на седиментация основно характеризират шелфовата зона на басейна. Отделни секвенции попадат или в плитката или в дълбоката шелфова зона. През долнокредния период басейнът се удълбочава, част от седиментите са характерни за пелагичната зона. Най-значителни различия във фациесите и обстановката на седиментоотлагане са открити в обхвата на Калов-Валанжинската секвенция от първи порядък, характеризираща сложната геодинамична еволюция на басейна през този период. Импулсивния характер на внасяне на кластичен материал при Ловешката Ургонска група (долна креда) би било предпоставка за образуване на колектори с потенциал за съхранение на природен газ и задържане на емисии от въглероден двуокис.

Ключови думи: Секвентостратиграфска интерпретация, Южномизийска периплатформа, Сондажно-геофизични данни

Introduction

The area of this study (Fig.1) covers the western part of South Moesian periplatform area located within the Central Northern Bulgaria (CNB). This unit is a secondary tectonic structure within the Moesian platform. This area is limited by the South Moesian fault to the north, which joins with the Krushovitsa-Gorsko Slivovo fault to the east. The south border is presented by Brestnitsa flexure. The territory is relatively well studied in geological aspect through multiple wells and geophysical studies at the end of the last century. Due to lack of modern computing technologies for processing and interpretation of seismic data, drilling workings in large numbers were used as the main approach in studying the petroleum perspectives of Northern Bulgaria. The main petroleum play covers the rocks of the Mesozoic section. After exploring the basics fund of anticlinal structures, the focus

logically shifts on the research and study of other types of stratigraphic and structural traps. This necessitated a more frequent use of seismic surveys as a particularly useful method for lateral tracking of sedimentary units including the elements of the petroleum system with a focus on the possible trapping bodies. The seismic data alone does not bring sufficient information without the required method and approach to interpretation. This requires the implementation of the sequence-stratigraphic analysis to give reasonable geological sense of seismic and drilling data. This analysis is complex and relies on the interpretation of seismic, well log and core data, as well as on field outcrops.

Comprehensive analyses of the Triassic sedimentary sequences are found in the articles of Mader, Çatalov (1992), Aydanliyski et al., (2004), Georgiev and Bakurdzhiev (2004). Tchoumatchenco (2002) separates two first-order Jurassic sequences. In the stratigraphic range of the Lower Cretaceous, within the range of the central and eastern Forebalkan area, partially within the South Moesian periplatform area, ten sequences of the third order with stratigraphic interval Berriasian-Valanginian and eight sequences in the Varremian-Aptian interval of the same order are described (Ivanov and Stoykova, 1997; Nikolov et al., 1998; Nikolov et al., 1998; Ciszak et al., 2000).

The main objectives of this article were to make a sequence stratigraphic analysis, to clarify the basin sedimentary filling and the typical depositional environments in the Mesozoic sediments based on available well data for an area falling within the South Moesian periplatform area. Four well sections within the Lukovit and Aglen areas were selected.

Regional geology

The South Moesian periplatform area represents the southern margin of the Moesian platform between the Balkan fold-thrust belt and the southern platform edge (Fig.1).

This area is defined as a transition zone (Bonchev et al., 1957) with different names – periplatform monocline (Garetskiy, 1968), pericratonic depression (Atanasov, 1973), and Targovishte-Provadiya step (Kalinko, 1976). In Monahov et al. (1981), along the Jurassic - Lower Cretaceous sediments, this area should be considered as the South Moesian periplatform area. Dabovski, Zagorchev (2009) present it as the South Moesian platform slope. It is more deeply buried and inclined to the south peripheral zone of the Bulgarian part of the Moesian platform.

The South Moesian periplatform area has a complex structural feature in which is dominated by the monoclinal south subsiding. Its formation starts from the beginning of Jurassic where the contemporary morphological image is shaped at the end of the Upper Jurassic and the Early Cretaceous periods. The geodynamic evolution of the area is marked by rift cycles in the Late Permian – Early Triassic, Late Triassic, Early Jurassic and Late Cretaceous periods that were repeatedly interrupted and followed by compression events (Georgiev et al., 2001). The major tectonic events and the deposition of a thicker diversion in the sediments were mainly

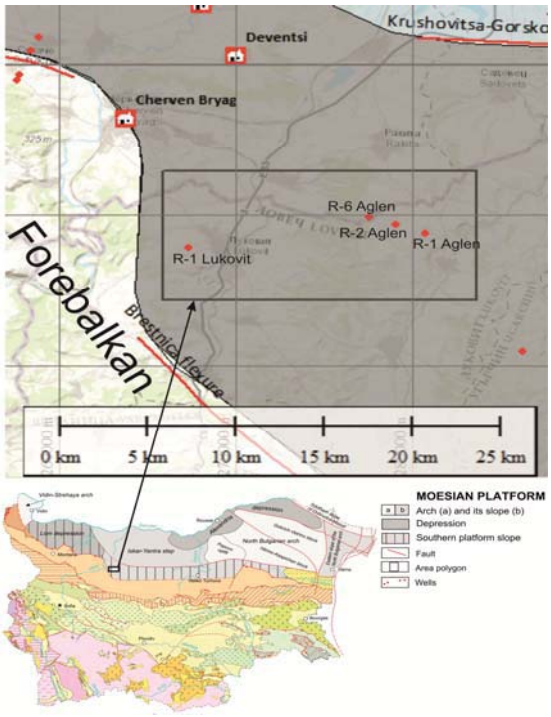

Fig. 1. Generalized tectonic map of Central North Bulgaria (Dabovski, Zagorchev, 2009) and Scheme of the studied area (Bokov and Atanasov, 1983).

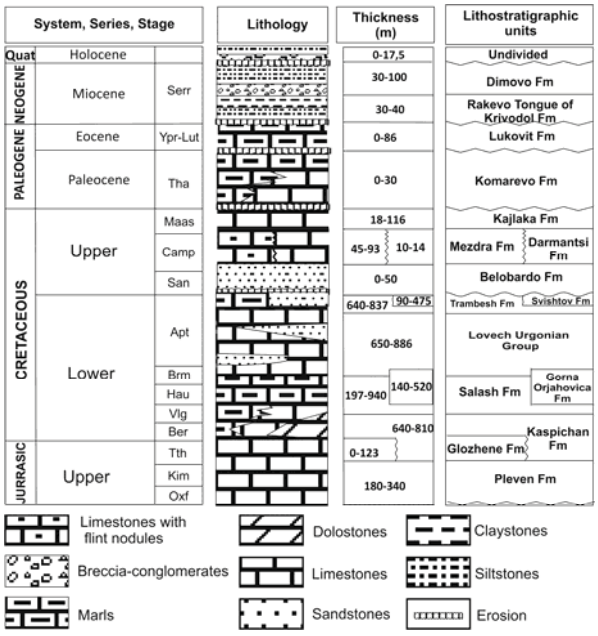

Fig. 2. Generalized lithostratigraphical scheme of sediments from the western part of the South Moesian platform slope (Bokov, 1983, with additions from the geological descriptions of R-1 Lukovit, R-1, 2, 6 Aglen).

through the Triassic, Lower-Middle Jurassic, Tithonian-Valanginian and to a lesser extent Late Cretaceous-Tertiary time (Botusharov, 2005). The sedimentary fill consists of Mesozoic rocks with a thickness of 4-6 km (Fig. 2) lying discordantly on a slightly deformed Paleozoic basement. They are covered by Paleogene, Neogene and Quaternary sediments and locally with Quaternary. The section has primarily a carbonate composition – limestones, clayey limestones, marls, and dolostones interbedded with relatively not so thick terrigenous deposits.

Methodology

To perform this analysis, well log data were used which include the curves of spontaneous potentials, deep laterolog resistivity, and gamma ray. They were processed by the Neuralog software, and were then imported in the Petrel software for further interpretation. The methodology of interpretation is entirely based on the concepts of the sequence-stratigraphic analysis (Mitchum and Van Wagoner. 1991; Posamentier et al. 1988a, 1988b). The presented well log sections are typical with their incomplete information, but are described in details according to the core and well cuttings.

Results

Based on studying the lithological descriptions and well log data, 5 sedimentary sequences (Fig. 3) formed within the transgressive-regressive cycles were separated.

Campanian-Maastrichtian second-order sequence

A sequence of the second order is separated. It covers the Campanian and Maastrichtian stages of the Upper Cretaceous. Its thickness reaches 187 m at the R-6 Aglen. The lower and upper sequence boundaries are erosive. It is composed of a highstand system tract, including the micritic limestones with flint concretions of the Mezdra formation (Fm) and the organogenic limestones of the Kaylaka Fm. The predominant part of the fossil remains in the Mezdra Fm is from organisms typical for the deep shelf environment (100-200m water column). While at the Kaylaka Fm - for shallow marine areas of the shelf, most likely as a result of the decrease of seawater towards the end of this system tract - the sequence is tracked at the four well sections.

Valanginian-Aptian second-order sequence

A Lower Cretaceous sequence of a second order is separated and comprises the stages from the Valanginian to the Aaptian. Its thickness reaches 2858 m at the R-1 Aglen. Only a highstand system track is outlined. The sequence begins with an erosion at the top of the Kaspichan Fm (at the R-1, 2, 6 Aglen), the Slivnitsa Fm (R-1 Lukovit), and ends again with erosion at the border of the Aptian-Upper Cretaceous. Within the scope of the sequence are the Salash Fm, the Gornooryahovo Fm, the Lovech Urgonian group, the Tramsbesh and the Svishtov Fm. Generally, the depositional environment is pelagic in the sediments of the Salash and the Gornooryahovo Fm, the latter being considered as a transitional shelf-deepwater setting because of the content of neritic fossil remains. The tendency of lowering the sea level can also be presumed with the deposition of a bed of clayey limestone in the upper parts of the Salash Fm (Fig. 3). The forming of the sediments of the Lovech Urgonian group (the Krushevo Fm, the Balgarene Fm, the Emen Fm, the Byala reka Fm, the Stratesh Fm, the Smochan Fm) is a direct reflection of the regressive development of the sedimentation basin towards the end of the Lower Cretaceous period when the subsiding rate was noticeably reduced and the adjacent elevated land on the south became the source of tremendous masses of diverse clastic and clay material. The sedimentation itself is with impulsive nature (Hrischev 1969, 1972). The sediments of the Trambesh Fm are formed in the shelf zone under a general regressive trend of the sea waters. Upward in the sedimentary section, the deposition of a bed of sandy sediments (presuming it is a wedge from the Roman Fm), subsequently the deposition of the Svishtov Fm inferring the reached eustatic minimum of the marine waters, increasing the influence of the alluvial systems from the south.

Callovian-Valanginian first-order sequence

Below the previous sequence, a sequence separated by Tchoumatchenco (2002) is observed with stratigraphic age Callovian-Valanginian. Based on the used well data, it is seen that its two boundaries are erosive. The thickness reaches 1453 m. It comprises a highstand system tract. Its sedimentary rocks have a carbonate composition (the Kaspichan Fm in the east, the Slivnitsa Fm and the Glozhene Fm in the west, the Pleven Fm in the east, the Yavorets Fm in the west). Tchoumatchenco (2002) relates the sediments of the Javorets Fm to the lowstand system tract, subsequently it is specified that they represent post-transgressive sediments typical for the highstand system tracts. The deposits of the Kaspichan Fm (at R-1, 2, 6 Aglen) are platform sediments deposited in a neritic environment. On the other hand, the limestones of the Slivnitsa Fm (at R-1 Lukovit) suggest the formation of submarine shallows in the pelagic parts of the basin.

Bajocian-Bathonian third-order sequence

It is tracked in the well sections of R-1, 2, 6 Aglen. It has the smallest thickness – 156 m and covers 2 stages - Bajocian and Bathonian from the Middle Jurassic. This circumstance implies the order of the sequence - third. It comprises two system tracts - a transgressive (TST) and a highstand (HST). The TST is composed of the sandy marls of the Bov Fm. The last 20 meters (4150-4170m at the R-1 Aglen) of this formation are characterized by increased values of the gamma ray log (GR). Generally, such anomaly could also be induced by micaceous sandstones and/or siltstones, but the other well logs (spontaneous potential and resistivity) do not confirm this.

Therefore, these anomalous values could be interpreted as an organic-rich sedimentary layer typical of the condensed section at TST. The radioactive elements that cause positive anomalies normally are sequestered by the organic matter (often cyanobacteria and phytoplankton). The top of this layer corresponds to the maximum flooding surface (Fig.3 - the green line). The transition to HST is marked by the deposition of clayey limestones of the Polaten Fm. The sediments are deposited in the shelf area of the basin.

Hettangian-Lower Bajocian second-order sequence

The sequence is totally transected by R-1, 2, 6 Aglen. It reaches up to 685 m thick at the R-6 Aglen. There is a stratigraphic range of Hettangian-Lower Bajocian and is of second order. Its boundaries are associated with erosion. Two system tracts (TST and HST) are distinguished. The transgressive system tract is represented by a condensed section - siltstones with glauconite and fossil remains-appertaining to the Bachiishte Fm. The latter is the thickest at R-1 Aglen - 15 m (4835-4850 m). GR values are high, reflecting the enrichment of glauconite and organic matter in this interval. The maximum flooding surface could be marked at the summit of the Bachiishte Fm. The highstand system tract comprises the sediments of the Ozirovo Fm and the Etropole Fm. Late sandstone intervals in the Etropole Fm could be

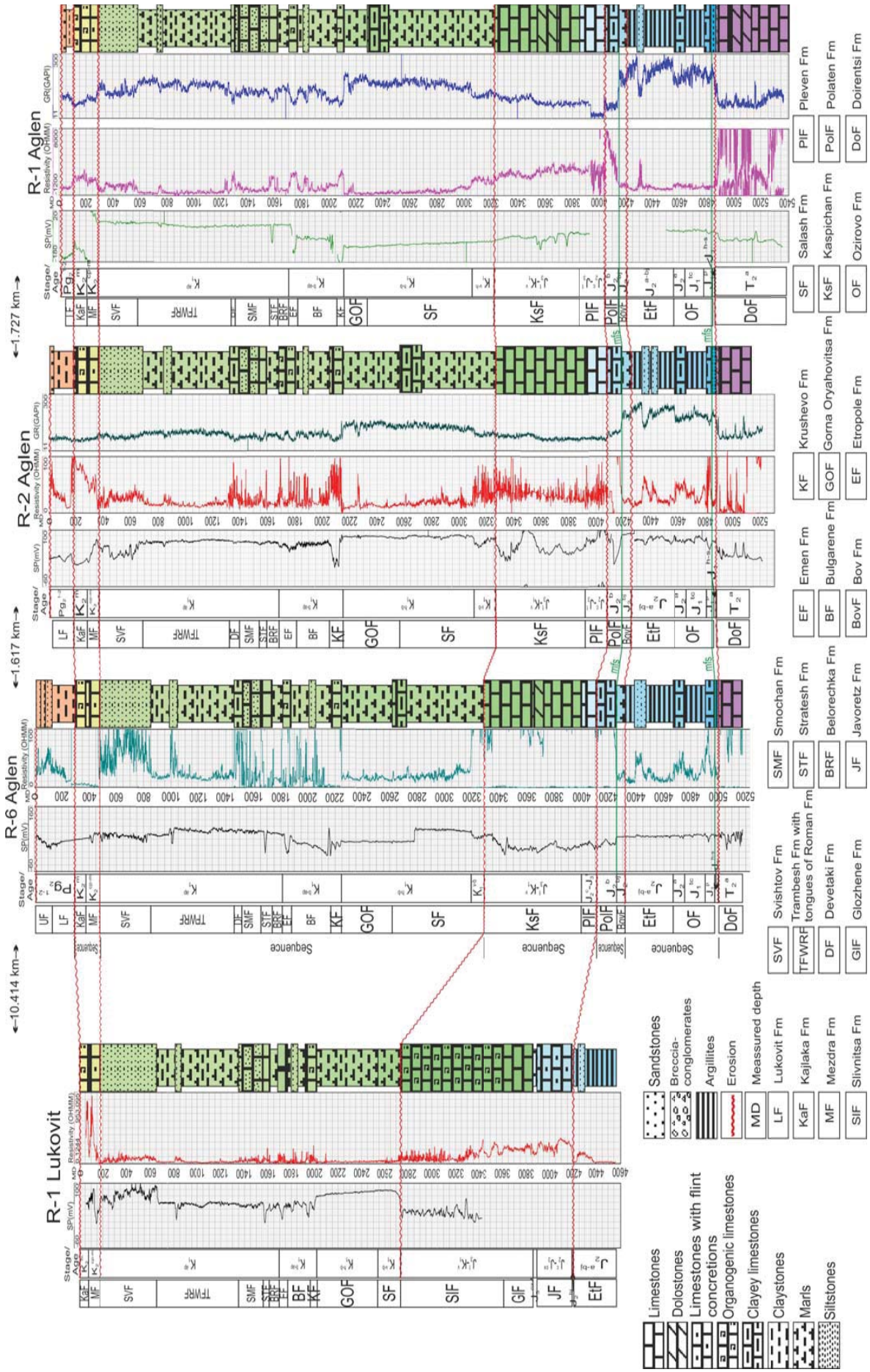

Fig. 3. Sedimentary sequences within the Mesozoic period interpreted on well log data (R-1 Lukovit; R-1, 2, 6 Aglen).

interpreted as a result of the reached eustatic minimum of the sea level and increasing the influence of the alluvial systems from the south. The sediments are deposited in the shelf area of the basin.

Conclusions

Based on the conducted study and the results in the Mesozoic section of the surveyed area, five sedimentary sequences from different orders (Campanian-Maastrichtian second-order sequence, Valanginian-Aptian second-order sequence, Callovian-Valanginian first-order sequence, Bajocian-Bathonian third-order sequence, Hettangian-Lower Bajocian second-order sequence) were distinguished along with their elements (system tracts) formed within transgressive-regressive cycles. Based on the analysis of the participating official lithostratigraphic units and well-log interpretation, the paleoenvironment of sedimentation is predicted for each individual sedimentary sequence.

The sedimentary sequences are predominantly with carbonate composition, with interbeds of terrigenous material, typical for the late stages of the highstand system tract at a reached eustatic minimum, increasing the influence of the source of the clastics from the south.

The paleoenvironments of deposition mainly represent the shelf area of the basin, with individual sequences falling either in the shallow or in the deep zone. During the Lower Cretaceous period, the depositional environment is represented by pelagic setting. The most significant differences in the facial appearance and sedimentation settings are found within the scope of the Callovian-Valanginian first-order sequence as a direct response to the complex geodynamic evolution of the basin during that period.The impulsive nature of importing a clastic material in the Lovech Urgonian group (Lower Cretaceous) would produce some collectors with the potential for storing natural gas or CO_2 sequestration.

It is difficult to pinpoint favorable reservoir bodies, especially when they have to be predicted within the HST. In this case, it is necessary to combine with seismic profiles in order to achieve a complete sequence-stratigraphic interpretation with emphasis on the petroleum system approach.

References

Айданлийски, Г., Д. Тронков, А. Щрасер. Цикличност в долнотриаската серия между ж.п. спирка Оплетня и мах. Сфражен. – В: Синьовски, Д. (ред), *Геоложки маршрути в северната част на Искърския пролом* С., Изд. В. Недков, 2004. - 90-101. (Aydanliyski, G., D. Tronkov, A. Shraser. Tsiklichnost v dolnotriaskata seria mezhdu zh.p. spirka Opletnya i mah. Sfrazhen. – V: Sinyovski, D. (red), Geolozhki marshruti v severnata chast na Iskarskia prolom S., Izd. V. Nedkov, 2004. – 90-101.)

Атанасов, А. Закономерности в строежа и нефтогазоносната перспективност на Северна България. – *Спис. Бълг. геол. д-во*, *34*, 3, 1973. - 247-271. (Atanasov, A. Zakonomersnosti v stroezha i neftogazonosnata perspektivnost na Severna Bulgaria. – Spis. Bulg. geol. d-vo, 34, 3, 1973. - 247-271.)

Боков, П., А. Атанасов. Геология и въглеводородна перспективност на Мизийската платформа в Централна Северна България, С., изд. Техника. 1983. (Bokov, P., A. Atanasov. Geologia i vaglevodorodna perspektivnost na Miziyskata platform v Tsentralna Severna Bulgaria, S., izd. Tehnika. 1983.)

Бончев, Ек., Ем. Белмустаков, М. Йорданов, Ю. Карагюлева. Главни линии в геоложкия строеж на Предбалкана между р. Янтра и Черно море. – *Изв.* Геол. инст. БАН, *5*, 1957. - 3-78. (Bonchev, Ek., Em. Belmustakov, M. Yordanov, Yu. Karagyuleva. 1957. Glavni linii v geolozhkia stroezh na Predbalkana mezhdu r. Yantra i Cherno more.- Izv. Geol. Inst. BAN, 5, 3-78.)

Ботушаров, Н. Перспективни нефтогазомайчини скали от западната-централна част на Южномизийската периплатформена област. Год. МГУ, Том 48, Св. I, 2005. - 17-23. (Botusharov, N. Perspektivni neftogazomaychini skali ot zapadnata-tsentralna chast na Yuzhnomiziyskata periplatformena oblast. God. MGU, Tom 48, Sv. I, 2005. - 17-23.)

Гарецкий, Р. Г. О южной границе Мизийской плиты (Болгария). – Докл. АН СССР, 179, 1, 1968. - 155-158. (Garetskiy, R. G. O yuzhnoy granitse Miziyskoy pliti (Bolgaria). – Dokl. AN SSSR, 179, 1, 1968. - 155-158.)

Георгиев, Г., Бакърджиев, И. Сеизмостратиграфска интерпретация на триаската секвенция в Източния Предбалкан. Год. Соф. у-т "Св. Кл. Охридски", ГГФ, кн. 1 – Геология, т. 96, 2004. - 87-102. (Georgiev, G., Bakardzhiev, I. Seizmostratigrafska interpretatsia na triaskata sekventsia v Iztochnia Predbalkan. God. Sof. u-t "Sv. Kl. Ohridski", GGF, kn. 1 – Geologia, t. 96. 2004. - 87-102.)

Дабовски, Х., Загорчев, И. Глава 5.1. Въведение: Мезозойска еволюция и алпийски строеж. – в: Загорчев, И., Дабовски, Х., Николов, Т. (ред.). Геология на България. Том II. Част 5. Мезозойска геология. Акад. изд. "Проф. М. Дринов", С.; 2009. - 13-37. (Dabovski, H., Zagorchev, I. Glava 5.1. Vavedenie: Mezozoyska evolyutsia i alpiyski stroezh. – v: Zagorchev, I., H. Dabovski, T. Nikolov, (red.). Geologia na Bulgaria. Tom II, Chast 5. Mezozoyska geologia. Akad. Izd. "Prof. M. Drinov", S.; 2009. - 13-37.)

Калинко, М. К. (ред.). Геология и нефтогазоносность Северной Болгарий. М., Недра, 1976. - 243 с. (Kalinko, M. K. (red.) Geologia I neftogazonosnost Severnoy Bolgarii, M. Nedra, 1976. – 243p.)

Монахов, И., С. Желев, Г. Георгиев. Нефтогазоносна перспективност на мезозойските наслаги от южната част на Североизточна България. – В: Геология и нефтогазоносност на Североизточна България (ред. Мандев, П., И. Начев). С., Техника, 1981. - 88-97. (Monahov, I., S. Zhelev, G. Georgiev. Neftogazonosna perspektivnost na mezozoiskite naslagi ot yuzhnata chast na Severoiztochna Bulgaria. – V: Geologia I neftogazonosnost na Severoiztochna Balgaria (red. Mandev, P., I. Nachev). S., Tehnika, 1981. - 88-97.)

Хрисчев, Х. Литоложки строеж и условия на образуване на Еменската варовикова свита (Ловешка ургонска група).

– Изв. Геол. инст., сер. стратигр. и литол., 18; 1969. - 171-205. (Hrischev, H. Litolozhki stroezh i uslovia na obrazuvane na Emenskata varovikova svita (Loveshka urgonska grupa). – Izv. Geol. inst., ser. stratigr. i litol., 18; 1969. - 171-205.)

Хрисчев, Х. Опит за палеогеографска реконструкция на Стратешката варовикова свита (Ловешка ургонска група). - Изв. Геол. инст., сер. стратигр. и литол., 21; 1972. - 207-220. (Hrischev, H. Opit za paleogeografska rekonstrukcia na Strateshkata varovikova svita (Loveshka urgonska grupa). – Izv. Geol. inst., ser. stratigr. i litol., 21; 1972. - 207-220.)

Ciszak, R., T. Nikolov, B. Peybernes, M. Ivanov, N. D. Mocurova, S. Calzada. Sequence stratigraphy of a transitional Valanginian and Hauterivian outcrop in NE Bulgaria and occurrence of the brachiopod Loriolithyris valdensis. – Batallera, Barcelona, 9; 2000. - 1-6.

Georgiev, G., C. Dabovski, G. Stanisheva-Vassileva. East Srednogorie-Balkan Rift Zone. – In: Peri-Tethys Memoir 6: PeriTethyan Rift/Wrench Basins and Passive Margins (Eds. P. A. Ziegler, W. Cavazza, A. H. F. Robertson, S. Crasquin-Soleau). Mem. Mus. Natn. Hist. Nat., Paris, *186*, 2001. - 259-293.

Ivanov, M., K. Stoykova. The Albian ammonites, nannofossils and sequence stratigraphy in Bulgaria.- Mineralia Slovaca, 29; 1997. - 295.

Mitchum, R. M. Jr., J. C. Van Wagoner. High-frequency sequences and their stacking patterns: sequence-stratigraphic evidence of high-frequency eustatic cycles. – Sedimentary geology , 70, 1991. - 131-160.

Mader, D., G. Ćatalov. Comparative palaeoenvironmental modelling of Buntsandstein braided river evolution in Bulgaria and Middle Europe. – Geologica Balc., 22, 6, 1992. - 21- 61.

Nikolov, T., B. Peybernes, R. Cizsak, M. Ivanov. Enregistrement sedimentaire de la tectonique extensive et de l'eustatisme dans le Cretace basal du Prebalkan central et oriental (Bulgarie). C. R. Acad. Sci., Paris, Sciences de la terre et des planets, 326, 1998. - 43-49.

Nikolov,T., M. Ivanov, K. Stoykova, B. Peybernes, R. Ciszak. Organisation sequentielle des depots du Tithonien superieur a l'Albien le long d'un transect Trojan-Pleven-Svistov (Bulgarie du Centre-Nord).– Сп. Бълг. геол. д-во, 59, 2; 1998. - 3-12.

Posamentier, H. W., M. T. Jervey, P. R. Vail. Eustatic controls on clastic deposition I – conceptual framework. In: Wigus et al. (eds.) Sea-level Changes: An Integrated Approach. Soc. Econ. Paleontol. Mineral. Spec. Publ. 42, 1988a. - 109-124.

Posamentier, H. W., P. R. Vail. Eustatic controls on clastic deposition II – sequence and system tract models. In: Wilgus et al. (eds.). Sea-level Changes: An Integrated Approach. Soc. Econ. Paleontol. Mineral. Spec. Publ. 42, 1988b. - 125-154.

Tchoumatchenco, P. Jurassic outcrop depositional sequence stratigraphy in western Bulgaria. – Geologica Balc., 32. 2-4; 2002. - 49-54.

The article is reviewed by Prof. Vassil Balinov, DSci. and Assoc. Prof. Dr Nikola Botusharov.

GEOLOGICAL FEATURES OF THE MESOZOIC SECTION BETWEEN THE VILLAGES OF STARO SELO AND STUDENA IN THE GOLO BARDO MOUNTAIN, WESTERN BULGARIA

Elitsa Ilieva

University of Mining and Geology "St. Ivan Rilski", 1700 Sofia; elicailieva@mgu.bg

ABSTRACT. The subject of this study is the Mesozoic section exposed on the road escarpment of the Struma highway that intersects the Golo Bardo Mountain between the villages of Staro Selo and Studena. The incision is predominated by Triassic, Jurassic and Lower Cretaceous sedimentary rocks which relate to the Formations of Svidol (Upper Olenekian), Mogila (Upper Olenekian – Lower Anizian), Pancharevo (Upper Olenekian – Lower Anizian), Bosnek (Anisian), Radomir (Anisian - Ladinian), Rusinovdel (Carnian-Norian), Gradets (Aalenian), Poletintsi (Middle Aalenian - Lower Bathonian), Gintsi (Lower Kimmeridgian), Drugan (Middle Kimmeridgian), Neshkovo (Middle-Upper Kimmeridgian), Kostel (Upper Kimmeridgian-Middle Tithonian) and a breccia conglomerate unit (Middle Oligocene). Structural-geological observations and interpretations of the obtained data were carried out, with special attention paid to the discontinuations of the sedimentary sequence. The normal superpositional relations are disturbed by a fault and fold tectonics, marking significant tectonic deformations related to several tectonic stages: the Late Kimmerian (T-J), the Austrian (K_1- K_2), the supposed Laramide (K_1-Pg), the Sava (Pg3-N), and the Neotectonic (N-Q) stage.

Keywords: Mesozoic section, Golo Bardo, tectonic deformations

ГЕОЛОЖКИ ОСОБЕНОСТИ НА МЕЗОЗОЙСКИЯ РАЗРЕЗ МЕЖДУ СЕЛАТА СТАРО СЕЛО И СТУДЕНА В ГОЛО БЪРДО, ЗАПАДНА БЪЛГАРИЯ

Елица Илиева

Минно-геоложки университет "Св. Иван Рилски", 1700 София; elicailieva@mgu.bg

РЕЗЮМЕ. Обект на изследване на настоящата работа е мезозойският разрез, който се разкрива в шкарпа на автомагистрала Струма, пресичаща планината Голо бърдо между селата Студена и Старо село. В разреза преобладават триаски, юрски и долнокредни седиментни скали, отнесени към Свидолска (горен Оленек), Могилска (горен Оленек-долен Аниз), Панчаревска (горен Оленек – долен Аниз), Боснекска (Аниз), Радомирска (Аниз – Ладин), Русиновделска (Карн – Нор), Градецка (Аален), Полатенска (среден Аален – долен Бат), Гинска (долен Кимеридж). Друганска (среден Кимеридж), Нешковска (среден – горен Кимеридж), Костелска (горен Кимеридж – среден Титон) свити и брекчо-конгломератна задруга (среден Олигоцен). Извършени са структурно-геоложки наблюдения и интерпретация на получените данни, като специално внимание е обърнато на прекъснатостите в разреза. Нормалните суперпозиционни отношения са нарушени от гънкови и разломни тектонски деформации, свързани с няколко тектонски фази: Къснокимерска (T-J), Австрийска (K_1- K_2), предполагаема Ларамийска (K_1-Pg), Савска (Pg_3-N) и Неотектонска (N-Q).

Ключови думи: Мезозойски разрез, Голо бърдо, тектонски деформации

Introduction

The main purpose of this work is to establish the nature of the relations between the lithostratigraphic units found in the Golo Bardo area. For this purpose, a section along the Struma highway, from the southern end of the village of Studena to the village of Staro Selo, is described. The article is a natural continuation of the problems discussed in our previous work – Ilieva, Zhelev (2010) and Ilieva, Dimitrov (2011).

In the first article, a new unit for the region was introduced – a brecco-conglomerate group with a continental, alluvial-prolavial-lymical character, which is a correlate of the Paleogene (Priabon - Oligocene) from the Pernik graben. It is a tectonic wedge in the dolomite limestones of the Middle Triassic Bosnek Fm, formed after the Paleogene during the Sava orogenesis.

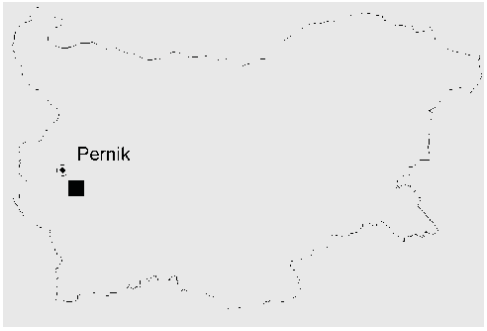

Fig. 1. Location of the Studena – Staro selo section.

It was found that the Mesozoic rocks in the area of the Golo Bardo mountain participate in large upright and open regional folds with the NW-SE direction of their axis (Ilieva, Ivanov, 2011). The new structural-geological observations show that the superpositional sediment relationships are not preserved anywhere, but a reversed layer of early bedding is observed.

Material and methodology

The presented study is based on structural and geological mapping of the outcrops along the Struma highway from the southern end of the village of Studena to the northern end of the village of Staro Selo (Fig. 1, Fig. 3). Planar and linear structural elements were measured and geometric modeling was performed using CAD software and stereographic software.

In the next stage, the observations of the section Studena - Staro Selo should be linked with observations in other outcrops from the region so that the regional distribution of already established structural relations could be confirmed.

State of the problem

The first information about Golo Burdo was given by E. Bonchev (1931), G. Bonchev (1936), S. Dimitrov, and Ts. Dimitrov (1931) who examined the tectonic structures of the Retro-Vitosha region. The research of Stefanov (1928, 1932, 1936a, b, 1943) is focused on the Triassic fauna as well as the Triassic lithostratigraphy of the Golo Bardo mountain. Detailed geological and structural-geological studies specific to the area are covered in the works of Moev (1967a, b). More recently, modern tectonic notions about the area are presented in the works of Zagorchev (1980, 1981, 1984, 1994, etc.) and Zagorchev et al. (1991). Sapunov et al. (1985) offer several distinct cross sections for the area associated with the Callovian-Upper Jurassic sediments. Subsequently, Budurov et al. (1995) elaborated detailed key sections for the Golo Bardo area, exploring for foraminifera and conodonts. The authors provided a large amount of paleontological data and significantly detailed the age intervals of the lithostratigraphical units in the area. The latest regional and geological ideas for the region were covered by Boudurov et al. (2009).

Palaeozoic, Triassic, Jurassic, Paleogene and Quaternary rocks are revealed in the studied area (Fig. 2). The stratigraphy of the area is considered in a number of literary sources. Within the boundary of the cross section belongs the Strouma diorite Fm (Stefanov, Dimitrov, 1936) of Neoproterozoic-Cambrian age. The subdivision of the Triassic lithostratigraphic units is given in detail in the works of Tronkov (1968, 1975, 1981, 1983).

The Triassic sediments in Golo Bardo are incorporated in several groups: the Petrohan Terrigenous group, the Iskar Carbonate Group, and a very limited Moesian Terrigenous-Carbonate Group, which is out of the area of the section. Jurassic sediments are discussed in numerous scientific publications by Sapunov (1969), Sapunov et al. (1985), as well as by Nikolov, Sapunov (1970), Dodekova et al. (1984), and others.

The Jurassic system is represented by the Gradets and Polaten Fm, the Neshkovo and Kostel Fm which are united in the Central Balkan Flish Group, while the Gintsi and Drugan Fm are united in the West Balkan Carbonate Group.

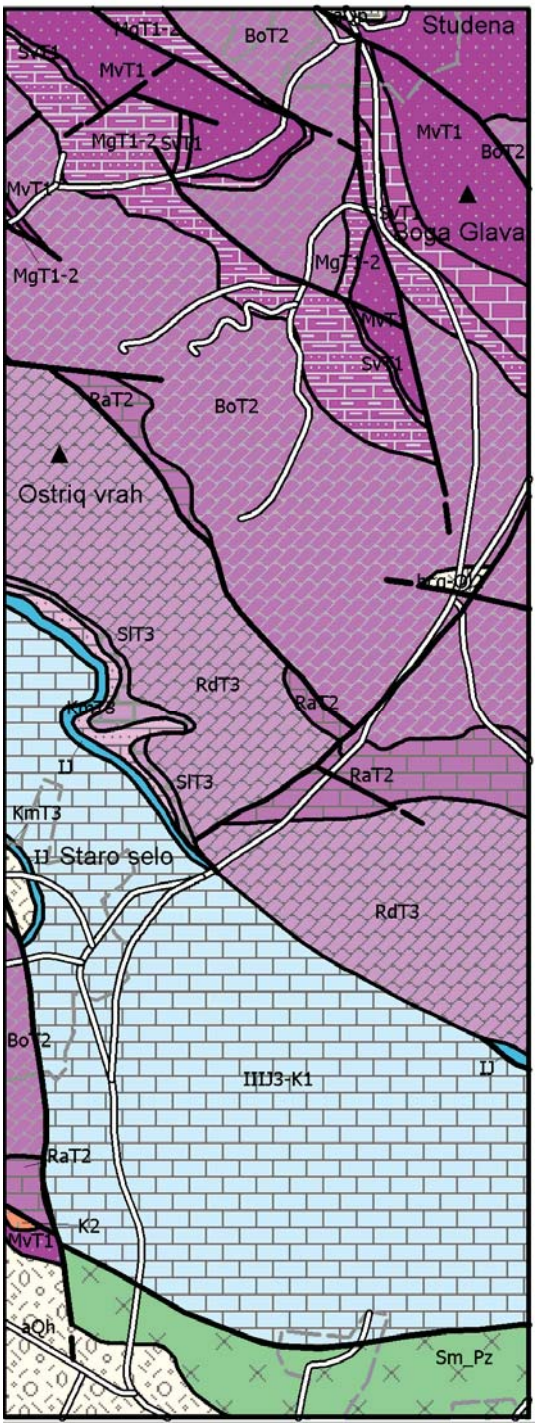

Fig. 2. Geologic map, scale 1:50 000 with amendments and supplements (Antonov et al., 2011 a, b). SmPz – Strouma diorite Fm, SvT_1 – Svidol Fm, MgT_{1-2} – Mogila Fm, PaT_{1-2} – Pancharevo Fm, BoT_2 – Bosnek Fm, RaT_2 – Radomir Fm, RdT_3 – Rusinovdel Fm, KmT_3 – Komshtitsa Fm, SlT_3 – Slaveeva Fm, IJ – Gradets, Polaten, Gintsi, Drugan Fm, $IIIJ_3$-K_1 Cenralbalkan Flish Group – Neshkovo and Kostel Fm, K_2 – granodiorite porphyry, bcg Ol_2 – breccia-conglomerate Fm, aQ_h – alluvial sediments.

Results

Description of the cross section

This section is located along the Struma highway, starting from the southern end of the village of Studena and ending at the village of Staro Selo (Fig. 3). The starting point (km 0 + 000) has the following coordinates: 675202 E and 4711063 N in WGS 84 coordinate system, UTM projection, zone 34. The western escarpment of the highway is mostly documented where the outcrops are more representative, and in some typical cases the eastern one also. The section shown on Figure 4 is drawn from south to north and represents the geological features of the Mesozoic section between the villages of Studena and Staro Selo. The geological description of the Mesozoic section between the villages of Studena and Staro Selo is given in Table 1.

Several cross sections from different authors have been done on the territory of the Golo Bardo mountain. The stratigraphic relations among Triassic, Jurassic and Cretaceous rocks revealed in the area are discussed in the work of Budurov et al. (1995), which describes three incisions in the area of Bosnek and Radomir. Investigating the geological development and the paleo-dynamics of Bulgaria through the Mesozoic and the Tertiary, they prove lateral differences in each cross section in Golo Bardo. It was found that the Jurassic sediments are transgressive and discordant with significant hiatus on the Triassic rocks.

Fig. 3. Location of the Studena – Staro selo section with the waypoints.

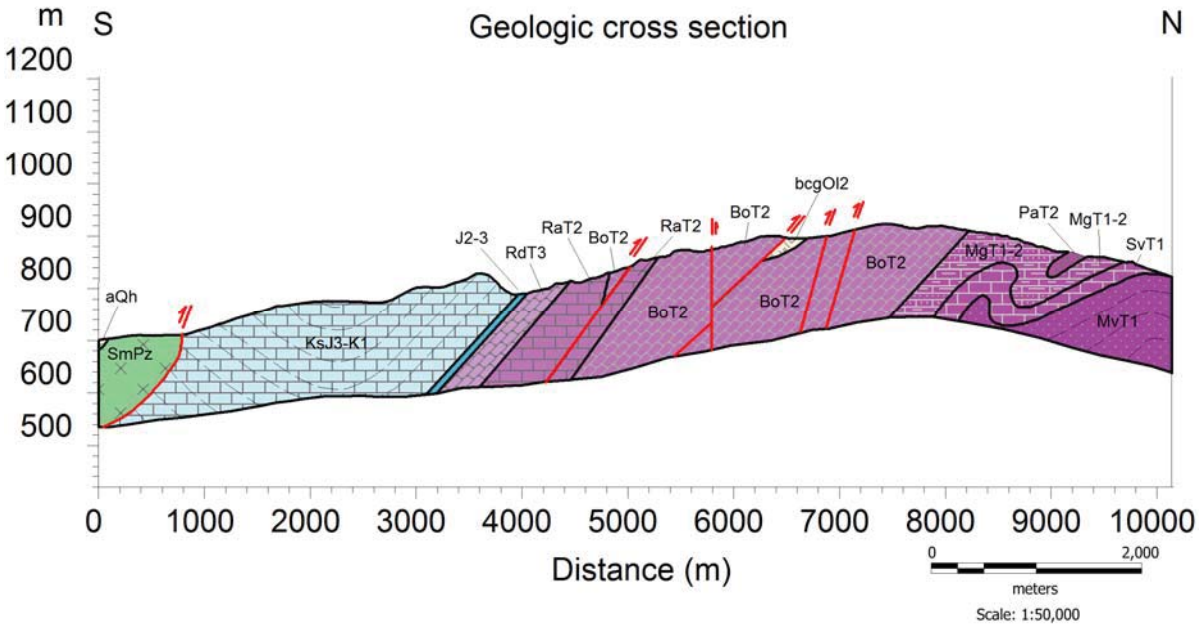

Fig. 4. Geologic cross section, scale 1:50 000. SmPz – Strouma diorite Fm, SvT_1 - Svidol Fm, MgT_{1-2} - Mogila Fm, PaT_{1-2} – Pancharevo Fm, BoT_2 – Bosnek Fm, RaT_2 – Radomir Fm, RdT_3 - Rusinovdel Fm, KmT_3 – Komshtitsa Fm, SlT_3 – Slaveeva Fm, IJ - Gradets, Poletintsi, Gintsi, Drugan Fm, $IIIJ_3$-K_1 Cenral Balkan flish group – Neshkovo and Kostel Fm, K_2 - granodiorite porphyry, $bcgOl_2$ – breccia-conglomerate Fm, aQ_h – alluvial sediments, red line – fault.

Figure 5 shows a geological map comprising the lithostratigraphic units and the fracture structures observed along the incision. It has been found that the Svidol Fm, described in the works of Goranov et al. (2002) and Antonov et al. (2011a, b), differs substantially from the initial description of Chatalov (1974) where it is characterized by an alternation of red, cream or gray carbonate rocks. According to Tronkov (1983), its lateral analogue - the Lyubash Fm, consisting of thin-layer allevrolite and sandy marls, limestones and limy sandstones - is observed in the abandoned quarry south of the village of Batanovtsi.

In the beginning of the section, beige sandy limestones and striped sandy limestones with muscovite (Fig. 7, d) are revealed which are not parts of the characteristic lithology of either the Svidol or the Lyubash Fm. Most likely, this is a multifacial lateral analogue that could be identified as an independent formation.

This requires more in-depth research, which will be reflected in a subsequent work. In this article, these rocks are described conditionally as Svidol? Formation.

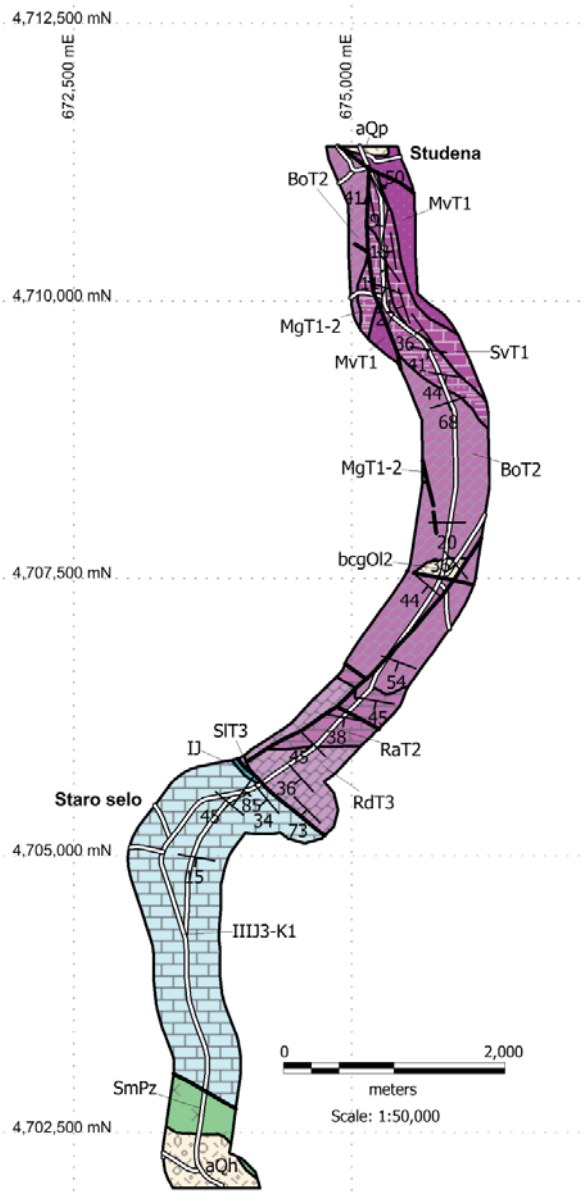

Fig. 5. Plan of the main structural elements observed at the Studena – Staro selo cross section, scale 1:50 000. SmPz – Strouma diorite Fm, SvT_1 - Svidol Fm, MgT_{1-2} - Mogila Fm, PaT_{1-2} – Pancharevo Fm, BoT_2 – Bosnek Fm, RaT_2 – Radomir Fm, RdT_3 - Rusinovdel Fm, KmT_3 – Komshtitsa Fm, SIT_3 – Slaveeva Fm, IJ - Gradets, Polaten, Gintsi, Drugan Fm, $IIIJ_3$-K_1 Cenral Balkan Flish Group – Neshkovo and Kostel Fm, K_2 - granodiorite porphyry, $bcgOl_2$ – breccia-conglomerate Fm, aQ_h – alluvial sediments. Bold line – fault.

Data from the conducted study showed that the tectonic contact between the black limestones of the Radomir Fm and the sugary dolomites of the Bosnek Fm, described by Zagorchev et al. (1991, 1994) and Antonov et al. (2011b), are not faulty. The observed folds (mainly in the Radomir Fm) of the contact between the two units are most probably the result of inter-formal slip in the process of tectonic deformation due to the different rheological properties of the rocks (Fig. 7, c). In places close to the contact, the limestones of the Radomir Fm are folded into isoklinal folds, but in most cases the contact is normal. The dolomites of the Bosnek Fm, on the other hand, are slightly fractured.

Structural-geological setting

The study revealed a complex picture of a folding interference in which folding events of different ages are partially co-axially overlaid so that later events mask the earlier effects.

Several tectonic stages have been set up in the Golo Bardo area. The demarcation of the Eo-Cimmerian tectonic stage from the Austrian is possible due to the pronounced azimuthal and angular unconformity between the Triassic and Jurassic-Lower Cretaceous stratigraphic sequence. The Laramide tectonic stage is not proven here because of the lack of Upper Cretaceous rocks, but it is established in the western parts of Golo Bardo. In the section where the research was carried out Sava tectonic stage was also found, through which a tectonic wedge of the breccia-conglomerate group was formed, which is all described by Ilieva, Zhelev (2010). The Neotectonic stage is manifested mainly by late faults that displace the structures, which have been already formed.

In a previous publication (Ilieva, Dimitrov, 2011), in two outcrops of the flish sediments of the Kostel Fm, the hinge of a lying fold was observed and the assumption of more such folds on a regional scale was made. In the present study, lying folds or a reversed layering was found. This means that the fold described is a local phenomenon, and on a regional scale the bedding can be considered normal.

Such folds of a lower order were found in the Pancharevo Fm PaT_{1-2} (Fig. 7a, b). They have a thigh orientation of limbs 240 to 250° and a direction of the axis – WNW-ESE. The type of the contact between the Pancharevo Fm and the older Mogila Fm (Fig. 7e) is normal lithological.

The diagrams of the cyclographic traces (Fig 6a, b) and the polar statistical diagrams of surface measurements in Triassic and Jurassic (Fig 6c, d) show values for their maxima, respectively, s_0-78 to 81/72° for Triasic sediments and s_0-46/50° for Jurassic ones. The difference in the dip directions is 23 - 35° and 18 - 22° in the dip. This indicates the existence of a clear azimuthal and angular unconformity between the Triassic and Jurassic-Lower Cretaceous tectonic stages.

The restoration of the primary geometry and age of the folds is associated with a certain difficulty because of the incompleteness of the outcrops. For this purpose, it is necessary to make a correlation of the structures on a regional scale and to use indirect data about the age of analogous deformations from other outcrops.

Table 1.

Geological description of the Mesozoic section along the Struma Highway between the villages of Studena and Staro Selo. The description is from north to south.

From (km)	To (km)	Lithostratigraphic unit	Index	Lithographic description	Layering orientation
0+000	0+088	Bosnek Formation	BoT_2	Strongly carced gray to dark gray dolomites and dolomite limestones of the Bosnek Fm	Unclear elements-
0+088	0+993	Svidol Formation?	SvT_1?	Beige sandy limestones, alternating with black sandy limestones with muscovite with multiple calcific lenses and veins	S_0-280/18°
0+993	1+436	No outcrops	-	No outcrops	-
1+436	1+678	Mogila Formation	MgT_{1-2}	Dark gray micritic limestones in places brecciated	S_0-241/38°
1+678	1+766	Pancharevo Formation	PaT_{1-2}	Light gray, hydrothermally altered sandy limestones with isoclinal metric folds. In the eastern escarpment of the road, under the limestones, are observed middle-layered, white to light gray, mica, quartz sandstones to gravelites	S_0-229/36°
1+766	2+020	Mogila Formation	MgT_{1-2}	Black intraclastic limestones	S_0-210/49°
2+020	2+406	Bosnek Formation	BoT_2	Light gray, striped dolomites	S_0-170/25°.
2+406	3+706	Bosnek Formation	BoT_2	Cracked, brecciated dolomites, forming screes	S_0-200/45°
3+706	3+786	Breccia-conglomerate Formation	$bcgOl_2$	Breccia-conglomerates and clays with lenticular layers of acidic tufts and limestones	S_0-200/45
3+786	4+886	Bosnek Formation	BoT_2	Bright, massive, locally striped, sugary dolomites	S_0-190/45°;
4+886	5+109	Radomir Formation	RaT_2	Dark limestones with abundant, but focused on separate levels, detrital component and bivalve fossils	S_0-190/36°
5+109	5+229	Bosnek Formation	BoT_2	Sugary, massive to striped dolomites of the Bosnek Fm on a contact with the black limestones of Radomir Fm	S_0-190/38°
5+229	5+637	Radomir Formation	RaT_2	Medium- to heavy-bedded sandy, bio-detrital light gray limestones with rare fine alevrolite layers. They are alternated with thin-bedded, carbonate, brownish alevrolite and black, aphanitic limestones	S_0-190/45°;
5+637	6+124	Rusinovdel Formation	RdT_3	Striped dolomites, medium-bedded, light and dark gray	S_0-225/45°
6+124	7+624	Kostel Formation (Cenral Balkan flish group)	KsJ_3-K_1 ($IIIJ_3$-K_1)	Flish alternation of medium-grained, fine-striped limey sandstones, alevrolites and argillites	S_0-220 /45°

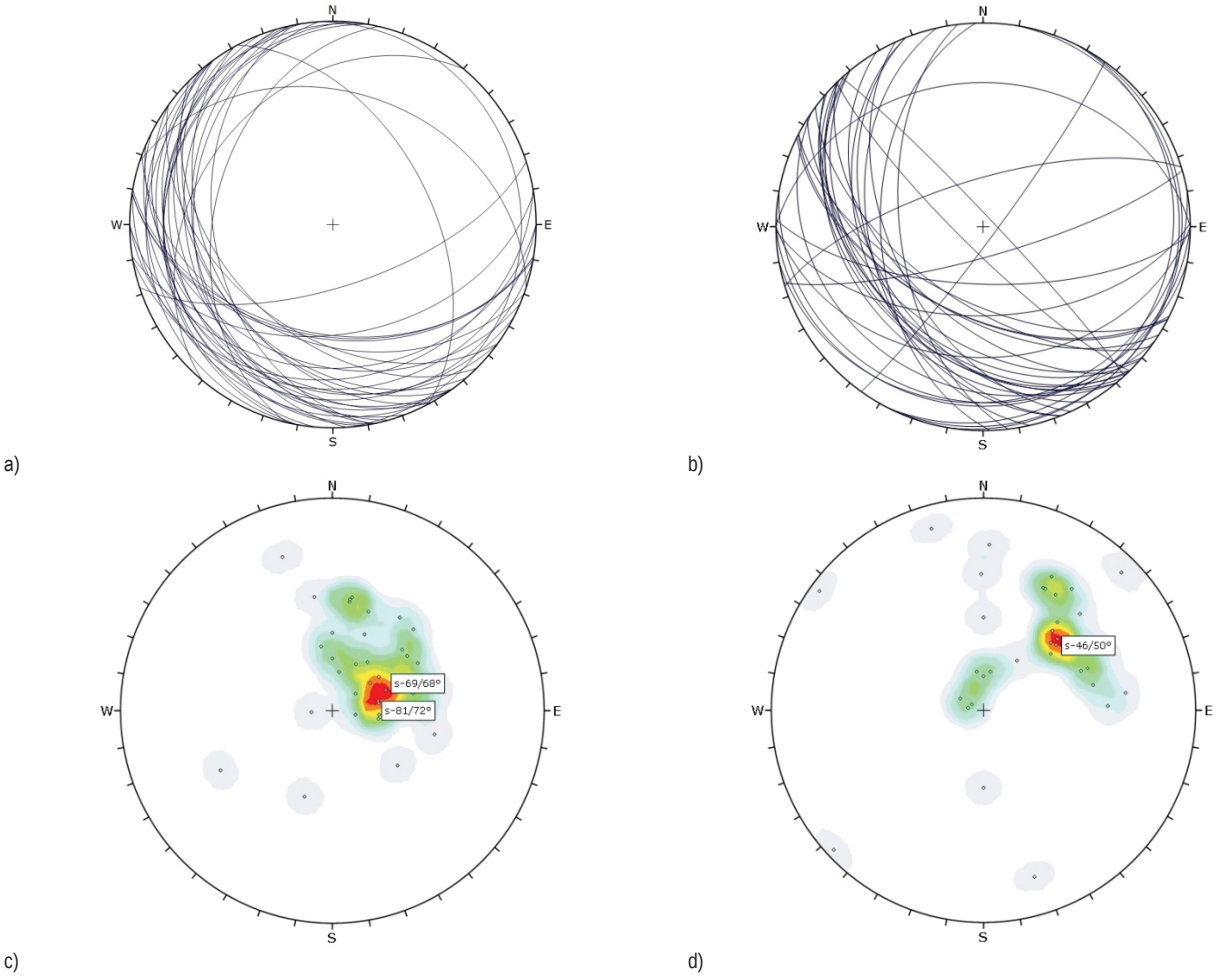

a) b) c) d)

Fig. 6. **a**) Diagram of the cyclographic traces of 37 planar surfaces in the Triassic sediments, b) Diagram of the cyclographic traces of 36 planar surfaces in the Jurassic sediments, c) Density diagram of poles of 37 planar surfaces in the Triassic sediments with the maxima, d) Density diagram of poles of 37 planar surfaces in the Jurassic sediments with the maxima

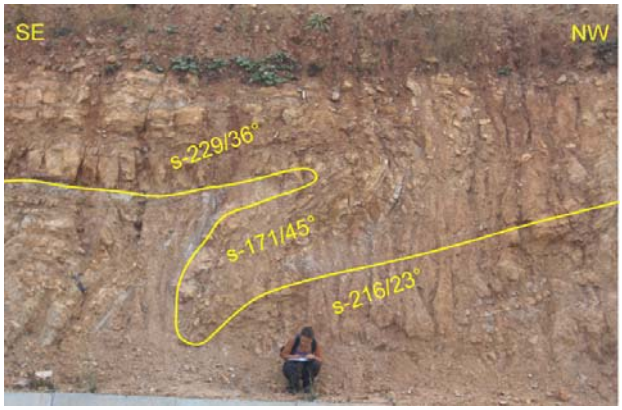

a)

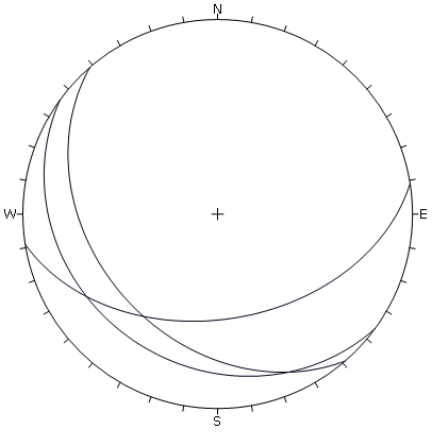

b)

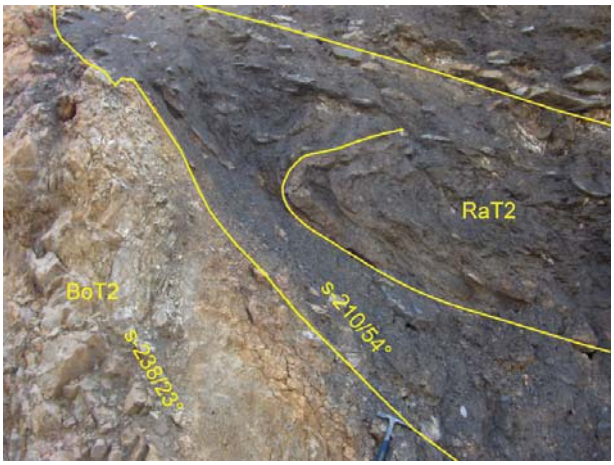

c)

d)

e)

Fig. 7. a) Lower-order fold in Pancharevo Fm (PaT_{1-2}), b) Diagram of the cyclographic traces of lower-order folds in Pancharevo Fm (PaT_{1-2}), c) Interfacial sliding between the dolomites of the Bosnek Fm and the limestones of the Radomir Fm, d) Sandy, striped limestones from the Svidol ? Fm, e) Contact between Pancharevo and Mogila Fm.

Conclusion

The described Studena - Staro Selo section revealed complex tectonic relationships between the lithostratigraphic units in the area. It has been found that Mesozoic sediments in the area are affected by several tectonic folding phases – Eo-Cimmerian, Austrian, Sava and Neotektonic. Regionally, the construction is dominated by large folds with NW-SE direction of the axes. The cross section shows the SW limb of a large conical to cylindrical fold that is refolded by younger folds. The demarcation of the Eo-Cimmerian tectonic stage by the Austrian stage is possibly due to the pronounced azimuthal and angular unconformity between the Triassic and the Jurassic-Lower Cretaceous tectonic stages.

Acknowledgments. I thank my colleagues from the Department of Geology and Geoinformatics for the critical remarks and valuable advice during the work on this article.

The research was funded through research project № ГПФ-208/2017 of the UMG "St. Ivan Rilski".

References

Антонов, М., П. Милованов, А. Попов, С. Герджиков, М. Дюлгеров. Обяснителна записка към геоложка карта на България, М1:50000. Картен лист К-34-59-А (Перник). – София, МОСВ, 2011а. - 40 с. (Antonov, M., P. Milovanov, A. Popov, S. Gerdzhikov, M. Dyulgerov. 2011. Obyasnitelna zapiska kam geolozhka karta na Bulgaria, M1:50000. Karten list K-34-59-A (Pernik). Sofia, MOSV, 2011a. - 40 p.)

Антонов, М., П. Милованов, А. Попов, С. Герджиков, М. Дюлгеров. Обяснителна записка към геоложка карта на България, М1:50000. Картен лист К-34-59-В (Дрен). – София, МОСВ, 2011б. - 46 с. (Antonov, M., P. Milovanov,

A. Popov, S. Gerdzhikov, M. Dyulgerov. 2011b. Obyasnitelna zapiska kam geolozhka karta na Bulgaria, M1:50000. Karten list K-34-59-V (Dren). Sofia, MOSV, 2011b. - 46 p.)

Бончев, Е. Тектонска скица на западната половина от южната окрайнина на Витоша. – Сп. на Бълг. Геол. д-во, 3, 1, 1931. - 1-14. (Bonchev, E. Tektonska skitsa na zapadnata polovina ot yuzhnata okrainina na Vitosha. – Sp. na Bulg. Geol. d-vo, 3, 1, 1931. - 1-14.)

Бончев, Г. Опит за тектонска синтеза на Западна България. – Geologica Balc., 2, 1, 1936. - 5-48. (Bonchev, G. Opit za tektonska sinteza na Zapadna Bulgaria. – Geologica Balc., 2, 1, 1936. -5-48.)

Будуров, К., Х. Дабовски, Е. Димитрова, М. Иванов, Б. Каменов, Л. Методиев, В. Минковска, Т. Николов, Н. Рускова, И. Сапунов, Д. Синьовски, Е. Василев, И. Загорчев. Геология на България. Част 5. Мезозойска геология. Акад. издат. М. Дринов, София, 2009. - 765 с. (Budurov, K., H. Dabovski, E. Dimitrova, M. Ivanov, B. Kamenov, L. Metodiev, V. Minkovska, T. Nikolov, N. Ruskova, I. Sapunov, D. Sinyovski, E. Vasilev, I. Zagorchev. Geologia na Bulgaria. Chast 5. Mezozoiska geologia. Akad. izdat. M. Drinov, Sofia, 2009. - 765 p.)

Димитров, С., Ц. Димитров. Указания за младокимерска фаза от алпийското планинообразуване в Югозападна България. – Сп. на Бълг. Геол. д-во, 3, 3; 1931. - 65-74. (Dimitrov, S., Ts. Dimitrov. Ukazaniya za mladokimerska faza ot alpiyskoto planinoobrazuvane v Yugozapadna Bulgaria. – Sp. na Bulg. Geol. d-vo, 3, 3; 1931. - 65-74.)

Димитров, С., Ц. Димитров. Указания за младокимерска фаза от алпийското планинообразуване в Югозападна България. – Сп. на Бълг. Геол. д-во, 3, 3; 1931. - 65-74. (Dimitrov, S., Ts. Dimitrov. Ukazaniya za mladokimerska faza ot alpiyskoto planinoobrazuvane v Yugozapadna Bulgaria. – Sp. na Bulg. Geol. d-vo, 3, 3; 1931. - 65-74.)

Додекова, Л., И. Сапунов, П. Чумаченко, Стратиграфия ааленских, байоских и батонских отложении в части Юго-Западной Болгарии. – Geologica Balc., 16, 3, 1984. - 23-40. (Dodekova, L., I. Sapunov, P. Chumachenko. Stratigrafiya aalenskih,, bayoskih I batonskih otlozhenii v chasti Yugo-Zapadnoi Bolgarii. - Geologica Balc., 16, 3, 1984. - 23-40.)

Загорчев, И. Раннеальпийские деформации в красноцветных отложениях Полетинско-Скринской разломной зоны. 1. Литостратиграфические особенности в свете структурных иследований. – Geologica Balc., 10, 2, 1980. - 37-60. (Zagorchev, I. Rannealpiyskie deformatsii v krasnotsvetnaih otlozheniyah Poletinsko-Skrinskoi razlomnoi zonai. 1. Litostartigraficheskie osobenosti v svete stukturnaih isledovanii. - Geologica Balc., 10, 2, 1980. - 37-60.)

Загорчев, И. Раннеальпийские деформации в красноцветных отложениях Полетинско-Скринской разломной зоны. 2. Строение и деформации северной части Влахинскога блока. – Geologica Balc., 11, 1; 1981. - 101-126. (Zagorchev, I. Rannealpiyskie deformatsii v krasnotsvetnaih otlozheniyah Poletinsko-Skrinskoi razlomnoi zonai. 2. Stroenie i deformatsii severnoi chacti Vlahinskogo bloka. - Geologica Balc., 11, 1; 1981. - 101-126.)

Загорчев, И. Доалпийски строеж на Югозападна България. В: Проблеми на геологията на ЮЗ България. С., Техника, 1984. -9-19. (Zagorchev, I. Doalpiyski stroezh na Yugozapadna Bulgariya. V: Problemi na geologiyata na YZ Bulgaria. S., Tehnika, 1984. - 9-19.)

Загорчев, И. Разпространение на пермските и долнотриаските червеноцветни комплекси в Югозападна България. – Сп. Бълг. геол д-во, 55, 3; 1994. - 37-53. (Zagorchev, I. Razprostranenie na permskite i dolnotriaskite chervenotsvetni kompleksi v Yugozapadna Bulgaria. – Sp. Bulg. geol d-vo, 55, 3; 1994. - 37-53.)

Загорчев, И., Р. Маринова, Д. Чунев, П. Чумаченко, И. Сапунов, С. Янев. Обяснителна записка към Геоложка карта на България в М 1: 100 000, к.л. Перник. – КГМР, Геология и геофизика АД, 1994. - 92 с. (Zagorchev, I., R. Marinova, D. Chunev, P. Chumachenko, I. Sapunov, S. Yanev. Obyasnitelna zapiska kum Geolozhka karta na Bulgaria v M 1: 100 000, k.l. Pernik. – KGMR, Geologiyai geofizika AD, 1994. - 92 p.)

Загорчев, И., Р. Маринова, Д. Чунев. Геоложка карта на България в М 1:100 000. Перник. Отпечатан ВТС, 1991. (Zagorchev, I., R. Marinova, D. Chunev. Geolozhka karta na Bulgaria v M 1:100 000. Pernik. Otpechatan VTS, 1991.)

Илиева, Е., В. Желев. Нови данни за геологията на Голо бърдо. – Год. МГУ, Геофизика и геология, 2010, -65-69. (Ilieva, E., V. Zhelev. Novi danni za geologiyata na Golo bardo. – God. MGU, Geofizika i geologiya, 2010, - 65-69.)

Илиева, Е., И. Димитров. Гънкова интерференция в мезозойските скали на Голо бърдо, Западна България. – Год. МГУ, Геофизика и геология, 2011, -39-44. (Ilieva, E., I. Dimitrov. Gankova interferentsiya v mezozoiskite skali na Golo bardo, Zapadna Bulgaria. – God. MGU, Geofizika i geologiya, 2011, - 39-44.)

Моев, М., Върху тектонския строеж на Голо бърдо. – Год. на Висшия минно-геоложки институт, София, 8, 5, 1967а. - 148-166. (Moev, M., Varkhu tektonskiya stroezh na Golo bardo. – God. na Visshiya minno-geolozhki institut, Sofia, 8,5, 1967a. - 148-166.)

Моев, М., Геоложки строеж на радомирското поле и Голо бърдо. – Годишник на Висшия минно-геоложки институт, София, 8, 5, 1967б. -167-181. (Moev, M., Geolozhki stroezh na radomirskoto pole i Golo bardo. – Godishnik na Visshiya minno-geolozhki institut, Sofia, 8, 5, 1967b. - 167-181.)

Николов, Т., И. Сапунов. О региональной стратиграфии верхней юры и части нижнего мела в Балканидах. – Докл. БАН, 23, 11, 1970. -.1397-1400. (Nikolov, T., I. Sapunov. O regionalnoi stratigrafii verhney yurai r chasti nizgnego mela v Balkanidah. - Dokl. BAN, 23, 11, 1970. - 1397-1400.)

Сапунов, И. Относно някои стратиграфически проблеми на юрската система в България. – Изв. Геол. Инст., 18, 1969. - 5-20. (Sapunov, I. Otnosno nyakoi stratigraficheski problemi na yurskata sistema v Bulgaria. – Izv. Geol. Inst., 18, 1969. - 5-20.)

Сапунов, И., П. Чумаченко, Л. Додекова, Д. Бакалова. Стратиграфия келловейских верхнеюрских отложений Югозападной Болгарии. – Geologica Balc., 15, 2, 1985. - 3-61. (Sapunov, I., L. Chumachenko, L. Dodekova, D. Bakalova. Stratigrafiya kelpoveiskih verhneyurskih

otlozheniy Yugozapadnoi Bolgarii. – Geologica Balc., 15, 2, 1985. - 3-61.)

Стефанов, А. Триаската фауна от Голо бърдо. – Тр. Бълг. природоизп. д-во, 13, 1928. - 143–152. (Stefanov, A. Triaskata fauna ot Golo bardo. – Tr. Bulg.prirodoizp. d-vo, 13, 1928. - 143–152.)

Стефанов, А. Върху стратиграфията на триасовата система в България с оглед на триаса от Голо-бърдо. – Тр. Бълг. природоизп. д-во, 15–16, 1932. - 227–246. (Stefanov, A. Varhu stratigrafiyata na triasovata sistema v Bulgaria s ogled na triasa ot Golo-bardo. – Tr. Bulg. prirodoizp. d-vo, 15–16, 1932. - 227–246.)

Стефанов, А. Триаската фауна от Голо-бърдо. 1. Brachiopoda. – Тр. Бълг. природоизп. д-во, 17, 1936a. - 144–152. (Stefanov, A. Triaskata fauna ot Golo-bardo. 1. Brachiopoda. – Tr. Bulg. prirodoizp. d-vo, 17, 1936a. - 144–152.)

Стефанов, А. Триаската фауна от Голо-бърдо. 2. Cephalopoda. – Изв. на Царските природонаучни инст. В София, 9, 1936b. - 147–166. (Stefanov, A. Triaskata fauna ot Golo-bardo. 2. Cephalopoda. – Izv. na Tsarskite prirodonauchni inst. V Sofia, 9, 1936b. - 147–166.)

Стефанов, А. Триаската фауна от Голо-бърдо. 3. Lamellibranchiata.– Сп. Бълг. геол. д-во, 14, 1943. -1–11. (Stefanov, A. Triaskata fauna ot Golo-bardo. 3. Lamellibranchiata.– Sp. Bulg. geol. d-vo, 14, 1943. -1–11.)

Стефанов, А., Ц. Димитров. Геологически изучавания в Кюстендилско. – Сп. Бълг. геол. д-во, 8, 3, 1936. -1-36. (Stefanov, A., Ts. Dimitrov. Geologicheski izuchavaniya v Kyustendilsko. – Sp. Bulg. geol. d-vo, 8, 3, 1936. -1-36.)

Тронков, Д. Границата долен триас – среден триас в България. – Изв. Геол. инст., сер. Палеонт, 17; 1968. - 113-131. (Tronkov, D. Granitsata dolen trias – sreden trias v Bulgaria. – Izv. Geol. inst., ser. Paleont, 17; 1968. - 113-131.)

Тронков, Д. Бележки върху стратиграфията на триаса в Голо бърдо. – Палеонтол., стратигр. и литол., 1, 1975. - 71-84. (Tronkov, D. Belezhki varhu stratigrafiyata na triasa v Golo bardo. – Paleontol., stratigr. i litol., 1, 1975. - 71-84.)

Тронков, Д. Стратиграфия триасовой системы в части Западного Средногорья (Югозападная Болгария). – Geologica Balc., 11, 1, 1981. - 3-20. (Tronkov, D. Stratigrafiya triasovoi sitemai v chasti Zapadnogo Srednogorya (Yugozapadnaya Balgariya) - Geologica Balc., 11, 1, 1981. - 3-20.)

Тонков, Д. Стратиграфские проблемы Искырской карбонатной групы (Триас) Юго-Западной Болгарии. – Geologica Balc., 5, 1983. - 91-100. (Tonkov, D. Stratigrafskie problemai Iskarskoi karbonatnoi grupai (Trias) Yugo-Zapadnoi Bolgarii. - Geologica Balc., 5, 1983. - 91-100.)

Чаталов, Г. Фации в Свидолской свите (нижний триас) Тетевенского антиклинория. – Докл. БАН, 27, 2, 1974. - 239-242. (Chatalov, G. Fatsii v Svidolskoy svite (nizhniy trias) Tetevenskogo antiklinoriya. - Dokl. BAN, 27, 2,)

Budurov, K., E. Trifonova, I. Zagorchev. The Triassic in Southwest Bulgaria. Stratigraphic correlation of key sections in the Iskar Carbonate Group. – Geologica Balc., 25, 1, 1995. - 27-59.

National Geofund Reports

Горанов, Е. и др. 2002. Геоложки доклад за изпълнение на геоложка задача „Геоложко картиране в М 1:25 000 със златометрия по вторичен ореол на Краищидната тектонска зона”. – Национален Геофонд. IV-483. (Goranov, E. i dr. 2002. Geolozhki doklad za izpalnenie na geolozhka zadacha "Geolozhko kartografirane v M 1:25 000 sas zlatometria po vtorichen oreol na Kraishtidnata tektonska zona". – Natsionalen Geofond. IV-483.)

The article is reviewed by Prof. DSc. Dimitar Sinyovsky and Assoc. Prof Dr. Ivan Dimitrov.

FRACTAL PROPERTIES OF THE ELEMENTS OF PLATE TECTONICS

Boyko Ranguelov[1], Yanko Ivanov[1]

[1]University of Mining and Geology "St. Ivan Rilski", 1700 Sofia, e-mail: branguelov@gmail.com

ABSTRACT. The new idea about possible fractal properties of the elements of plate tectonic is explored. The elements are divided according to their geodynamic properties - subduction, orogenesis, rifting, transform faulting, collision, etc. Area, linear and spot elements are considered as fractal objects and their fractal dimensions are established. If the hypothesis of the fractal characteristics of most elements of plate tectonics is correct, this could be a new direction of investigations related to the creation, development and the geological history of the main global tectonic units. The obtained results could be useful to the new approaches related to the search, exploration, and exploitation of ores, gas and oil, coal and all other aspects of geodynamics, the mining industry, and geology.

Keywords: fractal, tectonics, plates, subduction, rift, collision, transform fault, orogeny

ФРАКТАЛНИ СВОЙСТВА НА ЕЛЕМЕНТИТЕ ОТ ТЕКТОНИКАТА НА ПЛОЧИТЕ

Бойко Рангелов[1], Янко Иванов[1]

[1]Минно-геоложки университет "Св. Иван Рилски", 1700 София, e-mail: branguelov@gmail.com

РЕЗЮМЕ. Изследвана е нова идея за възможните фрактални свойства на различните елементи от тектоника на плочите. Елементите са разделени според техните геодинамични свойства - субдукция, орогенеза, рифтинг, трансформни разломи, колизия и др. Площните, линейните и точковите елементи са приети за фрактални субекти и са определени техните фрактални размерности. Ако хипотезата за фракталните характеристики е правилна, това би могло да даде нова насока на изследванията, свързани с образуването, развитието и геоложката история на тектонските плочи. Получените резултати са полезни за използването на нови подходи, свързани с търсенето, проучването и експлоатацията на рудни полезни изкопаеми, нефт и газ, въглища, както и във всички други аспекти на геодинамиката, минната индустрия и геологията.

Ключови думи: фрактал, тектоника, плочи, субдукция, рифт, колизия, трансформен разлом, ороген

Introduction

The present study is focused on the assessment of the fractal properties and the coefficients of the nonlinearity (fractal dimensions) of the spatial distribution of the major elements of Plate Tectonics.

The idea to investigate these properties was born from another research of the fractal properties of the used European-Mediterranean Seismotectonic Model (EMSM) generated by Jimenez et al. (2001). Some other publications by B. Ranguelov and joined teams (Ranguelov and Dimitrova, 2002, Ranguelov et al. 2003, 2004) suggested that such fractal properties are rather common in Geosciences. (Turcotte, 1986; Hirata, 1989).

The Plate Tectonics theory was built on the idea that major continental plates are moving over a substrate and have fragmentation as an explicit internal property. Later on, the theory of ocean spreading confirmed the effectiveness of this idea, including oceanic plates and all other elements – rifts, transform faults, subduction zones, etc.

The development of these theories led to their integration in a simple and highly effective model of the "Living Earth". The simple and elegant explanation of almost all geodynamic processes observed on the Earth, and fruitful practical applications of the Plate Tectonics, make it one of the most popular paradigms of recent Geosciences that is practically accepted by the science community. For first time Sorette and associates (Sorette and Pisarenko, 2003) suggested the idea of Fractal Plate Tectonics. They calculated the power low for 42 plates, known at that time. Much later Mallard (Mallard et al, 2016) explored the idea that subduction is the main driving mechanism and is responsible for the plate's fragmentation. So far, no one has investigated the fractal properties of all other components of plate tectonics.

Methodology and theoretical assumption

The classical example of a fractal object is defined by Mandelbrot (Mandelbrot, 1982). If the length of an object P is related to the measuring unit length l by the formula:

$$P \sim \ell^{1-D} \quad (1)$$

then P is a fractal and D is a parameter defined as the fractal dimension. This definition was given by B. Mandelbrot in the early 60-s of the 20-th century. His ideas support the view that many objects in nature cannot be described by simple geometric forms, and linear dimensions, but they have different levels of geometric fragmentation. It is expressed into the

irregularities of the different scales (sizes) – from very small to quite big ones. This makes the measuring unit an extremely important parameter because by measuring of the length, the surface or the volume of irregular geometric bodies could be obtained so that the measured size could vary hundred to thousand orders. This fact was first determined when measuring the coastal line length of West England and this gave Mandelbrot the idea to define the concept of a fractal.

Geology and geophysics accept that the definition of the different "fractals" as real physical objects is most often connected to fragmentation (Korvin, 1992). This reveals that each measurable object has a length, surface or volume, which depends on the measuring unit and the object's form (shape) irregularity. The smaller the measuring unit is, the bigger is the total value for the linear (surface, volume) dimension of the object and vice versa. The same is valid for 2D and 3D objects.

Another definition of a fractal dimension is related to the serial number of measurement to each of the measuring units used and the object dimensions. If the number of the concrete measurement with a selected linear unit is bigger than r, then it might be presented by:

$$N \sim r^{-D} \tag{2}$$

and the fractal is completely determined by D as its characteristic fractal dimension. Applying this definition for the elements of faulting and faults fragmentation, some authors use this idea to depict formal models of the earth crust fragmentation, which indicates the level of fracturing of the upper earth layers (Ranguelov, Dimitrova, 2002).

The theoretical approach for the linear case and for the 2D and 3D cases was developed by Turcotte (1986a) and Hirata, (1989). They focused the attention on the relations between the smallest measuring unit and the object's size in analyzing linear (1D), 2D and 3D objects (Fig. 1).

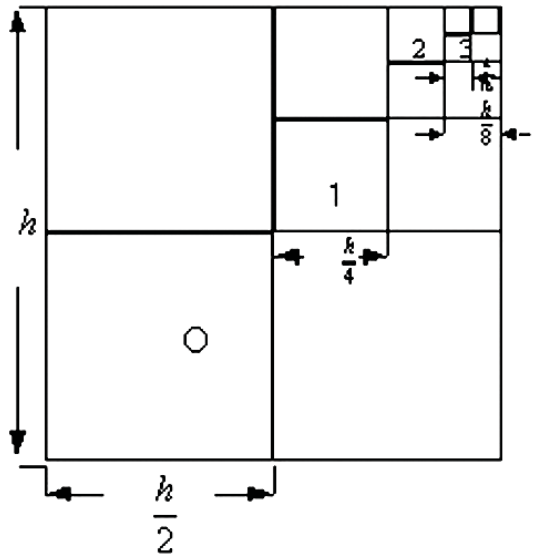

Fig. 1. 2D fractal scheme – each linear element is ½ of the larger one.

If l is the measuring unit and with m we denote the obtained value for N at each measuring cycle, then the common sum of the lengths N at level m according to Turcotte (Turcotte, 1986b) is:

$$N_m = (1 - p_c)\left(1 + \frac{n}{m} p_c + \left[\frac{n}{m} p_c\right]^2 \ldots \left[\frac{n}{m} p_c\right]^m\right) \tag{3}$$

where p_c denotes the probability for measuring of each length for the corresponding cycle of measuring.

Using formulas 1 and 2, we obtain the following formulae:

$$\frac{N_{m+1}}{N_m} = 2^D \tag{4}$$

for linear elements, and

$$\frac{N_{m+1}}{N_m} = \left(2^2\right)^D \tag{5}$$

for any area elements (surfaces).

Using this approach, we studied the elements of the Global Plate Tectonics model derived by Bird (2003). Following the outlined tectonic plates, orogens, rift zones, transform faults, subduction zones, and all other elements of the internationally recognized model, we investigated the possible fractal properties of all elements separately and calculated the fractal dimensions for each component.

Typology of the Components of Plate Tectonics and Graphical Fractal Analysis

The graphical fractal analysis has been performed after the separation of the major elements of the Plate tectonics theory - tectonic plates, orogens, rift zones, transform faults, subduction zones, etc. using the internationally recognized model by P. Bird. (2003). The methodology follows the algorithm presented in other publications (Ranguelov, 2010, Ranguelov et al. 2003, 2004):

- Presentation of the data for each selected element (total number, investigated parameter, dimensions – (only linear (1D) and surface sizes (2D) are considered)
- Calculation of the number for the graphics (selection of the calculation step for X and Y axes, scale on X and Y axes, values for each selected parameter).
- Presentation of the results on the graphics – on the X axis the semi-logarithmic scale is most convenient, on the Y axis z denotes in linear scale the numbers calculated for each element.
- In the next chapter the fractal dimensions will be calculated and results discussed.

The elements of the plate tectonics according to this theory have their common meaning and present some of the most important components under investigation – tectonic plates, rift zones, orogenies, subduction zones, collision zones, and transform faults. The typology and data, as well as the graphics are displayed below:

Tectonic Plates - total number - 52, investigated parameter - area size - Table 1.

Table 1.
Tectonic Plates and surface sizes

TYPE	N	TECTONIC PLATE	AREA [SQ. KM]
MAJOR (> 20M SQ. KM)	1	Pacific	104 600 300
	2	African	58 504 000
	3	Antarctic	58 202 000
	4	North American	55 501 000
	5	Eurasian	48 600 700
	6	Australian	46 000 600
	7	South American	41 800 900
MINOR [1M, 20M] SQ. KM	8	Somali	19 150 200
	9	Nazca	16 100 100
	10	Indian	12 450 000
	11	Sunda	8 900 200
	12	Philippine Sea	5 450 000
	13	Amurian	5 300 200
	14	Arabian	4 900 100
	15	Caribbean	3 000 800
	16	Okhotsk	3 000 200
	17	Cocos	2 950 090
	18	Yangtze	2 200 300
	19	Scotia	1 700 100
	20	Caroline	1 550 200
MICRO (< 1M SQ. KM)	21	North Andes	970 100
	22	Altiplano	830 070
	23	Banda Sea	700 200
	24	New Hebrides	650 400
	25	Anatolian	580 300
	26	Bird's Head	530 000
	27	Burma	520 100
	28	Kermadec	500 020
	29	Woodlark	450 200
	30	Woodlark	450 050
	31	Mariana	420 200
	32	Molucca Sea	420 070
	33	North Bismarck	390 000
	34	Timor	350 100
	35	Okinawa	330 080
	36	Aegean Sea	320 100
	37	South Bismarck	310 200
	38	Panama	270 070
	39	Juan de Fuca	260 100
	40	Tonga	250 050
	41	Balmoral Reef	200 080
	42	South Sandwich	180 400
	43	Easter	170 500
	44	Conway Reef	140 000
	45	Solomon Sea	130 070
	46	Niuafo'ou	120 400
	47	Maoke	120 200
	48	Rivera	100 120
	49	Juan Fernandez	100 090
	50	Shetland	70 010
	51	Galapagos	15 400
	52	Manus	8 060

The calculated number (z) is presented on Figure 2 in semi-logarithm scale.

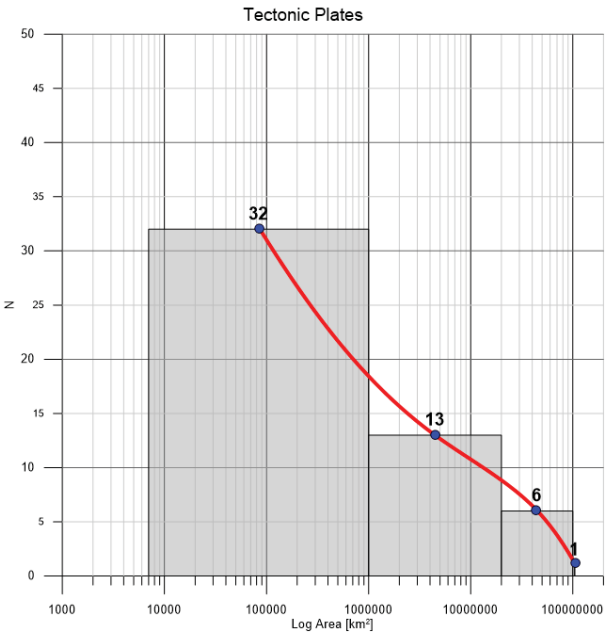

Fig. 2. Fractal distributions of the investigated tectonic plates.

Rift Zones - total number - 14; investigated parameter - lengths - Table 2

Table 2.
Rift Zones and lengths

N	RIFT	LENGTH [KM]
1	East African	5 350
2	Red Sea	2 400
3	West Antarctic	2 200
4	Keweenawan	2 000
5	Northern Cordilleran Volcanic Province	1 250
6	Gulf of California	1 130
7	Baikal	720
8	Rio Grande	660
9	Ottawa-Bonnechere Graben	520
10	Gulf of Suez	325

Table 2 - continued

N	RIFT	LENGTH [KM]
11	Upper Rhine	310
12	Reelfoot	240
13	Oslo	175
14	Gulf of Corinth	130

The calculated number (z) is presented on Figure 3 in semi-logarithm scale.

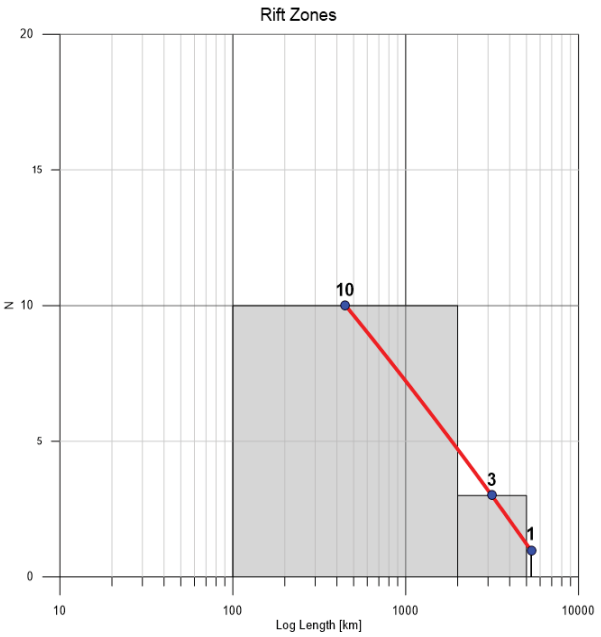

Fig. 3. Fractal distributions of the investigated rift zones.

Orogenies - total number - 13; investigated parameter - area size - Table 3

Table 3.
Orogens and surface sizes

N	OROGENS	AREA SIZE [SQ. KM]
1	Persia - Tibet - Burma	16 600 000
2	Ninety East - Sumatra	8 080 000
3	Alps	2 801 000
4	Alaska - Yukon	2 300 700
5	New Hebrides - Fiji	1 507 000
6	West Central Atlantic	1 501 100
7	Gorda - California - Nevada	1 350 100
8	Puna - Sierras Pampeanas	1 350 070
9	Peru	1 150 100
10	Philippines	1 000 070
11	Laptev Sea	420 000
12	Western Aleutians	190 000
13	Rivera - Cocos	24 000

The calculated number (z) is presented on Figure 4 in semi-logarithm scale.

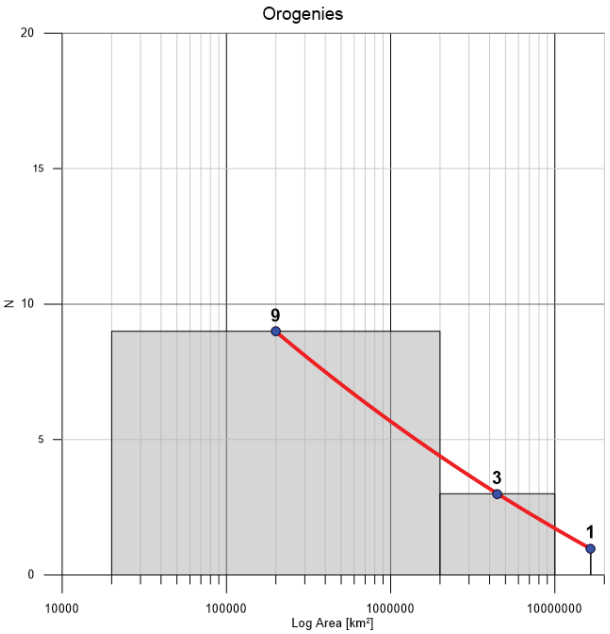

Fig. 4. Fractal distributions of the investigated orogens.

Subduction Zones - total number - 18; investigated parameter-area size - Table 4.

Table 4.
Subduction Zones and area sizes

N	SUBDUCTION ZONES	AREA SIZE [SQ. KM]
1	Nazca / South American	4 002 000
2	Pacific / Okhotsk	2 001 000
3	Indian, Australian / Sunda, Burma	1 600 300
4	Pacific / Australian	1 250 070
5	Pacific / Philippine Sea	1 100 100
6	Pacific / North American	900 100
7	Philippine Sea / Eurasian	780 090
8	Australia / New Hebrides	460 100
9	North America / Juan De Fuca	410 080
10	Solomon Sea / South Bismarck, Pacific	300 070
11	Aegean sea / Africa	250 900
12	Caroline / Bird's Head	250 010
13	Sunda Plate / Philippine Sea	200 100
14	South American / South Sandwich	140 000
15	Eurasian / Philippine Sea	60 100
16	Australian / Pacific	60 010
17	Antarctica / Scotia	35 100
18	Cocos / Caribbean	25 020

The calculated number (z) is presented on Figure 5 in semi logarithm scale.

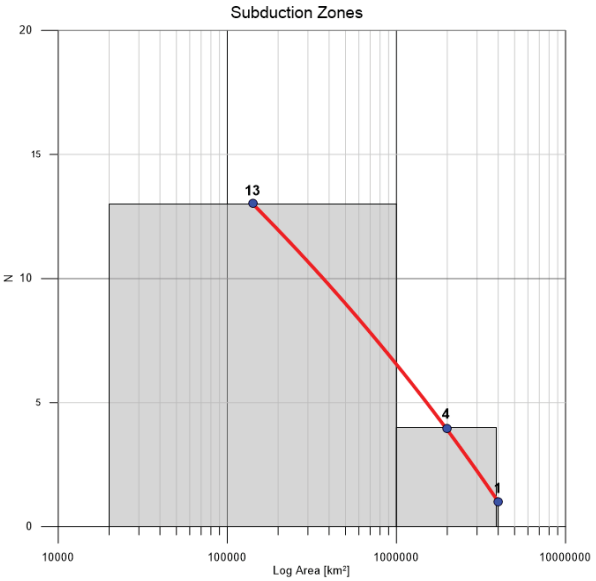

Fig. 5. Fractal distributions of the investigated subduction zones.

Major Collision Zones - number - 18, investigated parameter-area size - Table 5.

Table 5.
Major Collision Zones and area sizes

N	MAJOR COLLISION ZONES	AREA SIZE [SQ. KM]
1	Indo-Asian	2 502 000
2	Arabian-Eurasian	2 030 000
3	Izmir-Ankara-Erzincan	470 100
4	Maghrebides-Tell	460 200
5	Dinarides-Albanides-Hellemides	370 300
6	Apennines	200 400
7	Pyrenees	180 600
8	Carpathians	180 100
9	Beltics-rif	170 070
10	Molucca Sea	142 080
11	Western Alps	110 600
12	Eastern Alps	100 100
13	Inner Tauride Suture	75 000
14	Intra-Pontide Suture	50 300
15	Izu-Honshu	50 100
16	Taiwan	50 050
17	Balkanides	30 100
18	Hidaka	20 020

The calculated number (z) is presented on Figure 6 in semi logarithm scale.

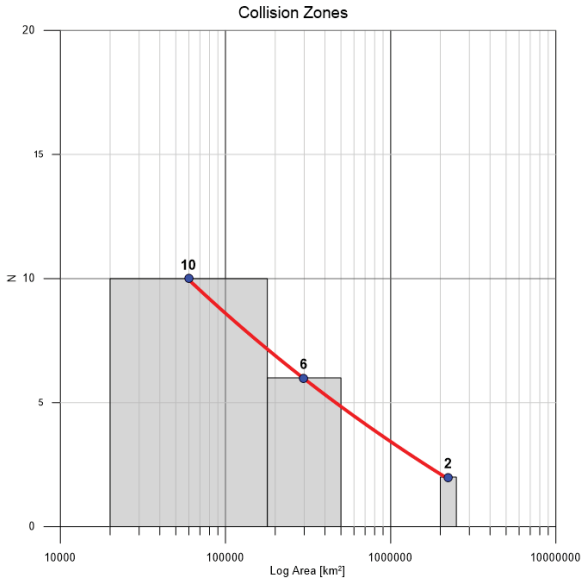

Fig. 6. Fractal distributions of the investigated collision zones.

Major Transform Faults - number - 18; investigated parameter-lengths - Table 6.

Table 6.
Major Transform Faults and lengths

N	MAJOR TRANSFORM FAULTS	LENGTH [KM]
1	Owen	1 840
2	Ulakhan	1 750
3	North Anatolian	1 160
4	San Andreas	1 100
5	Romanche	915
6	Queen Charlotte	830
7	Enriquillo-Plantain Garden	680
8	Puerto Rico	640
9	Walton	580
10	Dead Sea	555
11	Apline	550
12	Chaman	480
13	Rivera	400
14	St. Paul	385
15	Blanco	355
16	Ascension	275
17	Chain	255
18	Mendocino	240

The calculated number (z) is presented on Figure 7 in semi logarithm scale.

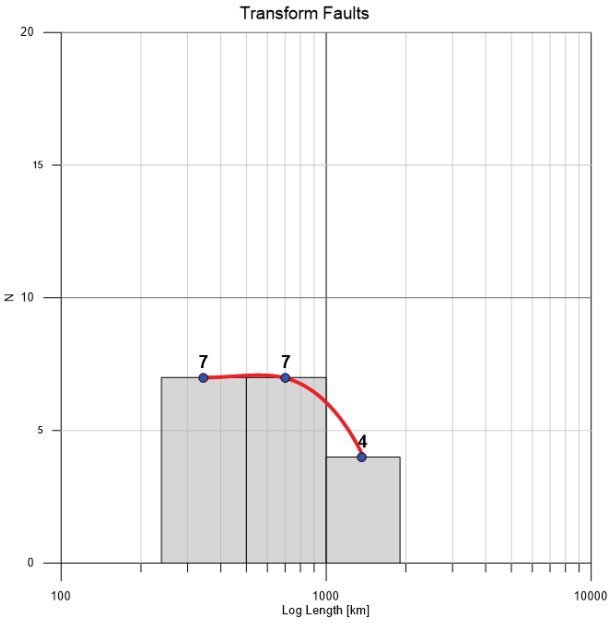

Fig. 7. "Fractal" distributions of the investigated transform faults.

Fractal Properties of Plate Tectonics

The fractal dimensions (D) have been calculated using the data from the graphics and tables. It is important to mention that all dimensions have negative numbers, but for easier perception are presented as positive values in the following table (Table 7).

Table 7.
Fractal Dimensions (linear and surfaces)

Plate Tectonics' Component	Linear	Surface	Notes
Tectonic Plates		3.01	High fragmentation
Rift Zones	1.81		Lowest fragmentation
Orogens		5.32	Highest fragmentation
Subduction Zones		3.07	High fragmentation
Major Collision Zones		3.28	High fragmentation
Major Transform Faults	N/A		Seems not to be a fractal

The analysis of the fractal dimension of all elements shows some specifics and trends and needs more details to be explained:

- All elements show relatively high fragmentation and strong non-linear trends.

- The linear expressed rift zones are characterized by the lowest fragmentation. It is difficult to explain why this peculiarity is demonstrated, but one probable explanation could be that this component of the plate tectonics is relatively younger than others mainly related to the oceanic crust fragmentation after the Pangea decay.

- Tectonic plates, subduction zones (mostly related to the ocean crust subducted parts of the Earth's crust), and collision zones have very similar non-linear behavior. The fractal dimensions are between 3 and 3.3. Thus, these elements show relative synergy between them and their fractal properties like geometric surfaces. The trends are rather clear.

- The most fragmented components are the orogens. This is relatively easy to explain because these elements are strongly variable in their surface sizes. In any case, so strong a fragmentation probably needs deeper geodynamic investigations to reveal geological reasons and relationships and to try to explain why such a peculiarity exists.

- The only component that seems not to be fractal (no fractal dimension) and could be extracted from this data is the transform faults. As linear elements dominated by horizontal movements of the plate convergence, these natural items probably have different origin, not so strictly related to the geodynamic evolution. This needs deeper research and investigations to reveal the origin and evolution of these faults.

- It is important to mention that a common task to these investigations is to discover if Plate Tectonics itself has fractal properties or not. The results of these investigations show that in general the main trends established due to the researched topic show clear fractal properties of the main plate tectonics components. The only exception (the transform faults) does not have a clear origin. It could be due to the limited data used, or it could have a more complicated source. This fact definitely requires a deeper research, integration and cooperation among the Geoscience societies.

Discussion and Discussed Questions

Following the calculated fractal dimensions and presented graphics of the investigated parameters of the plate tectonics, several disputable points appear and need some additional discussion. We appreciate any questions and topics under discussion. The main are presented as Q and R format:

- Are there fractal and non-fractal elements of the plate tectonics?
R: It seems that in general the Plate tectonics elements have clearly expressed fractal properties. The only exceptions discovered so far are the transform faults.

- Are the investigated objects enough for fractal analysis?
R: Some of them seem enough (for example - tectonic plates), others have values a little over 10. We consider that these numbers are enough to outline the trends of fractality and fragmentation of the investigated objects. Nevertheless, it is not possible to find larger objects of the Plate tectonics (which mean larger values to the right part of X). As this value is dominant for the calculation of the fractal dimensions, additional numbers to the left side (smaller in size objects) cannot change drastically the calculated values of D. McKenzie (McKenzie, 1972).

- There is an exception: transform faults which do not seem to have fractal properties.
R: This means that probably the fractal and non-fractal peculiarities will need deeper investigations including some not included in this study elements (for example "hot spots").

- What about hot spots? Why they are not included in this study?
R: The hot spots are a special component of the plate tectonics which cannot be easily explained. This is one of the reasons not to include them in this study. Another one is that there are too many established hot spots (some of them with origin which is not very clear) and this might distort the calculations. The topics will be investigated in future.

- Is there any possibility to investigate 3D objects about their fractal properties?
R: There is room for deeper investigations in the 3D domain. The thickness of the tectonic plates, the penetration depths of the subductions, the blocks (including their depths) limited by the faults (Papazachos, 1966, 1973) - these are only a few directions to the possibilities to extend similar investigations, but this needs much more uniform information from Geophysics (King, 1983).

- Why are triple junctions not included in this study?
R: Triple junctions are under a special investigation by Mallard and associates (Mallard et al, 2016) in an extended paper with good interpretation and we consider that this topic is solved.

- What is the physical meaning of the presence (or absence) of fractal properties of the Plate Tectonics?
R: Looks like Mother Nature has orchestrated the Earth's "chaos" in the proper manner and shows explicitly that all components in the recent geodynamics are interrelated and it is not easy to explain all processes acting in the Earth's interior.

Conclusions

The fractal analysis is performed to prove the strong non-linearity concerning the geometry distributions of the elements of Plate Tectonics.

The non-linear behavior of the linear and surface elements of the internationally recognized Plate Tectonic Model derived by P. Bird (2003) is discovered in this study. It shows that more punctual and refined methods of the mathematical analysis are useful tools to reveal the fine structure of the geodynamic models.

The discovered fractal properties of most elements of the Plate tectonics suggested that there is synergy among them and that probably they have deeper meaning for the Erath's geodynamic machine.

The lack of fractality in such a fine system for some investigated elements (transform faults, for example) needs deeper understanding of the physical evolution of our Planet.

References

Bird P., An updated digital model of plate boundaries. In: Geochemistry, Geophysics, Geosystems G3. AGU and the Geochemical Society, 4, 3, 2003. - 1027-1079.

Jimenez M., D. Giardini, G. Grunthal, SEASAME Working Group.Unified seismic hazard modeling throughout the Mediterranean region. In: Bolletino di Geofisica Teorica ed Applicata, 42,1-2, 2001. - 3-18.

Hirata T., Fractal dimension of fault system in Japan: Fractal structure in Rock geometry at various scales. In: Pure and Applied Geophysics., 131,1989. - 157-173.

King G., The accommodation of large strains in the upper lithosphere of the Earth and other solids by self-similar fault system. In: Pure and Applied Geophysics., 121, 1983. - 761-815.

Korvin G., Fractal models in the Earth Sciences. New York: Elsevier, 1992. - 236 p.

Mallard C., N. Coltice, M. Seton, R.D. Muller, P.Tackley, Subduction controls the distribution and fragmentation of Earth's tectonic plates. Nature, Nature Publishing Group, 535 (7610), 2016. - 140-143.

Mandelbrot B., The Fractal Geometry of Nature. San Francisco: W.H. Freeman & Co., 1982. - 368 p.

McKenzie D., Active tectonics of the Mediterranean Region. In: Geophysical Journal of Royal Astronomical Society, 30, 1972. - 1186-1193.

Papazachos B., Preliminary results of an investigation of crustal structure in SE Europe. In: Bulletin of the Seismological Society of America, 56, 1966. - 1368-1423.

Papazachos B., Distribution of seismic foci in the Mediterranean area and its tectonic implication. In: Geophysical Journal of Royal Astronomical Society, 33, 1973. - 1234-1345.

Ranguelov B., S. Dimitrova, Fractal model of the recent surface earth crust fragmentation in Bulgaria, In: Comptes Rendus de l'Academy Sciences Bulgaria. 55, 3, 2002. – 25-28.

Ranguelov B., Nonlinearities and fractal properties of the European-Mediteranean seismotectonic model. GEODYNAMICS & TECTONOPHYSICS., Vol. 1. № 3. 2010.- 225–230.

Ranguelov B., S. Dimitrova, D. Gospodinov, Fractal configuration of the Balkan seismotectonic model for seismic hazard assessment, In: Proceedings BPU-5, Vrnjacka Banja, Serbia and Montenegro, 2003. - 1377-1380.

Ranguelov B., S. Dimitrova, D. Gospodinov, E. Spassov, G. Lamykina, E. Papadimitriou, V. Karakostas, Fractal properties of the South Balkans seismotectonic model for seismic hazard assessment, In: Proceedings 5th Intl. Symposium on East Mediterranean Geology, Thessalonica, 2004. - 643-646.

Sornette D., Pisarenko, Fractal Plate Tectonics., Geophysical Research Letters, vol. 30, No3, 2003 - 1105-1118.

Turcotte D., Fractals and Fragmentation. In: Journal of Geophysical Research. 91, B2, 1986a. – 1921-1926.

Turcotte D., A fractal model of crustal deformation. In: Tectonophysics, 132, 1986b. -361-369.

The article is reviewed and recommended for publication by Prof. DSc. G. Mardirosian and Prof. Dr. I. Paskaleva.

THE EU ERASMUS+ *CABARET* PROJECT AND THE PARTICIPATION OF THE UNIVERSITY OF MINING AND GEOLOGY

Boyko Ranguelov

Mining and Geology University, 1700 Sofia, Bulgaria, e-mail: branguelov@gmail.com

ABSTRACT. The CABARET (CApacity Building in Asia for Resilience EducaTion) Project is funded by the European Union under the Erasmus+ program, to foster regional cooperation for more effective multi-hazard early warnings and increased disaster resilience among coastal communities. The goal of the Project is to strengthen the evidence-base in support of the implementation of the new framework. It is created by the participants of a consortium of 14 European and Asian higher educational institutions from nine countries - four from Europe and five from Asia. The participants are divided into two large groups: "program countries" (the European) and "partner countries" (from Asia as the continent that is mostly threatened by complex disasters, like earthquakes, tsunamis, hurricanes, flooding, etc.) The Intergovernmental Oceanographic Commission of UNESCO (IOC-UNESCO), the Asian Disaster Preparedness Center and the Federation of Sri Lankan Local Government Authorities are Associate Partners of the project, and will help to promote the benefits across Asia and beyond. The Project covers a three year period and intends for many meetings among participants for data and knowledge exchange, seminars, scientific conferences, and research work to be organized to facilitate the population through modern education. The MGU participation is active as co-chair of the WP7 - Learning and teaching tools methodologies and approaches to the multihazards early warning systems and sustainable development of the resilience education as well as most other working packages of the CABARET Project.

Key words: higher education, multihazards early warning systems (MHEW), Asia, Europe

ЕВРОПЕЙСКИ ERASMUS+ **ПРОЕКТ** *CABARET* **И УЧАСТИЕТО НА МИННО-ГЕОЛОЖКИ УНИВЕРСИТЕТ В НЕГО**

Бойко Рангелов

Минно-геоложки университет "Св. Иван Рилски", 1700 София, e-mail: branguelov@gmail.com

РЕЗЮМЕ. Проектът CABARET (CApacity Building in Asia for Resilience EducaTion) е финансиран от Европейската Комисия по програмата Erasmus +. Той има за основна цел да засили международното и междуконтинентално сътрудничество за по-ефективна устойчивост на обучението по една изключително важна тематика – създаване и използване на комплексни системи за ранно предупреждение от природни опесности. Създаден е консорциум от 14 европейски и азиатски институции от областта на висшето образование от 9 страни – 4 европейски и 5 азиатски. Те са разделени на две големи групи – „програмни" (4 от европейските страни) и „партньорски" (от Азия, като най застрашен континент от комплексни опасности – земетресения, цунами, тайфуни, наводнения и др.) страни. Проектът е планиран за 3 годишен период през който поредица от работни срещи, семинари, научни конференции и изследвания ще бъдат организирани за подпомагане на населението чрез модерно обучение. Участието на МГУ „Св.Иван Рилски" има административен (съръководител на работна група 7 – създаване на методологии за ефективно обучение на кадри с висше образование) и изследователски ангажимент. Основната част от изследванията ще бъдат в създаването на програми и лекционни курсове чрез иновативни методи на обучение в областта на кинематичните модели и разпространението на информацията в комплексните системи за ранно предупреждение.

Ключови думи: образование, комплексни системи за ранно предупреждение, Азия, Европа

Introduction

A new Erasmus+ project called CABARET explores the possibilities about sustainable education for the early warning systems covering multihazards events. Fourteen institutions from Bulgaria, Indonesia, Latvia, the Maldives, Malta, Myanmar, the Philippines, and Sri Lanka are included in the consortium along with the United Kingdom that hosts the University of Huddersfield's Global Disaster Resilience Centre, leading partner of the CABARET project (CABARET Project, 2016). The organization of the Project is constructed by two main groups of partners – so called "program countries" and so called "partner countries". There are also some associated partners – usually internationally recognized organizations - like ADPC, IOC (UNESCO), etc. The mutual cooperation is established to develop and use effectively the knowledge, experience and expertise, together with the education of the specialists, decision-makers, and population of the countries threatened by complex natural hazards, which has developed (or intend to do so in near future) early warning systems. The exploitation of the world positive practices and examples will be broadly incorporated in the educational platform. The structure of the Project suggests initial collection of data, gaps and needs definition of the threatened countries. Then assessment, scientific approach to the gaps and needs formulation and sustainable solutions will be preformed. The partner countries collect initial information and data. The program countries assess the need and gaps and produce recommendations. Both types of partners participate in the educational platform development, fulfilling needs, providing sustainability and producing manuals and other educational materials. The regional innovation hub is intended to use modern technologies in case of multihazards early warnings. The final purpose is to integrate the local needs, educational materials and multihazard early warning systems to the global initiative for people and infrastructure protection by the developed educational platform. Another very important aim of the Project is to build capacity for international and regional

cooperation among Asian HEIs (Higher Education Institutions) and European ones. The coordination, quality assurance and dissemination activities to bring the results to the wider public and scientific community are also among the purposes of the Project (Capacity building…, 2016). [http://ec.europa.eu/programmes/erasmus-plus/projects/]

General objectives and tasks

The General objective can be formulated in the following way:

- The capacity building for resilience education of some Asian countries related to the multihazards early warnings by use of world experience and European expertise
- Outlining of the gaps and needs for resilience education related to the complex early warnings
- Strengthening the cooperation among partner and program countries to provide highly reliable end effective resilience education of students in HEIs, between the decision makers and among the population
- Creation of an innovative hub for using the recent technologies ("smart sensors", satellite communications, smartphones, supercomputers, digital world and social networks) to provide resilent societies threatened by multihazards.
- Introduction of the innovative platforms for resilient education related to the multihazard early warning systems including on-line education at different levels, manuals, major on-line open courses, manuals, etc. to support the education and practical application to the costal societies.

All these tasks will be executed by seminars, on site education, on-line surveys, networking and frameworking workshops, etc. The extended dissesmination policy is intended to cover wide social groups and extended cooperation with economic and social partners.

Work Program

The Work Program of the project is intended to be executed within a 3-year period. All works to be performed are organized in several working packages.

Work Package 1 – Title: Intra- and inter-regional capacity building framework. This is the main package. It has coverage of all aspects of the Project, focusing on the current status of the countries' preparation, MHEWS in action or intended, questionnaire distribution about needs and gaps, and preparation of the country report called "country position paper" for the partner countries. The role of the program countries is to assess the reliability and the regional monitoring framework, as well as the outlined needs and gaps.

Work Package 2 – Title: Project management. The package deals with the project management and coordination between coordinator and partners, as well as among the partners. The creation of a Steering committee as executive body during the time of the project is intended. The visits about meetings, partners exchange and other actions as well as time schedules are also included.

Work Package 3 – Title: Quality assurance and monitoring. The package is targeted at the quality control and monitoring of all actions related to the Project activities. The data collected and assessment need to be done according the recent criteria of the scientific approach and to avoid negative influence of rumors and fake news.

Work Package 4 – Title: Regional innovation hub for multihazards early warning systems. The hub is one of the important issues of the Project because the fast development of the technologies, communications, and "smart sensors", as well as warning issues dissemination among the decision makers and population is a critical element to the effective functionality of any MHEW.

Work Package 5 – Title: Regional cooperation for multihazards early warning systems. This package is important from the point of view of the integration and unification of the local EWS on the regional and/or global level. The technologies transfer, warning issues, common protocols, unified data formats, etc. are important parts of the regional cooperation. It can serve as a pioneering work in this direction and to be a good example of the developed tools.

Work Package 6 – Title: Partnership with social and economic actors. Specific actions in this working package are very important because the partnership between social and economic partners and the educational communities can help the deeper understanding of the prevention and safety measures performed by the whole society.

Work Package 7 – Title: Learning and teaching tools methodologies and approaches. One of the most important packages targeted to all target groups. The created platform, MOOCs (Major On-line Open Courses), technical manuals and brochures, together with the use of the Internet abilities for distant education, are the modern tools for HEIs highly effective performance of the knowledge for real practical purposes.

Work Package 8 – Title: Dissemination and exploitation. The results obtained during the execution of the Project need to be largely distributed among specialists, scientific communities, HEIs (teaching staff and students), decision makers, and wide population about the MHEWS. All possible ways will be explored in these directions – workshops, meetings, conferences, newsletters, web-pages, social media, TV, newspapers and magazines, teaching programs and platforms, interviews, press-releases, etc. The dissemination topic is considered as one of the most important.

Achievements and deliverables

The work program is focused to produce and promote deferent types of deliverables as main products of the investigations, scientific analysis and practical results for larger use and performance. Among others the most important are:

- A regional monitoring and assessment network report (WP1)
- Country positions papers (WP1)
- Regional position paper(WP1)
- Organizing events (WP2)
- Interim and Closure Reports (WP2)
- Steering committee establishment (WP2)
- Quality board meetings and minutes (WP3)
- Quality plan (WP3)
- Independent evaluation reports(WP3)
- Partners' and participants' evaluation surveys and statistical analysis (WP3)
- Annual self-evaluation (WP3)
- Creation of a regional innovation hub (WP4)
- Sandpit events organization (WP4)
- Short-term scientific missions for innovations seminars (WP4)
- Innovation training workshops and materials (WP4)
- Capacity building roadmap for regional gaps and priorities (WP5)
- Regional cooperation training program and materials (WP5)
- Regional cooperation training events (WP5)
- University - social and economic partnership and secondment plan. (WP6)
- Secondments (WP6)
- University - social and economic partnership training events (WP6)
- Functional and technical specifications (WP7)
- Online regional capacity building platform (WP7)
- Manual for regional capacity building platform (WP7)
- Major On-line Open Courses (WP7)
- Dissemination and exploitation plan (WP8)
- Project website(WP8)
- Promotional kit (brochures, articles, press-release, posters) (WP8)
- Sustainability plan (WP8)
- Briefings on the Project (WP8)
- Training materials (WP8)
- Conference journals and papers (WP8)

Target groups

The target groups included in the project activities and achievements are divided into several groups:

- Teaching staff – an important group which must be educated in the best manner and should obtain maximum knowledge from the results of the project in order to be able to transfer this knowledge to others.
- Students – the main consumer of the knowledge and practices
- Technical staff – to learn the lessons and to apply the knowledge to the laboratories, maintaining staff and technical solutions.
- Trainees – important part of the educated components at all levels.
- Administrative staff – to have knowledge about correct solutions and effective management in any critical case and situation appearance.
- Librarians – for effective transfer of the knowledge to larger groups of people using literature.

Wide population is also a target group though not explicitly mentioned. The prevention could be effective if the whole population benefits from the project achievements.

Participation of the University of Mining and Geology

The project management provides different roles to the different participants. As a program country, Bulgaria participates in all gaps and need assessment procedures of the survey. The partner countries position papers will be integrated to the regional positions paper with the intensive participation and expertise use of the program countries. As an operative ruling body, the Steering Committee includes representatives from all participating institutions. In such way, MGU has a membership participant in the Steering committee. MGU together with the University of Maldives are leading partners in the working package 7 - Learning and teaching tools methodologies and approaches. In this frame, the UM will develop a resilient education platform and all other activities will be executed simultaneously. MGU will play an important role in:

- Multihazard early warning systems education – development and shearing software and hardware experience for the complex geological and meteorological marine hazards and risk reduction (Ranguelov, 2014; Parushev et al. 2015; Ranguelov, 2011, etc.).
- The process of sharing knowledge and experience, especially kinematic models of MHEWS. Such kinematic models (Ranguelov and Iliev, 2013) related to the earthquakes and tsunamis have been developed for Azerbaidjan (Baku case) (Ivanov et al., 2016) and Italy (Venice case – Parushev and Ranguelov, 2014). Several others have been produced during the execution of different projects – MARINGEOHAZARDS (Ranguelov et al, 2011), DACEA (Ranguelov, 2014), SCHEMA and SIMORA (Ranguelov, 2010; Ranguelov et al. 2011), etc.
- Education of any interested people at different levels – from the population to the higher educational institutions and decision makers (Ranguelov, 2013).
- Input preparation of the related topics for the other partners
- Involvement in the research of some examples and case studies for other partner countries (Ranguelov, 2011; Ranguelov et al. 2011)

The importance of the CABARET Project for MGU is as follows:

- cooperation with specialists from different countries with different environment and threats to the population and infrastructure
- exchange of knowledge and educational experience at different levels and creation of new tools for education about Natural and anthropogenic hazards
- development of a larger platform for prevention and protection activities and increasing the knowledge of the

specialists and population in the filed of Natural and Anthropogenic hazards and multiple hazards early warning systems (Ranguelov, 2011).

CONCLUSIONS

The participants in the CABARET Project believe in its pioneering role. The Project development, execution and deliverables and achievements reached are clearly outlined due to the following factors:

- Innovative approach to the capacity building of the sustainable education, international framework and specialized HEIs programs about use and effectiveness of the Multihazrds early warning systems and their application in everyday practice.
- The creation of a hub about the use of innovative technologies, smart sensors, fast early warnings communications, and new technologies like electronics, robotics, distant methods and imaginary, space technologies, etc. is an new approach in this direction.
- Educational platform, specific tools and specialized manuals for the educational aims, large application of the MOOCs and other innovative tools about higher education related to the MHEWS are among the first developed methodologies and approaches which could be rather useful to any other country, local or regional framework, as well as for everyday educational practice for the Integrated Coastal Areas Management.

Acknowledgments:

This work is supported by the CABARET Project No 573816-EPP-1-2016-1-UK-EPPKA2-CBHE-JP of EU Erasmus+ Program. The European Commission support for the production of this publication does not constitute an endorsement of the contents which reflects the views only of the authors, and the Commission cannot be held responsible for any use which may be made of the information contained therein.

References

Capacity Building in Asia for Resilience Education – CABARET Project. Detailed Description of the Project. Annex IV. Version 1. 2016, 201 p.

Ivanov Y., A. Kisyov, B. Ranguelov, Kinematic models and early warning systems (earthquakes and tsunamis) for Azerbaidjan (Baku case)., Ann. of M&G University, Vol. 59, Part I, Geology and Geophysics., 2016. - 95-100.

Parushev I., B. Ranguelov., General principles of the kinematic models used in eartly warning systems – earthquakes and tsunamis (VENICE CASE) ., Ann. of M&G University, Vol. 57, Part I, Geology and Geophysics., 2014. - 95-100.

Parushev I., B. Ranguelov, T. Iliev, E. Spasov, Kinematic modelling of idealized system for early registration and warning in case of an earthquake., In: Proc. 7th BgGS National Conference "GEOPHYSICS 2015" 2015. - 1-8. (on CD)

Ranguelov B., Atlas of the tsunami risk susceptible areas along the Northern Bulgarian Black Sea coast – Balchik site. 2010. 25 p.

Ranguelov, B. Natural hazards – nonlinearities and assessment, Acad. Publ. House (BAS), 2011, pp. 327.

Ranguelov B. Complex geophysical investigations – natural hazards, monitoring and early warning systems, on land and in the Black sea, In: Proc. of the 4th Int. scientific and technical conference "Geology and hydrocarbon potential of the Balkan-Black Sea region" 11 - 15 September, 2013, Varna, Bulgaria – 118-126

Ranguelov , B. Early warnings - Bulgarian experience in case of time deficit systems (earthquakes and tsunamis), Proceeding 1/2, 5th ICC&GIS 2014, 2014.,-. 738-745.

Ranguelov B., Radichev R., Dimovsky S., Oaie G., Dimitriu R., Diaconescu M., Palazov A., Dimitrov O., Shanov S., Dobrev N., MARINEGEOHAZARDS Project – key core elements of the early warning system in the Black Sea., Ann. of M&G University, Vol. 54, Part I, Geology and Geophysics, 2011. - 177-182.

Ranguelov, B., Iliev, T. A kinematical model of the Seismic Early Warning System (SEWS), Proc. 7th Balkan Geophysical Congress, Tirana, 7-10th October 2013. - (on CD).

http://ec.europa.eu/programmes/erasmus-plus/projects/eplus-project-details-page/?nodeRef=workspace://SpacesStore/5315e537-5ff2-42ed-888d-d8f3fb6ce86c (accessed 19 June 2017)

http://www.journalriskcrisis.com/mr-ranguelov-on-seismic-early-warning-systems/ (accessed 19 June 2017)

The article is reviewed and recommended for publication by Prof. DSc. G. Mardirosian and Prof. D-r. I. Paskaleva.

STUDY OF THE CAPABILITIES OF AVO-METHODS FOR THE DETECTION OF HYDROCARBON ACCUMULATIONS

Martin Toshev

University of Mining and Geology "St. Ivan Rilski", 1700 Sofia, E-mail: martin.toshev86@gmail.com

ABSTARCT. The AVO-methodology is based on the study and analysis of the wave field features related to the differing reflectance of the individual surfaces in the geological section. Several physical parameters of geological media are used: velocity of compressional wave, velocity of shear wave, density, acoustic impedance.
The software is based on the equation of Zoeppritz. This equation, re-processed by Aki-Richards, uses the linear relationship between the amplitudes of the reflected waves and $\sin^2\theta$, where θ is the angle of incidence of the seismic wave. The amplitude's change of reflected seismic waves, depending on the distance from the source point of seismic energy, has been investigated on real seismic data.
The presented study of the AVO-methodology possibilities for the identification of oil and gas deposits is based on the seismic, lithological and stratigraphic, and geological and geophysical data from the Galata gas field. In tectonic terms, the area falls on the southern board of the Varna Monocline, north of the Bliznatsi Fault. The data from a seismic line with south-north direction and materials from two wells were used. The AVO-anomalies studied are well correlated with the proven presence of hydrocarbon accumulations.

Keywords: AVO, incidence angle, acoustic impedance, anomalies.

ИЗСЛЕДВАНЕ НА ВЪЗМОЖНОСТИТЕ НА AVO-МЕТОДИТЕ ЗА ОТКРИВАНЕ НА ВЪГЛЕВОДОРОДНИ АКУМУЛАЦИИ

Мартин Тошев

Минно-геоложки университет "Св. Иван Рилски", 1700 София, E-mail: martin.toshev86@gmail.com

РЕЗЮМЕ. AVO-методиката се основава на изучаване и анализ на особеностите на вълновото поле, свързани с различаващата се отражателна способност на отделните повърхнини в геоложкия разрез. Използват се няколко от физическите параметри на геоложките среди: скорост на разпространение на надлъжните вълни (Vp), скорост на разпространение на напречните вълни (Vs), плътност на скалите (ρ), акустичен импеданс (ρ.Vp и ρ.Vs).
В основата на използвания софтуер е уравнението на Zoeppritz, преработено от Aki-Richards, където е заложена линейна връзка между амплитудите на отразените вълни и $\sin^2\theta$, където θ е ъгъл на падане на сеизмичната вълна. Изменението на амплитудите на отразените сеизмични вълни в зависимост от отдалечението от пункта на възбуждане на сеизмичната енергия, е изследвано върху реални сеизмични данни .
Представеното изучаване на възможностите на AVO-методиката за установяване на нефтогазови залежи е базирано върху сеизмичните, литолого-стратиграфските и сондажно-геофизичните данни от района на газовото находище Галата. В тектонско отношение площта попада върху южния борд на Варненската моноклинала, северно от Близнашкия разлом. Използвани са данните от един сеизмичен профил с направление юг-север и сондажно-геофизичните данни от два сондажа. Изучените AVO-аномалии добре се корелират с доказаното наличие на въглеводородни натрупвания.

Ключови думи: AVO, ъгъл на падане, акустичен импеданс, аномалии.

Introduction

The AVO-methodology is based on the study and analysis of the wave field characteristics related to the differing reflectance of the individual surfaces in the geological section. Several physical parameters of geological media are used: velocity of compressional wave (Vp), velocity of shear wave (Vs), density (ρ), acoustic impedance (ρ.Vp and ρ.Vs).

The presented study uses professional specialized software. The development of all programs that are used to extract the listed parameters of seismic data is based on Zoeppritz (1919) equation, revised by Aki & Richards (1980), and later simplified by Shuey (1985), wherein is set a linear relationship between the amplitudes of the reflected waves and $\sin^2\theta$ (where θ is is the angle of incidence of the seismic wave).

The aim of the present study with data from proven hydrocarbon accumulations is to present the capabilities of the AVO-methodology for the establishment of oil-gas deposits. For this purpose, seismic, lithological and stratigraphic, and geological and geophysical materials were used from the area of the Galata gas field.

In tectonic terms, the area falls on the southern board of the Varna Monocline, north of the Bliznatsi Fault (Fig. 1).Data from seismic line TX92-21 in direction south-north and well log materials of P-1 and P-2 Galata were used. It is interesting to note that the seismic line data used were recorded prior to the first well, discovered the deposits (late 1993 - early 1994) and before the start of its exploitation.

The Galata gas deposit is inserted in the platform carbonate sediments of the Paleocene, built by shallow algal limestones and in the Upper Cretaceous and Middle Eocene bio-clastic limestones.

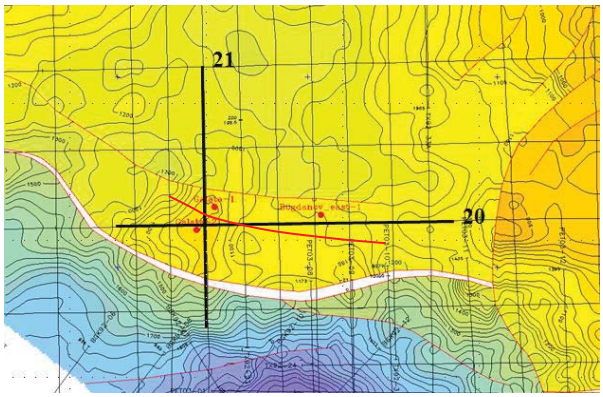

Fig. 1. Structural map of a seismic horizon attached to the top surface of the Paleocene

Figure 2 shows a fragment of the seismic section of line TX92-21 which crosses sequentially the Bliznatsi Fault from south to north, the area of the gas deposit and the F1 fault, limiting the Galata deposit from the north.

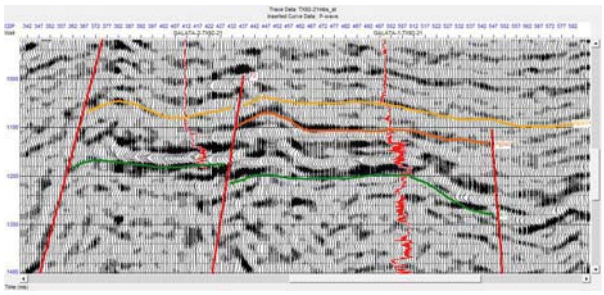

Fig. 2. Seismic section of a line TX92-21 with correlated P-wave curves from wells P-1 and P-2 in the Galata area

Across the line are correlated three seismic horizons attached to: the upper surface of Lower Cretaceous sediments (horizon K1), the upper surfaces of the Middle and Upper Eocene (horizons Pg2e2 and Pg2e3). Within the interval CDP-370 to CDP-515 of seismic line TX92-21 a local high amplitude anomaly was observed – a "bright spot". Anomalies of this type are so well-correlated with the existence of hydrocarbon accumulations that they are known as "direct hydrocarbon identifiers".

Methodology and preparation of data necessary for AVO study

The specialized profisional software used includes a set of programs for analysis of pre-stack seismic data for the purposes of evaluation and modeling of amplitude anomalies depending on offset. For AVO-processing of the Galata area chosen line TX92-21, the following seismic and well log information was used prepared in terms to be discoverable and matching the demands of AVO package:

- CDP Gathers records from seismic line TX92-21;
- Basic curve P-wave_corr_G1 (Fig. 3). This dependence of velocities of compression waves from the depth in P-1 Galata well was correlated with real seismic data from line TX92-21/CDP-505 with correlation coefficient 0.795 and frequency of impulse, with which is generated 28Hz synthetic trace;

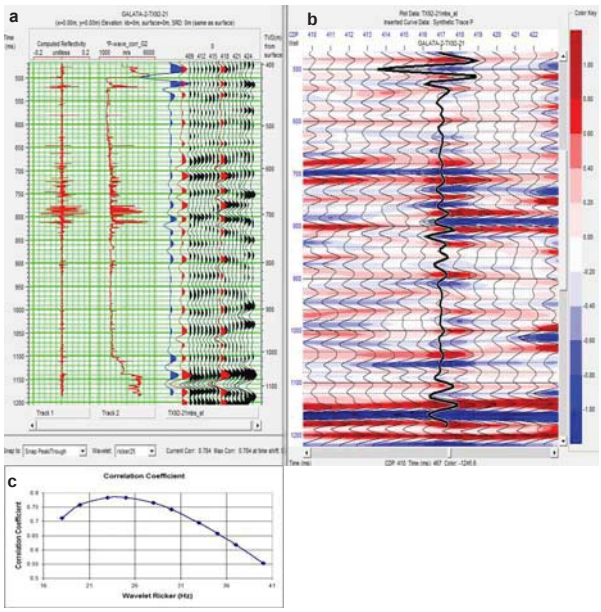

Fig. 3. Seismic line TX92-21
a/ Correlation between sonic log from P-1 Galata well and trace from the line; b/ Fragment of seismic section with synthetic trace generated from correlated P-wave curve of P-1 Galata; c/ Distribution of correlation coefficients for different frequencies of seismic impulse

- Basic curve P-wave_corr_G2 (Fig. 4). This dependence of velocities of compression waves from the depth in P-2 Galata well was correlated with real seismic data from line TX92-21/CDP-417 with correlation coefficient 0.784 and frequency of impulse, with which is generated 25 Hz synthetic trace;

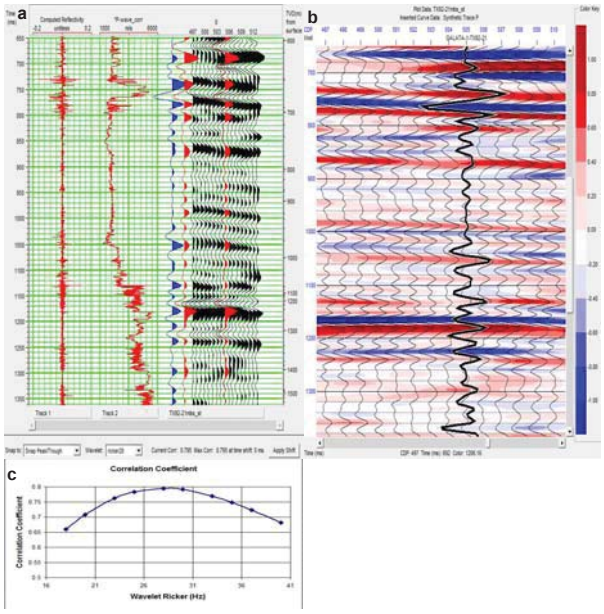

Fig. 4. Seismic line TX92-21
a/ Correlation between sonic log from P-2 Galata well and trace from the line; b/ Fragment of seismic section with synthetic trace generated from correlated P-wave curve of P-2 Galata; c/ Distribution of correlation coefficients for different frequencies of seismic impulse

- P-1 Galata well - original curve of natural Gamma ray (Fig. 5, a - Track1);
- P-1 Galata well - original curve of natural Gamma ray (Fig. 5,b - Track1)

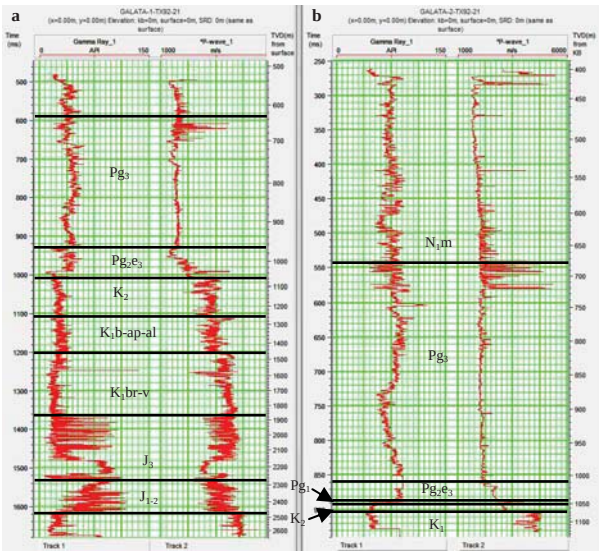

Fig. 5. Well log information, used for the current study; a/ **P**-1 Galata well; b/ **P**-2 Galata well)

- Density curve (Fig. 6,b), obtained from basic curve through Gardner's transformation;
- S-wave curve of the velocities of shear waves according to depth (Fig. 6,c), obtained through - Krief's - transformation of basic curves;
- Curve of Poisson's ratio coefficients (Fig. 6,d);
- Distribution of reflection coefficients, calculated from basic curve (Fig. 6,e);

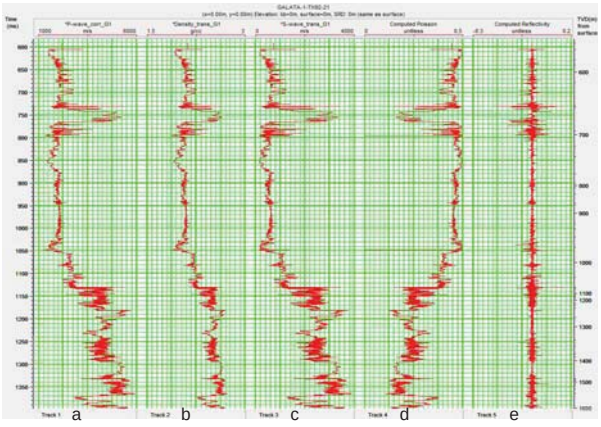

Fig. 6. **P**-1 Galata well– curves created by the correlated P-wave for the purposes of AVO developed methodologies
a/ basic curve P-wave_corr; b/ density curve from Gardner's – transformation of basic curve; c/ curve of velocities of S-wave from Krief's – transformation of basic curve; d/ curve of Poisson's ratio coefficient; **e**/ Distribution of reflection coefficients calculated of basic curve

The last four described curves are transformations of P-wave_corr_G-1 curve used for P-1 Galata. Analogical set of curves (not presented here) was prepared and used for P-2 Galata well.

AVO-technology gives the opportunity to perform three group of researches:

- AVO-modeling of gas or oil saturation;
- AVO-technics based on reflection capability of seismic boarders in geological section;
- AVO-analysis of rock properties in the section.

AVO-modeling of gas saturation

AVO-modeling precedes possible AVO area studies aiming at prediction of changes which would occur in the characteristics of the wave field with change of the fluid filling collectors in the geological section.

Figure 7 presents AVO-modeling on well data P-1 Galata. The correlated P-wave_corr_G1 is used at constant density ρ = 2.22 g/cm^3 and porosity ϕ = 24% for water saturation 5%, 30% и 100%.

On the curve obtained at the lowest water saturation (5%), there was a significant decrease of the velocities in the target area (interval with Middle Eocene aged) by about 17% compared to the 100% water saturation velocity. This would create anomalous impedance values approximate 1100 m/s. g/cm^3.

For each AVO model in Figure 7 were presented also synthetic records with a maximum offset of 1996m, as is the maximum offset in line TX92-21, which significantly exceeds incidence angle 30º. The nature of the resulting synthetic records largely explains the deep Mute applied to standard seismic data processing in the line.

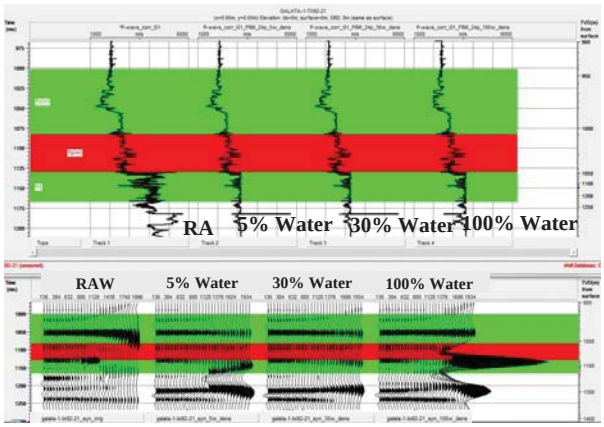

Fig. 7. AVO-modeling at water saturation 5, 30, 100%, constant density 2.22g/cm^3 for target area and porosity 24% (P-1 Galata well)

AVO-techniques based on the reflectivity of seismic boundaries in the geological section

All theoretical developments (the equations of Zoeppritz, 1919; Aki & Richards, 1980 etc.) which serve as the basis for applied AVO-techniques are proven to be valid for incidence angle up to 30º. In order to determine the range of offsets to meet the limitation condition described, a gradient analysis was made on a real record (CDP-470) by seismic line TX92-21 (Fig. 8.a). The same procedure is repeated on a synthetic record by data from the P-wave_corr_G1 curve from the P-1 Galata well (Fig. 8.b). In both cases it can be seen that the offset satisfying the condition of the incidence angle does not exceed 30º, is small - no more than 1150 m. This does not allow us to use such well-functioning AVO-techniques based

on the reflectance of reflective surfaces in the geological section, such as near and far sections, and angle stacks for different incidence angles.

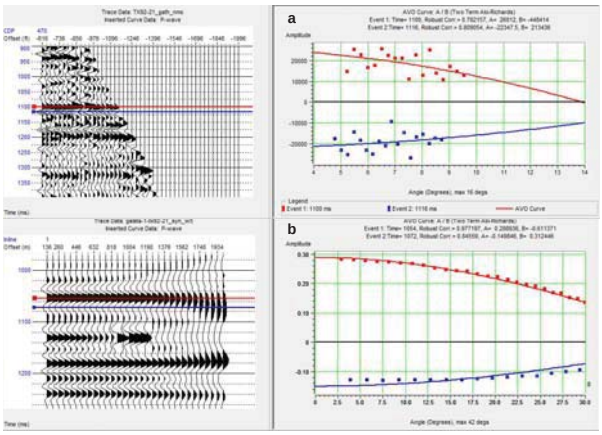

Fig. 8. Gradient analysis
a/ on real data from CDP-470 on line TX92-21; b / on synthetic data from P-wave curve P-1 Galata well

AVO-analysis of the properties of the rocks in the section

In areas with favorable rock features, it is possible to detect hydrocarbons directly - using standard seismic data. However, not all areas have so favorable physical properties on the rocks that the seismic amplitudes in the Post-Stack Migrating data provide information on the reservoir quality and the presence of hydrocarbons. In such cases, it is useful to apply complex AVO-techniques to see how the amplitudes of pre-stack data vary depending on the offset. Here are shown the sections of four AVO-properties of the rocks in Galata area: Intercept (A) (Fig. 9), Gradient (B) (Fig. 10), Poisson's Ratio (Fig. 12) and Fluid Factor (Fig. 13).

AVO-Property Intercept (A) and Gradient (B)

The intercept is the intersection of the best match line with axis at zero distance source-receiver (zero offset) or the zero incidence angle. This is the amplitude of the zero offset directly related to the reflection coefficient (Ostrander, 1984). In this sense, the section of the property Intercept (A) represents the variation of the reflection coefficient of the P-waves on the line induced by the lateral variation of the physical parameters of the geological media contacting the reflecting surface. For a simple cumulative trace, the amplitude value of a certain time is averaged for the amplitudes of all offsets. Thus, this averaging eliminates the amplitude of information that is carried by each offset. On the other hand, however, information about the change of offset amplitude is used in the calculation of the "intercept-trace". In this sense, the intercept-section can be considered as a more informative section than the conventional one in the sense of amplitude anomalies.

The gradient is the slope of the best match line. A section of AVO-property Gradient (B) describes from CDP-trace to the next CDP-trace, along the line, the reflection coefficient is changed according to the offset. The anomalous values are related to the local variation of the wave velocities above and below the reflecting surface. The large change in the Vp / Vs ratio causes high gradient values. Since the presence of gas in porous rocks strongly influences the Vp / Vs ratio, the gradient section is a good indicator of such reservoirs.

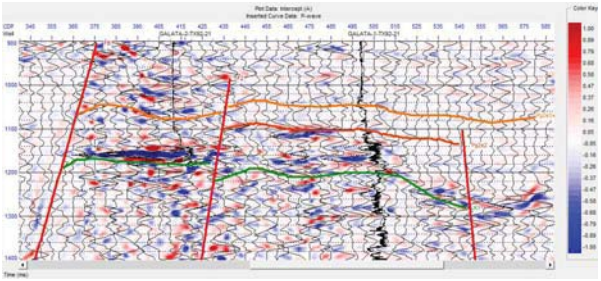

Fig. 9. Section of AVO-property Intercept (A)

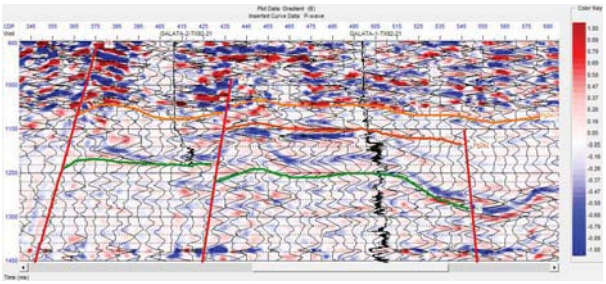

Fig. 10. Section of AVO-property Gradient (B)

AVO-Analysis - Crossplot (A / B)

Figure 11 present the result of the AVO-analysis Crossplot that implements the interconnection between AVO-properties Intercept (A) and Gradient (B). Reflections from the upper surface of water-saturated sediments are plotted around linear dependence (wet trend), passing through the start of the coordinate system. Its slope depends on the average Poisson's coefficient. Reflections from the upper surface of hydrocarbon accumulations are grouped under the wet trend, and reflections from the lower surface of the reservoir - above it (Castagna, & Swan, 1997). The two marked areas –blue (F) and yellow (E) - correlate very well with the gas-saturated intervals on the cross-section shown on Fig. 11,d, where the two wells P-1 and P-2 Galata are located.

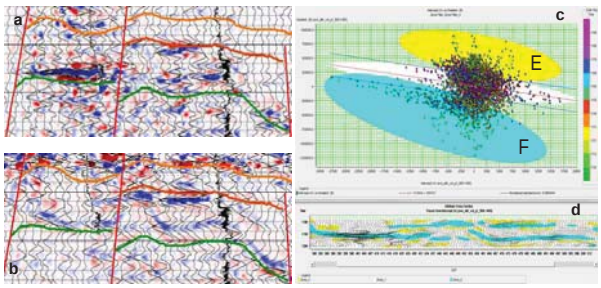

Fig. 11. AVO - analysis crossplot A/B
a/ Fragment of AVO-property Intercept (A) in target zone (line TX92-21); b/ Fragment of AVO-property Gradient (B) in target zone (line TX92-21); c/ **A**VO - Crossplot in target zone (line TX92-21); d/ AVO Cross-section in target zone (line TX92-21)

AVO-Property Poisson's Ratio

In Figure 12, the AVO-indicator Poisson's Ratio Coefficients are considered for the "bright spot" anomaly only. Generally, the velocities of clays and sandstones are not significantly different. The presence of fluid in a collector can cause a difference in the velocities of the P- and S- waves, and hence

the anomalous values of the Poisson's Ratio coefficient (Koefoed, 1955).

AVO - Property Fluid Factor

Figure 13 shows the AVO-indicator Fluid Factor. The AVO-property Fluid Factor is defined by Castagna (Castagna, 1993) as a deviation from the calculated on drilling data dependence Vp/Vs for water-saturated clayey rocks and sandstones.

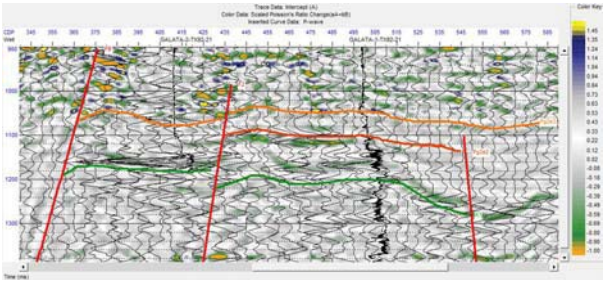

Fig. 12. Section of AVO-property Poisson's Ratio

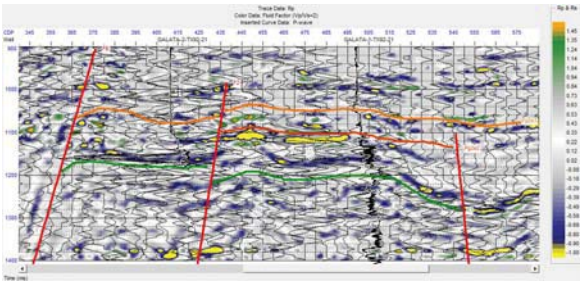

Fig. 13. Section of AVO-property Fluid Factor

Conclusion

The results of all AVO-techniques give rise to several important conclusions:

- At each section of the AVO-properties, it is noticeable that the anomalies appear on a lower noisy background than the standard section;
- The described amplitude anomaly "bright spot" in the standard seismic section TX92-21 appears to be an anomalous area of the Intercept (A) and Gradient (B) sections, in view of the fact that both are related to variations in the reflection coefficient;
- The sections of the AVO-properties show a more detailed division of the gas-saturated interval and an uneven distribution of the rocks collector properties in the target zone, including sediments of the following periods: Upper Cretaceous, Paleocene, and Middle Eocene. The gas-saturated section interval in the tectonic block P-2 Galata well is one attached to the limestone of the Paleocene and Upper Cretaceous, while in the northern block (the area of P-1 Galata), the main anomalous zone is attached to the upper part of the Middle Eocene, but a significant improvement in the capacity characteristics of the collector is also recorded at the lower part of the Eocene;
- An important result is obtained from the AVO-technology AVO-analysis Crossplot, where the upper and lower surface of the intervals with a substantial gas-saturation is observed well on the image of Figure 11,d- Cross-section
- The anomalous zones in the tectonic block, where is located P-1 Galata well around the CDP-450, mark an area, where a future well would be in a more favorable structural position and as collector quality as compared to the P-1 Galata well position. This is particularly well illustrated by the sections from AVO-properties: Poisson's Ratio (Fig. 12) and Fluid Factor (Fig. 13).

In conclusion, it can be noted that the interpretation of amplitudes of pre-stack data is extremely effective in reducing the risk when choosing a location for a search or exploitation drilling.

Acknowledgements

I would like to express my gratitude to Rexim Seis Ltd. (www.reximseis.com) for the provided software products and real seismic data with the help of which the experimental studies were carried out.

References

Aki, K. & P.G. Richards. Quantitative Seismology. - W.H. Freeman and Co., 1980. - 202-228.

Castagna, J. P. Rock physics - the link between rock properties and AVO response. - In: Offset dependent reflectivity – theory and practice of AVO analysis (eds. J. P. Castagna & M. M. Backus). Investigations in Geophysics, 8, 1993. Society of Exploration Geophy-sicists.

Castagna, J. P. & H. W. Swan. Principles of AVO. Crossplotting. The Leading Edge, 16, 1997. - 337-42.

Koefoed, O. On the effect of Poisson's ratios of rock strata on the reflection coefficients of plane waves. - Geophysical Prospecting, 3, 1955. - 381-387.

Ostrander, W.J. Plane-wave reflection coefficients for gas sands at nonnormal angles of incidence. - Geophysics, 49, 1984. - 1637-1648.

Shuey, R. T. A simplification of the Zoeppritz equations. - Geophysics, 50, 1985. - 609-14.

Zoeppritz, K. Uber reflexion und durchgang seismischer Wellen durch Unstetigkerlsflaschen. Uber Erdbebenwellen VIIB. Nachrichten der Koniglichen Gesellschaft der Wissenschaften zu Gottingen. - Math. Phys., K1, 1919. - 57-84.

The article is reviewed by Prof. Dr. Boyko Rangelov and Prof. Stefan Dimovski, DSc.

A GEOPHYSICAL APPROACH FOR MAPPING OF ABANDONED MINING WORKINGS AND UNCONSOLIDATED ZONES IN COAL MINING AREAS

Stefan Dimovski[1], Nikolay Stoyanov[1], Christian Tzankov[1], Atanas Kisyov[1]

[1]University of Mining and Geology "St. Ivan Rilski", Sofia 1700; dimovski@mgu.bg, nts@mgu.bg, ch.tzankov@gmail.com, at.kisyov@gmail.com

ABSTRACT. Coal mining is the cause of significant changes in the geotechnical and hydrogeological conditions in the subsurface areas affected by it. This creates serious problems with the ground stability, rapid rise of groundwater level and concentrated or scattered water surface inflows. The proposed geophysical approach for mapping of abandoned mining workings and unconsolidated zones in the problem areas is based on the application of electrical resistivity tomography (ERT). This approach is approbated during the localization of abandoned mining workings (galleries, collapsed zones, cracked areas and pillars) developed throughout the many years of coal mining in the region of Pernik northern neighborhoods. The presented results confirm the applicability of the proposed methodology of field data measurement, analysis and interpretation.

Keywords: electrical resistivity tomography, abandoned mining workings, unconsolidated zones

ГЕОФИЗИЧЕН ПОДХОД ЗА КАРТИРАНЕ НА СТАРИ МИННИ ИЗРАБОТКИ И РАЗУПЛЪТНЕНИ ЗОНИ ВЪВ ВЪГЛЕДОБИВНИ РАЙОНИ

Стефан Димовски[1], Николай Стоянов[1], Християн Цанков[1], Атанас Кисьов[1]

[1]Минно-геоложки университет "Св. Иван Рилски", София 1700; dimovski@mgu.bg, nts@mgu.bg, ch.tzankov@gmail.com, at.kisyov@gmail.com

РЕЗЮМЕ. Подземният въгледобив е причина за значителни промени в геотехническите и хидрогеоложките условия в засегнатите от него части от подповърхностното пространство. Това създава сериозни проблеми с устойчивостта на земната основа, бързо покачване на подземните води и съсредоточени или разсеяни водопроявления на земната повърхност. Предложеният геофизичен подход за картиране на стари минни изработки и разуплътнени зони в проблемните участъци се базира на прилагането на електротомографски изследвания. Подходът е апробиран при картирането на отработените пространства (галерии, обрушени зони, напукани зони и целици) по време на многогодишния подземен въгледобив в района на северните квартали на гр. Перник. Представените резултати потвърждават приложимостта на методиката на измерване, анализ и интерпретация на данните.

Ключови думи: електротомографски изследвания, стари минни изработки, разуплътнени зони

Introduction

The mining activities in the Pernik coal basin are the cause of significant changes in the geotechnical and hydrogeological conditions in the subsurface areas affected by it. They create serious problems with the ground stability, rapid rise of groundwater level and concentrated or scattered water surface inflows. Some of the most affected areas in the region are Pernik northern neighborhoods Rudnichar, Dimova mahala, Beli breg (Figs. 1 and 2).

Geophysical methods can be successfully applied for the detailed study of the near-surface geological section (Dimovski et al., 2007). They fulfil the results from the borehole investigations and allow correct interpolation of the general behavior of the present formations. Electrical resistivity methods have wide application for the detailed mapping of the near-surface section. Their geological efficiency is connected to the rocks differentiation according to electrical resistivity. For a precise geoelectrical section the rocks electrical resistivity is tied to the existing preconditions for presence of ionic conductivity (Dimovski et al., 2008; Shanov et al., 2009).

The main task of the performed geophysical studies is to detail the near-surface hydrogeological section in the studied area down to a depth of 40-50 m. More specifically, the results have to provide the possibility to outline, with sufficient reliability, the spatial boundaries of layers and zones characterized by different lithological and grain-size characteristics, as well as by different degree of water-permeability and water-saturation. It is also necessary to establish the potential presence and to define the extent of unconsolidated zones and cavities in the subsurface section.

The main objectives of the geophysical research are to map the spatial boundaries of the determined low-rank hydrogeological units (HGU) in the affected by the coal mining parts of the Paleogene coal bearing complex and to determine the boundary between the unsaturated zone (zone of aeration) and the water-saturated zone.

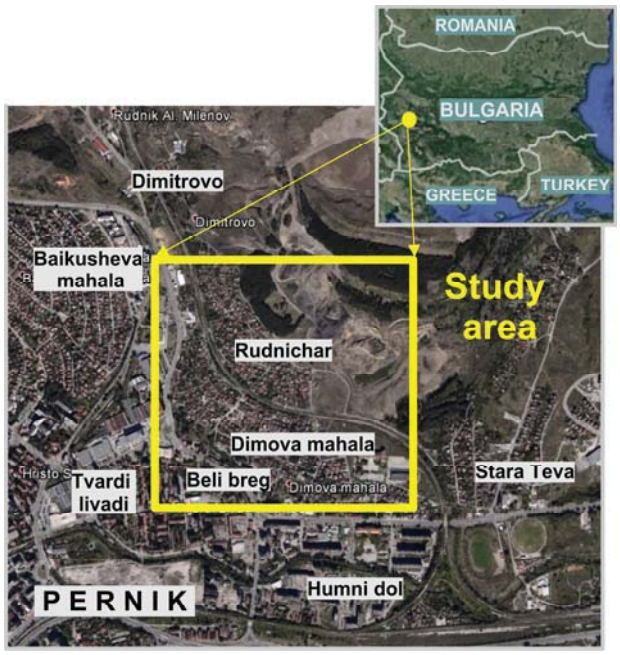

Fig. 1. Location of the study area in the region of Pernik – neighborhoods Rudnichar, Dimova mahala, Beli breg

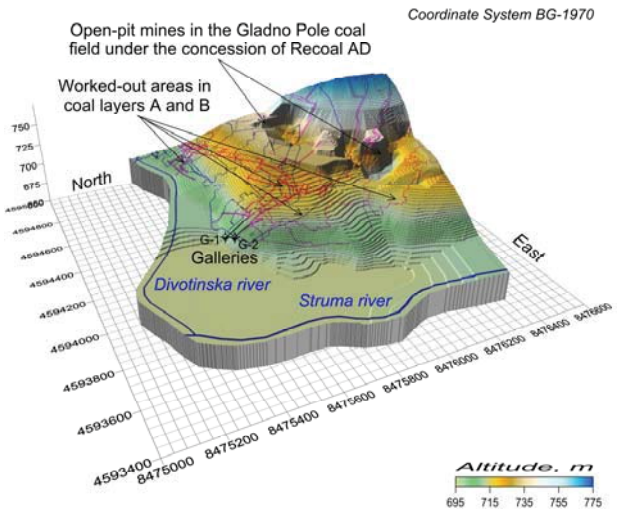

Fig. 2. Geomorphologic map with the location of the abandoned mining workings in the region of Pernik – neighborhoods Rudnichar, Dimova mahala, Beli breg

Basic elements of the electrical tomography surveying technique

Electrical resistivity tomography (ERT) is a new and rapidly evolving technology for the non-invasive imaging of the near-surface section. This method, based on the use of modern equipment, optimal measuring techniques (Griffiths et al., 1990), and computer processing of acquired data (Loke, 1999). From a series of electrodes, low frequency electrical current is injected into the subsurface, and the resulting potential distribution is measured. A large variety of different source and receiver positions are used to sample the target section (Griffiths and Barker, 1993).

The true resistivities in the subsurface area are determined by the computer program RES2DINV (Loke, 2001). For this purpose, the resistivity values measured by the field equipment in different points (having particular electrodes location) have to be transferred into apparent resistivity values after taking into consideration the array geometry. The computer program uses as input data the information about the electrodes location on the surface and the apparent resistivity values in each measured point. On this basis the program automatically divides the subsurface area into a given number of rectangular blocks. Then, applying the least-squares method, the resistivity of each block is determined in such a way that the calculated apparent resistivity values for the composed model fit in the best possible way the measured electric field.

The so determined geoelectrical model can be transformed into a geological one on the base of:

- General information of the geological and hydrogeological conditions in the studied region.
- Reference data for the electrical resistivity of different rock types (Keller and Frischknecht, 1966; Daniels and Alberty, 1966).
- Data from the drilled boreholes.

Surveying results, analysis and interpretation

When planning the number, length and location of the geophysical lines, the available archive data for the coal mining accomplished in the past (maps, schemes, plans and mine surveys), as well as data from the drilling activities performed in 2012-2015 are taken into account. The lines cover comparatively evenly the territory of the Pernik neighborhood Rudnichar, which is a prerequisite for a better determination of the spatial boundaries of the low-rank HGU in the Paleogene coal bearing complex.

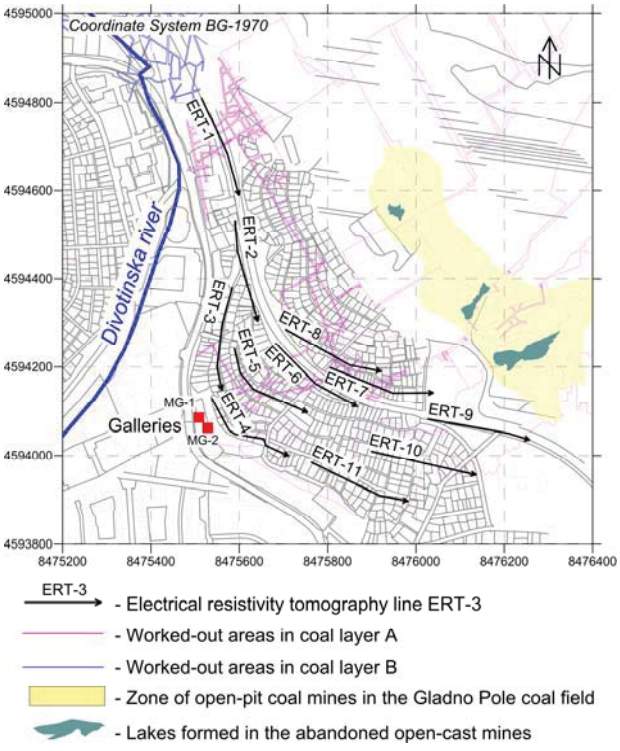

Fig. 3. Cadastral plan with the location of the geophysical surveying lines in the region of Pernik northern neighborhoods

The field measurements were performed along eleven lines having a total length of 2530 m (each ERT line has a length of 230 m). The location of the geophysical surveying lines in the area under study is illustrated in Figure 3. The four-electrode Wenner-Schlumberger array was applied. The measurements were performed applying Terrameter SAS 1000, a resistivity and IP instrument produced by ABEM. The processing of the acquired data and the interpretation of the obtained results are performed by members of the Departments of Applied Geophysics and Hydrogeology and Engineering Geology, University of Mining and Geology "St. Ivan Rilski", Sofia. A case of water surface inflow and moments from the field measurements are illustrated in Figure 4 and Figure 5.

Fig. 4. Water surface inflow through the exit of mining gallery MG-1 in the region of Pernik neighborhood Dimova mahala

Fig. 5. Moments from the field measurements in the region of Pernik neighborhood Rudnichar

The analysis of the results is in accordance with the geological sections recorded in the drilled boreholes and the available information about the past coal mining activities in the area.

The electrical resistivity sections obtained along the eleven studied lines are illustrated in Figure 6, Figure 7, and Figure 8. The performed analysis gives reason the following conclusions to be made:

1. The geoelectrical section along all lines is consistent regarding the electrical resistivity distribution in depth.

2. The electrical resistivity of the varieties composing the studied near-surface section changes in a relatively narrow range – from about 30 Ωm up to more than 120 Ωm.

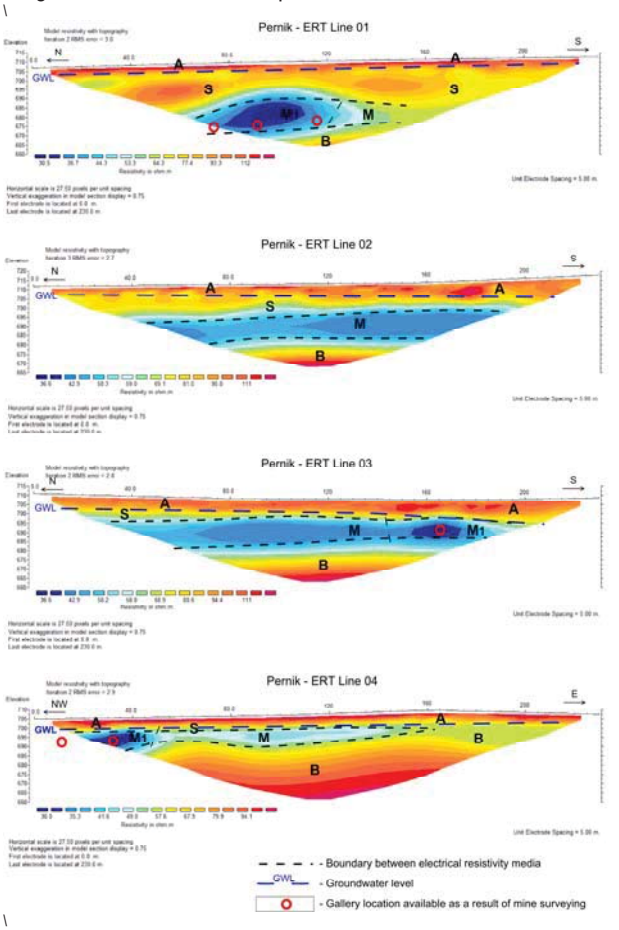

Fig. 6. Electrical resistivity sections obtained along lines ERT-1, ERT-2, ERT-3 and ERT-4

3. It can be summarized that the studied geoelectrical section is represented by five electrical resistivity media, mapping five zones and two sub-zones, each characterized by different degree of unconsolidation, water-saturation and water-permeability. Most probably, these zones are mapping the spatial boundaries of the low-rank HGU determined down to a depth of 50 m in the range of the affected by the coal mining parts of the Paleogene coal bearing complex.

4. The differentiated electrical resistivity media, zones and sub-zones in the sections along the eleven studied lines are the following:

The first electrical resistivity media (Zone A) is located in the upper part of the near-surface sections along all lines. It is characterized by the highest values of the electrical resistivity for the studied geoelectrical section – in the range from 75 Ωm up to more than 120 Ωm. It most likely maps the spread of the unsaturated zone (zone of aeration) in the consolidated near-surface part of the Paleogene coal bearing complex.

The second electrical resistivity media (Zone S) is situated just underneath *Zone A* in the range of the affected by the underground coal mining parts of the Paleogene complex. It is characterized by a little bit lower values of the electrical resistivity – in the range from 55 Ωm up to 80 Ωm. *Zone S*

probably shows the spread of the partially unconsolidated water-saturated areas above the abandoned mining workings that comprise the low-rank HGU *upper anthropogenic complex 2 – Anthr cmx - up2.*

The third electrical resistivity media (Zone M1) is determined in the depth interval from 16 m down to 35 m in the sections along lines ERT-1, ERT-5, ERT-6, ERT-7, ERT-8, and along lines ERT-3 and ERT-4 – in the depth interval from 7 m down to 20 m. The values of the electrical resistivity in this zone are the lowest for the studied geoelectrical section – in the range from 30 Ωm up to 50 Ωm, sometimes a little bit higher. Most probably *Zone M1* denotes the location of the galleries and the worked-out area in coal layers A and B. The galleries locations available as a result of mine surveying in the past are illustrated by red circles on the presented geoelectrical sections (Figs. 4 and 6). This media is water-saturated. In the scope of *Zone M1* enter two low-rank HGU – *lower anthropogenic complex 2 (Anthr cmx - l2)* and *lower anthropogenic complex 4 (Anthr cmx - l4).*

In the section along line ERT-5, in the upper part of the third electrical resistivity media, a high-ohmic region *(Sub-zone aM1)* is established. It is characterized by values of the electrical resistivity in the range from 45 Ωm up to 70 Ωm (Fig. 7). *Sub-zone aM1* most probably maps the unsaturated part of *Zone M1* that is located above groundwater level.

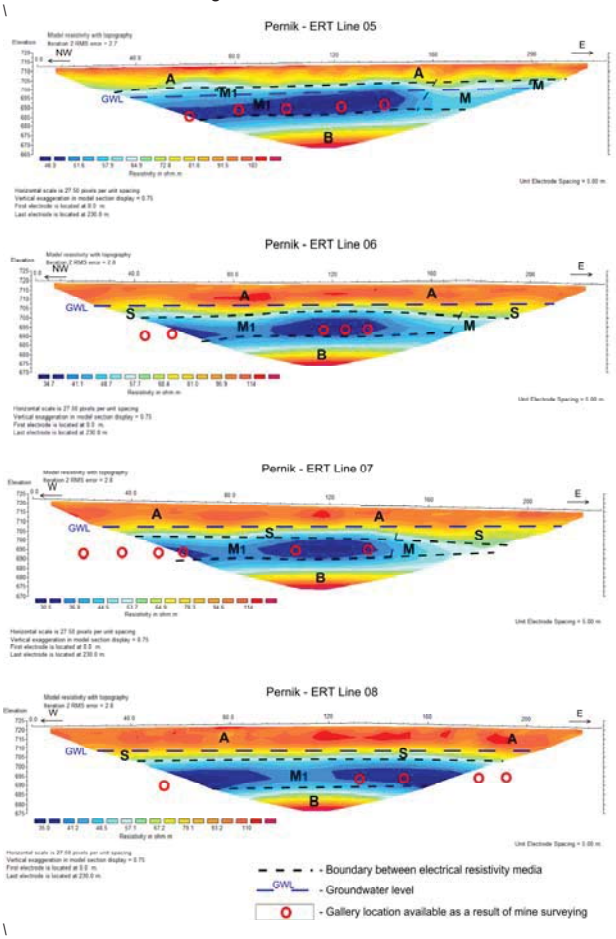

Fig. 7. Electrical resistivity sections obtained along lines ERT-5, ERT-6, ERT-7 and ERT-8

The forth electrical resistivity media (Zone M) is expressed in the sections along all lines (with the exception of line ERT-8) in a fairly wide range – in the depth interval from 3 m down to 32 m, most frequently in the interval from 5 m down to 25 m. It has a little bit higher values of the electrical resistivity than the ones characteristic for *Zone M1* – in the range from 50 Ωm up to 70 Ωm, however in separate regions outside these limits. This zone includes the water-saturated parts of the worked-out areas in coal layers A and B (mining workings, collapsed zones, cracked areas and pillars) that comprise two low-rank HGU – *lower anthropogenic complex 1 (Anthr cmx – l1)* and *lower anthropogenic complex 3 (Anthr cmx – l3).*

In the eastern end of the section along line ERT-5, in the upper part of the forth electrical resistivity media, a high-ohmic region *(Sub-zone aM)* is established. It is characterized by values of the electrical resistivity in the range from 50 Ωm up to 80 Ωm (Fig. 7). In this case, *Sub-zone aM* probably reveals the spread of the unsaturated part of *Zone M* that is located above groundwater level.

The fifth electrical resistivity media (Zone B) maps the deep parts, in some cases also the periphery, of the sections along all lines. It is characterized by comparatively high values of the electrical resistivity – in the range from 75 Ωm up to more than 120 Ωm. Most probably *Zone B* denotes the relatively stable, unaffected by the coal mining, parts of the Paleogene coal bearing complex. This zone comprises the low-rank HGU *Paleogene coal bearing complex in natural state – Pg cmx.*

5. The groundwater level in the sections along all lines (with the exception of line ERT-5) is marked by the boundary between Zone A and Zone S. At some locations in the sections along lines ERT-4, ERT-9, ERT-10 and ERT-11, the groundwater level is mapped by the boundary between Zone A and Zone B, and in the section along lines ERT-5 – by the lower of boundaries of Sub-zone $^{a}M_1$ and Sub-zone ^{a}M. The groundwater level is presented by a dotted blue line on the presented geoelectrical sections (Figs. 6, 7, 8).

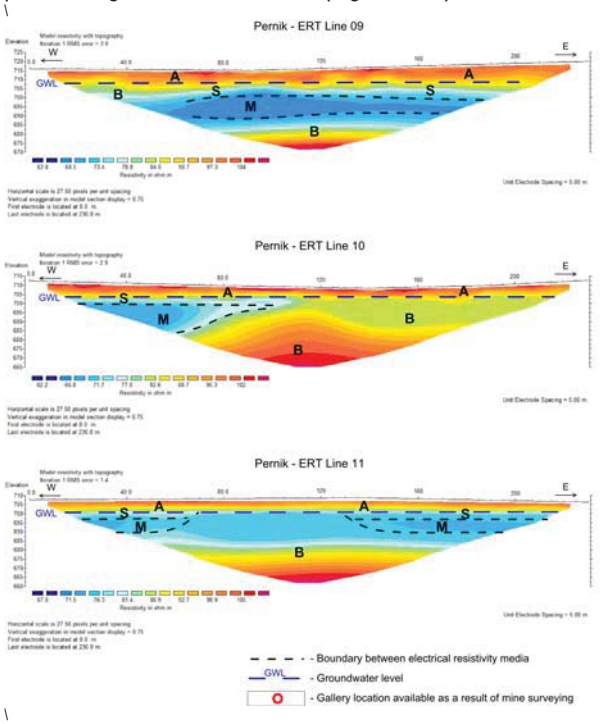

Fig. 8. Electrical resistivity sections obtained along lines ERT-9, ERT-10 and ERT-11

In accordance with one of the main objectives of the performed study, on the base of the derived electrical resistivity sections along the eleven surveyed lines and the detected geoelectrical borders, structural maps are developed concerning the top and the bottom of the areas affected by coal mining (*Zone M₁* and *Zone M*) – Figure 9 and Figure 10. These surfaces are revealing the spatial boundaries of the four determined low-rank HGU of the lower anthropogenic complex: *Anthr cmx – l1, Anthr cmx – l2, Anthr cmx – l3* and *Anthr cmx – l4*.

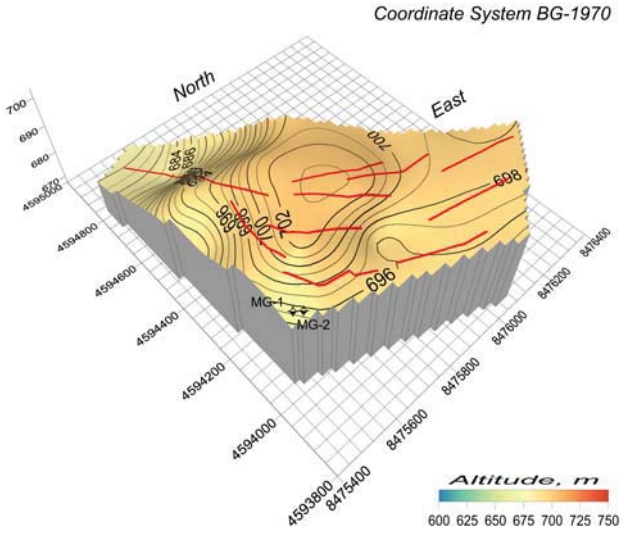

Fig. 9. Structural map of the top of low-rank HGU of the lower anthropogenic complex – *Anthr cmx – l1, Anthr cmx – l2, Anthr cmx – l3* and *Anthr cmx – l4*

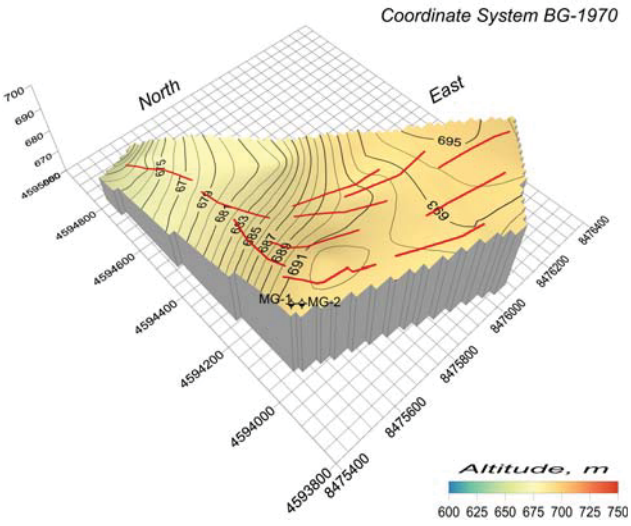

Fig. 10. Structural map of the bottom of low-rank HGU of the lower anthropogenic complex – *Anthr cmx – l1, Anthr cmx – l2, Anthr cmx – l3* and *Anthr cmx – l4*

The determined spatial boundaries of the low-rank HGU in the range of the affected by the coal mining parts of the Paleogene coal bearing complex are implemented in the development of a numerical 3-D hydrogeological model. This model is applied for estimating the changes in the hydrogeological conditions, the rise of groundwater level and the quantity of groundwater drained by concentrated or scattered water surface inflows.

Conclusions

The achieved practical results are confirming the geological effectiveness of the discussed approach for data acquiring, analysis and interpretation.

Five zones and two sub-zones, each characterized by different degree of unconsolidation, water-saturation and water-permeability are separated. These zones map the spatial boundaries of the low-rank HGU determined down to a depth of 50 m in the range of the affected by the coal mining parts of the Paleogene coal bearing complex.

The obtained results are implemented in the development of a numerical 3-D hydrogeological model that is applied for estimating the changes in the hydrogeological conditions, the rise of groundwater level and the quantity of groundwater drained by concentrated or scattered water surface inflows.

References

Daniels F., R. A. Alberty. Physical chemistry. John Wiley and Sons, Inc., 1966. - 674 p.

Dimovski, S., N. Stoyanov, Ch. Gyurov. Efficiency of electrotomography surveying for geoelectrical mapping of near-surface geological section. – BULAQUA Journal, 4, 2007. - 47-55.

Dimovski, S., N. Stoyanov, S. Kostyanev. Application of electrical resistivity techniques for investigation of landslides. – Proceedings of the First International Conference on Remote Sensing Techniques in Disaster Management and Emergency Response in the Mediterranean Region, EARSeL, Zadar, Croatia, 2008. - 241-251.

Griffiths, D. H., J. Turnbull, A. I. Olayinka. Two-dimensional resistivity mapping with a computer-controlled array. – First Break, 8, 1990. - 121-129.

Griffiths, D. H., R. D. Barker. Two-dimensional resistivity imaging and modeling in areas of complex geology. – Journal of Applied Geophysics, 29, 1993. - 211-226.

Keller G.V., F.C. Frischknecht. Electrical methods in geophysical prospecting. Pergamon Press Inc., Oxford, 1966. - 517 p.

Loke, M.H. Electrical Imaging Surveys for Environmental and Engineering Studies. A Practical Guide to 2-D Surveys. Penang, Malaysia, 1999. - 67 p.

Loke, M.H. A practical guide to RES2DINV ver. 3.4; Rapid 2-D resistivity & IP inversion using the least-squares method. Geotomo Software, Penang, Malaysia, 2001. - 129 p.

Shanov, S., A. Mitev, A. Benderev, K. Kostov, B. Mihailova. Electrical survey for detailed characterizing of underground karst: Example from Iskar River (Western Bulgaria). 5th Congress of Balkan Geophysical Society — Belgrade, Serbia, Geophysics the cross road. EAGE, 10-16 May 2009. (on CD).

The article is reviewed by Prof. Dr. Aleksey Benderev and Prof. Dr. Radoslav Varbanov.

MATHEMATICAL FLOW MODEL OF THE MERICHLERI THERMO-MINERAL FIELD

Nikolay Stoyanov[1], Stefan Zeinelov[1]

[1]University of Mining and Geology "St. Ivan Rilski", Sofia 1700; nts@mgu.bg; stefan.zeynelov@gmail.com

ABSTRACT. A generalized conceptual scheme of the thermo-mineral field "Merichleri" is presented that is based on data from its exploitation and on the contemporary ideas for the geological and tectonic characteristics of its imbedding structures. This concept is implemented in the composed three-dimensional model of the flow field in the studied region. The modeled area covers a territory of 4.5 km^2 and includes the upper part of the thermo-mineral reservoir to a depth of 450 m and its periferial low water-bearing zone. Three hydrogeological units fall within these margins: a volcanogenic fault-fissure drainage complex, a volcanogenic fissure complex, and a low water-bearing fissure complex. By the developed mathematical model are estimated the water balance revenue and expenditure elements and is performed a quantitative assessment of the field water resources. The boundaries of the sanitary protection zone around the existing facility for extraction of thermo-mineral waters are deternined. The computer programs Modflow and Modpath are used for the model development.

Keywords: hydrogeological model, mineral water resources, thermo-mineral field.

МАТЕМАТИЧЕСКИ ФИЛТРАЦИОНЕН МОДЕЛ НА ТЕРМОМИНЕРАЛНО НАХОДИЩЕ „МЕРИЧЛЕРИ"

Николай Стоянов[1], Стефан Зейнелов[1]

[1]Минно-геоложки университет "Св. Иван Рилски", София 1700; nts@mgu.bg; stefan.zeynelov@gmail.com

РЕЗЮМЕ. Представена е обща концептуална схема на термоминерално находище „Меричлери", базирана на данни за неговата експлоатация и на съвременните представи за геолого-тектонския строеж на вместващите го структури. Концепцията е имплементирана в съставения тримерен модел на филтрационното поле в района на находището. Моделната област обхваща горната част термоминералния резервоар до дълбочина 450 m и периферна на него слабо водоносна зона на обща площ 4,5 km^2. В тези граници попадат три хидрогеоложки единици: вулканогенен разломно-пукнатинен дренажен комплекс, вулканогенен пукнатинен комплекс и пукнатинен слабо водоносен комплекс. С математическия модел са определени приходните и разходните елементи на водния баланс и е направена количествена оценка на водните ресурси на находището. Определени са границите на санитарно-охранителната зона около действащото съоръжение за добив на термоминерални води. При разработването на модела са използвани компютърните програми Modflow и Modpath.

Ключови думи: хидрогеоложки модел, ресурси на минерални води, термоминерално находище

Introduction

The exceptional balneological properties of the water in the Merichleri thermo-mineral field and its close similarity to the water in Karlovi Vari, Chech Republic, have been the main reason for active exploitation and serious scientific research in this water field for the past 100-120 years. The works of various scientific researchers during this period focus on the genesis, the physical and chemical properties, the abstraction and the use of the mineral water (Azmanov, 1940; Shterev, 1964; Petrov, 1964; Petrov et al., 1970; Pencheva et al., 1998). Some unpublished archived materials (reports, statements and notes) contain detailed data from the prospecting of this field, data about the mineral water sources used in the past and information about the only existing borehole C-3x (Geshev and Denkov, 1972; Dobreva, 1997; Neykov, 2017).

The general schemes and estimates presented in referenced sources do not provide satisfactory answers to a number of important questions regarding the properties of the hydrogeological units comprising and bordering the field, the structure of the sub-surface flow, the mineral water balance and resources, the boundaries of the sanitary protection zones (SPZ) surrounding the water sources, etc. Resolving these tasks by conventional or analytical models is not always efficient. Given the high level of heterogeneity of the hydrogeological structure and the more complex boundary conditions prevailing in the Merichleri field, detailed simulation of specific hydrogeological conditions at the required level of precision would require the use of digital 3D models. The limitation of this approach, arising from insufficient volume of data, can be successfully compensated by the use of calibration procedures.

Mathematical digital 3D models have been used to re-create the complex hydrogeological situation in the Merichleri field. These models have determined the flow structure, have produced quantitative balance and resource estimations of the field, and have defined the boundaries of the SPZ around the C-3x borehole. Modflow and Modpath computer software has been applied for this purpose. (McDonald and Harbaugh, 1988; Pollack, 1994.). Scientific publications and archived materials concerning the field have been used as well (Shterev, 1964; Petrov et al., 1970; Stoyanov, 2015; Geshev and Denkov, 1972; Dobreva, 1997; Petrov, 1998; Neykov, 2017).

General information about the Merichleri field

With its genetic features, chemical components and gas content, the Merichleri thermo-mineral field belongs to the group of carbon-acidic nitrous mineral water fields. Initially, the mineral water with TDS of 6.4 g/l had been flowing from the Solentsi natural spring in the Merichlerska river flood plain, 3 km to the south-east of the village of Merichleri. The spring was capped in 1907 and had a flow-rate of approximately 1 l/s at drainage elevation of 150.8 m. Following the Chirpan big earthquake in 1928, the spring dried up, the shocks having opened new underground mineral water discharges along the Merichleri river valley and along the faults running parallel to the Maritsa river, around 20 m below the capped elevation. "Merichleri" type water had surfaced briefly in the Chernokonevo residential area of the town of Dimitrovgrad. Water of similar composition was discovered in 1937, although of lower temperature (20°C), poorer mineral composition (5.1 g/l) and reduced CO_2 content. This water was capped by a 16 m concrete shaft, using a flow-rate of around 0.2 l/s. Two 300 and 220 m long boreholes were drilled in 1958-59 near the old capping structure. The mineral water found there was 33-36°C in temperature and identical in composition to the water in the dried-up spring, and with pumping flow-rate per unit drowdown of 2-4 (l/s)/m. The water entered the boreholes at depths of 40 and 80 m through wide joints, with the water level being established at a depth of 2.5-3.0 m. In the period between 1965 and 1968, the Committee for Geology and Mineral Resources (CGMR) drilled and studied in detail the C-3x exploration borehole - so far the only source for extraction of mineral water from the Merichleri field. This 371 m long borehole runs through wide joints and several fault zones in the 40-70 m and 270-300 m intervals. The static level is established at 5.5 m and the pumping rate per unit drowdown is 5.6 (l/s)/m. TDS of the extracted water is 6.4 g/l, very close in composition to the water that disappeared after the earthquake, but with a higher temperature of 45°C. Its type is sulphate-carbonaceous, sodium, fluorine and boron. The water contains around 500 mg/l of diluted CO_2, and 30% of N_2 are established in the spontaneous gas. So far, the resource estimates for the field have been based on observations of mineral water rate, chemical composition and temperatures.

The conceptual model

Considering the modern geological and tectonic ideas of the region (Boyanov et al., 1993a,b) and based on the available information about the source of mineral water, the following general concept about the hydrogeological conditions in the thermo-mineral water field has been adopted (Fig. 1).

Main mineral water reservoir

It is assumed that the main reservoir was formed among the very deeply bedded Proterosoic metamorphites, Paleozoic granites and, partially, Mid-Triassic limestones of the Upper Thracian depression rock foundation (Shterev, 1964). The "Merichleri" type of water is regarded as one manifestation of a common mineral basin buried underneath at more than 1,000 m thick Tertiary complex. In chemical composition, in particular, regarding the content of sulphites and chlorides, this water does not correlate to the composition of the hosting rocks, and only the fluorine can be related to the type of the main collector. Most likely, buried water has penetrated the Pre-Tertiary bedding of ancient Eocene and Pliocene water basins. It is assumed that the water in the ancient basins had been sodium-glauberite in composition, with a very low content of chlorides, subsequently, following geological and tectonic changes and climate alteration, undergoing substantial metamorphosis which has continued during their stay in the main collector. The presence of CO_2 is related to the Oligocene volcanic processes which have also changed the composition of micro-components.

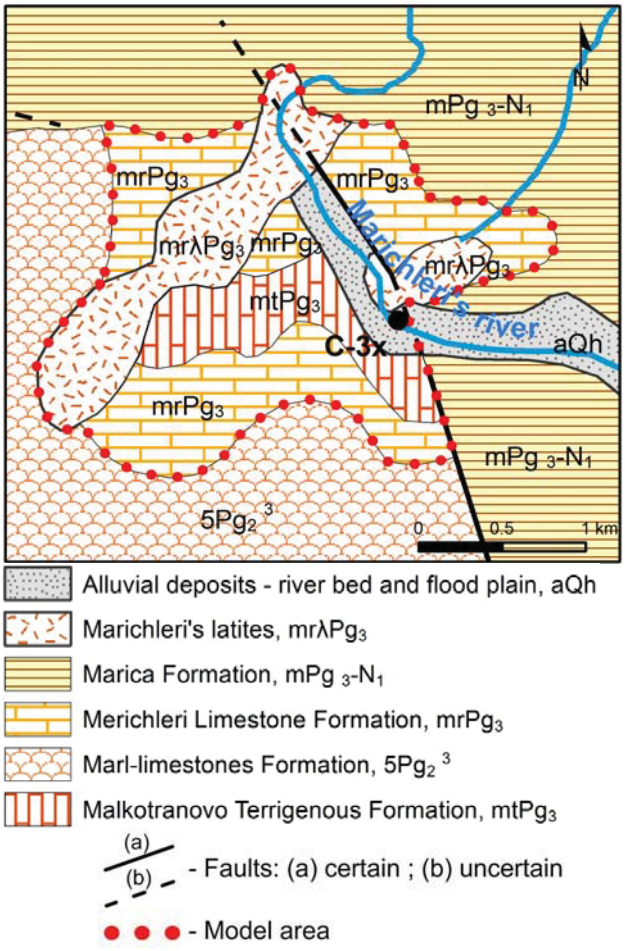

Fig. 1. Geological map in the region Merichleri thermo-mineral field. Location of the C-3x mineral water borehole
(by the Geological map of Bulgaria M 1:100000. Map of the Chirpan area and map of the Dimitrovgrad area.)

Secondary mineral water reservoir and peripheral zone

According to the accepted assumption, two hydrogeological units can be delineated at a depth of 300-400 m in the accessed and peripheral parts of the mineral water reservoir:

- *A volcanogenic fault-fissure drainage complex - secondary mineral water reservoir.* It is formed in subvolcanogenic Upper-Oligocene bodies latites defined as Meirchleri's latites ($mr\lambda Pg_3$). They are embedded and cut across the terigenic-carbonaceous sediments of the Merichleri limestone Formation ($mrPg_3$), the Malkotranovo terigenous Formation ($mtPg_3$), and, also, sediment and pyroclastic materials of the underlying Eocene-Oligocene complexes (Fig. 1). The Merichleri's latites are highly fractured and faulted, with strongly manifested traces of hydrothermal activity. The mineral water from the main reservoir flows toward the surface and circulates mainly

through a complex system of sub-meridional and sub-parallel intersecting fault and downthrow-fault structures. These structures and the fissured volcanogenic bodies are regarded as a secondary reservoir of the Merichleri field. The deeply lying faults and downthrow faults are not only the main path along which the deeply accumulating thermo-mineral water flows, but are also the main factors determining the quantity and quality of the resources in the field. There are two components in the mineral water flow direction: (a) ascending thermo-mineral flow along faults from the main reservoir toward the surface, and (b) horizontal flow into the secondary reservoir mainly along the fault-downthrow fault sub-meridional structures. In general, the horizontal flow direction is S-SE toward the main regional draining structure - the Maritsa fault zone. The average hydraulic gradient is, approximately, 1.2E-04. Two hydrogeological units of lower order can be differentiated by the flow properties of the media:

- *A tectonic highly conductive zone:* This zone includes the fault-downthrow fault structures.
- *A fractured poor water-bearing zone:* This zone includes the main part of the subvolcanogenic complex outside the the tectonic structures.

The secondary reservoir is recharged by the ascending thermo-mineral flow from the main reservoir and by a lateral flow along a fault from the north. The adjoining low water-bearing complex of shallow cold water supplied from the Merichlerska river plain and from precipitation provides a very limited level of recharging. The average precipitation total - 606 mm in the Dimitrovgrad gauging station (Koleva and Peneva, 1990) and the water permeability of the surface layer lead to the assumption that the average recharge rate (W) in the tectonic highly conductive zone is around 2.0E-04 m/d, and around 1.0E-04 m/d in the fractured poor water-bearing zone. The main part of the water accumulated in the secondary reservoir leaves the field, draining underground toward the Maritsa fault zone and, partially, toward some of the neighbouring water-bearing complexes. Another smaller portion of the mineral water is abstracted from the C-3x mineral water borehole.

- *A fractured poor water-bearing complex - peripheral zone*. This zone includes the sediments of the Merichleri limestone Formation ($mrPg_3$) and the Malkotranovo terigenous Formation ($mtPg_3$) in the upper part of the cross section, and is assumed to comprise rocks of varying composition and genesis at depth. In an upward direction, the section includes Upper Eocene and Lower Oligocene rock complexes, attributed by stratigraphic study to the Marl-limestones Formation ($5Pg_2^3$) – organogenic and sandy limestones and marls; the formation of the first medium-acidic volcanism (Pg_2^3) – tuffs, tuffites and latites, and the formation of the first acidic voclanism (Pg_3) – tuffs, tuffites, tuff-sandstones, sandstones, siltstones and limestones. These rocks are fractured and secondarily altered at varying degrees. As a whole, the water bearing capacity of this rock complex is very low. The water in the areas close to the surface is cold and fresh, while at depth and near the secondary reservoir, it has a higher temperature and altered chemical composition. This zone is recharged by fresh cold water from the Palaeogene karst aquifer, by water from the Merichlerska river flood plain, by precipitation, and by water from the secondary reservoir. The lower permeability of the layer close to the surface leads to the assumption of a lower recharge rate W - approximately 5.0E-05 m/d. The peripheral zone is drained by the fault-downthrow fault structures which control the groundwater flows, to the south, toward the Palaeogene karst aquifer.

Boundary hydrogeological units

Looked at in plan, the field borders on two high-order hydrogeological units: A Palaeogene karst aquifer (on the western and southern borders) and a Palaeogene-Neogene complex of low water-bearing capacity (on the northern and eastern boundaries).

- *The Palaeogene karst aquifer.* This aquifer was formed within highly fractured and karsted carbonaceous sediments of the Marl-limestones Formation ($5Pg_2^3$) and the formation of the first acidic voclanism (Pg_3). It marks the western and southern boundaries of the field. This aquifer is among the highest ranking and economically most important fresh-water bearing reservoirs in the Dimitrovgrad and Chirpan areas. Its average transmissivity is approximately 500 m^2/d and the hydraulic conductivity most frequently is between 5 and 8 m/d. Generally, the groundwater flow direction is S-SW, and the average hydraulic gradient is 5.0E-4.
- *The Palaeogene-Neogene complex of low water-bearing capacity.* This complex was formed among the Oligocene-Miocene sediments of the Maritsa Formation (mPg_3-N_1). The section is represented by thick layers of clay, thin layers and lenses of sandy clays and clayey sands, coal slates and coals with a total thickness of around 350-400 m and more. Generally, the permeability of this sediment complex is very low and it acts as a virtually water-tight lateral boundary around the field on the north and east.

Composing of the 3D flow model

The 3D flow model (FM3D) is a three-dimensional simulation of the flow structure in the Merichleri field accounting for specific hydrogeological conditions and for all external impacts, including the impact of the C-3x borehole. The general ideas and input parameters used in the making up of the model are as follows:

- FM3D was developed using Modflow software in accordance with the conceptual model.
- The model area covers the exploited part of the mineral water field, with a total area of 4.5 km^2. A non-uniform orthogonal network was used to establish the spatial discretisation. This network is denser around the C-3x borehole where the gradients are the highest.
- FM3D includes three model layers - ML-1, ML-2 and ML-3 (Fig. 2). Each model layer delineates 3 model zones which are used for a comparatively accurate determination of the spatial boundaries of the hydrogeological units identified in the field (Fig. 3). The hydraulic conductivity (k) and active porosity (n_0) values set for each model zone are presented in Table 2.
- The regional flow was modelled for an Order III boundary condition using the *General Head Boundary* (GHB) scheme for the outer boundaries of the model. The conductance along the boundaries has been calculated based on the depth and hydraulic conductivity for the zone to which the

respective model cell belongs. The boundary hydraulic head were set in the following manner: (1) The general direction of the horizontal flow is to the south-west toward the Maritsa Fault zone, with an average gradient of around 1.2E-04; (2) Some of the groundwater flow is oriented toward the large fault-downthrow fault zones in the south-eastern part of the model area.

- Recharging through infiltration was set as a constant value in all cells of the first model layer - W = $4x10^{-5}$ m/d. The boundary condition *Recharge* is used for this. The flow rate values in the three model zones are as follows: MZ-1.1 – $W_{1.1}$ = 2.0E-04 m/d; MZ-1.2 – $W_{1.2}$ = 1.0E-04 m/d; MZ-1.3 – $W_{1.3}$ = 5.0E-05 m/d.
- The ascending flow from the main reservoir was set at the bottom of the ML-3 layer, within the MZ-3.3 model zone, with an Order II boundary condition following the *Specified Flow* scheme. The initially set flow value was adjusted during model calibration.
- The C-3x borehole was simulated as a three-dimensional object with the relevant coordinates and structural features (diameter, depth, position of the water intake, etc.) The model was set with a constant pumping rate of Q = 5 l/s, using an Order II boundary condition following the *Specified Flow* scheme.

The FM3D model was calibrated using the following: (1) data about the static water levels in exploration boreholes and in the C-3x borehole; (2) pumping tests data. The calibration procedure involved varying of the initial conditions and flow velocities for each model zone, and, also, the hydraulic head and transmissivity along the outer boundaries.

Table 1.
Hydrogeological units, model layers and model zones

Hydrogeological unit		Geological unit	Lithological characteristics	Geological index	Model layer	Model zone
1st rank	2nd rank					
Volcanogenic fault-fissure drainage complex (secondary reservoir)	Tectonic highly conductive zone	Meirchleri's latites	amphibole-biotin-pyroxenes latites	mrλPg_3	ML-1 ML-2 ML-3	MZ-1.1 MZ-2.1 MZ-3.1
	Fractured poor water-bearing zone					MZ-1.2 MZ-2.2 MZ-3.2
Fractured poor water-bearing complex (peripheral zone)	-	Meirchleri limestone Formation, Malkotranovo terrigenous Formation, Upper Eocene and Lower Oligocene rock complexes *	limestones, marls, sandstones, conglomerates, tuffs, tuffites, siltstones, tuff-sandstones	mrPg_3 mtPg_3 Pg_2^3- Pg_3	ML-1 ML-2 ML-3	MZ-1.3 MZ-2.3 MZ-3.3

* *Note*: Upper Eocene and Lower Oligocene rock complexes of the peripheral zone includes deep parts of the Marl-limestones Formation ($5Pg_2^3$), formation of the first medium-acidic volcanism (Pg_2^3) and formation of the first acidic volcanism (Pg_3).

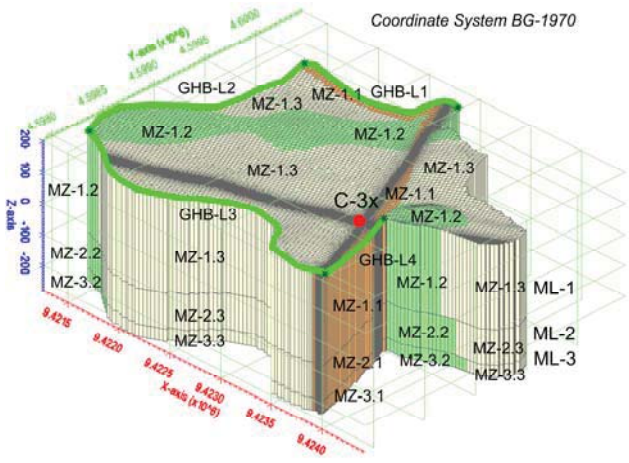

Fig. 2. Geometry of model layers and zones. Boundary conditions

Table 2.
Hydraulic conductivity (k) and active porosity (n_0) of the model layers and zones

Hydrogeological unit	Model zone	k, m/d	n_0, -
Tectonic highly conductive zone (secondary reservoir)	MZ-1.1 MZ-2.1 MZ-3.1	3.3E00	8.0E-03
Fractured poor water-bearing zone (secondary reservoir)	MZ-1.2 MZ-2.2 MZ-3.2	7.5E-01	7.0E-03
Fractured poor water-bearing complex (peripheral zone)	MZ-1.3 MZ-2.3 MZ-3.3	4.5E-01	5.0E-03

Note: The values of k and n_0 are determined using literature data based on the type of litological kinds and a performed qualitative analysis of the character, size and filling of the fissures in the rock mass, as well as the characteristics of the products of the weathering processes and the secondary change (Spitz and Moreno, 1996; Stoyanov, 2015).

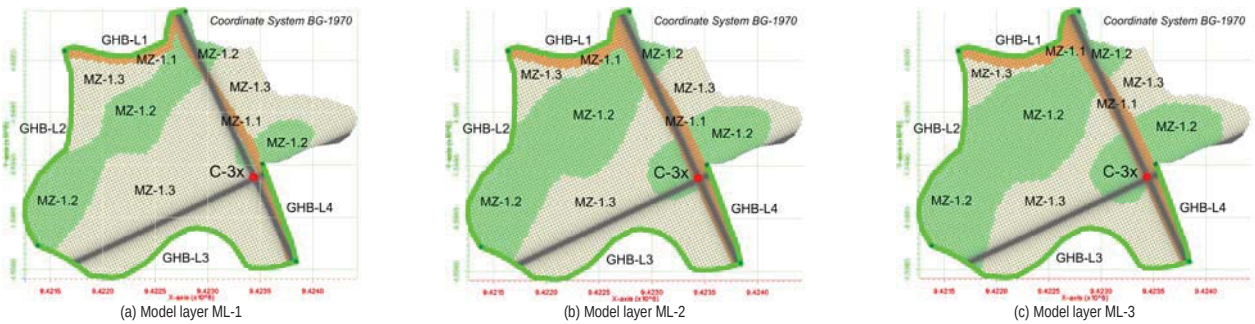

(a) Model layer ML-1 (b) Model layer ML-2 (c) Model layer ML-3

Fig. 3. Model zones and boundary conditions in model layers ML-1, ML-2 and ML-3

Table 3.
Boundary conditions

Boundary	Type	Part	Length, m	Average conductance C_{av}, m^2/d
North – simulate a flow coming at through faults from the Paleogene karst aquifer	GHB	GHB-L1	1310	100
West – simulate an Inflow from the Paleogene karst aquifer	GHB	GHB-L2	1965	50
South – simulate a flow draining from the field into the Paleogene karst aquifer	GHB	GHB-L3	2919	20
South-East – simulate a flow from the field draining at depth through faults	GHB	GHB-L4	1005	500
Note: In addition another external boundary condition is set: Recharge from precipitation and from the river flood plain in all cells of the model laye ML-1				

Table 4.
Water balance of the volcanogenic fault-fissure drainage complex - secondary mineral water reservoir

flow in, Q_i^{in}, L/S		flow out, Q_i^{out}, L/S	
THE THERMO-MINERAL FLOW ASCENDING FROM THE MAIN RESERVOIR	17.25	DRAINING TO THE ADJACENT AQUIFERS AND AT DEPTH THROUGH FAULTS	18.25
INFLOW FROM THE FRACTURED POOR WATER-BEARING COMPLEX (PERIPHERAL ZONE)	5.27	DRAINING TO THE FRACTURED POOR WATER-BEARING COMPLEX (PERIPHERAL ZONE)	5.29
INFLOW FROM THE ADJACENT AQUIFERS	3.85	PUMPING RATE OF THE C-3X MINERAL WATER BOREHOLE	5.0
Recharge from precipitation and from the river flood plain	2.18		
Total flow in:	28.55	Total flow out:	28.54
Difference 0.04 %			

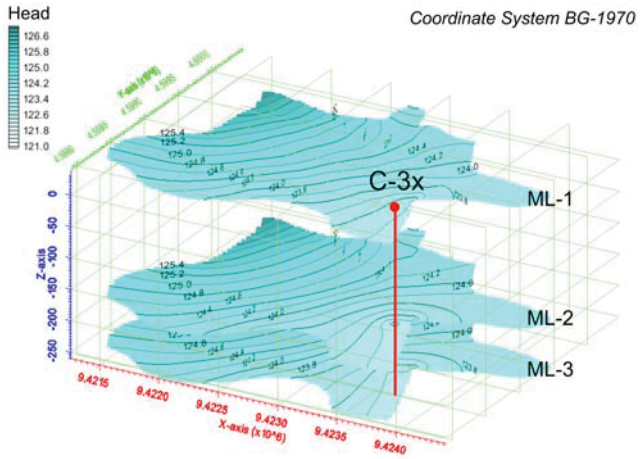

Fig. 4. Flow structure in model layers ML-1, ML-2 and ML-3

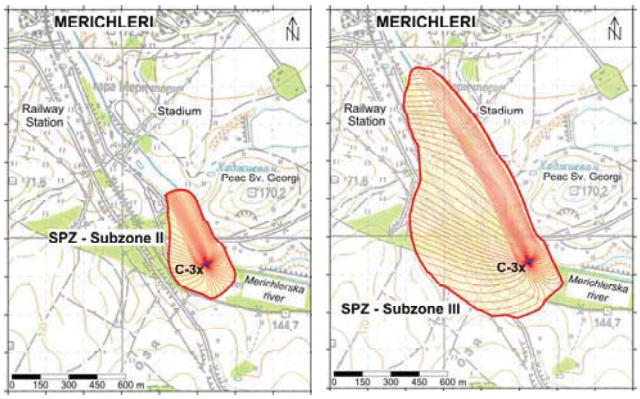

(a) SOZ – Subzone II (b) SOZ – Subzone III

Fig.5. Boundaries of SOZ around the C-3x borehole in the Merichleri thermo-mineral field

Model solution results

Flow structure

FM3D was used to produce a mathematical simulation of the flow structure. The resulting solution for the distribution of hydraulic heads in the three model layers is presented in Figure 4. This flow structure illustrates the hydrodynamic situation of the field during uninterrupted operation of the C-3x borehole.

Water balance. Mineral water resources

Table 4 presents a summary of the FM3D generated quantitative estimates for the water-balance elements in the field. The results allow the following important conclusions about the water resources in the Merichleri field:

- The mineral water resources of the volcanogenic fault-fractured draining complex, which is the secondary reservoir, are 28.55 l/s.
- Approximately 60% of the resource is formed by the ascending thermo-mineral flow from the main reservoir. Another 18% enter via the peripheral zone around the secondary reservoir. The remaining 22% are from adjacent aquifers, from precipitation and from the river flood plain.
- The regional resources of the field, assumed as equal to the thermo-mineral flow ascending from the main reservoir, are 17.25 l/s.
- Mineral water is extracted via the C-3x borehole at a constant pumping rate of 5 l/s and with an operational drawdown of 1.85 m. This mode of operation is optimal and ensures that the composition and temperature of the extracted water are preserved. The remaining resources in the field drain (disperse) at depth through various faults into adjacent aquifers and into the peripheral zone.

Models to determine the SPZ boundaries

The boundaries of sanitary protection zone (SPZ) - Subzone II and Subzone III around the C-3x mineral water borehole have been determined using Modpath software. This software created two migration models, MP3D-1 and MP3D-2, based on the FM3D generated model solution of the flow structure. The porosity n_0 values assumed for the modelled areas of both models were based on reference data (Spitz and Moreno, 1996), in accordance with the lithological features and the secondary alterations comprising the hydrogeological units (Table 2). MP3D-1 was used to determine the boundaries of Subzone II over a calculation period of 400 days, and MP3D-2 was used to determine the boundaries of Subzone III over a

calculation period of 25 years. These periods are consistent with Bulgaria's current regulatory documents. The boundaries of subzones are presented in Figure 5a and Figure 5b.

Conclusion

The elaborated 3D model has successfully determined the complex structure of the flow area and has generated a quantitative estimate of the water balance and of the resources in the Merichleri thermo-mineral field, and, also, the optimal abstraction parameters and the sanitary protection zone boundaries. The model estimations allow for a better understanding of the mineral water formation and movement mechanisms, and produce new data about the mineral water resources. The results are also of high practical importance for the efficient operation of the Merichleri field. This model is a universal facility and can be used to predict higher abstraction rates of mineral water by means of new boreholes or by increased flow-rate at the C-3x borehole, without changing the composition or temperature of the extracted water or without disturbance to the ecological balance. The research approach presented here would be useful for resolving of similar tasks of hydrogeological nature.

References

Азманов, А. Българските минерални извори. С., Държавна печатница, 1940. – 256 с. (Azmanov, A. Balgarskite mineralni izvori. S., Darzhavna pechatnitsa, 1940. – 256 p.)

Боянов, Ив., Ж. Шиляфова, А. Горанов, М. Русева. Обяснителна записка към геоложка карта на България М 1:100000. Картен лист Димитровград. С., КГМР, ГИ БАН, Геология и Геофизика АД, 1993 а. – 67 с. (Boyanov, Iv., Zh. Shilyafova, A. Goranov, M. Ruseva. Obyasnitelna zapiska kam geolozhka karta na Bulgaria M 1:100000. Karten list Dimitrovgrad. Sofia, KGMR, GI BAN, Geologia i Geofizika AD, 1993 a. – 67 p.)

Боянов, Ив., Ж. Шиляфова, А. Горанов, М. Русева, Т. Ненов. Обяснителна записка към геоложка карта на България М 1:100000. Картен лист Чирпан. С., КГМР, ГИ БАН, Геология и Геофизика АД, 1993 б. – 56 с. (Boyanov, Iv., Zh. Shilyafova, A. Goranov, M. Ruseva, T. Nenov. Obyasnitelna zapiska kam geolozhka karta na Bulgaria M 1:100000. Karten list Chirpan. Sofia, KGMR, GI BAN, Geologia i Geofizika AD, 1993 b. – 56 p.)

Колева, Ек., Р. Пенева. Климатичен справочник. Валежи в България, С., БАН, 1990. – 169 с. (Koleva, Ek., R. Peneva. Klimatichen spravochnik. Valezhi v Bulgaria. S., BAN, 1990. – 169 p.)

Петров П. Основни закономерности в разпространението на минералните води в България. – Трудове върху геологията на България, 3, 1964. – 83-158. (Petrov, P. Osnovni zakonomernosti v razprostranenieto na mineralnite vodi v Bulgaria. – Trudove varhu geologiata na Bulgaria, 3, 1964. – 83-168.)

Петров, П., Св. Мартинов, К. Лимонадов, Юл. Страка. Хидрогеоложки проучвания на минералните води в България. С., Техника, 1970. – 196 с. (Petrov, P., Sv. Martinov, K. Limonadov, Yul. Straka. Hidrogeolozhki prouchvania na mineralnite vodi v Bulgaria, S., Technika, 1970. – 196 p.)

Стоянов, Н. Математически филтрационен модел на термоминерално находище „Хасковски минерални бани“. – Годишник на Минно-геоложки университет “Св. Ив. Рилски” - София, 58, I, 2015. – 190-195. (Stoyanov, N. Matematicheski filtrazionen model na termomineralno nahodishte “Haskovski mineralni bani”. – Godishnik na Minno-geolozhki universitet “Sv. Iv. Rilski” - Sofia, 58, I, 2015. – 190-195.)

Щерев, К., Минералните води в България. С., Наука и изкуство, 1964. – 172 с. (Shterev, K. Mineralnite vodi v Bulgaria. S., Nauka i izkustvo, 1964. – 172 p.)

McDonald, J. M., Harbaugh, A. W. A modular three-dimensional finite-difference flow model. Techniques of water resources investigations of the USGS - Book No 6, Denver, USGS, 1988. – 586 p.

Pentcheva, E., Van't dack, L., Veldeman, E., Hristov, V., Gijbels, R. Hydrogeochemical characteristics of geothermal systems in South Bulgaria. Universiteit Antwerpen (UIA), Belgium, 1998. – 121 p.

Pollack, D. W. User's Guide for Modpath, V.3: A particle tracking post-processing package for Modflow, the USGS finite-difference ground-water flow model, Open file rep. 94-464, Denver, USGS, 1994. – 56 p.

Spitz, K., J. Moreno. A practical guide to groundwater and solute modeling. New York, JW&S, Inc., 1996. – 460 p.

ARCHIVED MATERIALS - REPORTS, STATEMENTS AND NOTES

Гешев, Г., Б. Денков. Доклад за резултатите от проведените хидрогеоложки проучвания на въглекисело находище – с. Меричлери и находище при гр. Харманли. Ямбол, ДСО „Геоложки проучвания“, 1972. – Архив МОСВ. (Geshev, G., B. Denkov. Doklad za rezultatite ot provedenite hidrogeolozhki prouchvania na vaglekiselo nahodishte – s. Merichleri i nahodiste pri gr. Harmanli. Yambol, DSO “Geolozhki prouchvania”, 1972. – Arhiv MOSV.)

Добрева, Д. Хидротермални ресурси в Горнотракийския басейн, С., БАН, 1997. – Архив ГИ-БАН. (Dobreva, D. Hidrotermalni resursi v Gornotrakiyskia baseyn, S., BAN, 1997. – Arhiv GI BAN.)

Нейков, Н. (ред.). Доклад за преоценка на експлоатационните ресурси и определяне на зона за защита на находището на минерална вода № 44 - „Меричлери“. Пловдив, Водоканалпроект АД, 2017. - Архив Община Меричлери. (Neykov, N. (red.) Doklad za preozenka na eksploatazionnite resursi i opredelyane na zona na zashtita na nahodisteto na mineralna voda № 44 – “Merichleri”. Plovdiv, Vodokanalproekt AD, 2017. – Arhiv Obstina Merichleri.)

Петров П. (ред). Преоценка на ресурсите на геотермална енергия в България – Дог. N 69/06.04.1998 на МОСВ с ГИ БАН. С., БАН, 1998. – Архив МОСВ. (Petrov, P. (red.). Preotsenka na resursite na geotermalna energia v Bulgaria – Dog. N 69/06.04.1998 na MOSV s GI BAN. S., BAN, 1998. – Arhiv MOSV.)

The article is reviewed by Prof. Dr. Aleksey Benderev and Prof. Mihail Galabov, DSc.

APPLICATION OF HYPERSPECTRAL VEGETATION INDICES FOR DISEASE DETECTION IN YOUNG APPLE TREES

Kalinka Velichkova[1], Dora Krezhova[2]

[1]University of Mining and Geology "St. Ivan Rilski", 1700 Sofia, e-mail: k.velichkova@mgu.bg
[2] Space Research and Technology Institute, Bulgarian academy of sciences, 1113Sofia, e-mail: dkrezhova@stil.bas.bg

ABSTRACT: Recent advances in hyperspectral remote sensing make it possible to develope new ways for monitoring of plant ecosystems and environment changes as well as for detection of plant diseases under field conditions. Hyperspectral (narrow-band) vegetation indices (Vis) have been shown to provide additional information being decisive in characterizing the physiological state, biochemical composition, physical structure,, and water content of the plants. The present study aims to determine narrow spectral bands that are best suited for characterizing the influence of a viral infection (at an early stage) on young apple trees, cultivar Florina, infected with Apple Stem Grooving Virus (ASGV). An empirical-statistical approach was developed and applied on hyperspectral reflectance data collected by means of a portable fiber-optics spectrometer USB2000 in the visible and near infrared spectral ranges (450-1000 nm) with a spectral resolution of 1.5 nm. Several narrow-band VIs - normalized difference vegetation index (NDVI), modified NDVI (mNDVI), simple ratio (SR), photochemical reflectance index (PRI), chlorophyll/pigment related indices (Chl $_{red\ edge}$, Chl $_{green}$), pigment index (PI), chlorophyll absorption ratio index (CARI), modified CARI (MCARI), and disease index f_d were selected and calculated for estimation of the applicability of the indices to detect changes that occured in the physiological state of the trees infected with ASGV. Statistical analyses (Students' t-test and F-test) were applied to assess the sensitivity of the VIs. Indices CARI, Chl $_{red\ edge}$, and PRI gave the best results.

Keywords: Remote sensing, hyperspectral leaf reflectance, vegetation indices, apple stem grooving virus (ASGV)

ПРИЛОЖЕНИЕ НА ХИПЕРСПЕКТРАЛНИ ВЕГЕТАЦИОННИ ИНДЕКСИ ЗА УСТАНОВЯВАНЕ НА ЗАБОЛЯВАНЕ НА МЛАДИ ЯБЪЛКОВИ ДЪРВЕТА

Калинка Величкова[1], Дора Крежова[2]
[1]Минно-геоложки университет "Св. Иван Рилски", 1700София, e-mail:k.velichkova@mgu.bg
[2] Институт за космически изследвания и технологии – Българска академия на науките, 1113 София, e-mail: dkrezhova@stil.bas.bg

РЕЗЮМЕ: Последните постижения в хиперспектралните дистанционни изследвания дават възможност за развитие на нови начини за мониториране на растителните екосистеми, на промените в околната средаи за откриване на болести по растенията. Хиперспектралните (теснолентови) вегетационни индекси (ВИ) предоставят допълнителна информация, която се оказа от решаващо значение при характеризиране на физиологичното състояние, биохимичния състав, физическата структура и водно съдържание на растенията. Настоящото изследване има за цел да определи теснолентови спектрални ленти, които са най-подходящи за характеризиране на влиянието на вирусна инфекция върху млади ябълкови дървета, сорт Флорина, заразени с вируса на ябълковото стъблено набраздяване (ASGV). Спектралните данни за отразена от листата радиация са регистрирани с портативенспектрометър USB2000 във видимата и близката инфрачервена области (450-1000 nm) със спектрална резделителна способност 1,5 nm. Разработен и приложен е емпирично-статистически подход върху тези данни и са изчислени и оценени няколко теснолентови ВИ: нормирана разлика (NDVI), модифициран NDVI (mNDVI), просто съотношение (SR), фотохимичен (PRI), два хлорофилни индекса (Chl red edge, Chl green), пигментен (PI), абсорбция на хлорофил (CARI) и негова модификация (MCARI), и индекс на болестта fd. За оценка на чувствителността на ВИ към промените във физиологичното състояние на заразените с ASGV дървета са приложени статистически анализи чрез t-тест на Стюдънт и F-тест). Най-добри резултати дадоха индексите CARI, Chl $_{red\ edge}$, and PRI.

Ключови думи: Дистанционни изследвания, хиперспектрално отражение от листа на растения, вегетационни индекси, вирус на ябълковото стъблено набраздяване

Introduction

Precise estimates of the plant diseases and their effect on the quality and quantity of crop production are important for horticulture, precision agriculture, as well as for basic and applied plant researches. Reliable and timely assessments of plant disease occurrence and spread are the basis for planning plant protection activities in field or greenhouse production.

Remote sensing data and techniques have already proven to be relevant to many requirements of agricultural applications. Different studies and experiments demonstrated their usefulness and feasibility to address various agricultural issues, such as crop classification and mapping, predicting crop yield, soil survey, irrigation planning, and damage assessment by disaster, pest or diseases (Wang et al., 2010; Usha and Bhupinder, 2013; Krezhova et al., 2017). Remote sensing methods are widely used in managing abiotic stresses, such as nitrogen and water deficiency, salinity and herbicide stress, in order to improve crop yield. When it comes to biotic stress, remote sensing is only able to assess the damage from diseases; and yet, it is not useful for preventing the losses. Therefore, further research is needed to investigate the early detection of biotic stress in plants before the occurrence of visible symptoms.

Recent hyperspectral remote sensing (HRS) techniques based on leaf reflectance measurements are successfully used to derive meaningful biophysical variables related to plant physiological state, like the concentration of foliar pigments (Panigada et al., 2010), nitrogen concentration (Fava et al., 2009), water content (Colombo et al., 2008), leaf structure (Monteiro et al., 2012), etc.

Spectral reflectance of plants in the visible (VIS) and near infrared (NIR) regions of the electromagnetic spectrum is primarily affected by plant pigments, mainly chlorophylls (Chls) and carotenoids, and cellular structure of the leaves. Chls absorb light energy and transfer it into the photosynthetic apparatus. Carotenoids (yellow pigments) can also contribute energy to the photosynthetic system. Chls tend to decline more rapidly than carotenoids when plants are under stress or during leaf senescence (Gitelson and Merzlyak, 1996). From the optical point of view, these pigments have different spectral behaviour, with specific absorption features at different wavelengths, which allows remote sensing techniques to discriminate their respective effects on vegetation reflectance spectra.Thus, the variations in leaf pigment content provide useful information concerning the state of the plants.

The increasing importance of hyperspectral reflectance data motivated researches for defining optimal wavebands to estimate changes in plant physiological state (Stellacci et al., 2016). The complexity of a rich hyperspectral dataset requires techniques for reduction of such large volumes of data, characterized by redundancy of information due to the high degree of correlation of neighbouring wavebands (Thenkabail et al., 2012; Rinaldi et al., 2014). Finding efficient solutions is essential for exploiting the full potential of hyperspectral data. Most of the approaches proposed are based on optical vegetation indices (VIs) that summarize the information contained in the reflectance spectrum through mathematical combinations of reflectance at different wavelengths. Large number of narrowband VIs, derived from hyperspectral measurements, was developed allowing several combinations for each biophysical variable (Wang et al., 2012). The use of VIs may improve the sensitivity to vegetation parameters investigated minimizing the influence of extraneous factors.

In recent years, researchers have studied various spectral vegetation indices to detect different vegetation diseases (Delalieux et al., 2009; Ranjan et al., 2012; Velichkova et al., 2016). Efficient use of spectral data in detecting plant disease depends on the application. The spectral regions from 400 to 700 nm and 700 to 1100 nm are mainly influenced by leaf composition of pigments, structure, and water content (Mahlein et al., 2013). The effects of a disease on the pigments and structure of a plant and the change in their spectral responses enable spectroradiometry and remote sensing techniques to detect plant disease effectively (Oerke et al., 2016).

The aim of this study is to detect a biotic stress (latent viral infection) on young apple trees caused by apple stem grooving virus (ASGV) in an early stage without visual symptoms. An empirical-statistical approach was applied on hyperspectral leaf reflectance data on the basis of calculation of several narrowband vegetation indices and evaluation of their sensitivity to the changes in the physiological state of the infected trees.

Materials and methods

Plant material

Young (one-year-old) apple trees, cultivar Florina, grown in a small non-commercial orchard were used for investigations. The trees were without disease symptoms on the aerial parts and organs. In the summer, a few trees (about 25) were checked trough Double Antibody Sandwich Enzyme Linked Immunosorbent Assay (DAS-ELISA) for the presence of viruses. Some of them were infected with ASGV. For data analysis we chose five trees – four infected to different degrees with ASGV and one non-infected that was adopted as control tree.

Spectral measurements

Leaf reflectance spectra of the five apple trees were collected using a portable fiber-optic spectrometer USB2000 (Ocean Optics, 2017) in the spectral range 450-1000 nm at a spectral resolution of 1.5 nm (bandwidth at half maximum). The measurements were carried out on an experimental setup in a laboratory. The light signal from the freshly detached leaves is guided to the entrance lens of the spectrometer by a-meter-long fiber-optic cable directed perpendicular to the measured surface. As a source of light, a halogen lamp providing homogeneous illumination of measured leaf areas was used. Leaf reflectance measurements were made at about 10 cm above the illuminated sides of 25 to 30 leaves on the healthy and infected leaves from each tree. At the beginning of each measurement, the emitted spectrum of the light source was registered from a diffuse reflectance standard. Spectral analyses were carried out in spectral range 450-850 nm at 1130 narrow spectral bands (0.3 nm). The spectral reflectance characteristics (SRC) of the investigated leaves were determined as the ratio between the reflected from leaves radiation and this one reflected from the standard.

Narrowband vegetation indices used in this study

VIs were commonly calculated from combinations of reflectance at two or three spectral bands (most common in red and NIR spectral ranges) in order to obtain a single value (index) that is related to the vegetation growth.

For assesment of the changes in the physiological state of the apple trees infected with ASVG, we selected ten narrowband VIs, given in Table 1. VIs included were applied at the leaf level and were expected to be related to photosynthetic activity, biomass, Chl content and plant stress.

Normalized Difference Vegetation Index (NDVI) was first proposed by Rouse et al. (1974) and is one of the most known and widely used VIs. It is based on the contrast between reflectance in the red region due to maximum absorption of foliar pigments (Chls and carotenoids) and reflectance in NIR where the maximum of the reflection caused by leaf cellular structure and biomass has appeared (Davenport and Nicholson, 1993). NDVI is affected by plant photosynthetic activity, total plant cover, plant and soil moisture and is commonly used for estimation of plant ''greenness''. In most of the researches NDVI shows non-linear relationship with biophysical parameters such as green leaf area index (LAI) and biomass (Baret and Guyot, 1991).

Table 1
Calculated narrowband vegetation indices for detection of ASGV virus infection on apples trees

Index	Equation	Full name	Reference
NDVI	$(R_{NIR}– R_{red})/(R_{NIR}+R_{red})$, NIR=845 nm, red=665 nm	Normalized Difference Vegetation Index	Rouse et al. (1974)
mNDVI	$(R_{750}– R_{705})/(R_{750}+ R_{705})$	Modified Normalized Difference Vegetation Index	Jurgens (2010)
SR	R_{NIR}/R_{red} NIR = 760 nm, red=695 nm	Simple Ratio	Tucker (1979)
CARI	$(R_{700} – R_{670})-0.2(R_{700} – R_{550})$	Chlorophyll Absorption Ratio Index	Kim (1994)
MCARI	$[(R_{700} – R_{670})-0.2(R_{700} – R_{550})](R_{700}/R_{670})$	Modified Chlorophyll Absorption Ratio Index	Daughtry (2000)
$CI_{red\ edge}$	$(R_{NIR}/R_{red\ edge}) – 1$ red edge=714 nm, NIR=760 nm	Chlorophyll Index at green range	Gitelson et al. (2005)
CI_{green}	$(R_{NIR}/R_{green}) – 1$ green=550 nm, NIR=760 nm	Chlorophyll Index at red edge	Gitelson et al. (2005)
PI	R_{NIR}/R_{red} NIR=677 nm and red=554 nm	Pigment index	Tilley et al. (2003)
PRI	$(R_{531}– R_{570})/(R_{531} + R_{570})$	Photochemical Reflectance Index	Gamon et al. (1992)
f_D	$R_{500} / (R_{500}+ R_{570})$	Index of disease	

Modified NDVI (mNDVI) with wavelength of 705 nm was an improved version of NDVI (Sims and Gamon, 2002). It was developed to eliminate the effects of surface reflectance by incorporating the blue band. This VI is more strongly correlated with total Chl content and eliminates the effect of surface reflectance. Li et al. (2015) found that mNDVI is very sensitive to minor changes in the vegetation canopy, gap fraction, and senescence, and has been used for precision agriculture, forest monitoring,, and vegetation stress detection. The value of this index is between -1 and 1, as the values in range 0.2 to 0.7 are an indicator for green vegetation (Snirer, 2013).

The simple ratio index (SR) (Jordan, 1969) is probably the first index and is the most commonly used to derive LAI for a forest canopy. When it is calculated at wavelengths 760 and 695 nm (SR in this case was called also Carter index), it is specialized narrow band index for the monitoring of stress (Tucker, 1979). Its value is in the interval 0 – 30 (Snirer, 2013).

Chlorophyll Absorption Ratio Index (CARI) was first developed by Kim et al. (1994) and measures the magnitude (depth) of Chl absorption at the red region (670 nm) where the maximum of Chl absorption is, to the green (550 nm) and red-edge (700 nm) regions of the spectrum, where absorption of the photosynthetic pigments is minimum. By CARI, a reduction of the variability of the photosynthetically active radiation due to the presence of diverse non-photosynthetic materials could be achieved (Wu et al., 2009).

Modified Chlorophyll Absorption Ratio Index (MCARI) was proposed by Daughtry et al. (2000).It was designed to measure photosynthetically active radiation related to Chl absorption in red and red-edge regions. Thus, it is mostly affected by Chl variability, showing high sensitivity even at high chlorophyll levels (Haboudane et al., 2004). Authors found that MCARI has a great potential for LAI predictions, because 60% of MCARI variation is due to the LAI, although they did not consider NIR band in its formula.

Photochemical Reflectance Index (PRI) was developed by Gamon et al. (1992) to estimate rapid changes in the relative levels of carotenoid pigments (particularly xanthophylls). Carotenoid pigments indicate if photosynthetic light was used efficiently. Thus PRI determines directly light use efficiency by remote sensing (Raddi et al., 2005). PRI is used in studying vegetation productivity and stress. Its value ranges from -1 to 1. The common range for green vegetation is from - 0.2 to 0.2 (Snirer, 2013).

Chl Index at green range (Chl_{green}) and Chl Index at red edge ($Chl_{red\ edge}$) belong to three-band model for non-invasive estimation of Chl and carotenoid contents. Both were proposed and studied by Gitelson et al. (2003, 2005). Because of the strong linear correlation with Chl content, the Chl_{green} could be applied for estimation of canopy Chlcontent at any leafscale, under a wide range of canopy conditions and seasonal changes and variation in photosynthesis patterns (Thanyapraneedkul et al., 2012). $Chl_{red\ edge}$ did not depend on the crop type and exhibited low sensitivity to soil background effects. It was a suitable surrogate of Green LAI as it objectively responded to changes in both leaf area and foliar chlorophyll content (Wu et al., 2009).

The leaf pigment vegetation indices (PIs) were designed to provide a measure of stress-related pigments present in vegetation, such as carotenoids and anthocyanins, which tend to be present in higher concentrations when vegetation is in a weakened state. PIs do not quantity Chl, which is measured using the greenness indices. Applications of PIs include crop monitoring, ecosystem studies, analyses of canopy stress, and precision agriculture (Sims and Gamon, 2002).

Disease indices f_D are specific for singular study. As f_D increased, the reflectance decreased significantly in NIR regions.

Data analyses

For the assessment of the sensitivity of considered 10 VIs (Table 1) to changes in the physiological state of apple trees

infected with ASGV, statistical analyses (extended Student t-test and Fisher-test) were performed by applying a two-step procedure. To produce reliable conclusions, these tests require normally distributed data; therefore, the VIs datasets were preliminary tested for normality with the Shapiro-Wilk test at a significant level of 0.05.

As a first step, the Student two-sample t-test was carried out to determine the statistical significance of the differences between the values of the calculated 10 VIs for infected trees against the control ones. The differences are affirmed as statistically significant at level $p < 0.05$.

Then, we applied the Fisher's Least Significant Difference (LSD) test. Accordingly, the difference between two mean values is declared statistically significant at a given level of significance if found to exceed the value of LSD. In our case the value $LSD_{0.05}$ is calculated from the expression

$$LSD_{0.05} = t_{0,05}.s_d ,$$

where: $t_{0,05}$ is tabulated t-value at the level of significance 0,05 with degrees of freedom n_1+n_2-2, (n_1 and n_2 are the numbers of the control sample and the infected sample, respectively), and s_d is the pool standard deviation of the difference between the means.

Results and discussion

The averaged (over 30 measured areas) SRCs of the control apple trees and four trees infected by ASRG are shown in Figure 1. SRCs of the infected trees differ against the control trees in several spectral ranges: green (520–580 nm, maximum reflectivity of green vegetation), red (640–680 nm, maximum chlorophyll absorption), red edge (680–720 nm, maximum slope of the reflectance spectra), and NIR (720–770 nm, plateau of the characteristics). In all spectral ranges, the SRCs values are higher than the control. The differences at green and NIR regions are most significant.

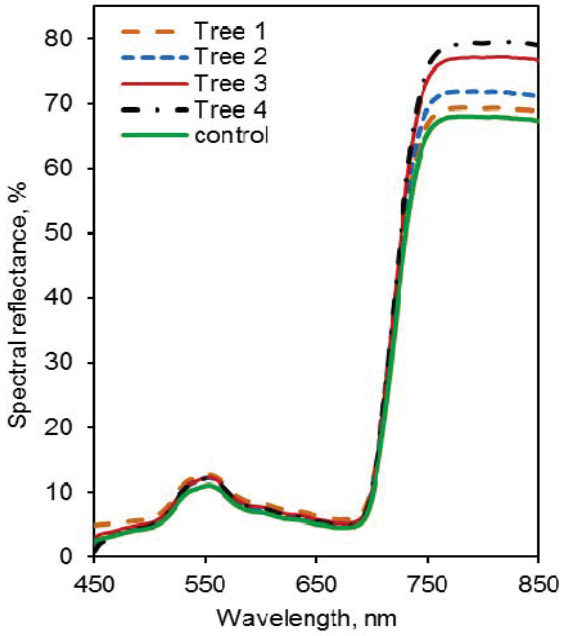

Fig. 1. Averaged SRC of leaves of five studied apple trees

We checked the VIs datasets for normality by means of Shapiro-Wilk test investigating the values of skewness and kurtosis. The standard error (SE) and the value of the ratios skewness/SE_{skew} and kurtosis/SE_{kurt} were calculated and they are within the interval (-1.96; +1.96), so that data are normally distributed. In Figure 2, we exemplify results from the Shapiro-Wilk test at a significance level 0.05 applied to the pigment index (PI) dataset for apple tree 4.

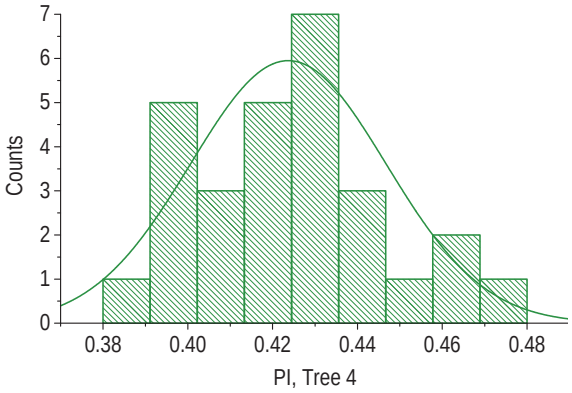

Fig. 2. The distribution of pigment VI dataset for tree 4 infected by ASGV

Figure 3 shows box plots summarizing the results of assessment of the normality of PI datasets derived from hyperspectral reflectance data of control and four infected trees. The results show that VIs datasets satisfy the normal distribution reasonably well.

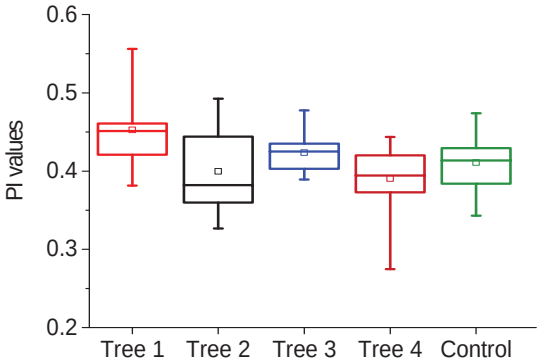

Fig. 3. Box plots ofPI datasets of all investigated trees: median (line across box), mean value (small empty square box), minimum and maximum values (lower and upper ends of the whisker, respectively), interquartile range containing 50% of values (box)

Student t-test was performed at a level of statistical significance $p<0.05$ for assessment of the significance of the differences between mean of sets of the calculated VI values of control and infected trees. Mean values, p-values, F-values, and LSD for the sets of hyperspectral VIs used in the study are shown in Table 2. F-values are calculated as a ratio of variances (squares of standard deviations) of two compared groups (healthy and infected).

Table 2.
Mean values, p-values, F-values, and LSD for the sets of hyperspectral VIs used in the study

tree	1	2	3	4	1	2	3	4	1	2	3	4
NDVI					mNDVI				SR			
Mean healthy	0.870	0,870	0.870	0.870	0.644	0.644	0.644	0.644	10.325	10.325	10.325	10.325
Mean infected	0.842	0,871	0.869	0.863	0.609	0,625	0.643	0.636	8.588	10,328	10.336	11.256
F-ratio	1.747	2,390	1.486	2.969	2.177	9,081	1.676	2.601	1.625	5,700	1.064	5.730
p	ns	*	ns	ns	ns	***	ns	ns	ns	***	ns	***
LSD	0.006	0,005	0.004	0.006	0.011	0,016	0.009	0.010	0.315	0,484	0.290	0.516
difference	0.028	0,001	0.001	0.013	0.034	0,019	0.001	0.012	1.738	0,003	0.011	0.931
CARI					MCARI				Chl_{green}			
Mean healthy	5.176	5,176	5.176	5.176	18.910	18.910	18.910	18.910	5.176	5.176	5.176	5.176
Mean infected	5.753	5,980	5.712	5.921	19.616	23,401	20.739	22.824	4.509	5,080	5.298	5.613
F-ratio	2.318	7,388	1.002	2.506	1.941	6,528	1.075	2.532	1.057	5,816	1.008	3.619
p	*	***	ns	*	ns	***	*	*	ns	***	ns	**
LSD	0.396	0,493	0.261	0.346	1.920	2,400	1.320	1.779	0.239	0,342	0.200	0.302
difference	0.576	0,804	0.536	0.744	0.707	4,492	1.830	3.915	0.667	0,095	0.123	0.437
$Chl_{red\ edge}$					PI				PRI			
Mean healthy	1.482	1.482	1.482	1.482	0.411	0.411	0.411	0.411	0.027	0,027	0.027	0.027
Mean infected	1.328	1,362	1.479	1.561	0.453	0,400	0.424	0.390	0.028	0,326	0.026	0.022
F-ratio	2.128	8,074	1.792	2.692	1.684	1,823	2.544	1.093	9.090	2,679	2.427	13.772
p	ns	***	ns	*	ns	ns	*	ns	***	*	*	***
LSD	0.074	0,098	0.058	0.068	0.025	0,020	0.015	0.019	0.005	0,009	0.002	0.005
difference	0.154	0,120	0.003	0.080	0.042	0,011	0.013	0.021	0.001	0,005	0.001	0.005

*ns – no statistical significance; * - p<0.05; ** - p<0.01; *** - p<0.001*

The results show that NDVI is insensitive to ASGV viral infection at an early stage. The mean NDVI values of control and infected trees are close (about 0.85). In healthy leaves, NDVI values are positive and have a maximum value of 1. The higher values are an indicator for more amount of biomass and more Chl content. In our case, mean NDVI values of infected trees weakly decrease against the control and this VI can be used as a measure of the greenness and vigour of the vegetation.

Index mNDVI is also insensitive to the infection. Its values decrease when the vegetation is subject to a state of stress. The values in range from 0.2 to 0.7 are an indicator for green vegetation. In our case, the values are between 0.64 and 0.61 (for infected trees) and the decrease is not significant. This is due to the fact that no visual symptoms occured in the infected leaves but still mNDVI indicates slight changes in its physiological state.

Pigment VI (PI) appears less sensitive since it indicates that no changes occured in the ratio Chl/carotenoids. This is the reason why VIs SR, Chl_{green} and $Chl_{red\ edge}$ also do not show good results for detection of viral infection at an early stage.The changes in SRCs (Fig. 1) of infected trees in green spectral range around 550 nm (maximum of the reflectivity of green vegetation due to Chl content) are not statistically significant for trees 1, 3, and 4 (with lower ASGV content). The results of serological test DAS-ELISA applied on ifected trees for the presence of ASGV are displayed in Figure 4. Disease index f_d calculated for reflectance in the choosen wavelengths proved to be not suitable for this investigation and the results are not shown in Table 2.

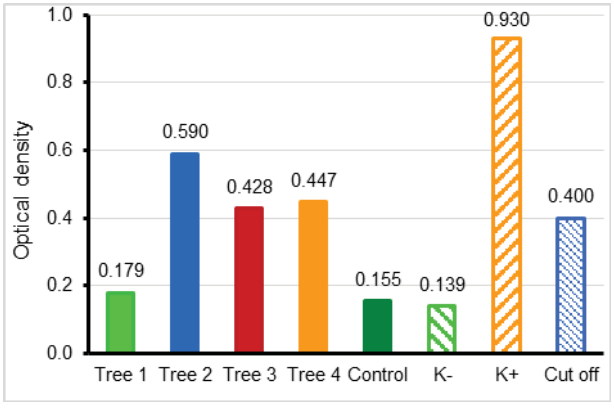

Fig. 4. Results of DAS-ELISA test on leaf samples from infected with ASGV young apple trees

Indices PRI, CARI, and MCARI show the best results. PRI directly determined light use efficiency by remote sensing data - leaf reflectance at 531nm, where changes in xcantophyll cycle are manifested as narrow absorbtion feature and are an indicator for the changes in the physiological state of the

plants. CARI and MCARI were designed to measure the Chl influence in the green, red and red-edge regions. In our case, average SRCs of infected trees differ more significant against the control (Fig. 1) in these regions. The mean values of both VIs increase for all infected trees.

The normalised differences of mean values of 10 VIs calculated from spectral data of infected trees against the control tree are presented in Figure 5. It is seen that differences are highest for tree 2 and tree 4 in correspondence with the ASGV concentration.

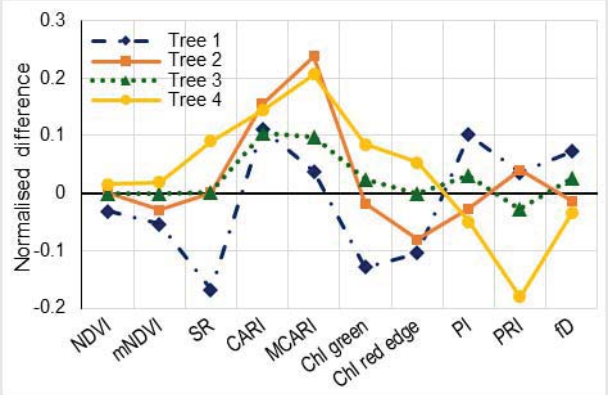

Fig. 5. Normalized differences of vegetation indices of the infected apple trees against the control tree

Conclusions

Ten hyperspectral vegetation indices were tested to explore their potential in assessment of influence of viral infection, caused by ASGV, at an early stage. In principle, all considered vegetation indices should be suitable to detect differences in the reflection between healthy and diseased plants. Different narrow band combinations were applied to derive from the indices better sensitivity to changes in physiological state (biophysical variables) such as Chl and pigment contents, cell structure, vegetation vigour, etc. Statistical methods were implemented to assess their sensitivity. Thus, for the investigation of the ASGV infection, two of the indices (NDVI and mNDVI) were found inapplicable. The sensitivity of other indices, such as SR, Chl_{green} and $Chl_{red\ edge}$, was not very high. PRI, CARI, and MCARI showed the best results as the differences of SRCs of infected trees in the selected wavebands were more significant.

This paper has shown that the selection of optimal narrow spectral bands that were better adjusted to study of a given application, allows to reduce the amount of hyperspectral data and computer time used for their proccesing, sometimes making the data interpretation easier.

References

Baret, F., G. Guyot. Potentials and limits of vegetation indices for LAI and APAR assessment. - Remote Sens. Environ., 35, 1991. - 161-173.

Colombo, R. R., M. Meroni, A. Marchesi, L. Busetto, M. Rossini, C. Giardino, C. Panigada. Estimation of leaf and canopy water content in poplar plantations by means of hyperspectral indices and inverse modeling. - Remote Sens. Environ., 112, 2008. - 1820-1834.

Daughtry, C. S. T., C. L. Walthall, M. S. Kim, E. Brown de Colstoun, J. E. McMurtrey III. Estimating corn leaf chlorophyll concentration from leaf and canopy reflectance. - Remote Sens. Environ., 74, 2000.- 229-239.

Davenport, M. L., S. E. Nicholson. On the relation between rainfall and the Normalized Difference Vegetation Index for diverse vegetation types in East Africa. - International Journal of Remote Sensing, 14, 1993. - 2369-2389.

Delalieux, S., B. Somers, W. W. Verstraeten, J. A. N. Aardt, W. Keulemans, P. Coppin. Hyperspectral indices to diagnose leaf biotic stress of apple plants considering leaf phenology. - Int. J. Remote Sens., 30, 2009. -1 887-1912. DOI: 10.1080/01431160802541556

Fava, F., R. Colombo, S. Bocchi, M. Meroni, M. Sitzia, N. Fois, C. Zucca. Identification of hyperspectral vegetation indices for Mediterranean pasture characterization. - Int. J. Applied Earth Observ. and Geoinform., 11, 4, 2009. - 233-243.

Gamon, J., J. Penuelas, C. Field. A narrow-waveband spectral index that tracks diurnal changes in photosynthetic efficiency. - Remote Sens. Environ., 41, 1992. - 35-44.

Gitelson, A. A., M. N. Merzlyak. Signature analysis of leaf reflectance spectra: algorithm development for remote sensing of chlorophyll. - J. Plant Physiol., 148, 1996. - 494-500.

Gitelson, A. A., U. Gritz, M. N. Merzlyak. Relationships between leaf chlorophyll content and spectral reflectance and algorithms for non-destructive chlorophyll assessment in higher plant leaves. - J. Plant Physiol., 160, 3, 2003. - 271-282.

Gitelson, A. A., A. Viña, V. Ciganda, D. C. Rundquist, T. J. Arkebauer, Remote estimation of canopy chlorophyll content in crops. - Geophys. Res. Lett., 32, L08403, 2005.

Haboudane, D., J. R. Miller, E. Pattey, P. J. Zarco-Tejada, I. B. Strachan. Hyperspectral vegetation indices and novel algorithms for predicting green LAI of crop canopies: Modeling and validation in the context of precision agriculture. - Remote Sensing of EnvironmentRemote Sens. Environ., 90, 2004. - 337-352.

Jordan, C. F. Derivation of leaf area index from quality of light on the forest floor. - Ecology, 50, 1969. – 663-666.

Jurgens, C. The modified normalized difference vegetation index (mNDVI) a new index to determine frost damages in agriculture based on Landsat TM data. - Int. J. Remote Sens., 18, 17, 1997. - 3583-3594, published online 25 Nov, 2010.

Kim, M. S. The Use of Narrow Spectral Bands for Improving Remote Sensing Estimation of Fractionally Absorbed Photosynthetically Active Radiation (fAPAR). Masters Thesis. Department of Geography, Universityof Maryland, College Park, MD, 1994.

Krezhova, D., K. Velichkova, N. Petrov. The effect of plant diseases on hyperspectral leaf reflectance and biophysical parameters. - In Proceedings of the 5th International conference of radiation and dosimetry in various fields of research (RAD-2017), Budva, Montenegro (in press), 2017.

Li. J., L. Pu, M. Zhu, X. Dai, Y. Xu, X. Chen, L. Zhang, R. Zhang. Monitoring soil salt content using HJ-1A hyperspectral data: A case study of coastal areas in Rudong County, Eastern China. - Chin. Geogra. Sci., 25, 2, 2015. - 213-223. DOI: 10.1007/s11769-014-0693-2

Mahlein, A. K., T. Rumpf, P. Welke, H. W. Dehne, L. Plümer, U. Steiner, E. C. Oerke. Development of spectral indices for detecting and identifying plant diseases. – Remote Sens. Environ., 128, 2013. - 21-30.

Monteiro, P. F. C., R. A. Filho, A. C. Xavier, R. O. C. Monteiro. Assessing biophysical variable parameters of bean crop with hyperspectral measurements Priscylla. - Sci. Agric., 69, 2, 2012. - 87-94.

Oerke, E.-C., K. Herzog, R. Toepfer. Hyperspectral phenotyping of the reaction of grapevine genotypes to Plasmopara viticola, - J. Exp. Bot., 67, 18, 2016. - 5529-5543.

Ocean Optics. 2017.

https://oceanoptics.com/wp-content/uploads/OEM-Data-Sheet-USB2000-.pdf

Panigada, C., M. Rossini, L. Busetto, M. Meroni, F. Fava, R. Colombo. Chlorophyll concentration mapping with MIVIS data to assess crown discoloration in the Ticino Park oak forest. - Int. J. Remote Sens., 31, 12, 2010. - 3307-3332.

Raddi, S., S. Cortes, I. Pippi, F. Magnani. Estimation of vegetation photochemical processes: an application of the photochemical reflectance index at the San Rossore test site. In: Proc. of the 3rd ESA CHRIS/Proba Workshop, 21–23 March, 2005, ESRIN,Frascati, Italy, (ESA SP-593, June 2005), H. Lacoste Ed.,ESTEC, Noordwijk, 2005.

Ranjan, R., U. K. Chopra, R. N. Sahoo, A. K. Singh, S. Pradhan. Assessment of plant nitrogen stress through hyperspectral indices. - Int. J. Remote Sens., 22, 20, 2012. -6342-6360. DOI: 10.1080/01431161.2012.687473

Rinaldi, M., A. Castrignanò, D. De Benedetto, D. Sollitto, S. Ruggieri, P. Garofalo, F. Santoro, B. Figorito, S. Gualano, R. Tamborrino. Discrimination of tomato plants under different irrigation regimes: analysis of hyperspectral sensor data. - Envirometrics, 26, 2014. - 77-88.

Rouse, J. W., R. H. Haas, J. A. Schell, D. W. Deering, J. C. Harlan. Monitoring the vernal advancement of retrogradation of natural vegetation, Greenbelt, MD, USA: NASA/GSFC, 1974, Type III Final Report, 371.

Sims, D. A., J.A. Gamon. Relationships between leaf pigment content and spectral reflectance across a wide range of species, leaf structures and developmental stages. - Rem. Sens. Environ.,81, 2002. - 337-354.

Snirer, E. Hyperspectral remote sensing of individual gravesites - exploring the effects of cadaver decomposition on vegetation and soil spectra. A thesis submitted to McGill University in partial fulfillment of the requirements of the degree of Masters of Science. Department of Geography McGill University, Montreal, August, 2013.

Stellacci, A. M., A. Castrignanò, A. Troccoli, B. Basso, G. Buttafuoco. Selecting optimal hyperspectral bands to discriminate nitrogen status in durum wheat: a comparison of statistical approaches.–Environ. Monit. Assess., -188, 3, 2016. -199. DOI: 10.1007/s10661-016-5171-0

Thanyapraneedkul, J., K. Muramatsu, M. Daigo, S. Furumi, N. Soyama, K. N. Nasahara , H. Muraoka, H. M. Noda, S. Nagai, T. Maeda, M. Mano, Y. Mizoguchi. A vegetation index to estimate terrestrial gross primary production capacity for the Global Change Observation Mission-Climate (GCOM-C)/Second-Generation Global Imager (SGLI) Satellite Sensor. - Remote Sens., 4, 12, 2012. - 3689-3720. DOI:10.3390/rs4123689

Thenkabail, P. S., J. G. Lyon, A. Huete. Advances in hyperspectral remote sensing of vegetation agricultural crops. In: Hyperspectral remote sensing of vegetation. A. Thenkabail, P. S. Lyon and J. G. Huete Eds., USA: CRC Press, Boca Raton (FL), 2012.

Tilley, D. R., M. Ahmed, J. Son, H. Badrinarayanan. Hyperspectral reflectance of emergent macrophytes as an indicator of water column ammonia in an oligohaline, subtropical marsh. - Ecol. Eng., 21, 2-3, 2003. – 153-163.

Tucker, C. J. Red and photographic infrared linear combinations for monitoring vegetation. - Remote Sens. Environ., 8, 1979. - 127-150.

Usha, K., S. Bhupinder. Potential applications of remote sensing in horticulture. A review.- Sci. Horticul.,153, 2013. - 71-83.

Velichkova, K., D. Krezhova, S. Maneva. Spectrometric measurements of reflected radiation in ecology research. In: Annual of the University of Mining and Geology “St. Ivan Rilski”, 59, Part I, Geology and Geophysics, 2016. - 196-201.

Wang, K., S. E. Franklin, X. Guo, M. Cattet. Remote sensing of ecology, biodiversity and conservation: A review from the perspective of remote sensing specialists. - Sensors,10, 2010. - 9647-9667.

Wang, W., X. Yao, X. F. Yao, Y. C. Tian, X. J. Liu, J. Ni, W. X. Cao, Y. Zhu. Estimating leaf nitrogen concentration with three-band vegetation indices in rice and wheat. - Field Crops Research, 129, 2012. – 90-98.

DOI: https://doi.org/10.1093/jxb/erw318

Wu, C., Z. Niu, Q. Tang, W. Huang, B. Rivard, J. Feng. Remote estimation of gross primary production in wheat using chlorophyll-related vegetation indices. - Agricultural and Forest Meteorology, 149, 2009. – 1015-1021.

The article is reviewed by Prof. Stefan Dimovski, DSc. and Assoc. Prof. Dr. Maya Vazkicheva.

HYPERSPECTRAL MEASUREMENTS OF ROCKS AND SOILS IN CENTRAL SREDNOGORIE

Denitsa Borisova[1], Banush Banushev[2], Hristo Nikolov[1], Roumen Nedkov [1], Daniela Avetisyan[1]

[1]Space Research and Technology Institute, Bulgarian Academy of Sciences /SRTI-BAS/, 1113 Sofia; dborisova@stil.bas.bg
[2]University of Mining and Geology "St. Ivan Rilski", 1700 Sofia; banushev@mgu.bg

ABSTRACT. Remote sensing is the technique of acquiring, processing, and interpreting images and multi channels spectral data, acquired from optical imager sensors mounted on aircraft and satellite platforms recording the interaction between investigated objects and electromagnetic energy. Remote sensing application in Earth observation begins with the design and development of equipment for carrying out research of the monitored objects remotely and without disturbing their integrity. Ground-truth data in Earth observation of the environment and in the remote sensing investigations are very important. In this work, remote sensing images are used for mineral exploration in different applications for mapping geology and recognizing soils and rocks by their spectral signatures. We used Landsat, ASTER, and Sentinel satellites images to interpret structures, soils and rocks. For data verification, the hyper-spectral systems USB 2000 and NIRQUEST 512.2 of Ocean Optics Inc. are used in laboratory and field spectrometric measurements. They make it possible to define the finest spectral characteristics of soil minerals and rocks for their identification. The obtained spectral data are compared with similar data from different instruments for Earth observation included in the spectral libraries. They correspond to the shape of the spectral signature in the same spectral range obtained with other spectrometers. These promising results encourage us to plan the next campaigns for the field spectroscopy measurements in different regions of Bulgaria.

Keywords: remote sensing, in-situ spectrometric measurements, spectral data, Earth observation, data verification

ХИПЕРСПЕКТРАЛНИ ИЗМЕРВАНИЯ НА СКАЛИ И ПОЧВИ В ЦЕНТРАЛНО СРЕДНОГОРИЕ

Деница Борисова[1], Бануш Банушев[2], Христо Николов[1], Румен Недков [1], Даниела Аветисян[1]

[1]Институт за космически изследвания и технологии, Българска академия на науките, 1113 София; dborisova@stil.bas.bg

[2]Минно-геоложки университет "Св. Иван Рилски", 1700 София; banushev@mgu.bg

РЕЗЮМЕ. Дистанционните изследвания са техника за получаване, обработка и интерпретация на изображения и многоканални спектрални данни, придобити от оптични сензори, монтирани на самолети и сателитни платформи, които регистрират взаимодействието между изследваните обекти и електромагнитната енергия. Приложението на дистанционните изследвания в наблюдението на Земята започва с проектирането и разработването на оборудване за извършване на изследванията на наблюдаваните обекти от разстояние и без да се нарушава тяхната цялост. Наземните данни са много важни при наблюдението на Земята. В тази работа изображенията от дистанционните наблюдения се използват в различни приложения - за проучване на минерални ресурси, за геоложки картографиране и за разпознаване на почвите и скалите чрез техните спектрални характеристики. Използвани са спътникови изображения от ресурните спътнинци Landsat, ASTER и Sentinel, с цел разпознаване на скални разкрития и почви. За проверка на данните са използвани спектрометричните системи USB 2000 и NIRQUEST 512.2 на Ocean Optics Inc., чрез които са проведени лабораторни и полеви спектрометрични измервания. Те осигуряват определянето на най-добрите спектрални характеристики на минералите в почвите и на скалите, които да послужат за разпознаването им при интерпретацията на спътниковите изображения. Получените спектрални данни се сравняват с подобни данни от различни инструменти за наблюдение на Земята, включени в спектрални библиотеки. Те съответстват на формата на спектралните характеристики в същия спектрален диапазон, получен с други спектрометри. Тези обещаващи резултати ни насърчават да планираме следващите кампании за полеви спектрометрични измервания в различни региони на България.

Ключови думи: дистанционни изследвания, in-situ спектрометрични измервания, спектрални данни, наблюдения на Земята, верификация на данни

Introduction

Ground-truth data in Earth observation of the environment and in the remote sensing investigations are very important. Remote sensing images are used in the present paper for supporting mineral exploration and mapping geology and for recognizing soils and rocks by their spectral signatures. We used ASTER, Landsat, and Sentinel satellites images for interpreting both, rocks and soils. For data verification, the hyper-spectral systems USB 2000 and NIRQUEST 512.2 of Ocean Optics Inc. are applied for in-situ (laboratory and field) spectrometric measurements. They provide spectral data for defining the finest spectral characteristics of soil minerals and rocks for their identification. The obtained spectral data are compared with similar data from different instruments for Earth observation included in the spectral libraries, such as USGS and JPL data base. They correspond to the shape of the spectral signature in the same spectral range obtained with other spectrometers. These promising results encourage us to plan the next campaigns for collecting mineral, rock, and soil samples for the laboratory and for the field spectrometric measurements in different regions of Bulgaria.

MATERIALS AND METHODS

Landsat 8 Operational Land Imager

Landsat 8 Operational Land Imager (OLI) images consist of nine spectral bands with a spatial resolution of 30 meters for Bands 1 to 7 and 9. The ultra blue Band 1 is useful for coastal and aerosol studies. Band 9 is useful for cirrus cloud detection. The resolution for Band 8 (panchromatic) is 15 meters. The approximate scene size is 170 km north-south by 183 km east-west (106 mi by 114 mi) (https://landsat.usgs.gov/what-are-band-designations-landsat-satellites, July 2017).

ASTER Instrument

The Advanced Spaceborne Thermal Emission and Reflection Radiometer (ASTER) is an imaging instrument onboard Terra, the satellite of NASA's Earth Observing System (EOS) launched in December 1999. ASTER is a cooperative effort between NASA, Japan's Ministry of Economy, Trade and Industry (METI), and Japan Space Systems (J-spacesystems). ASTER data is used to create detailed maps of land surface temperature, reflectance, and elevation. The coordinated system of EOS satellites, including Terra, is a major component of NASA's Science Mission Directorate and the Earth Science Division. The goal of NASA Earth Science is to develop a scientific understanding of the Earth as an integrated system, its response to change, and to better predict variability and trends in climate, weather, and natural hazards (http://asterweb.jpl.nasa.gov/index.asp, July 2017).

The ASTER instrument consists of three separate instrument subsystems. Each subsystem operates in a different spectral region, has its own telescope(s), and was built by a different Japanese company. ASTER's three subsystems are: the Visible and Near Infrared (VNIR), the Shortwave Infrared (SWIR), and the Thermal Infrared (TIR). In our study, were used data from the subsystem in the SWIR region.

SENTINEL-2 Multispectral Instrument

The Sentinel-2 Multispectral Instrument (MSI) will sample 13 spectral bands: four bands at 10 metres, six bands at 20 meters, and three bands at 60-meter spatial resolution. The acquired data, mission coverage and high revisit frequency provides for the generation of geo-information at local, regional, national, and international scales. The data is designed to be modified and adapted by users interested in thematic areas (https://earth.esa.int/web/sentinel/user-guides/sentinel-2-msi/overview, July 2017).

Instruments Characteristics

The ASTER bands are overlaid on the atmosphere model presented on Figure 1.

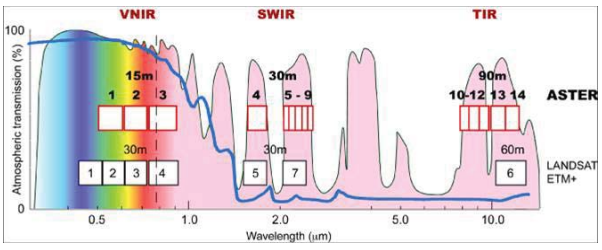

Fig. 1. ASTER bands (http://asterweb.jpl.nasa.gov/images/spectrum.jpg, July 2017)

SENTINEL-2 data is complementary to existing missions including LANDSAT (Fig. 2) and SPOT.

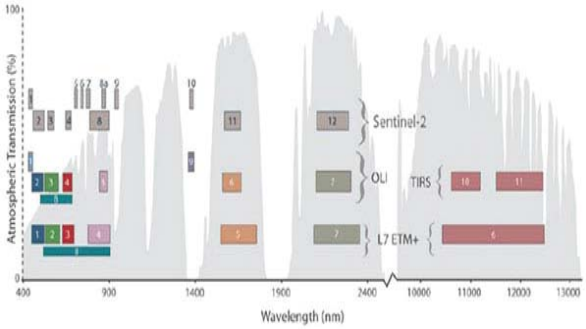

Fig. 2. Sentinel-2 and Landsat spectral bands (https://earth.esa.int/web/sentinel/user-guides/sentinel-2-msi/overview, July 2017)

Field and laboratory instruments

For data verification, the hyper-spectral systems USB 2000 (TOMS) and NIRQuest 512.2 of Ocean Optics Inc. are used in the field and the laboratory (in-situ) spectrometric measurements. The field reflectance spectral signatures were obtained with a TOMS (Thematically Oriented Multi-channel Spectrometer) designed and constructed in the Remote Sensing System Department at the Space Research and Technology Institute – Bulgarian Academy of Sciences in collaboration with Alabama State University USA (Petkov et al., 2005). A high-performance optical bench, low-noise electronics, and various grating options make NIRQuest Spectrometers the best choice for modular NIR spectroscopy. This small footprint spectrometer is available in several different models that cover various wavelength ranges between 900 nm and 2500 nm. As with most Ocean Optics designs, the NIRQuest can be customized for your specific application with various grating, slit and mirror options. The NIRQuest is ideal for applications ranging from analyzing moisture content in food and beverage products to analyzing trace metals in wastewater and laser characterization among others. The NIRQuest 512.2 was used in the laboratory spectrometric measurements (https://oceanoptics.com/wp-content/uploads/OEM-Data-Sheet-NIRQuest.pdf, July 2017).

ASTER Spectral Library

The ASTER spectral library includes data from three other spectral libraries: the Johns Hopkins University (JHU) Spectral Library, the Jet Propulsion Laboratory (JPL) Spectral Library, and the United States Geological Survey (USGS - Reston) Spectral Library.

In the present study, we used data from the ASTER spectral library for comparing the obtained infrared spectral data from ASTER instrument onboard of the airborne platform and the same data from laboratory measurements for the same rock samples included in the spectral libraries (Baldridge et al., 2009).

Region of Interest (RoI)

The total area of the said region is about 600 km^2 located in the central part of Bulgaria. In this work, the region of interest is Central Srednogorie (Fig. 3). This zone is located in the central part of Bulgaria and belongs to Apuseni-Banat-Timok-

Srednogorie belt, into which one of Europe's richest porphyry Cu and Cu-Au epithermal deposits are located (Strashimirov et al., 2002; Popov et al., 2012). In the Srednogorie zone, situated 60-90 km east of Sofia, the ore deposits exploited contain mainly Cu and Cu-Au-Mo. In this region, 150 ore deposits, ore occurrences and mineral indications are found and documented.

Fig. 3. Metallogenic zones in Bulgaria (after Bogdanov, 1982; Bird et al., 2010)

About 10 km south of the town of Zlatitsa, on the road to Panagyurishte, an outcrop of the South Bulgarian granitoids are embedded in metamorphic rocks of the Proto-Rhodope group. To the South, Bulgarian granitoids intrusive bodies concerned with Palaeozoic ages, different sizes and composition, are divided into three intrusive complexes. The first set includes intrusive granites, grano-diorites, and small bodies of diorite and quartz-diorites. The Smilovene, Hissar and Poibrene plutons are included in this complex. The composition of the second intrusive complex includes amphibole-biotite, biotite, and light granites. The Koprivshtitsa, Klissura, and Matenitsa plutons belong to this complex. The third intrusive complex is represented by granular biotite, biotite-muscovite, and pegmatite granitoids. In this complex, the Strelcha, Karavelovo, Lesichovo, and Varshilo plutons are presented (Dabovski et al., 1972). In the point of field measurement, biotite granites of the Northwest Koprivshtitsa pluton are revealed. They are light gray, sometimes rusty colored by iron hydroxides, medium- to coarse-grained, with a clear lineal porphyroid parallelism. They are formed by K-feldspar, plagioclase, quartz, biotite, apatite, and zircon (Banushev et al., 2012).

Results and Discussion

Reference spectra

Reference spectra of granites, grano-diorites, and related soil types were obtained from the USGS and JPL spectral libraries. The USGS spectral library contains reference spectra for rocks and soils that represent different localities around the world but most of them are presented in one particle size (Clark et al., 2007).

Spectral analysis

According to specific features of the spectral signatures, the USGS and JPL reference spectra of granites, grano-diorites, and related soil types that are closest to granites, grano-diorites and related soil types in the RoI were analyzed.

In Figure 4a, the spectral reflectance signatures of granite (blue line reflects 23-33%), brown soils (brown line reflects 2-29%), and grass as green vegetation (green line typical reflective maximum at 0.55 μm and (0.76-0.85) μm and at least 0.67 μm) taken from the USGS spectral library (Baldridge et al., 2009) are presented. They represent reference spectral reflectance characteristics and are used for comparative interpretation of the results acquired during the field hyper-spectral measurements.

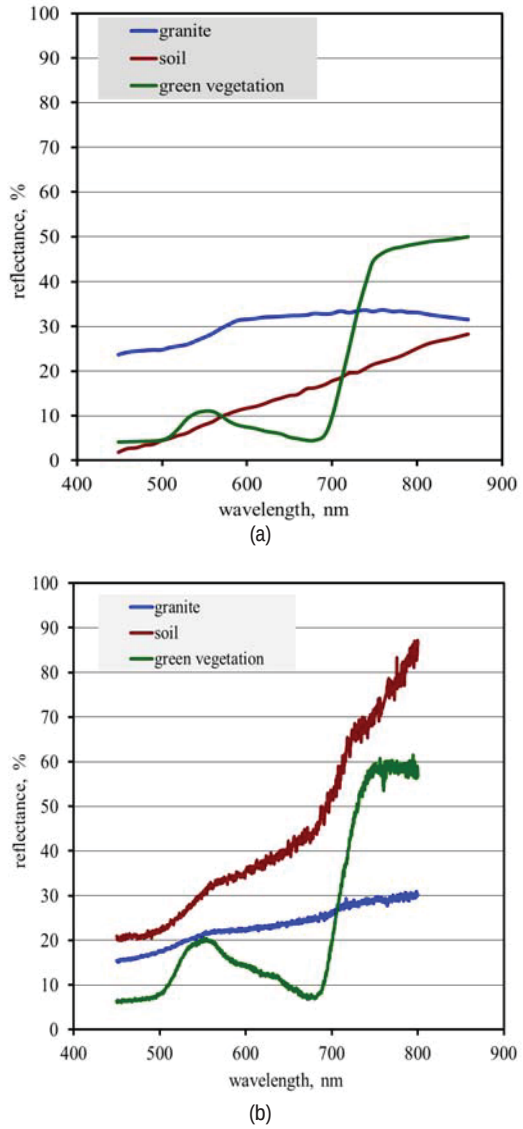

Fig. 4. Plot of spectral reflectance signatures of granites, related soil types and green vegetation obtained from: (a) ASTER reference library (Baldridge et al., 2009) and (b) TOMS field hyper-spectral measurements

Figure 4b shows the spectral reflectance characteristics of granite, brown forest soil, and green vegetation obtained in the field hyper-spectral measurements using the TOMS spectrometric system. The reflectance spectra of granites and brown forest soil show significant differences in value range (0.6-0.8) μm.

The infrared spectra of granite have increased water vapor, which causes a observable saw tooth appearance in the short wavelength region of the spectra (2-3) μm. Results show that it has an absorption feature around 1.9 μm (Fig. 5). The 1.9 μm feature is covered by atmospheric (water) absorption (Curran et al., 2001). This minimum in the spectral characteristics could be found in laboratory spectral data because of the higher amount of energy reaching the instrument detector.

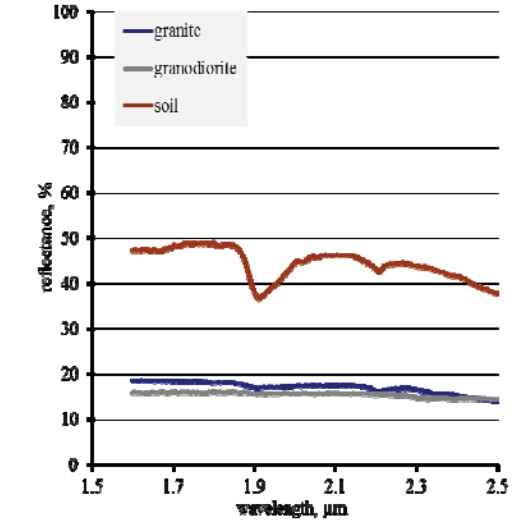

(a)

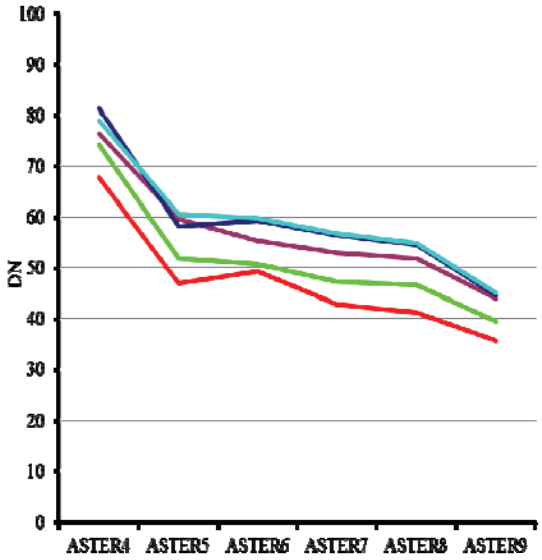

(b)

Fig. 5. Plots of infrared spectra of: (a) granites, grano-diorites, and related soil from ASTER library (Baldridge et al., 2009); (b) RoI from ASTER instrument

The ASTER spectra of exposed granites in RoI (green line in Figure 5) have the same trend as reference spectra from the spectral library. Since there are no detectors in the spectral range (1.8-2.1) μm, the missing spectral data could be the cause for misinterpretation of the infrared spectral data. Therefore, additional in-situ laboratory and field spectrometric measurements in this spectral range have to be planned and performed.

Figure 6a presents a Landsat 8 image (November 2015) of the RoI with three ground control points /GCPs/ for studied land covers. The GCPs include soil and rocks. Figure 6b demonstrates the spectral reflectance curves for each GCP obtained from Landsat 8. For better interpretation and classification of soils and rocks in mountain regions, the described measurements complete the methodologies explained in Avetisyan (2015) and Avetisyan and Nedkov (2015).

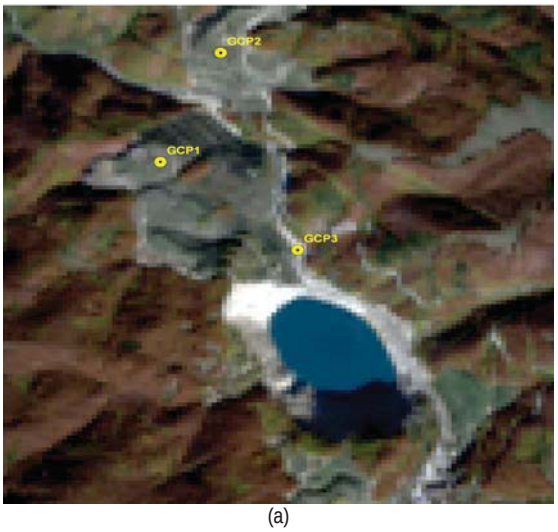

(a)

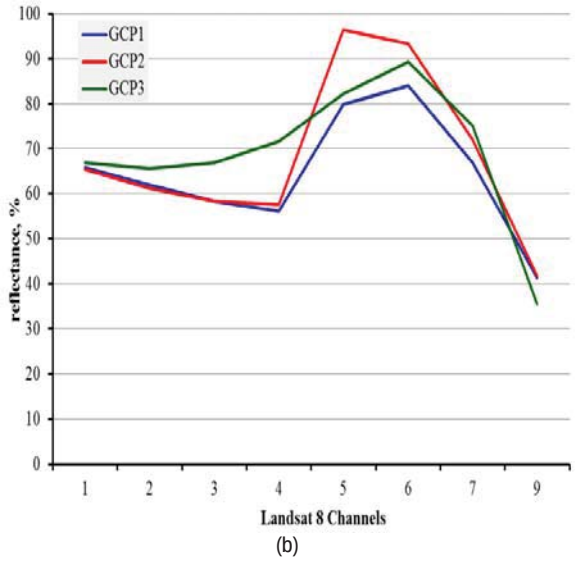

(b)

Fig. 6. Landsat 8 image of the RoI in 2015 with GCPs (1-3) (a) and relating spectral signatures (b)

A Sentinel-2 MSI image (August 2015) of the RoI with three ground control points /GCPs/ for studied land covers that are identical as those on Landsat 8 image is presented in Figure 7a. GCP1 and GCP2 include mainly soil and rocks. In GCP3, the three main land cover types – rocks, soils, and vegetation – are included. Figure 7b demonstrates the spectral reflectance curves for each GCP obtained from Sentinel-2 MSI.

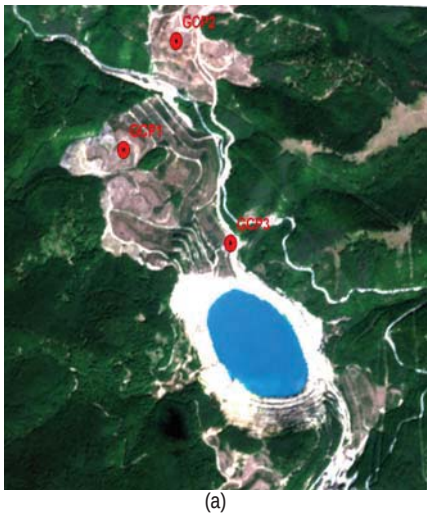

(a)

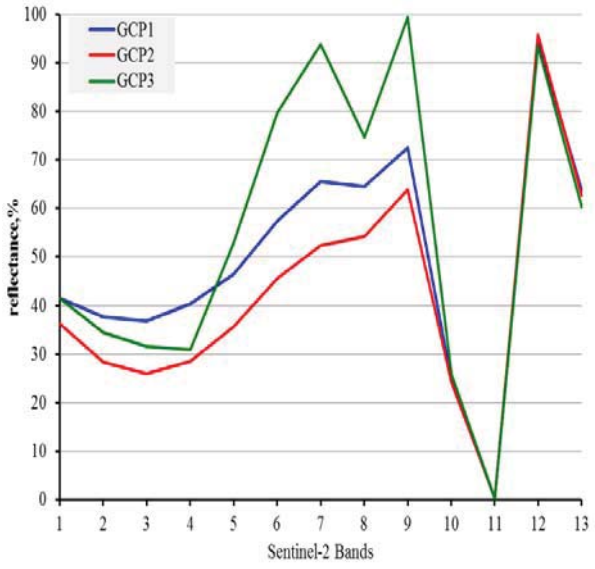

(b)

Fig. 7. Sentinel-2 MSI image of the RoI in 2015 with GCPs (1-3) (a) and relating spectral signatures (b)

Conclusions

Multispectral data from three different spectrometric systems – ASTER on satellite Terra, OLI on satellite Landsat 8, and MSI on satellite Sentinel-2 - were used in this study to identify exposed rocks and soils in the Central Srednogorie region, Bulgaria. For data verification, the hyper-spectral systems TOMS (USB 2000) and NIRQuest 512.2 of Ocean Optics Inc. were used in performing in-situ (the laboratory and the field) spectrometric measurements. The results show that the suggested methods for analyzing the spectral data could be useful for identifying exposed rocks and soils. Theoretical and analytical techniques that have been developed for the analysis of the laboratory spectral data were also applied to field spectral data. The shape of the spectral curves acquired during the laboratory and the field measurements confirmed this promising technique in satellite data verification.

References

Банушев, Б., С. Приставова, Р. Костов, Р. Паздерав, Н. Цанкова, Е. Раева, С. Малинова. Ръководство за учебни практики по минералогия и петрография. ИК "Св. Иван Рилски", София, 2012. (Banushev, B., S. Pristavova, R. Kostov, R. Pazderav, N. Tsankova, E. Raeva, S. Malinova. Rakovodstvo za uchebni praktiki po mineralogiya i petrografiya. IK "Sv. Ivan Rilski", Sofia, 2012)

Дабовски, Х., И. Загорчев, М. Русева, Д. Чунев. Палеозойски гранитоиди в Сащинска Средна гора. Год. УГП, 16, 1972. - 57-92. (Dabovski, H., I. Zagorchev, M. Ruseva, D. Chunev. Paleozojski granitoidi v Sashtinska Sredna gora. God. UGP, 16, 1972. - 57-92.)

Попов, П., С. Страшимиров, К. Попов, М. Каназирски, К. Богданов, Р. Радичев, С. Димовски, С. Стойков. Геология и металогения на Панагюрския руден район. София, Изд. къща „Св. Ив. Рилски", 2012. – 227стр (Popov, P., S. Strashimirov, K. Popov, M. Kanazirski, K. Bogdanov, R. Radichev, S. Dimovski, S. Stoykov. Geologiya i metallogeniya na Panagyurskiya ruden rayon. Sofia, Izd.kashta "St. Ivan Rilski", 2012. – 227p.)

Avetisyan, D. Assessment of vegetation cover degradation and soil erosion in Chuprene Reserve (Northwestern Bulgaria) using remote sensing and geographical information systems. Ecological Engineering and Environment Protection, 1, 2015. – 47-56.

Avetisyan, D., R. Nedkov. Determining the magnitude and direction of land cover changes in the semi-natural areas of Haskovo Region, Southeast Bulgaria. – Geoscience and Remote Sensing Symposium 2015, IEEE International, 2015. – 4637-4640.

Baldridge, A. M., S. J. Hook, C. I. Grove and G. Rivera. The ASTER Spectral Library Version 2.0. – Remote Sensing of Environment, 113, 2009. – 711-715.

Bird, G., P. Brewer, M. Macklin, M. Nikolova, T. Kotsev, M. Mollov, C. Swain. Dispersal of contaminant metals in the mining-affected Danube and Maritsa drainage basins, Bulgaria, Eastern Europe. – Water Air and Soil Pollution, 206 (1-4), 2010. – 105-127.

Bogdanov, B. Bulgaria. – In: Mineral Deposits of Europe. Vol.2. Southeast Europe (Eds. Dunning, F., W. Mykura, D. Slater). The Mineralog. Society, London, 1982. – 215-232.

Curran, P.J., J.L. Dungan, D.L. Peterson. Estimating the foliar biochemical concentration of leaves with reflectance spectrometry testing the Kokaly and Clark methodologies. - Remote Sens. Environ. 76, 2001. – 349-359.

Petkov, D., H. Nikolov, G. Georgiev. Thematically Oriented Multichannel Spectrometer (TOMS). – Aerospace Res. in Bulgaria, 20, 2005. – 51-54.

Strashimirov, S., R. Petrunov, M. Kanazirski. Porphyry-copper mineralisation in the central Srednogorie zone, Bulgaria. – Mineralium Deposita, 37, 2002. – 587-598.

http://asterweb.jpl.nasa.gov/index.asp, July 2017

http://asterweb.jpl.nasa.gov/images/spectrum.jpg, July 2017

https://earth.esa.int/web/sentinel/user-guides/sentinel-2-msi/overview, July 2017

https://landsat.usgs.gov/what-are-band-designations-landsat-satellites, July 2017

https://oceanoptics.com/wp-content/uploads/OEM-Data-Sheet-NIRQuest.pdf, July 2017

The article is reviewed by Prof. Stefan Dimovski, DSci. and Assist. Prof. Dr. Hristiyan Tsankov

EXTENSIONAL REACTIVATION OF A FORMER COMPRESSIONAL FAULT ZONE: AN EXAMPLE FROM THE EASTERN PART OF THE ZLATITSA GRABEN

Yanko Gerdzhikov[1], Zornitsa Dotseva[1], Dian Vangelov[1]

[1] Sofia University "St. Kl. Ohridski", 15 Tzar Osvoboditel Blvd, 1504 Sofia, Bulgaria, e-mail: janko@gea.uni-sofia.bg

ABSTRACT. The formation of the grabens and the uplift of the Stara Planina Mountain are morphological features, related to the translations along the normal faults, situated along the southern foot of the mountain. Most often, the normal fault zone is rather well expressed as a prominent mountain front, thus indicating active tectonics along the normal fault zone. The subject of this study is the easternmost part of the fault zone in the Zlatitsa graben. The area provides good outcrops of rocks that are situated along the mountain front and thus it can be assumed that complete profiles along the normal fault zone can be observed. The structural analysis of the related tectonites indicates evolution that is more complex. Within the fault zone, two different parts are characterized in terms of thickness, as well as related tectonites. Within the western part, a several-meter-thick cataclasite zone affects the Paleozoic gneisses. Numerous folds, as well as some slip planes indicate an earlier, probably severely overprinted, phase of compressional top-to-the-north shear. The easternmost parts of the zone are characterized by 1-2 m thick fault core surrounded by brecciated and silicified granitic host rocks. Rare Riedel shears within the fault core indicate extensional shearing. However, our data are incompatible with the interpretation of this fault zone as a product of only extensional tectonics. Based on: 1/ the presence of folded cataclasites; 2/ the presence of sporadic top-to-the-south slip surfaces; 3/ large thickness of the fault zone and evidence for an intensive hydrothermal alteration, it can be argued that the studied zone represents an older compressional fault zone reactivated during the youngest tectonic face. These results are in line with the data from the Karlovo graben and the western part of the Zlatitsa graben.

Keywords: Zlatitsa graben, normal fault, fault zone, reactivation, tectonic inheritance

ЕКСТЕНЗИОННА РЕАКТИВАЦИЯ НА КОМПРЕСИОННИ РАЗЛОМНИ ЗОНИ: ПРИМЕР ОТ ИЗТОЧНАТА ЧАСТ НА ЗЛАТИШКИЯ ГРАБЕН

Янко Герджиков[1], Зорница Доцева[1], Диан Вангелов[1]

[1] Софийски Университет "Св. Кл. Охридски", бул. „Цар Освободител" 15, 1504 София, e-mail: janko@gea.uni-sofia.bg

РЕЗЮМЕ. Издигането на Стара планина и формирането на грабени в южното подножие са породени от транслациите по система от разседи в южния Старопланински склон. В повечето случаи тези разседи са морфоложки изразени като ясно обособен планински фронт, което наред с други геоморфоложки белези индикира съвременната активност на разсяданията. Обект на настоящото изследване е източната част на разседната зона, в района на изток от с. Антон, където има много добра разкритост на скалите от участъка на планинския фронт и са достъпни почти пълни профили през разломната зона. Проведените структурни изследвания индикират сложна еволюция на скалите от тектонската зона, маркираща планинския фронт. Получените данни са несъвместими с интерпретацията на разломната зона, като структура породена само от екстензионни срязвания. Аргументите за това са: 1/ наличие на нагънати катаклазити; 2/ присъствие на спорадични южновергетни срязвания; 3/ значителната дебелина на разломната зона и белезите за интензивна хидротермална промяна. На базата на тези факти, считаме че изследваната тектонска зона представлява екстензионно реактивирана компресионна зона. Тези резултати потвърждават аналогични изводи, направени при изучаването на разседните сегменти в Карловско и западната част на Златишкия грабен.

Ключови думи: Златишки грабен, разсед, разломна зона, реактивация, тектонско унаследяване

Introduction

In recent years, significant advances have been made in understanding the tectonic evolution of the Zlatitsa-Etropole area in the Stara Planina Mountain and situated along the southern mountain foot of the Zlatitsa graben (recent overview in Antonov et al., 2010a, 2010b; see also Gerdzhikov et al., 2012; Kunov et al., 2017; etc.). These studies demonstrate that the contemporary structure of the area is defined by several tectonic phases, of major importance being the Variscan, Early Alpine (J3-K1), Late Alpine (Pc-Eo) and post-Late Oligocene extensions. From an orogenic point of view, within a very narrow E-W trending belt locked between the Vezhen pluton and the Zlatitsa graben (width in map view between 6,5 and 0,3 km), structures can be observed that attributed to these tectonic phases of different age. Besides, in the area to the NE of the village of Anton, these structures are overlapping (e.g. Antonov et al., 2010). This spatial proximity and even overlapping is an indicator for possible structural inheritance and reactivation. Such ideas have been proposed earlier (Bonchev, Karagyuleva, 1961), but solid structural arguments for this supposition are not available. Here we present results of our structural studies of the easternmost part of the fault zone that coincides with the normal fault zone controlling the formation of the Zlatitsa graben. These data indicate prolonged structural evolution and are incompatible with the interpretation of the fault-related rocks along the mountain front as a product of a single tectonic event.

Geological setting

The Zlatitsa graben is part of the system of grabens situated along the southern margin of the Stara Planina Mountain (e.g. Tsankov et al., 1996; Roy et al., 1996). The basin is elongated in E-W direction and has a length of about 35 km. Situated between the Stara Planina and the Sredna Gora Mountains, the basin can be characterized as inter-montane (Fig.1), filled by a continental succession without a well-studied thickness. From a structural point of view, this extensional structure is controlled mainly by a south-dipping fault that is traced along the southern slope of the Stara Planina Mountain. This normal fault (referred to as the Zlatitsa graben normal fault – ZGNF) has a pronounced geomorphological expression as it is marked by a prominent mountain front (term defined in Bull and McFadden, 1977) with mean slope angles between 18–34°. Along with other qualitative and quantitative tectonic geomorphological characteristics (Mishev et al., 1962; Gerdxhikov et al., 2012), this is strong argument for the contemporary activity of the fault zone. Importantly, low-temperature FT geochronological data indicate that the extension along this fault zone initiated in Late Oligocene time (Kunov et al., 2017).

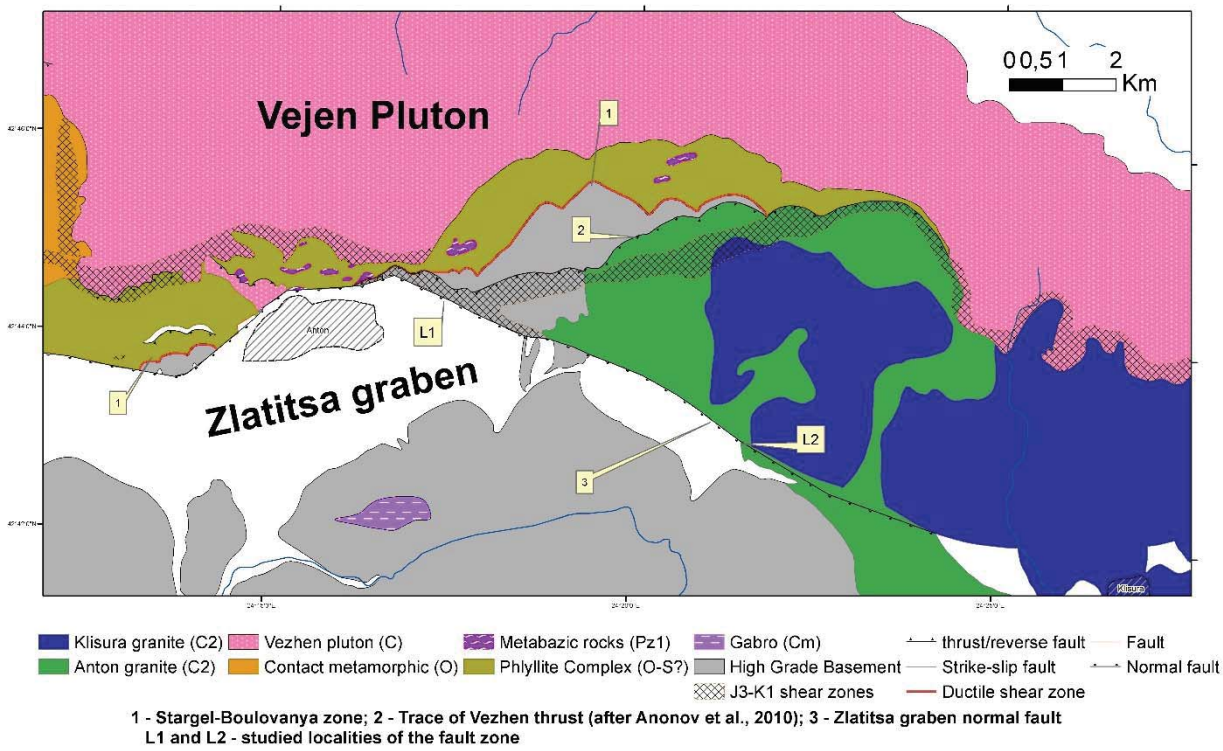

Fig. 1. Geological map of the Zlatitsa graben with the location of the studied part of the Zlatitsa graben normal fault

On the basis of the Zlatitsa graben normal fault trace in map view, three geometrical segments (in the sence of Peackok et al., 2016) can be defined – western(~11 km), central (14.5 km) and eastern (12.5 km). The subject of the current research is the well-outcropped eastern segment of the Zlatitsa graben normal fault. Here, the zone is completely hosted within the Variscan basement and is at least partially covered by Quaternary alluvium, delluvium, and colluvium deposits. The Variscan basement is represented by metamorphic rocks and granitoids. In the metamorphic basement, two complexes are distinguished that differ in grade and evolution: the high-grade basement (the Central Srednogorie High-Grade metamorphic complex – Gerdzhikov et al., 2008; the Pirdop Complex – Antonov et al., 2010) and the low-grade phyllite dominated complex (Phyllite formation, Antonov et al., 2010).

The area to the northeast of the village of Anton (Fig. 1) is a real tectonic knot that telescopes four tectonic zones which differ in age (Antonov et al., 2010). The Variscan Stargel-Boluvanya zone and the Early Alpine north-vergentmetre-decametre scale shear zones are with a penetrative character. The translations along the Variscan zone led to the juxtaposition of the high- and low-grade basement units and to the creation of the regional-scale, stable, south-dipping planar fabric. While the Stargel-Boluvanya zone is well-mapped (e.g. Antonov et al., 2010), the extent of the Early Alpine shear zones is not yet well-known. They are traced as east-west striking lens-like high-strain domains, mainly hosted within the gneissic basement. Traditionally, the Vezhen thrust is regarded as a representative of the Late Alpine north-vergent compressional structure (Bonchev and Karagyuleva, 1963; Antonov et al., 2010). It is important to note that the existence and the exact trace of this structure are topics of debate (e.g. Gerdzhikov et al., 2008; Antonov et al., 2010). The latest contribution (Antonov et al., 2010) suggested the NE trend of this zone and its possible merger/connection with the other tectonic zones along the mountain front that coincides with the Zlatitsa graben normal fault.

New structural geological studies were carried out in this segment that allowed us to revise the previously reported (Glabadanidu et al., 2012) architecture and significance of the fault zone.

Fault zone structure and related tectonites

The studied segment of the Zlatitsa graben normal fault strikes east-southeast (115º) and dips moderately at 30-40º to the south. Outcrop conditions are highly variable. From the village of Anton to the valley of the Vartopska river, the whole zone, or at least the upper parts of it, are covered by colluvium or alluvium sediments. To the east, the zone is completely hosted in the Late Variscan granites, yet there are no perfect outcrop conditions along the zone. Field data indicate that the thickness and characteristics of the zone are highly dependent on the type of the protoliths. Thus, in the western part, where the zone cuts the Variscan gneissic basement, the zone is represented by up to 10 m of a brecciated and strongly cataclastically reworked rock volume. To the east, the zone cuts through more competent granitoids and here the thick damage zone hosts a comparatively narrow fault core.

Fault zone in the gneissic basement

Two large outcrops in the westernmost part of the studied area provide nice opportunities to study the fault zone that coincides with the mountain front. In both of them, the fault-related rocks are covered by alluvium or colluvium. We interpret these rocks as an exhumed footwall of the Zlatitsa graben normal fault. Most probably the youngest fault strands are covered and masked by Holocene sediments. Locality 1 (at 24.29065, 42.73946) represents a deca-meter scale 3D outcrop along the slopes of a deeply incised river valley. The footwall consists of two micas, often highly weathered, and fractured gneisses. Most often the foliation is strongly folded, but in places with more consistent orientation, foliation dips to the southwest (200-230º/50-60º). Two domains are distinguished within the fault zone: heterogeneously faulted and ultracataclastic (Fig. 2).

In domain 1, the gneisses are strongly fractured and host several levels of black cataclasites to ultracataclasites. The black color of the strongly cataclastically reworked gneisses is due to the extreme crushing of the rock mass, along with processes of diffusive mass transfer and growth of chlorite. In the ultracataclastic domain 2, the dominant rock type is represented by chlorite-rich cataclasites and ultracataclasites that host clasts of the protolith that are sized of up to a decimeter. Cataclastic and ultracataclastic tectonites are strongly affected by centimeter- meter-scale folding. The orientation of the fold axes displays some spread, but the main NW-SE trend can be detected (Fig. 3a). A possible reason for this spread is the presence of numerous centimeter-scale shear zones and slip surfaces that are abundant in the ultracataclastic domain. Importantly, the orientation of these structures differs in terms of strike and dip to the mean orientation of the eastern segment of the Zlatitsa graben normal fault (Fig. 3b). It was not possible to detect linear fabric on the shear surfaces. Structures as Riedel shears and C-S mesoscale mélanges (Kusky, Bradley, 1999) indicate that most of them are extensional, yet such features also point to the presence of compressional, top-to-the-north, NE shear.

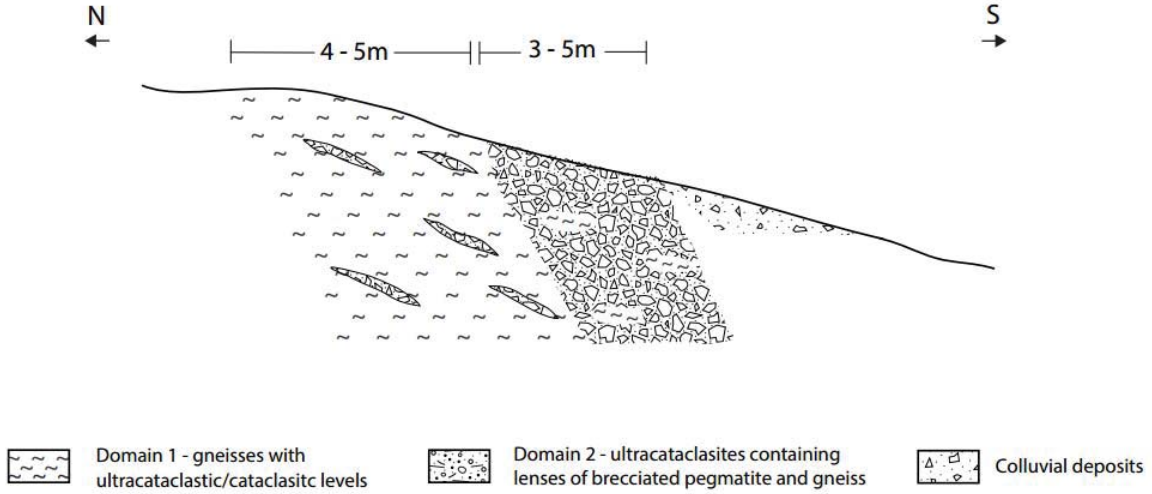

Fig.2. Overview of the main components of the fault zone developed in the gneissic basement from Locality 1

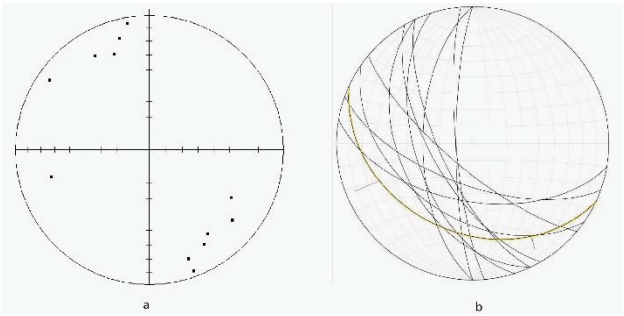

Fig.3. Stereo-plots. a) fold axes from Locality 1; b) slip surfaces from the ultracataclastic domain (Locality 1). Arrows mark the great circle representing the orientation of the eastern segment of ZGNF. Equal area, lower hemisphere

About 250 m eastwards (at 24.29271, 42.73863), there are good outcrops of a heterogeneously faulted domain from Locality 1. They are covered by colluvium, so the upper parts of the fault zone are masked. Again, the brecciated and cataclastically reworked gneisses are affected by folds with axes trending NW-SE. Non-penetrative Riedel shears (slip planes) as well as imbricated shear-bounded lens fragments indicate compressional, north-vergent shear (Fig. 4).

Fig.4. Folded cataclasites (folded surfaces underlined by dash white line) and slip planes indicating N-vergent shear. North is to the left

Fault zone in the granite

For the purpose of the description of the zone, we can define three elements: footwall zone, fault core and hanging wall zone. This cross-sectional architecture is centered on the identified in the field single, narrow zone built up of breccias, cataclasites, and gauge. The type locality of the fault core is easily accessible on the main road E-871 (Locality 2, at, 42.71829; L2 in Fig. 1) where the zone strikes 125^{o} and dips 40-45^{o} to the south.

The footwall of the zone is well-outcropped. Here, the intensity of the brittle overprint varies from rather weak to very strong. In weakly deformed parts, the protholite is affected by a network of fractures and weak brecciation and does not display strong hydrothermal overprint. The intensively overprinted parts of the footwall are brecciated, dissected by discrete south-dipping fault, and often silicified. Usually, it is difficult to obtain a clear view of the original fabric of these rocks. Still, at a few places, it is clear that the brittle zone overprints foliated to weakly foliated granites. In the uppermost part of the footwall, there are 2-4 m thick levels of brecciated and strongly silicified granite with extremely fine-grained grey-greenish matrix.

The hanging wall is often covered by colluvium and more rarely by alluvial deposits. The immediate hanging wall is built by the same granites. They are also strongly brecciated and contain planes that shallowly (35^{o}) dip to the southslip, trending 100^{o}.

The core of the zone is about 1 m thick and is characterized by great heterogeneity. The dominant lithology is represented by cohesive, matrix-supported, grey-greenish tectonite that contains angular or oval-shaped clasts with long axes of up to several centimeters. A coarse cataclastic foliation that is co-planar with weak color layering is observed. Due to the heterogeneity of these tectonites, their precise classification is almost impossible. According to the classification of Woodcock Mort (2008), they fit within the categories of chaotic breccias and cataclasites. Both types of tectonites do not show systematic spatial relations either to the cataclastic foliation, or to other structural discontinuities. Most probably their “mixing” is the result of a heterogeneous strain distribution. The uppermost level of these grey cataclastic rocks is a rather strong and resistent ot erosion. It forms a pronounced “crust” that preserves the fault core from erosion. The strong cohesion of this rock type is due to the presence of calcite cement and abundant calcite veins. Microfabric studies reveal the intensive influx of carbonate-rich fluids into the strongly fractured rock mass.

Another type of tectonite is dark grey to black ultracataclasite that forms 2-3 irregular layers (up to 25cm thick) parallel to the cataclastic foliation. The ultracataclasite is affected by strong foliation that corresponds to closely spaced mesoscale fractures and shear surfaces. On the scale of the specimen, these tectonites are clast-free. Clasts that vary in size are observed in thin sections. Some of them are well-rounded, a feature suggesting very strong attrition. Some clasts are overgrown by newly formed chlorite that is also abundant in the matrix. The foliation is defined by sub-parallel alignment of 1) elongation of newly grown phyllosilicate phases; 2) lensoidal clasts of the protholite; 3) vaguely defined pressure solution seams marked by enrichment of insoluble constituents; 4/ elongated beards of phyllosilicates upon clasts.

While the distinguished tectonite types (grey chaotic breccias, grey cataclasites and black ultracataclasites) most often interlayer parallel to the cataclastic foliation, there are field relations that suggest mutually cross-cutting relations. We observed decimeter-meter-scale blocks of the breccias embeded into the black ultracataclasites, as well as presence of black ultracataclasite clasts into grey breccias. All these relations are documented in a single large outcrop with areal extent of >1 000m^{2}. Most probably they are the result of a protracted period of successive slip events occurring in different conditions of fluid availability and strain rate. Of course, it cannot be excluded that they result from overlapping products of different tectonic phases.

During the first inspection of the outcrop in 2005, we recorded the existence of polished surface/s with almost down-dip lineation (160/30). Later field work was not able to record again these data. In down-dip sections, orthogonal to the foliation, available along several 1-1.2 m deep gullies, we observed Riedel shears that are steeper (40–50°) to the cataclastic foliation and in some cases displace the faint layering within breccias. Because we were unable to observe any marks on the fault/shear surfaces,these Riedel shears are the only kinematic indicator that confirms the extensional character of the shearing.

Discussion

Were the tectonites, localized along the mountain front, formed during the single tectonic phase?

It is well known that brittle faults often record long history and, once formed, they are mechanically weak zones that accommodate later strain increments (e.g. Holdsworth et al., 1997). Besides, it is demonstrated that previously existing structural anisotropy exerts strong control on the geometry of faulting in the continental crust (Buttler et al. 2008). These possibilities are still unrecognized in the case with the fault network in the studied area.

The data reported in this contribution refer to the fault-related rocks situated immediately on the mountain front. They can be regarded as a result of a single tectonic phase related to post-Oligocene extensional tectonics. Yet, field data argue for re-appraisal of this most conventional idea. There are data and arguments that motivate a negative answer to the posed question.

First, the obtained data from the fault zone in the gneissic basement - such as the large thickness of the zone, the existence of folds affecting cataclasites, as well as the presence of north-vergent shears - are incompatible with the interpretation of the studied fault zone as completely related to the extensional movements related to the Zlatitsa graben normal fault. Most probably, the studied tectonites represent an old compressional zone related to a Late Alpine compression.

Second, despite of the fact that it is not that conclusive, the data from the tectonite fabric in the granite basement are also incompatible with the simplest tectonic scenario. Arguments supporting this view can be the significant width of the zone and the data for very strong fluid infiltrations not only in the fault core, but in the brecciated host rocks, too.

Third, the reported features of the fault zone within the granite basement bear a strong similarity with the observed features along the normal fault at the same tectonic-geomorphological position from the neighboring Karlovo graben. The normal fault along the southern slope of the StaraPlanina Mountain in the Karlovo area is most often represented by cataclastic rocks that are up to 1-2 m thick, strongly hydrothermally altered (silicified or carbonatization), and resistant to weathering. Due to their mechanical properties, the normal fault is often marked by the upper surface of these altered rocks that appear on the crust. A similar crust is present at the uppermost levels of the studied segment of the Zlatitsa graben normal fault where the zone cuts the granite basement. Importantly, a detailed field work along the southern foot of the Stara Planina Mountain in the area of the Karlovo graben clearly demonstrated that the normal fault zone, controlling the contemporary uplift, reactivates Late Alpine thrust surfaces (Balkanska and Gerdzhikov, 2010). Data from the western part of the graben (between the villages of Bunovo and Chelopech) also clearly indicate extensional reactivation of a former south-dipping compressional fault array that is rather wide in this part (Dotseva et al., 2016).

Conclusions

The mountain front in the eastern part of the Zlatitsa graben is marked by a complex and long-living tectonic zone. This conclusion is in line with the suggestions of Tsankov et al. (1996) and the data from the neighboring Karlovo graben (Vangelov et al., 2010; Balkanska and Gerdzhikov, 2010).

In the light of our new results, it can be concluded that the application of the classical tripartite model of the fault zone architecture (Chester et al., 1993) cannot be applied to the Zlatitsa graben normal fault. It is obvious that the model of the fault architecture that was previously reported by us (Glabadanidu et al., 2012) is too simplistic. Structural data clearly indicate the extensional character of the last movements in the fault core in the granite basement. The specific features for the zone are the lack of pronounced lineation, as well as meso-and macro-scale corrugations and polished fault mirrors.

Despite being well-outcropped, we did not find incohesive tectonites along the studied geometric segment of the Zlatitsa graben normal fault. This can be explained by the migration of active fault strands toward the interior of the graben, thus exhuming the main fault zone along the mountain front. Thus, we follow the model of Stewart and Hancock (1988) of the “intrafault-zone hanging wall collapse”.

Acknowledgements

The study started within the frame of the project funded by the Ministry of Education and Science Grant (VU-13/06). Dr Radulovis thanked for the useful insights into the subject.

References

Вангелов, Д., Я. Герджиков, К. Бонев, С. Николов. Предварителни данни за формирането и еволюцията на Карловския басейн. - Год. СУ, Геол.-геогр. факултет, 102, 1, 2010. - 71-106. (Vangelov, D., I. Gerdzhikov, K. Bonev, S. Nikolov. Predvaritelni danni za formiraneto i evolyutsiyata na Karlovskiya basein. – God. SU, Geol.-geogr. fakultet, 102, 1, 2010. – 71-106.)

Герджиков, Я., Д. Вангелов, И. Глабаданиду. Един подценен геоложки риск: дебритните потоци. – Сп. на Бълг. геол. дружество - 73, 1-3, 2012. -85-104. (Gerdzhikov, I., D. Vangelov, I. Glabadanidu. Edin podtsenen geolozhki risk: debritnite pototsi. – Sp. na Bulg. geol. druzhestvo -73, 1-3, 2012. -85-104).

Мишев, К., В. Попов, Ц. Михайлов. Морфология и неотектоника на старопланинското подножие между праговете Гълъбец и Козница. – Изв. Геогр. инст., VI, 1962. - 43–61. (Mishev, K., V. Popov, Ts. Mihailov. Morfologiya i neotektonika na staroplaninskoto podnozhie mezhdu pragovete Galabets i Koznitsa. - Izv. Geogr. Inst., VI, 1962. - 43–61.)

Antonov, M., S. Gerdzhikov, L. Metodiev, Ch. Kiselinov, V. Sirakov, V. Valev. 2010. Explanatory note to the Geological Map of the Republic of Bulgaria in Scale 1:50 000. Map Sheet K-35-37-B (Pirdop). Sofia, Geocomplex, 99 p.

Balkanska, E., I. Gerdzhikov, 2010. New data on the structure of Botev Vrah thrust along the southern foot of Central

Stara Planina Mountain. Comptes Rendus Academy bulgare des Sciences 63 (10), 1485–1492.

Bonchev, E., J. Karagyuleva. 1961. Das Srednogorije antiklinorium und die Staraplanina-granituberschiebungsdecke. *Trav. sur la géologie. de la Bulgarie*, 2, 31–42.

Bull, W. B., L. D. McFadden. 1977. Tectonic geomorphology north and south of the Garlock Fault, California, in Geomorphology in Arid Regions: Annual Binghamton Conference, D.O. Doehring, ed., State University of New York at Binghamton, 115–136.

Butler, R. W. H., C. E. Bond, Z. K. Shipton, R. R. Jones, M. Casey, , 2008. Fabric anisotropy controls faulting in the continental crust. *Journal of the Geological Society 165*, 449–452.

Caine, J. S., R. L. Bruhn, C. B. Forster, 2010. Internal structure, fault rocks, and inferences regarding deformation, fluid flow, and mineralization in the seismogenic Stillwater normal fault, Dixie Valley, Nevada. *Journal of Structural Geology*, Fault Zones 32, 1576–1589.

Chester, F. M., J. P. Evans, and R. L. Biegel, (1993). Internal structure and weakening mechanisms of the San Andreas fault. Journal of Geophysical Research 98: doi: 10.1029/92JB01866

Dotseva, Z., D. Vangelov, I. Gerdzhikov, D. Dancheva, 2016. Bunovo-Anton Fault Zone – an array of fault segments or remnants of a Late Alpine fault zone? National Conference "Geosciences 2016", Sofia, December 2016,

Faulkner, D. R., C. A. L. Jackson, R. J. Lunn, R. W. Schlische, Z. K. Shipton, C. A. J. Wibberley, M. O. Withjack, 2010. A review of recent developments concerning the structure, mechanics and fluid flow properties of fault zones. *Journal of Structural Geology*, Fault Zones 32, 1557–1575

Géraud, Y., M. Diraison, N. Orellana, 2006. Fault zone geometry of a mature active normal fault: A potential high permeability channel (Pirgaki fault, Corinth rift, Greece). *Tectonophysics*, Natural Laboratories on Seismogenic Faults 426, 61–76.

Glabadanidu, I., I. Gerdzhikov, D. Vangelov, 2012. Structural and tectonic geomorphological studies in Zlatitsa graben, Central Bulgaria, National Conference "Geosciences 2012", Sofia, December 2012, 107-108.

Holdsworth, R.E., C. A. Butler, A. M. Roberts, 1997. The recognition of reactivation during continental deformation. *J. Geol. Soc*. *154*, 73–78

Kunov, A., I. Gerdzhikov, D. Vangelov, E. Balkanska, A. Lazarova, S. Georgiev, D. Stockli, E. Blunt, R. E. Holdsworth, C. A. Butler, A. M. Roberts, 1997. The recognition of reactivation during continental deformation. *J. Geol. Soc*. *154*, 73–78

Kunov, A., I. Gerdzhikov, D. Vangelov, E. Balkanska, A. Lazarova, S. Georgiev, D. Stockli, E. Blunt, 2017. First thermochronological constraints on the Cenozoic extension along the Balkan Fold-Thrust Belt (Central Stara Planina Mountain, Bulgaria). Int. J. Earth Sci. (in press).

Kusky, T. M., & D. C. Bradley, 1999. Kinematic analysis of mélange fabrics: examples and applications from the McHugh Complex, Kenai Peninsula, Alaska. *Journal of Structural Geology*, *21*, 1773-1796.

Peacock, D., C. Nixon, A. Rotevatn, D. Sanderson, & L. Zuluaga, 2016. Glossary of fault and other fracture networks. Journal of Structural Geology 92, 12-29.

Rowe, C.D., W. A. Griffith, 2015. Do faults preserve a record of seismic slip: A second opinion. *Journal of Structural Geology 78,* 1–26. doi:10.1016/j.jsg.2015.06.006

Roy, M., L. H. Royden, B. C. Burchfield, Ts. Tsankov, R. Nakov. 1996. Flexural uplift of the Stara planina range, Central Bulgaria. –Basin Research, 8, 143-156.

Stewart, I. S. and P. L. Hancock, (1988), Normal fault zone evolution and fault scarp degradation in the Aegean region. Basin Research, 1: 139–153. doi:10.1111/j.1365-2117.1988.tb00011.x

Tsankov, Ts., D. Angelova, R. Nakov, B. C. Burchfiel, L. Royden. 1996. The Sub-Balkan graben system of central Bulgaria. *Basin Research, 8*, 125-142.

Vangelov D, I. Gerdzhikov, K. Bonev, S. Nikolov, 2010. Preliminary data of the Karlovo Basin formation and evolution. *Ann. Sofia University*, 102, 1, 71-106. (in Bulgarian)

Woodcock, N., K. Mort, 2008. Classification of fault breccias and related fault rocks. Geological Magazine, 145(3), 435-440.

This article was reviewed by Prof. DSc. Dimitar Sinyovski and Assoc. Prof. Dr. Ivan Dimitrov.

DEFORMATION PROPERTIES OF THE PLIOCENE CLAYS FROM THE SOFIA BASIN

Stefcho Stoynev[1], Antonio Lakov[1]

[1]University of Mining and Geology "St. Ivan Rilski", Sofia 1700; stoynev@mail.bg

ABSTRACT. The intensive construction works during the recent years are related to deeper foundation works. These require more precise determination of the strength and strain parameters of the mottled and bluish-green clays of Pliocene sediments from the Sofia basin. The article discusses the deformation parameters of the Pliocene clays and sands from the site of the 200 m high 'Capital Fort' building in Sofia obtained from laboratory and elastimeter field tests. Their comparison revealed that the elastimetric deformation modules are much higher than the oedometric modules used as a common practice. Their application in the design will allow a considerable improvement in the foundation of the buildings and structures.

Keywords: Pliocene clays, elastimetric test, oedometric test, modules, comparison

ДЕФОРМАЦИОННИ СВОЙСТВА НА ПЛИОЦЕНСКИТЕ ГЛИНИ ОТ СОФИЙСКИЯ БАСЕЙН

Стефчо Стойнев[1], Антонио Лаков[1]

[1]Минно-геоложки университет "Св. Иван Рилски", София 1700; stoynev@mail.bg

РЕЗЮМЕ. Интензивното строителство на високи сгради в София през последните години налага все по-дълбоко фундиране. Това изисква и по-точно определяне на якостно-деформационните свойства пъстрите и синьозелените глини и пясъци, изградащи плиоценските отложения на Софийския басейн. В статията са разгледани деформационните свойства на плиоценските глини и пясъци за територията на площадката на 200 m високата сграда „Капитал форт" в гр. София, определени чрез лабораторни и пресиометрични полеви изследвания. Направеният сравнителен анализ, показва, че еластиметричните деформационни модули на плиоценските материали са значително по-високи от използваните в инженерната практика компресионни модули. Тяхното използване позволява значително оптимизиране на проектите за фундиране на сградите и съоръженията.

Ключови думи: плиоценски глини, еластиметричен опит, компресионен опит, модули, сравнение

Introduction

It is a long-term practice in Bulgaria to derive the soil deformation modules from laboratory oedometric tests while pressure-meter tests and their variation of elastimetric tests were rarely conducted due to their specific equipment and high price the tests. The national Ordnance № 1 (1996) allowed the deformation module of the massif to be obtained by multiplication of the tangent oedometric module for 0.2 MPa load by a factor from 2 (normally used as safe value) to 5 (practically not applied). Higher factors are accepted after comparative justification but that was rarely practiced. The purpose of this study is to make a comparative analysis of the deformation modules of the Pliocene clays and sands obtained from laboratory and elastimeter field tests from the site of the 200 m high 'Capital Fort' building in Sofia that is currently under construction.

The site is located on the south-east outskirts of the town next to 'Tsarigradsko shosse' Boulevard (Fig. 1). The building will be 200 m high including 4 underground levels buried at 14-15 m depth. The seismic structural design requires a raft foundation on 35 m long piles with 180 cm diameter. As previous experience for depth up to 30-35 m was available for the adjacent existing 120 m high building, additional drilling of 3 boreholes with a length of 80 m and 1 borehole 101 m deep

Fig. 1. Location of the studied site (Google Earth)

was completed. The boreholes were used for establishing the geological structure at a greater depth, for sampling for new laboratory tests, for carrying out SPT's and elastimeter tests in the boreholes, as well as for seismic sounding in the deepest borehole.

Geological structure of the site

The area is located in the southeast periphery of the Sofia Pliocene graben-type basin. The basis of the graben is built up mainly by intrusive rocks forming irregular step-like denivelated blocks. In the graben, a sedimentary basin of the Crimean type

was formed, which was gradually filled up by lacustrine sediments in the center part and mixed with alluvial materials in the peripheral areas. The total thickness of the Pliocene complex ranges from 250 to 500 m. They form the Pliocene clay-sandy formation (the so called 'Lozenets Series') including two lithological complexes that have been established in its upper section:

The lower (gray-green) complex is built up by irregular alternation from thick hard clays, sandy clays, clayey sands, and well-graded sands. The upper (yellow-brown) complex includes a series of alternating mottled clays, sandy clays, sands, and gravels.

The Pliocene materials are covered with Quaternary deposits presented mainly by dark brown to gray-black deluvial silty clays and gravel with sandy-clayey filling. The site is covered by an artificial embankment with limited thickness.

Based on the drilling and the laboratory data, the following layers (geotechnical soil types) were distinguished on the site:

- Layer 1 – Artificial embankment;
- Layer 2 – Buried top soil;
- Layer 3 – Deluvial brown clayey silt (clSi) and silty clay (siCl) to sandy (sa) - Quaternary;
- Layer 4 – Well-graded medium (MGr) to fine (FGr) gravel with sandy silty (sasi), silty sandy (sisa) filling - Quaternary;
- Layer 5 – Mottled clayey silt (clSi), sandy silt (saSi), hard – Pliocene;
- Layer 6 – Fine silty to clayey sand (siFSa and clFSa), medium dense to dense – Pliocene;
- Layer 7 – Medium silty (sMFSa), dense to very dense – Pliocene.

The Pliocene layers occur at a depth from 10 m as an alternation from 1-2 m up to 4-5 m thick intervals of the main layers but frequently they are interlayered by the others. As Layer 6 usually occurs only as separate comparatively thin intervals within Layers 5 and 7, its deformation properties will not be considered separately.

Oedomertic tests

The laboratory oedometric tests were carried out according to the requirements of CD CEN ISO/ 17892-5:2007 at load increments of 5, 12, 25, 50, 100, 200, 400 and 800 kPa and 24 hour consolidation for each of them. For the purposes of the software design of the piled foundation, the pre-consolidation pressures and the compression coefficient values were not considered. The oedometric modules were calculated as secant to the compression curve within the loading intervals and were referred to the mid-point stress values. In total, 9 tests were carried out for Layer 5 and 5 tests for Layer 7. The obtained oedometric modules (E_{oed}) – average, minimum and maximum values - are presented in Table 1.

Table 1.
Oedometric test modules for Layers 5 and 7.

Mean load increments values, MPa	Oedometric modules E_{oed}, MPa					
	Layer 5 (9 tests)			Layer 7 (5 tests)		
	Ave.	Min.	Max.	Ave.	Min.	Max.
0.075	2.63	0.71	5.52	2.63	0.71	2.63
0.15	2.77	1.06	5.30	2.77	1.06	2.77
0.30	3.37	1.56	5.94	3.37	1.56	3.37
0.60	4.67	2.454	8.00	4.67	2.45	4.67

The average scatter of the minimum and maximum values from the average ones are (-1.4).SD and (+2.0).SD for Layer 5 and (-1.15).SD and (+1.5).SD for Layer 7 respectively (SD is the standard deviation). The broader range of variation of the eodometric modules for Layer 5, though more samples were tested from it, is explained with the higher variations in its grain-size distribution.

Elastimetric tests

The elastimetric tests were carried out with the OYO-Elastimeter-100 model 4141 device with a logger for direct measurement of the radial deformations and a manual pressure pump unit (Fig. 2).

Fig. 2. OYO-Elastimeter-100 model 4141 device

The device is compatible to the requirements of ASTM D4719-07. A probe with a length of 60 cm and stiffness of 5 MPa was used. Prior to the site tests, initial calibration of the device was carried out in thick-walled steel tubes and proper corrections were input in the logger. The pre-boring procedures included casing of the borehole to 1.5 m above the test level with an external diameter of 112 mm. Pre-drilling 1,5 times the test interval with a 76 mm rotary core barrel. The probe was installed in the middle of the test interval and initial pressure was applied. After achieving good contact with the borehole wall, the test was carried out with 0.1 MPa pressure increments applied for a period of 2 min. The readings of the radial displacements were electronically logged and processed according to the device specifications. A test curve 'radial deformation R' vs 'Pressure p' was plotted and its linear section was identified. Typical test curve from the site in presented in Figure 3.

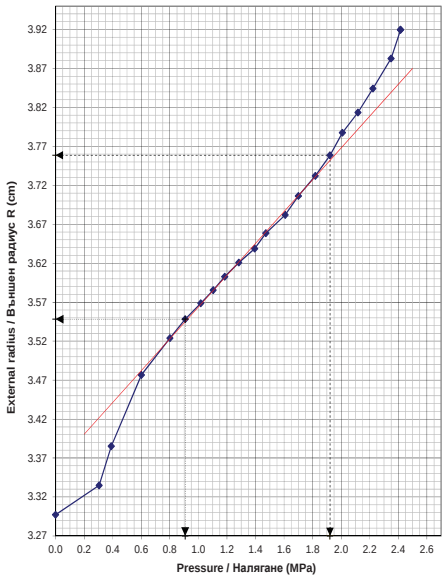

Fig. 3. Elastimeter test curve

Table 2.
Elastimetric modules for Layers 5 and 7

Layer 5				
Borehole	Test no.	Depth, m	(0÷Δp)/2, MPa	E_{el}, MPa
MC-7a	1	17.70	0.51	22.89
MC-7a	3	30.70	0.98	102.3
MC-8a	1	16.20	0.58	15.3
MC-8a	2	20.70	0.90	46.3
MC-9a	1	15.80	0.95	27.2
		Average		42.8
		Min.		15.3
		Max.		102.3
		N		5
		SD		31.48
		t_α		2.57
		E_{el}k (lower)		6.6
		E_{el}k (upper)		79.0
Layer 7				
Borehole	Test no.	Depth, m	(0÷Δp)/2, MPa	E_{el}, MPa
7a	2	21.80	0.57	89.07
7a	4	37.40	0.55	116.74
7a	5	52.60	1.30	108.89
7a	6	65.60	1.39	97.52
8a	3	31.40	0.70	66.68
8a	4	48.50	0.88	59.33
8a*	5	70.50	1.19	69.45
9a	2	20.40	0.51	29.36
9a	3	26.10	1.05	46.63
9a	4	34.00	0.55	75.46
9a	5	52.40	1.31	74.88
9a	6	68.10	1.01	58.32
		Average		74.4
		Min.		29.4
		Max.		116.7
		N		12
		SD		24.33
		t_α		2.18
		E_{el}k (lower)		59.1
		E_{el}k (upper)		89.7

The deformation modulus value E_{el} is calculated as:

$$E_{el} = (1+\mu).R_m.(\Delta p/\Delta R),$$

where: $\Delta p/\Delta R$ is the slope of the linear section; R_m is the mean radius of the probe for the center of the linear section; μ is the Poisson's coefficient assumed to be 0.3.

In total, 5 elastimetric tests were conducted in Layer 5 and 12 tests in Layer 7. The values for the deformation modules are presented in Table 2. The table includes the middle point of the stress ranges of linear deformation $(0\div\Delta p)/2$ as well.

Some basic statistics are added to the table in order to determine the lower and upper characteristic values of the deformation modules for 95% two-sided confidence level. According to Eurocode EN 1990, the characteristic values of the elasimetric modules are determined as follows:

$$E_{elK} = E_{ave} \pm k \times SD$$

where SD is the standard deviation value and 'k' is a coefficient, determined by the following formula:

$$k = t_\alpha \times \sqrt{\frac{1}{N}}$$

where N is the count of the values.

Comparison between oedometric and elastimetric modules

The average oedometric modules and the elastimetric modules for each layer are plotted towards the mean stress values of the secant and linear portions of the stress-strain test curves respectively (Fig. 4a and b). Simple linear trend lines are added to the oedometric values to illustrate the trends of E_{oed} increase with the vertical load increments.

The test results show clearly that the oedometric modules are with much lower values than the elastimetric ones. The lowest ratios E_{el}/E_{eod} for the maximum oedometric vs minimum elastimetric values are at least in the orders of 3 times for Layer 5 and 6 times for Layer 7 but the highest ratios exceed 20-24 times. A certain decrease of this ratio may be expected for oedometric modules derived for test stress levels higher than 0.8 MPa (to 1.6 MP and 3.2 MPa) that may approach the minimum elastimetric modules values, but for the average ones the ratio will be still at least 3-5 times. Further, we should mention that the elastimentric modules characterize a real linear behaviour of the soil base that, in the case of vertical foundation loading, may be considered as 'quazi-elastic' which allows the application of the elastic theory in the foundation design.

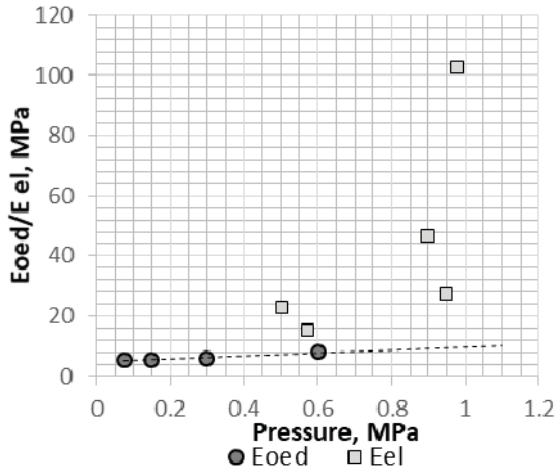

(a) For Layer 5

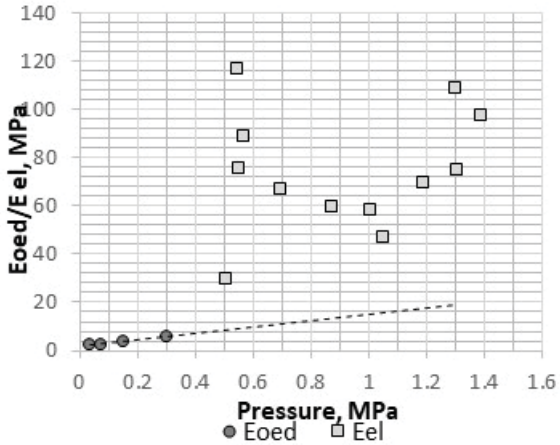

(b) For Layer 7

Fig. 4. Plots with oedometric modules (E_{oed}) and elastimetric modules (E_{el}) vs mean pressures for Layer 5 (a) and Layer 7 (b)

These differences can be explained by several scale effect factors:

- much faster and complete one-dimensional consolidation of the oedometric specimen due to its minor thickness (filtration path) and much pressure-effective gradients (above 300) that practically overpass the soil's initial gradient ($I_{crit.}$);
- complex partial 3-dimentional radial consolidation around the borehole wall with pressure gradients that decrease in radial direction even beyond the critical one and a practically 'infinite' flow path.
- the laboratory test specimen is usually affected by different manipulations related to drilling, sampling, transportation and cutting in the test ring that result in less intactness and lower stiffness relative to its size that the borehole walls and the soil base itself.

Conclusions

The elastimetric tests produce a stress-strain stress in the soils much more adequate to its behaviour as foundation base. The elastimetric modules for the Pliocene sediments from the studied site are much higher compared to the oedometric modules. For high vertical loads (0.5-0.6 MPa and more), the ratio factor is at least 3-5. For lower vertical loads, the oedometric modules should be factored at least by values of 5 to 10. These factors may be applied in general to the oedometric modules for the Pliocenie clays and sands on other sites in the town of Sofia that will allow significant improvement of the foundation design.

References

ASTM D4719-07. Standard Test Methods for Prebored Pressuremeter Testing in Soils.

CD CEN ISO / 17892-5:2007 Geotechnical investigation and testing - Laboratory testing of soil - Part 5: Incremental loading oedometer test.

EN 1990:2002 Eurocode - Basis of structural design.

The article is reviewed by Prof. Stefan Dimovski, DSc. and Assoc. Prof. Dr. Nikolay Stoyanov.

GEODYNAMIC CONDITIONS OF THE LANDSLIDE AT THE VILLAGE OF SIPEY, KARDZHALI MUNICIPALITY

Antonio Lakov[1], Stefcho Stoynev[1]

[1]University of Mining and Geology "St. Ivan Rilski", 1700 Sofia; tony_ lakov@abv.bg

ABSTRACT. The geomorphology and the geological structure of Eastern Rhodopes contribute to the development of landslide processes. Most frequently they are related to the extended areas built up by tuffs and bentonite clays. On the territory of Kardzhali municipality only, more than 30 landslides have been registered. In the spring of 2015, due to the intensive rainfall and snow melting, 8 new landslides were triggered. The landslide in the village of Sipey is one of the largest in the region – with an area of about 20 dka. Its activation resulted in the complete destruction of living houses, roads, water electricity supply lines. The landslide is developed in the tuffs that build up the geological section in the region. The article analyses the actual geodynamic conditions of the landslide, its mechanism and development, and the triggering factors. Based on the results from the stability calculations, landslide forces are obtained and recommendations for reinforcement are made.

Keywords: landslides, stability, reinforcement

ГЕОДИНАМИЧНИ УСЛОВИЯ НА СВЛАЧИЩЕТО В СЕЛО СИПЕЙ, ОБЩИНА КЪРДЖАЛИ

Антонио Лаков[1], Стефчо Стойнев[1]

[1]Минно-геоложки университет "Св. Иван Рилски", 1700 София; tony_ lakov@abv.bg

РЕЗЮМЕ. Геоморфологията и геоложкият строеж на Източните Родопи благоприятстват развитието на свлачищни процеси. Най-често те са привързани към разпространението на туфите и бентонитовите глини, които изграждат геоложкия разрез на значителни територии. Само на територията на община Кърджали са регистрирани повече от 30 броя свлачища, а в резултат на интензивните валежи и снеготопенето през пролетта на 2015 година се активизираха 8 броя свлачищни циркуса. Свлачището в село Сипей е едно от най-голямите по обхват свлачища в района – около 20 dka. В резултат от активизацията на свлачищните процеси са напълно разрушени жилищни сгради, пътната и ВиК инфраструктура и е прекъснато ел. захранване. Свлачищните процеси са свързани с разпространението на туфите и туфобрекчите, които изграждат геоложкия разрез в района. В статията е направен анализ на съвременното геодинамично състояние на свлачището, механизма и динамиката на развитие на свлачищните процеси и причините, които са обусловили развитието им. Въз основа на резултатите от стабилитетните изчисления са направени препоръки за укрепване и са оразмерени противосвлачищните съоръжения.

Ключови думи: свлачища, устойчивост, укрепване

Introduction

The area of the Eastern Rhodope is affected by numerous landslides, associated with the highly dismembered relief and the wide affiliation of the tuffs and bentonite clays in the geological section. On the territory of Kardzhali municipality only, more than 30 landslides have been registered. In the spring of 2015, due to the intensive rainfall and snow melting, 8 new landslides were triggered. The landslide in the village of Sipey is one of the largest in the region – with an area of about 20 dka (Fig.1). The first signs of landslide processes in this area were detected in 2014. Subsequently, their range significantly expanded. The landslide processes resulted in the destruction of a section of about 150 meters from "Georgi Popmarinov" Str. (one of the inletting streets in the village), water supply and sewage facilities, high electricity network poles, and four living houses. The landslide processes are currently active and their future development can affect more living houses and widen the destroyed part of the road.

Geomorphological characteristics and geological structure

The village of Sipey is located north-east from the town of Kardzhali. The relief is of low-mountain to hilly type. It is part of the Eastern Rhodope massif. The altitude is between 300 and 325 m. The Paleogene terrigenous and volcanic sediments which fill up the Eastern Rhodope Paleogene depression form smooth relief forms. Only the lava flows keep a sharper relief, forming protruding hills or plates. The gullies and rivers are mainly erosional, with V-shaped valley profiles. The village of Sipey is located at the top of the right valley slope of the Arda River, just below the ridge of its watershed.

In a geological and structural aspect, the region refers to the Eastern Rhodope Paleogene depression. Its filling includes two rock complexes. Continental sediments (calcareous-sandstone complex) and marine sediments (marl-limestone complex) are specific for the lower complex. It refers to the late Eocene.The second complex is represented by the alternation of medium acidic and acidic volcanites, with reef limestone bands and

large sandstone bodies (eg. the Dzhebel complex). A triple alternation of medium acidic (andesite) and acidic (rhyolite) complexes is observed in the entire section of this complex. The thickness of the Paleogene deposits is over 2000 m.

The geological section of the landslide is built up of the second Medium acidic volcanic complex, which is lithologically represented by medium-acid tuffs and a reef limestone series. Bentonite clay bands can be found as a result of hydrothermal meta-somatic processes. These are well extended, with a thickness from a few centimeters up to more than 15 m. The bentonites are white to light-colored.

The Quaternary cover is represented by deluvial and deluvial-elluvial silty and silty-sandy clays with a thickness of up to 4.0 - 5.0 m.

Hydrogeological conditions

The groundwater is bound to the tuff horizons. They are hydraulically connected in a single aquifer. Due to the different weathering degree of the tuffs and the presence of bentonite clay interlayers, it is with a rather complex regime. At the upper part of the landslide, the groundwater levels occur at a depth of 12.6-14.5 m getting to 3.5 m down the slope. At the road zone, their depth is from 4.20 to 8.60 m. The aquifer is slightly pressurized (from 0.5 m to 5.3 m) due to the different permeability of tuffs with different weathering degrees, as well as due to the presence of bentonite interlayers that act as local aquitards. The permeability coefficient of the aquifer varies between 0.1 m/d and 2.0 m/d. The average permeability coefficient of the bentonite clays is $0{,}30.10^{-6}$ m/d. In wet seasons, the water levels rise significantly and reach the terrain surface of the negative relief forms. During the study of the landslide in February 2015 (when the slide was activated), the water levels reached the surface of the two wells located in the area.

Landslide description

The landslide has affected terrains with an area of about 20 dka in the western part of the village of Sipey. The first signs of landslide processes in this area were detected in the end of 2014. Subsequently, their range widened significantly. The areas affected by the landslide processes are characterized by an undulating relief, clearly marked main landslide scarps with a height of 1.5-2.5 m, toe elevation, numerous inside scarps, and open cracks. The electric poles within its range were inclined and the living houses located were with serious constructive damages that made them uninhabitable. The landslide processes are in an active stage of development. There is an actual danger that they will increase their area (observed in the summer months of 2015), which will lead to the destruction of more living houses and infrastructural facilities in the area, and an increase of the range of the destroyed part of the road. The landslide is developed in highly weathered tuffs and the sliding surface is located along the contact with the base from bentonite clays. It has a linear shape, with an average inclination of about 11° and at depth between 4.50 and 6.50 meters from the surface. The landslide itself has a circular contour.

It is triggered mainly by the massive saturation of the clays from the weathering crust of the Paleogene tuffs due to the heavy rainfall in the area by the end of 2014 and the beginning of 2015. As a result, groundwater level reached the terrain surface in the negative relief forms leading to a considerable decrease of strength properties. The uncontrolled water leakage from the artificial water basin located in the north part above the landslide had an additional unfavorable influence over the stability of the terrains in the area. Household water was discharged in the low relief parts, due to the lack of sewerage network, and also contributed for the saturation of the landslide materials.

Engineering geological characteristics

The following layers (engineering soil types) are divided in the geological section (Fig. 2):

- *Layer 1* – Gravel embankment (crusted stone). It was executed during the building of the road and has limited area distribution. Its width varies between 1.0 and 1.30 meters.
- *Layer 1b* – Clay, grey-black, organic. The clay builds the top part of the natural Quaternary covering. Its average thickness is 1.20 – 1.50 meters.
- *Layer 2* – Highly weathered tuffs, yellow-green to rusty, silty to silty-sandy with gravel. The layer builds up the top level of the Oligocene tuff and materials. The weathering processes have changed the tuffs to clays and gravely clays. Their thickness varies from 7.0–9.0 m in the top part of the landslide to 3.0 – 5.0 m in its lower part. The layer is subjected to the landslide processes and the sliding surface is developed in its base.
- *Layer 3* – Bentonite clay, grey-green to beige, hard. The clays occur as continuous interlayers in the tuffs with thickness from 5.5–9.0 m down slope to 8.0–15.0 m in the middle and top parts of the slope. The clays are fissured and crushed in some areas. The strong sensitivity during the interaction with water is typical for the bentonite clays. They swell significantly and their strength properties present a thixotropic behaviour.
- *Layer 4* – Tuffs, weathered. They build the weathering crust of the second horizon of tuffs under the bentonite clays at a depth from 8.0–9.0 m in the toe and middle part of the landslide up to 12,0–15,0 m in its top part. The layer thickness is 0.5–2.0 m. The tuffs and tufts are highly weathered to hard gravely clays and to gravel with clayey-sandy filling.
- *Layer 5* – Tuffs, slightly weathered gray. They build the basic part of the geological section. The tuffs are slightly weathered, irregularly interlayered by thin clay bands (up to 0.10 m thick). They are sensitive to interaction with water up to complete disintegration.

The soil type geotechnical properties are shown in Table 1.

Landslide stability assessment

According to the characteristics of the landslide, the model of sliding along parallel to the terrain sliding surface was adopted (as in Naredba № 12, or Ordnance№ 12), but taking into account the active earth pressure in the top part of the landslide. The general stability scheme is given in Figure 3.

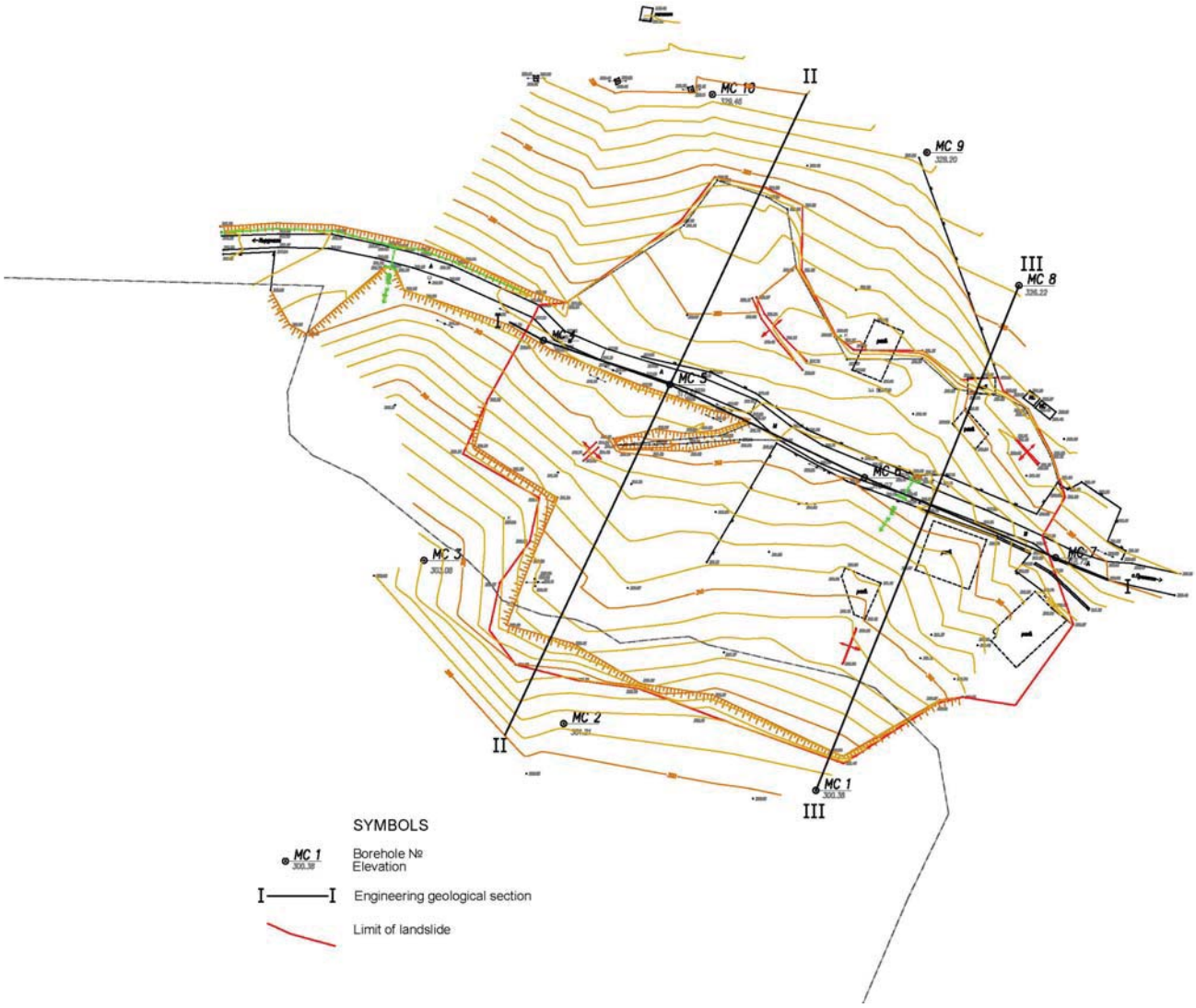

Fig. 1. Terrain situation with landslide boundaries and exploratory work location

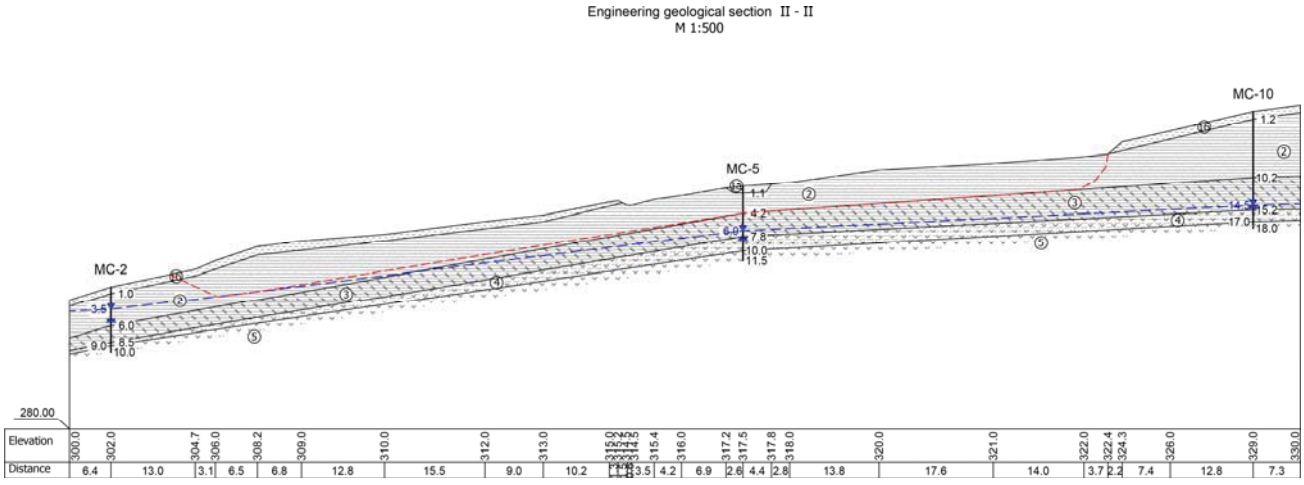

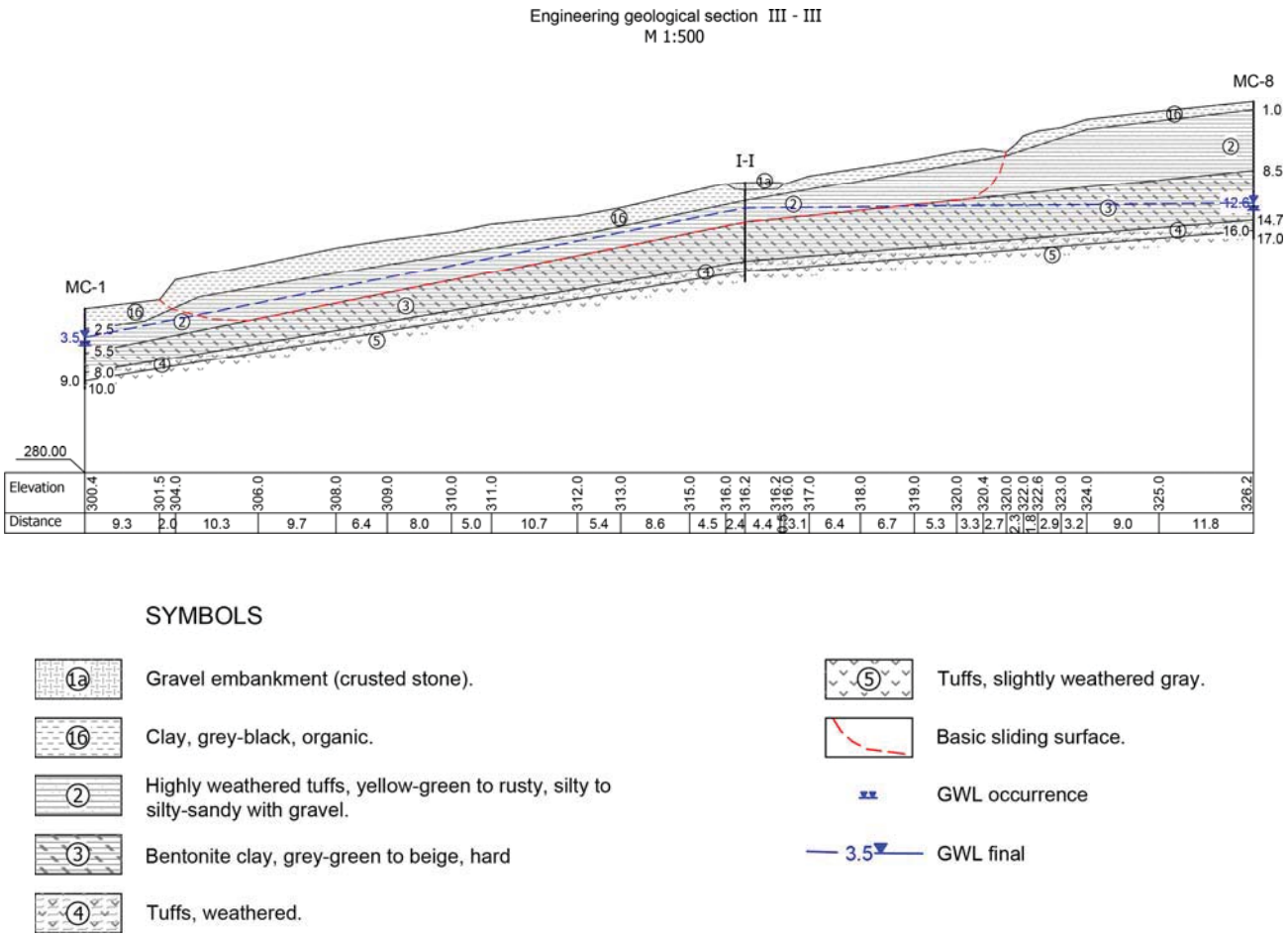

Fig. 2. Engineering geological sections. (The layer indices are given below)

Table 1.
Geotechnical properties of the soil types

SOIL PARAMETERS		Layers №					
		1	1б	2	3	4	5
Bulk density	ρ_n, g/cm^3	1.90	1.69	1.70	1.62	1.64	210
Plasticity index	Ip, %	-	-	22.0	54.3	19.4	-
Consistency index	Ic	-	-	0.65	0.87	1.04	-
Peak shear strength (characteristics)							
Angle of internal friction	ϕ_k, °	-	-	14.2	13	18	23
Cohesion κPa	C_k, kPa	-	-	25.1	25.8	37.9	49.6
Residual shear strength (characteristics)							
Angle of internal friction	ϕ_k, °	-	-	12.0	12.0	-	-
Cohesion κPa	C_k, kPa	-	-	16.1	19.3	-	-

Remark: The characteristic values of the friction angle and the cohesion are obtained through statistical processing of the results from plane shear tests in aTaylor type apparatus in a consolidated-drained state.

For profiles II-II and III-III with lengths of 100 m and 145 m, an average depth of the sliding surface of 5.5 m and average slope of about 11 degrees were estimated.

Since the landslide surface is attached to the base of layer 2, the corresponding average density values γ=17.0 kN/m^3 and the characteristic values of the residual shear strength are used in the stability calculations. The maximum water saturation of the massif ($h=h_w$) is considered.

The calculated safety factors for both profiles are F=1.55 and F=1.30, respectively. These values do not correspond to the actual active state of the landslide. Back calculations are made in order to establish a more realistic value for the cohesion, corresponding to a safety factor of F=1.00. The obtained values for both profiles are respectively C = 12.2 kPa for F=0.997 (along profile II-II) and C = 12.0 kPa for F=1.003 (along profile III-III), the lower is considered to be characteristic for the landslide.

The slope stability defined by the above mentioned shear parameters, without the presence of groundwater, results in safety factors of F=1.48 and F=1.51, respectively. This shows that the groundwater is the basic factor for triggering the landslide processes. So, for a major approach for its stabilization, we should consider the construction of a trench fishbone drainage system inside the landslide body. Considering the fact that the excavation works will be carried out in an active landslide, it is technologically appropriate for the depth of the trenches to be limited to 3.0 m. Assuming a curvilinear depression line between the drainage members, the average design decrease of the groundwater level in the slope is estimated to be 2.5 m from the surface corresponding in the calculations to h_w = 3.0 m.

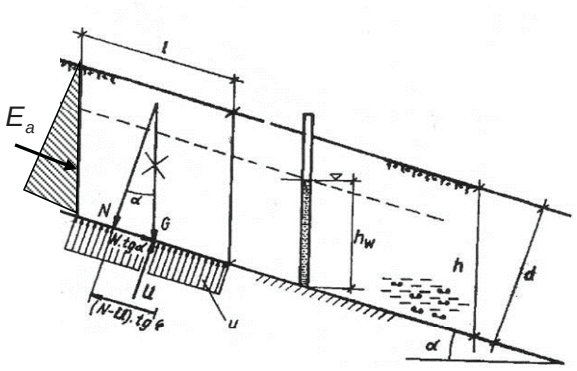

Fig. 3. General calculation scheme for parallel sliding

$$F = \frac{(1 - r_u)\gamma . h . \cos^2 \alpha . tg\,\phi . l + c . l}{\gamma . h . \sin \alpha . \cos^2 \alpha . l + E_a}$$

където :

$$r_u = \frac{\gamma_w h_w}{\gamma_n h};$$

$$E_a = \frac{\gamma . h^2}{2} K_a ; K_a = \frac{\cos^2 \alpha}{\left[\cos^2 \alpha + \cos(\varphi + \alpha)\cos(\varphi - \alpha)\right]}$$

The design stability calculations were performed according to the requirements of Eurocode 7 and National Annex EN 1997-1: 2005 / NA Amendment 1. DA3 design approach is applied using a partial resistance coefficient γR = 1.0. For a basic load combination in accordance with the National Annex EN 1997-1 / NA, the following partial factors to the soil parameters are applied – $\gamma\gamma$ = 1.0, $\gamma\varphi$ = 1.25, and γC = 1.25.

The obtained results for the stability factors for profile II-II and profile III-III are F=0.975 and F=0.992, respectively. These values are close to but still lower than the limit value for F=1.00 and they show that the slopes in both sections are still unstable under the specified conditions.

Since the main purpose of the landslide stabilization is to restore the road and limit the development of the landslide process, it was accepted to construct an anchored pile wall located at the up-slope side shoulder of the road.

The necessary anti-landslide forces R along the two profiles are determined through back calculations to achieve a minimum safety factor of F=1.00. For lengths of the landslide blocks above the line of the support structure 37.0 m and 62.0 m, the obtained values are R = 116 kN/m and R = 94 kN/m.

Calculations for earthquake conditions are performed in a serviceability state with partial factors on the soil parameters $\gamma\gamma$ = $\gamma\varphi$ = γC = 1.0. The seismic coefficient for the stability calculations is obtained by the formula:

$$K_C = 0{,}5 . aR . \gamma I . S = 0{,}5 . 0{,}11 . 1{,}0 . 1{,}2 = 0{,}066,$$

where: aR is the reference seismic acceleration for the region, according to the National seismic zoning; γI is the coefficient of significance, equal to 1.0; S is the amplification coefficient that, according to Eurocode 8 and National Annex EN 1998-1 / NA1 for the established Soil Ground C, is S=1.2.

For these conditions, the obtained values of the anti-landslide force for profile II-II is R=167 kN/m, and for profile III-III it is R=184 kN/m. As far as they are higher than the determined for a basic load combination, the maximum value R=184 kN/m is accepted as a design value for the whole landslide.

Conclusions

The analysis of the slope stability conditions in the studied area, including the road section passing through and the results from the landslide stability calculations, shows that it must be stabilized. In particular, the stability of the road and the limiting of the landslide development towards the buildings in the eastern boundary of the landslide should be assured. Based on the established engineering-geological conditions and the stability calculations, the following are recommended as most efficient anti-sliding measures:

- Construction of a 3 m deep buried trench fish bone drainage system inside the landslide body;
- Construction of a reinforcement anchored pile wall along the up-slope side road shoulder. It should be designed to counteract a force of 184 KN/m. The wall will ensure the

protection of the road, and limit the development of the down-slope landslide process;

- Construction of an overloading embankment from coarse-grained aggregates just above the pile wall with a height of 1.5 m in order to prevent the danger of the landslide overflowing over the wall;
- Repairing the water basin in the area above the landslide to stop water leakage in the landslide body;
- Inspection of the sewers of the living houses in the area and eliminating their discharge into the landslide body;
- Construction of a ditch with bottom drainage along the road and leading the surface waters outside the landslide area;
- Restoring of the drain-pipe in the eastern part of the landslide;
- Performing a vertical planning for grouting the opened cracks and regenerating a gentle surface slope that will allow the quick down-slope flow of the surface waters.

References

Наредба № 12 за проектиране на геозащитни строежи, сгради и съоръжения в свлачищни райони, 2001. (Naredba No 12 za proektirane na geozashtitni stroezhi, sgradi i saorazheniya v svlachishtni rayoni, 2001.)

Eurocode 7 - Geotechnical design - Part 1: General rules - National annex to BDS EN 1997-1:2005

Eurocode 8: Design of structures for earthquake resistance. National annex EN 1998-1/NA. March 2012.

The article is reviewed by Prof. Stefan Dimovski, DSc. and Prof. Dr. Radoslav Varbanov.

MERCURY BIOMONITORING WITH MOSS FROM THE ALMADÉN MINING DISTRICT, SOUTH CENTRAL SPAIN

Iva Miteva[1], Pablo Higueras[2] and Jose Maria Esbri[3]

[1] University of Mining and Geology "St. Ivan Rilski", 1700 Sofia, Bulgaria, e-mail: iva.i.miteva@gmail.com
[2] Universidad de Castilla-La Mancha, Plaza M. Meca 1, 13400 Almadén, Spain, E-mail: Pablo.Higueras@uclm.es
[3] Universidad de Castilla-La Mancha, Plaza M. Meca 1, 13400 Almadén, Spain, E-mail: JoseMaria.Esbri@uclm.es

ABSTRACT: The migration of chemical elements in the environment is inevitable. Therefore, the elements that can cause damage to human health must constantly be observed. Mercury is one of the elements whose toxicity imposes persistent monitoring. For this reason, there are a couple of active and passive monitoring methods to observe its behavior. Like other vegetation, mosses accumulate mercury in their structure which is related to the concentration of this element in the air. Mosses are highly valued for observation purposes in Almadén. The town is famous for the largest mercury deposit in the world and thus requires constant monitoring.

Keywords: mercury, mosses, biomonitoring, Almadén, thermal speciation.

БИОМОНИТОРИНГ НА ЖИВАК С МЪХОВЕ ОТ МИННИЯ РАЙОН НА АЛМАДЕН, ЮЖНАТА ЧАСТ НА ЦЕНТРАЛНА ИСПАНИЯ

Ива Митева[1], Пабло Игерас[2] и Хосе Мария Есбри[3]
[1] Минно-геоложки университет "Св. Иван Рилски", 1700 София, E-mail: iva.i.miteva@gmail.com
[2] Университет де Кастиля-Ла Манча, Плаза М. Мека 1, 13400 Алмаден, Испания, E-mail: Pablo.Higueras@uclm.es
[3] Университет де Кастиля-Ла Манча, Плаза М. Мека 1, 13400 Алмаден, Испания, E-mail: JoseMaria.Esbri@uclm.es

РЕЗЮМЕ. Миграцията на химическите елементи в околната среда е неизбежна. Следователно тези елементи, които могат да застрашат човешкото здраве, трябва да бъдат следени постоянно. Живакът е един от тези елементи, чиято токсичност налага непрестанен мониторинг. Поради тази причина има няколко активни и пасивни методи за мониторинг, с които да се следи поведението на токсичните елементи. Подобно на друга растителност, мъховете приемат живак от въздуха и го натрупват в своята структура. Концентрацията на живак във въздуха е свързана със съдържанието му в мъховете. Тяхната полза е високо ценена за наблюдение на Алмаден – най-голямото живачно находище в света.

Ключови думи: живак, мъхове, биомониторинг, Алмаден, термично сортиране.

Introduction

Mosses are highly adaptable and widespread in nature. They have the ability to uptake airborne heavy metals and POPs from the atmosphere which makes them highly valued for passive biomonitoring (Bargagli, 2016). Atmospheric mercury is in a dynamic equilibrium with moss tissues, reflecting variations of total gaseous mercury in their concentrations on mosses tissues (Boquete et al., 2013). There are a great number of studies applying this capacity of mosses to biomonitor atmospheric mercury, not only mercury dispersion patterns around mercury mining sites (Huckabee et al., 1983; Plouffe et al., 2004; Qiu et al., 2005; Ping et al. 2008) or industrial areas (Boquete et al., 2013; Varela et al., 2014), but also on a larger scale to an entire country like Norway (Steinnes et al., 2003) or on a still larger scale to a whole continent like Europe (Harmens et al., 2010, 2015). There are protocols to make biomonitoring studies using mosses (Frontasyeva et al., 2014), and a lot of discussions on whether these protocols are adequate and based on scientific criteria or not (Fernandez et al., 2015). Nowadays, biomonitoring atmospheric mercury using mosses is a common issue. One of the most important places requiring constant monitoring on the ambient is the Almadén district area (Esbri et al., 2016). The mercury in the ore body is in the form of cinnabar (HgS). The district is about 300 km^2 with an estimated total content of mercury before mining of around 250 000 t. The mining works in the district began in Roman times, around 2000 years ago, and continued without interruption until 2003. In 2005, the European Union forbade the mining and production of mercury because of its toxicity. Depending on the form and bond related with the other elements, mercury can be extremely poisonous or not so toxic. Nowadays, the mine is reclaimed and has a status of a world heritage site in the list of UNESCO (UNESCO, 2012). It is well-known that mining industry cannot extract all the useful compounds of the ore bodies. Also, the way of extraction of mercury through evaporation and liquefaction emits a huge amount of Hg which is accumulated in the surrounding soils (Higueras et al., 2006). In the atmosphere, 95% of mercury can be found as Hg^0 which is a stable and highly mobile form (Schroeder and Munthe, 1998). The significantly smaller amount is in the water-soluble state which is characterized by low mobility because of its reaction with gaseous compounds, such as $HgCl_2$, HgO. Based on

laboratory experiments, it has been proved that mosses take up Hg^0 rapidly and linearly and that the metal becomes strongly bound with almost no losses for a couple of weeks. The reason for this retention is that the accepted Hg^0 is transformed into water-soluble Hg^{2+}[cita]. Because of the volatile character and mobility of mercury, the area requires constant monitoring to ensure the health of the citizens of the town.

Materials and methods

Sampling network was designed to cover populated areas, the main atmospheric mercury source (Almadén mining center), secondary sources (cinnabar monuments or polluted roads), and local background locations. Figure 1 displays sampling areas, sampling points, and TGM measurement points on the Almadén area.

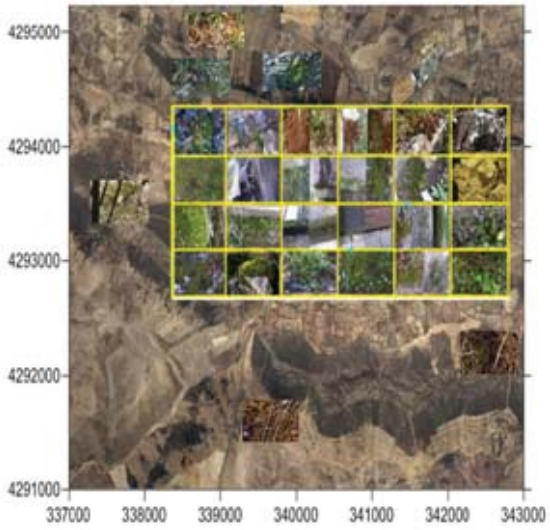

Fig. 1. Sampling network with the sampling moss

In order to acquire realistic information about TGM contents in the atmosphere of Almadén, It was necessary to make air measurements in day and night hours. These measurements were carried out by Atomic Absorption Spectrometry using Lumex R - 915+ equipment that takes 1 TGM data and is able to detect mercury concentrations between 2 ng m^{-3} and 25,000 ng m^{-3}. The seasonal change can strongly affect the survey (Esbri et al., 2016). Spring is the most suitable season for collecting mosses because they are wet and newborn, and TGM has higher contents than in autumn and winter. The mosses for this survey were collected in April of 2017. Mercury accumulation becomes bigger in time. To avoid this, only the youngest and greenest mosses were taken. Samples were collected from each square of the coordinate network plus some extra material to close the anomaly area. Figure 1 represents the place and the species of moss samples. According to Fernandez et al., (2015) there is a difference in atmospheric moss uptake depending on the moss species. For this survey, only the average concentrations are taken.

The samples were temporarily stored in a carton envelope with the help of a chemical spoon and using nitrile gloves. They were brought to the laboratory on the same day. The samples were immediately washed and dried in a laboratory oven at 35ºC for 7 days. The mosses were washed carefully with ultra pure water. The inclusion of ash and soil particles in the moss body may influence the final result. To avoid inaccuracies as much as possible, soil particles were removed carefully. Immediately after washing, samples were put in polypropylene jars and left in the laboratory drying oven until they completely dried. Samples stayed in the oven for one week under the temperature of 35 ^{0}C. This temperature was required because of the volatile character of Hg, to avoid losses of mercury. After this week, samples were sealed with parafilm. To prevent the growth of microorganisms, the samples were put into a fridge at a temperature of below -15ºC. After all these steps, the samples were ready for analyses. The sample had to be homogenized and put into flasks.

The total mercury analysis was achieved by Atomic Absorption Spectrometry, using a Lumex RA-915+ equipment; with its PYRO-915 pyrolysis attachment BCR-62 CRM was analyzed simultaneously to ensure the quality of measurements.

Results

For this survey, 39 moss samples were taken, collected around the whole area and the expected main gaseous mercury source in the eastern part of the town. Table 1 represents the average concentration in each sample. According to Fernandez (2002b), the essential number of samples must not be less than 30. Sample №17 of section C1 is with extremely high concentration of around 800 ppm. The reason for that anomaly level is the cinnabar rock with extremely rich liquid mercury.

The concentration of mercury in the air is different throughout the hours of day and night. This strong variability has influence over the uptake rates in mosses. The influence of weathering conditions, too, affects Hg concentrations. To better understand this variability, the air measurements are taken throughout day and night. The result of them is shown in Figure 3. Red spot №1 is exactly under the mine so that it is expected to be with high concentrations. Two reasons may have influence on the results for red spot №2 – the windrose and the outcrop. There is a polluted road east of the town that is covered with residues from the ore which create the anomaly in №3.

According to the results from the mosses, the mercury pollution is stronger in the first 300 m near the mine. One of the main reasons is the fact that this area is very rich in mercury and a big amount of it is still in the soil. The second reason is the way of extraction through frying of the ore. The results were expected which confirm that the pollution in area is strictly observed and that moss biomonitoring is sensible and in accordance with active monitoring techniques.

Table 1.
Main mercury data of studied sites

Sector	TGM (ng m^{-3})	Sector	TGM (ng m^{-3})
F3	43.5	B2	159.6
F1	46.9	D1	92.0
E1	88.2	D1	112.8
BB	98.5	D2	78.0
F3	0.3	D2	47.4
F4	80.1	E3	63.5
E4	100.5	E3	55.3
AA	93.4	D3	86.5
A3	0	D3	136.7
A4	0	C3	139.7
D4	27.1	C3	145.9
C4	85.1	B3	173.3
B4	91.8	MA 001 Residencial area	55.2
B3	47.3	MA 00 University	47.1
C2	138.2	AA	127.0
C1	227.7	BB	35.8
A1	37.8	BB1	28.6
CASTLE OF VIRGEN	102.6	BB2	6.6
A2	153.8	CC	35.2
B1	180.2		

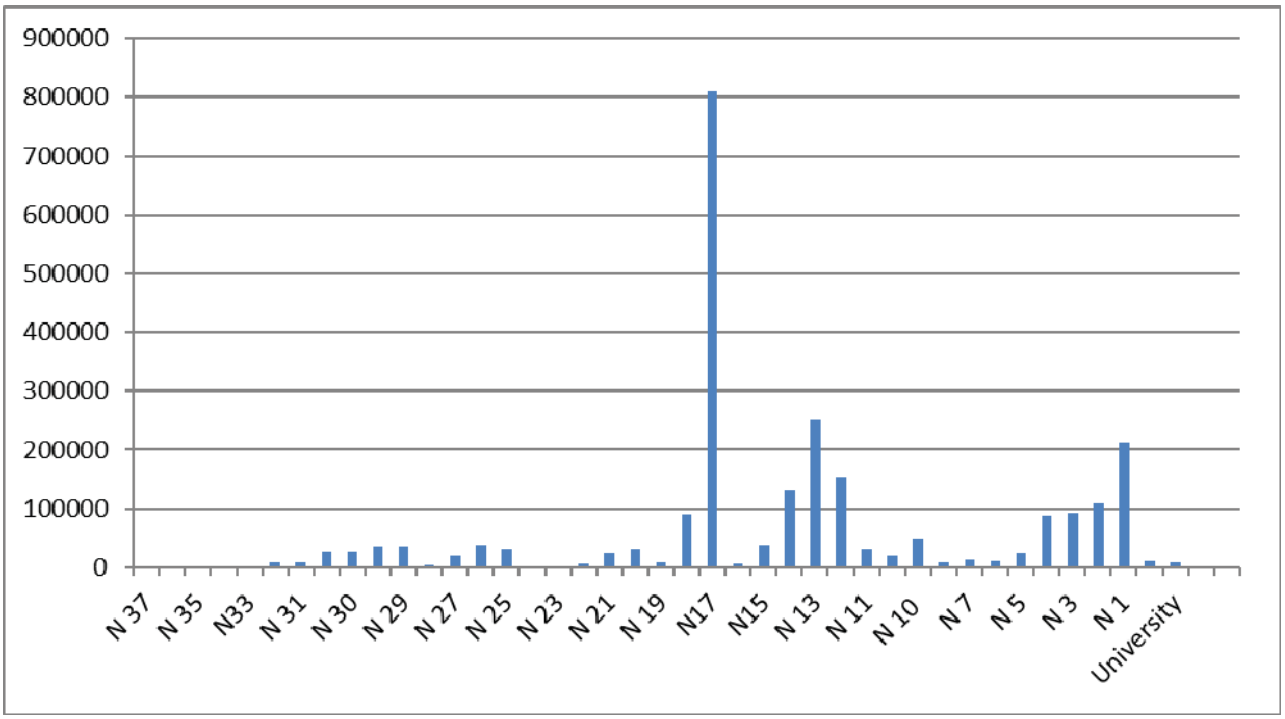

Fig. 2. Average mercury concentration in TGM (ng m^{-3})

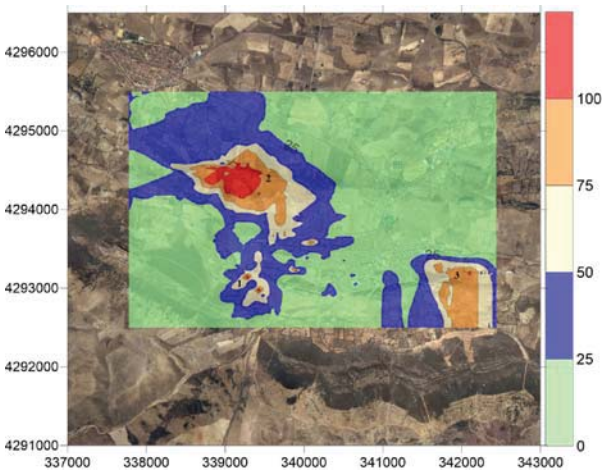

Fig. 3. Total gaseous mercury concentration measured with Lumex R - 915+ equipment

Conclusion

It seems that mosses are more appropriate for monitoring gaseous mercury over a longer period than direct measurements. These organisms provide information of where the main mercury source is and of the preferential dispersion pattern in the studied area.

References

Bargagli, R. Moss and lichen biomonitoring of atmospheric mercury: A review. Science of the Total Environment, 572, 2016. - 216-231.

Boquete, M. T., J. A. Fernández, A. Carballeira, J. R. Aboal. Assessing the tolerance of the terrestrial moss Pseudoscleropodium purum to high levels of atmospheric heavy metals: a reciprocal transplant study. Sci. Total Environ. 461-462, 2013. - 552–559.

Esbrí, J. M., A. Martínez-Coronado & P. L. Higueras. Temporal variations in gaseous elemental mercury concentrations at a contaminated site: Main factors affecting nocturnal maxima in daily cycles. Atmospheric Environment, 125, 2016. - 8-14.

Fernández, J. A., M. T. Boquete, A. Carballeira & J. R. Aboal. A critical review of protocols for moss biomonitoring of atmospheric deposition: Sampling and sample preparation. Science of the Total Environment, 517, 2015. - 132-150.

Frontasyeva, M., H. Harmens. The participants of the ICP Vegetation, 2014. Heavy metals, nitrogen and POPs in European mosses: 2015 survey. Monitoring Manual.

Harmens, H., D. A. Norris, E. Steinnes, E. Kubin, J. Piispanen, R. Alber et al. Mosses as biomonitors of atmospheric heavy metal deposition: spatial patterns and temporal trends in Europe. Environ. Pollut. 158, 2010. - 3144–3156.

Harmens, H., D. A. Norris, K. Sharps, G. Mills, R. Alber, Y. Aleksiayenak, O. Blum et al. Heavy metal and nitrogen concentrations in mosses are declining across Europe whilst some “hotspots” remain in 2010. Environ. Pollut. 200, 2015. - 93–104.

Higueras, P., R. Oyarzun, J. Lillo, J. C. Sánchez-Hernández, J. A. Molina, J. M. Esbrí & S. Lorenzo. The Almadén district (Spain): Anatomy of one of the world's largest Hg-contaminated sites. Science of the Total Environment, 356, 1-3, 2006. - 112-124.

Huckabee, J. W., F. Sanz Diaz, S. A. Janzen, & J. Solomon, Distribution of mercury in vegetation at Almadén, Spain. Environmental Pollution. Series A, Ecological and Biological, 30, 3, 1983. - 211-224.

Ping, Li, X. Feng, , L. Shang, G. Qiu, B. Meng, P. Liang & H. Zhang. Mercury pollution from artisanal mercury mining in Tongren, Guizhou, China. Applied Geochemistry, 23, 8, 2008. - 2055-2064.

Plouffe, A., P. E. Rasmussen, G. E. M. Hall, & P. Pelchat. Mercury and antimony in soils and non-vascular plants near two past-producing mercury mines, British Columbia, Canada. Geochemistry: Exploration, Environment, Analysis, 4, 4, 2004. - 353-364.

Qiu, G., X. Feng, S. Wang & L. Shang. Mercury and methylmercury in riparian soil, sediments, mine-waste calcines, and moss from abandoned Hg mines in East Guizhou province, Southwestern China. Applied Geochemistry, 20, 3, 2005. - 627-638.

Schroeder, W. H., J. Munthe. Atmospheric mercury – an overview. Atmospheric Environment, 32, 1998. - pp. 809-822.

Steinnes, E., T. Berg, T. E. Sjϕbakk.. Temporal and spatial trends in Hg deposition monitored by moss analysis. Sci. Total Environ. 304, 2003. - 215–219.

UNESCO. Decisions report – 36th session of the World Heritage Committee (Saint Petersburg). Available at, 2012. http://whc.unesco.org/archive/2012/whc12-36com-19e.pdf. Last accessed (06/07/2017).

Varela, Z., J. R. Aboal, A. Carballeira, C. Real & J. A. Fernández. Use of a moss biomonitoring method to compile emission inventories for small-scale industries. Journal of Hazardous Materials, 275, 2014. - 72-78.

This article was reviewed by Prof. Dr. Irena Kostova and Assoc. Prof. Dr. Anatoliy Angelov.

GEODYNAMIC CONDITIONS OF THE TERRAINS FROM THE EASTERN ZONE OF THE TOWN OF ORYAHOVO

Stefcho Stoynev[1], Anotnio Lakov[1]

[1]University of Mining and Geology "St. Ivan Rilski", Sofia 1700; stoynev@mail.bg

ABSTRACT. A considerable area of the town of Oryahovo is situated on an ancient landslide that affects the middle and the lower zones of the bank of the Danube. The ancient landslide circus extends from the central and eastern zones of the town and goes outside the town regulation. Secondary sliding movements are periodically triggered in zones from the ancient landslide body. In 2006 and 2014, two landslides were triggered that disturbed practically the entire river bank slope, being the largest in this country for the past years. Massive shearing zones and ground settlements we induced resulting in the complete destruction of buildings and infrastructure, including the main road Oryahovo – Leskovets. The article analyses the actual geodynamic conditions of the sliding processes, their mechanism and development pattern, the geometry of the two landslide circuses. The results of the study are used in the landslides stabilization design.

Keywords: landslides, stability, reinforcement

ГЕОДИНАМИЧНО СЪСТОЯНИЕ НА ТЕРЕНИТЕ В ИЗТОЧНАТА ЧАСТ НА ГРАД ОРЯХОВО

Стефчо Стойнев[1], Антонио Лаков[1]

[1]Минно-геоложки университет "Св. Иван Рилски", София 1700; stoynev@mail.bg

РЕЗЮМЕ. Значителна част от град Оряхово е разположена върху древно свлачище, което е засегнало средната и долна част на долинния склон на река Дунав. Древният свлачищен циркус обхваща централната и източна част на града и продължава извън пределите му. В тялото на древното свлачище периодично се активизират вторични свлачищни процеси, които обхващат отделни части от него. През 2006 и 2014 година в източната част на града се активираха две свлачища, които обхванаха практически целия долинен склон и са най-големите по обхват, формирани на територията на нашата страна в последните години. Те причиниха мащабни срязвания и пропадания на земната основа, придружени с цялостно разрушаване на сгради и инфраструктура, включително и главния път Оряхово – Лесковец. В статията е направен анализ на съвременното геодинамично състояние на терените в източната част на гр. Оряхово, анализирани са причините, които са обусловили активизацията на свлачищните процеси, изяснен е механизмът и динамиката на развитие на свлачищните процеси, геометрията на двата свлачищни циркуса. Резултатите от изследването са използвани при изготвянето на проектните решения за стабилизиране на свлачищата.

Ключови думи: свлачища, устойчивост, укрепване

Introduction

The town of Oryahovo is located in the western part of the Danube hilly plain. A major part of the town is located on the high Danube bank that is affected by landslide processes. They are of two types – ancient, temporarily stabilized, and contemporary, active. The origin and development of the ancient landslides are related to the paleo-valley of the Danube, embedded at a much lower hypsometric level than the present erosion base. The ancient processes began with the formation of a prism (or prisms) at the bottom part of the paleo-valley of the Danube, as the landslide process was of spreading type and developed along a weak zone (or surface) embedded into the calcareous Pliocene sediments from the basis of their geological profile. The sinking of the prism caused gradual upstream loosening of the massif and realization of new concessive surfaces up the slope with approximate circular configuration. These surfaces developed to the depth the basic one, but some ran through the massif at a higher level, into the hard-plastic Pliocene clays. There are also analyses that these sliding processes were accompanied by seismogenic events. The dynamics of the landslide processes during the late Holocene subsided due to the change of the paleographic environment and the landslide bodies were erosionally denudated. The original mechanism of the landslide processes had formed stepped landslide levels most of which gradually altered their terrain contours to circular shapes due to superimposed sliding processes. The constant slow movements of the landslide body (without considering the faster ones localized in different smaller areas), point out to the fact that this large ancient landslide structure is unlikely to be completely stabilized over time and to the present day.

The contemporary stability of the terrains in the town is highly influenced by active landslide processes. They are developed into separate areas from the body of the ancient landslide. The sliding surfaces are developed most commonly in the ancient landslide body without reaching its basic sliding area. The contemporary landslides lead to disturbances in the resistance of the buildings and facilities and to destruction of the infrastructure. The contemporary landslides which affect the eastern part of the town are with the largest range in the region of Oryahovo. They fall within the ancient landslide structure – landslide Quarters "Iztok" (Fig. 1). Two larger circuses are distinguished into the body of the ancient landslide: one of them is circus "Iztok", registration No. VRC 31.54.020.02.22,

and the other is “Voynishki poroi”, registration No. VRC 31.54.020.02.17. The circus “Sredna zona” is inserted as a smaller one between them. The circus “Voynishki poroi” (the easternmost part of the ancient landslide) is outside the urban territory. All three circuses are structurally and geodynamically bound together and the temporary activization of each one affects the neighboring ones. Numerous smaller or larger secondary circuses are superimposed on them.

Geological and tectonic structure

The region of the town of Oryahovo falls into the Lom’s graben depression where the axis to the Ogosta River valey directs southeast. The Kozloduy structure and its adjoining Kozloduy-Glozhen synclinal are overlapped in the region's depression. On top of the upper Cretaceous sediments, the syncline limb takes the shape of a graben, as it lies southeast with an inclination of 5-7.5 degrees. The upper stratigraphic horizons of the Neogene complex are occupied mainly by two formations – Furen /Sarmath/ and Beloslatina Formation /Meot-Pont/, which covers it. The Furen formation, with an average thickness of about 50-70 m, includes clayey-sandy horizons banded by sandy limestones and calcareous sandstones. The clayey layers are represented by ochres, grey-green and rusty coloured clays, mainly silty and sandy plastic. They are irregularly but relatively often banded by terrigen coarse-graded deposits – lenses and bands of clayey sands, from aleuritic to coarse water saturated sands. Bands, coatings, and grains of iron hydroxides, as well as organic admixtures, are often found in the layer.

During the Miocene-Pliocene period, the fine-grained deposits of the Furen formation were mainly transgressively deposited over the Beloslatina formation. Their facies is continental, including plastic clays with layers of slightly cemented brecco-conglomerates or clayey sandstones. They have an average thickness of about 20-30 m. The Pliocene basin ends with alternating rusty colored clays and sandy layers that mark the end of the sub-aquatic sedimentation. The coarse-grained composition, the rhythmic shift, and the increased ferrite content of these sediments suggest significant shallowing cycles of the basin. At a depth of about 30 m in the Danube river terrace and beyond a depth of 100 m at the top of the slope of the valley, the described formations lie over a calcareous complex from organogenic and detritic limestones and soft (chalk) limestones, banded by calcareous clays and clayey marl from the bottom horizon of the Furen Formation or the Florentine Formation. The Neogene deposits are covered by loess from the so called Danube loess province. Its thickness next to the Danube bank is in the range of 50-60 m. The maximum thickness of up to 85 m of loess is in the area of the town of Oryahovo.

Hydrogeological conditions

The hydrogeological conditions in the area of the ancient landslide are determined by the groundwater accumulated in the Pliocene complex. The groundwater is bound to the sandy deposits and the limestone-sandstone layers. The water-bearing complex is multilayered, pressurized. It is structurally built by continuous alternations of low-permeable clayey layers and the more permeable sandy and rocky water-bearing layers. The high plasticity of the clayey layers creates local aquitards. At a depth of over 100 m from the terrain, the aquifer complex hydraulically contacts with the underlying calcareous horizon.

The recharge of the aquifers is infiltrational, coming from the extensive loess plateau and the landslide slope surface. The groundwater flow is generally directed north with an average gradient of 0.15-0.20. The groundwater drains in the Danube. The aquifer is spatially well-developed. The local disruptions of the aquifer intervals due to the landslide processes create partially pressurized zones. The clayey layers in the aquifer structure in some sections are partial aquitards, but the hydraulic connection between the aquifers is rapidly recovers as a result of the sediment composition and their disruption from the landslide processes. The infiltrational recharge of the groundwater from the ancient landslide area is about 13.0 l/sec. (Kuzmanov, K. et al., 2014, Stoynev, S. et al., 2017).

Geodynamical conditions

The first registered problems and corresponding geological surveys in the area are from the mid-twentieth century. The stabilization activities during these years are mainly related to the construction of water draining facilities. New cyclic activations were periodically recorded until the realization of the largest ones, affecting significant territories in the eastern part of the town – the landslide named “Iztok” in 2006, and the landslide named “Sredna zona” in 2013-2014. Despite the activities undertaken and the numerous supporting structures, the contemporary landslide processes are still active, affecting new terrains in westerly direction. As a result of the contemporary landslides, the infrastructure and the living houses in the area are practically destroyed, as well as a significant part of the supporting facilities.

The landslide development of the terrains within the ancient landslide is divided into three stages - from 1954 to 2005, from 2005 to 2011, and after 2011.

- ***1st stage*** – the deformations of the ancient landslide were quite even, at a rate of – 0.10-0.25 mm/d. The total displacements of the terrain alternate in a small range – from 97 cm to 102 cm, i.e. within about 600 m of the length of the landslide, the total movement was within 1.0 m. The displacements of the terrain were almost parallel in direction and gradually increased from the north to the south. The rate of the deformations in the steep Danubian slope was the slowest – it varied between 0.03-0.05 mm/d, which indicated slight activity. In a southerly direction, towards the gentler landslide slope, where the average inclination of the terrain is between 6-12 degrees, the terrain deformations were considerably greater – the average rate was 0.20 mm/d. The main movement of the landslide was north-northeast with a zone affected to the approximate elevations of 75-78. Local active slides that are usually located on the more steep slopes were formed over the years within the range of the landslide, such as the landslide processes realized north from “N. Obretenov” Str. in 2004. In order to ensure the stability

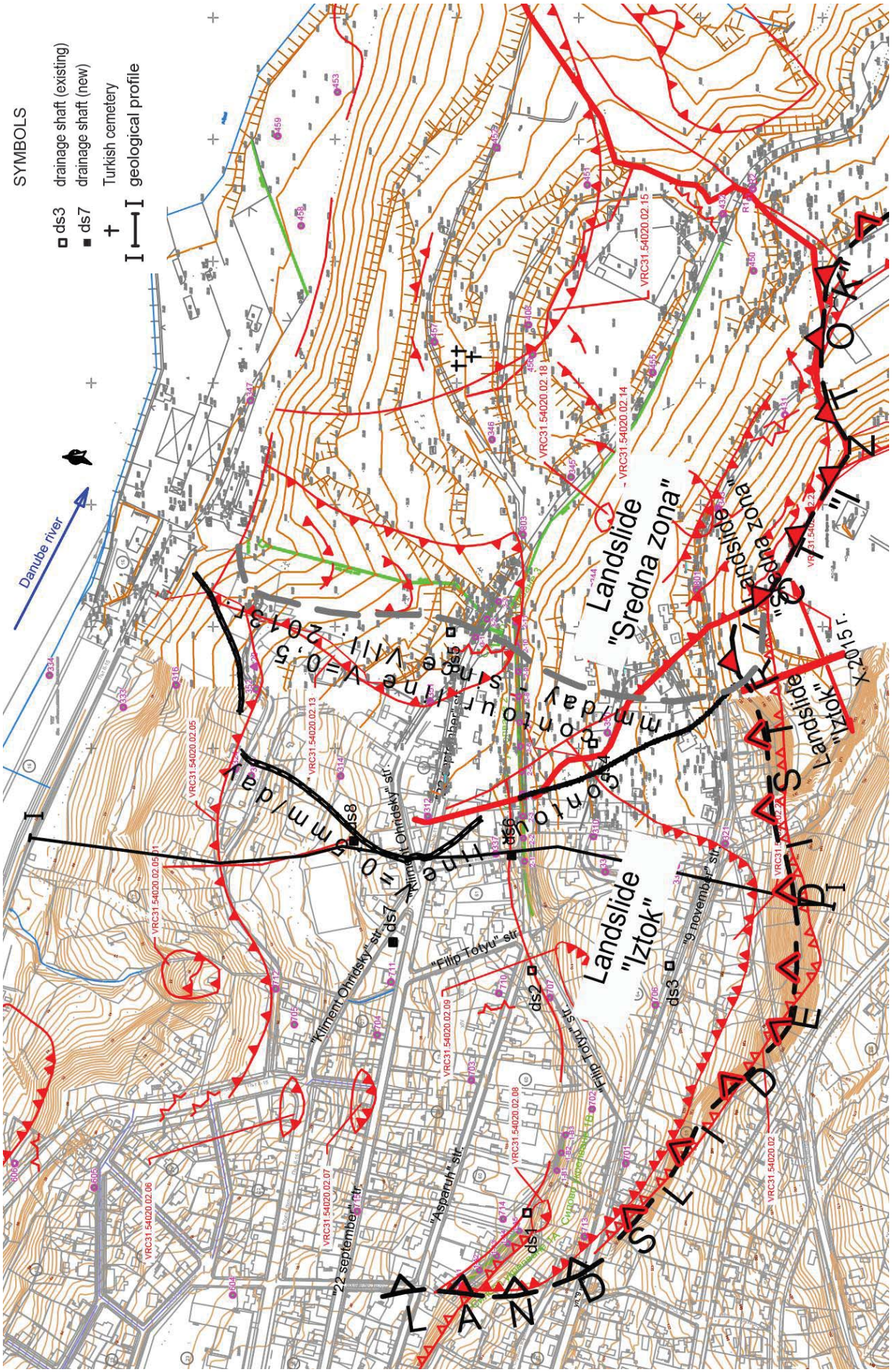

Fig. 1. Geodynamic map of the landslide area in the eastern part of the town of Oryahovo

of the terrains, numerous ground water draining activities were carried out. In the 1950s, trench drains with a depth of 4.0 - 5.0 meters were built in the area of the main landslide. Subsequently, several groups of horizontal drainage boreholes (HDB) with a length of up to 150-160 meters were drilled up. During the 1980s, a construction of drainage shafts with built-in HDBs began. In the eastern part of the quarter, in "9th November" Str., a section of the so-called 'dropping wells' that conducted the drained groundwater from the Pliocene horizon within the Sarmatian limestones was drilled (KNIIBKS "Vodokanalproekt", 1989).

- ***2nd stage*** – it began with the activation of the landslide processes in the western part of the ancient landslide and the formation of the "Iztok" landslide. The activation began in December 2005 and the most intensive landslide deformations were in the period February-April 2006. The landslide impacted an area of about 550 meters wide and about 250 meters long, as it covered the valley between "Asparuh" Str. and the main scarp of the ancient landslide (fig. 1). The formed contemporary landslide was embedded within the ancient one, with a well-expressed prism at the head contoured by vertically stepped fractures with a gap of 0.5 to 1.0 meters. In the north direction, towards the Danube bank, the terrains were visibly more stable and influenced only by the deep sliding movements. The data from the investigations show that the activation of the landslide processes developed on two levels – deep, in the area of the ancient sliding surfaces, and shallow, in the upper parts of the ancient landslide body (fig. 2). In the range of the head prisms, weak zones were found at a depth of about 90 meters, and in the north direction they were at a depth of about 60 meters. The contemporary deep sliding surfaces were formed along the ancient disturbed areas, also probably associated with old prisms of active pressure. Their inclination was about 5 degrees and they developed in the Pliocene Sarmatian clays and the mottled limestone-carbonate layers. The toe passive prism was in the Danube and was related to its contemporary erosion base of the river. The slope stability analysis showed that the safety factor along the deep surfaces was near the equilibrium limit F=1.02, which also corresponded to the processes of slow movements. The shallower landslides, which determined the contemporary geodynamical state of the terrain, covered the slope area above "Asparuh" Str., reaching the prisms of active pressure in the south ("9th November" Str.). The terrains were heavily cracked, as the buildings that fell within reach were completely destroyed. The maximum deformations of the terrain reached a speed of 30-40 cm/day. Its development was related to natural factors, such as the geological structure and the primary structural disturbance of the bank from the ancient landslides, the significant infiltration of groundwater, and the additional hydrostatic pressure resulting from the torrential rainfall in this period (a total of 1073 mm), as well as to technogenic factors, such as damage of the water-supply pipeline along "Asparuh" Str. and, above all, to the non-operating drainage system built in the area of the ancient landslide scarp. Due to lack of maintenance and prevention, the drainage sewers were blocked and this caused them to fill up with water, resulting in additional water saturation of the Pliocene materials (Stoynev, S. et al., 2006).

To ensure the stability of the landslide emergency drainage activities were undertaken to restore the functioning of the existing drainage system. New vertical drop wells were drilled in the area of the landslide main scarp and also two drainage shafts with 50-70 meters lengths of HDBs were constructed. To ensure the stability of the shallow contemporary landslides, four anchored pile systems were constructed. As a result of these, the terrains in the area of the landslide were stabilized and the deformations returned to levels close to those before the activation of landslide processes – 0.1-0.5 mm/day ("Geozashtita Pleven", 2016).

- ***3rd stage*** – it began with the activation of the landslide processes east of the "Zelena bara" gully, in the area of the "Sredna zona" water basin. The active landslide processes started in 2011, but by 2013 they had a relatively low movement rate – 2.5 mm/day, starting to form a prism of active pressure in the area directly below the "Sredna zona" water basin. Significant activation of the landslide processes occurred in the spring of 2014. The main landslide scarp was formed at about 20 meters north of the "Sredna zona" reservoir. The width of the scarp reached up to 250 meters and the developed systematic cracks in this area formed a distinctive prism of active pressure. Another heavily cracked area of the terrain started from the main road Oryahovo-Leskovets and ended under the Turkish cemetery. The cracks with an azimuth between 110-130 degrees and 70-80 degrees formed two sinking prismatic blocks, and the northern one was more distinctive (Fig. 1). In depth, the two described prisms may have formed a common peak of the prism of active pressure. In general, the terrain in and around the former town park area was heavily cracked, as smaller or larger cracks rapidly changed their direction and the area got a mosaic pattern of terrain deformations. The formed landslide body had a typical circular shape, appearing in a well-defined arc of the main scarp and pear-shaped body in the northern direction. Its width reached up to 700 m, as its length was within that range or more. There were three main areas of the landslide – a sunken upper part with a length of up to 200 m; a central plain area, and an elevated toe zone (the "Iztok" park) at the slightly inclined terrains in the north extending to the steep valley slope and strip from the Danube aquatory with a length of about 200 m. The total deformation in the range of the toe zone increased to over 11.5 m and a corresponding rate of 20 mm/d. Similar numbers were detected in the western part of the "Iztok" park. The main road to Leskovets between the gorges of "Zelena bara" and "Voynishki poroi" was shifted in the north-northeast direction by 10.3 and 6.8 meters respectively. (Kuzmanov, K. et al., 2014; "Geozashtita Pleven", 2016).

The structure of the landslide body, depending on the construction of the landslide slope and the spatial arrangement of the sliding surfaces, was of a block-type type (Fig. 2). The entire eolian-delluvial horizon and the Pliocene-Sarmatian sediments were affected. The main deep sliding surface has also entered the layered calcareous-marl horizon. The thickness of the landslide body varied from 90-95 meters to 110 meters, and the area with the most active movements was at a depth of 20-42 meters. They were of a mixed mechanism– both formed bottom to top and top to bottom, with translational and cylindrical type sliding surfaces. Embedded smaller and with different volumes, landslide bodies were developed inside the main landslide: above the main road Oryahovo-Leskovets, along the "Zelena bara" gorge, and down the steep Danube slope.

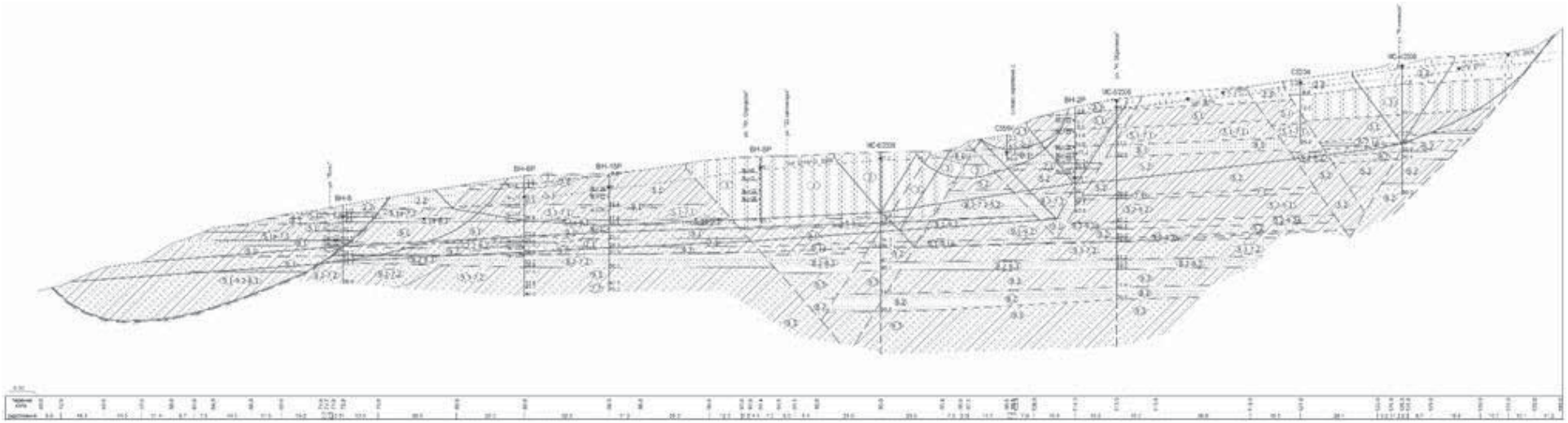

SYMBOLS

Layer 1 - Embankment /Embankment materials/

Layer 2.2 - Si. Silty formations - sandy and typical loess, with macrospores, subsident, slightly moist to moist.

Layer 2.3 - Si. Sandy formations - sandy and typical loess, slightly subsident to non-subsident, moist to water-saturated.

Layer 3 - clSi. Uniform to mottled delapsive formations, priority including loess soils, as well as colluvial clayey sands and Pleistocene and Pliocene clays.

Layer 4 - siCl. Loess clays, brown to red-brown, hard.

Layer 5 - siCl. Clays, silty, medium to hard-plastic, beige-rusty with whitish streaks and spots, grey-whitish to grey-green in some areas, stiff to hard. Rusty-brown and grey clays are included, as well as brown with dark streaks and spots. There are concretions and deposits of dark hydroxides and organic admixtures.
Layer 5.1 - decompressed layers with lower density and **layer 5.2** - well-compressed.

Layer 5.1a (9.1a) - Cl. Clays with high plasticity, dark-rusty, dark-brown to grey-black and multicolored, stiff to hard with organic admixtures, with disturbed structure in some areas.

Layer 6 - siCl. Gravely clays, medium-plastic, hard to very hard with presence of fine and medium-grained angular gravel, often with amorphous limestone deposits.

Layer 7.1 - sasiCl. Clays with low plasticity and clayey sands, rusty with whitish streaks and spots in some areas, stiff to hard. Nests of well-graded sands, fine to coarse-grained, clayey to varying degrees are limited in the layer. The texture is laminated in some sections - alternation of light and dark streaks. The variety has a predominant Pliocene age.

Layer 7.2 - sasiCl. Clays with low plasticity and clayey sands, rusty with whitish streaks and spots in some areas, predominantly very hard. Nests of well-graded sands, as well as thin bands of sandy limestones are limited in the layer. The variety has a Sarmatian age.

Layer 8.1 - siMSa. Sand - predominantly medium-grained, rusty to whitish, silty to coarse in nests and lenses, well-graded, variously sorted, medium-dense to dense, slightly moist to moist. The formation has a predominant Pliocene age.

Layer 8.2 - siFSa/saCl. Sand - predominantly fine, silty, well-graded, variously sorted, rusty, ocher to whitish, very dense, water-saturated. Bands of clayey sands and rarely clays with low plasticity are included. Thin bands of calcareous sandstones and limestones are episodically present. The formation has a predominant Sarmatian age.

Layer 8.3 - siFSa/saCl. Analogical to layer 8.2, but with higher percentage of limestones and calcareous sandstones (an average of about 30-50% from the layer), as well as aleruite sands and clayey sands, very dense (semi-bonded).

Layer 9.1 - siCl. Clays with medium and low plasticity, beige-rusty, ochre with whitish streaks and spots, grey-green or whitish in some areas, stiff and hard. Thin bands of clay with lower plasticity are rarely included. Thin bands of darker clays which refer to **variety 9.1a** (organic admixtures content) are found in the layer.

Layer 9.2 - siCl. Clays with medium and high plasticity, beige-rusty, ochre with whitish streaks and spots, grey-green or whitish in some areas, hard and very hard, tough. Thin bands of clay with lower plasticity are rarely included. They build lower layers of the Sarmatian formation.

Layer 9.3 - siCl. Clays similar to layer 9.2 with higher litification degree

BH-5P — Borehole No.5, equipped as a piezometer (from this survey).
MC-6/2006 — Archive borehole No.6 from 2006.
C35/04 — Archive borehole No.35 from 2004.

Groundwater level

N=21 — Penetration resistance - 21 percussions for an interval of 30cm.

Contemporary slipping surfaces and areas with a different active variety

Ancient disturbed areas

Fig. 2. Engineering geological sections. (The layer indices are given below)

Except for the natural geological causes, the significant activation of the "Sredna zona" landslide was provoked by the additional water saturation of the slope. During the spring and autumn of 2014, there was a significant amount of rainfall in the region, as the total amount in the same year reached high values of more than 1000 mm/m^2. The water quantities that leaked and infiltrated slowly into the soil from the "Sredna zona" basin should be considered as well.

The activation of the "Sredna zona" landslide grearly influenced the "Iztok" landslide as the boundary between them (Fig. 2) was shifted significantly in the western direction. The relocation exceeded 200 m along the "22nd September" Str. The landslide processes affected zones beyond "Bolnichno dere" and the deformations progressed towards the building of the secondary school. At its eastern end, the deformations were directed north at a rate of 0.06 mm/d, in total of 4.6 cm and a terrain elevation of 1.6 cm.

Just as during the period 1984-2004, the Danube steep bank north from the "Lale" Str., suffered from slow and relatively small deformations. The total extent in its middle area for the period was 6 cm, with an average displacement rate of 0.11 mm/d. Above it, at the top of the slope, along the "Lale" Str., the terrain displacements were considerably bigger –in total of 30-40 cm and corresponding rates of 0.5-0.6 mm/d (Stoynev, S et al., 2017).

Conclusions

The analysis of the state of the terrains located in the area of the ancient landslide "Iztok" allows for the following conclusions:

- The ancient landslide is not fully stabilized, as the terrain is subject to slow deformations, possibly due to creeping processes along a deep bedded sliding surface (65 to 110 m) that is lithologically predefined by the semi-calcareous limestone horizon;
- The current state of the terrain of the ancient landslide circus is defined by the activation of the "Iztok" and "Sredna zona" landslides. Their geometry is different as the active landslide surface of the "Iztok" landslide is in the depth range of 15-20 m and that of the "Sredna zona" landslide is in the depth range of 20-42 m;
- The basic reasons for the current activation of the landslide processes are connected with the natural geological conditions (strength properties of the Neogene deposits and their structural disturbance by the ancient landslides), as well as with the saturation of the slope from intensive rainfall, typical for the region of Oryahovo, and from the leakage of the water supply network. The accumulated stresses in the slope from the deep creeping processes along the ancient sliding surface have influenced the activation of the current sliding processes as well;
- The underground water balance in the landslide body shows that the constructed drainage facilities drain an insignificant quantity of the ground water – just about 30% of the rechargement of the landslide body coming from the loess plateau. This shows the incomplete efficiency of the constructed drainage shafts, dropping wells, and HDS;
- Due to the different geometry of the two contemporary landslides and their mutual influence, a significant part of the constructed anti-landslide structures and drainage systems are destroyed.

The current state of the terrains from the ancient landslide and the patterns of development of the landslide processes show that it is necessary to apply new approaches to reduce the landslide activity and stabilize the structure. For example:

- Priority shall be given to surface drainage facilities. Over the years, this approach has been neglected, but the analysis of the processes in the area suggests that such facilities are quite efficient. A large quantity of the drained groundwater in the area through deep shafts, drains, HDS, etc., is discharged into the "Zelena bara" and "Bolnichno dere" gorges. This constant flow maintains the adjacent landslides in continuous active state. It was not realized that over the years this practice resulted in draining away the groundwater from a higher level and recharging the lower landslide level with the same quantities. The upper landslide levels and the two gorges are elements from the large-scale landslide structure described, which is continuously drained in its lower parts. The constant active state of the "Zelena bara" and the "Bolnichno dere" landslide slowly disturbs the slope along the Danube bank and activates prisms of active pressure which restart slow landslide processes. The accumulation of stresses in the upper slope zones ("9th November" Str., "N. Obretenov" Str.) results in their cyclic movements (usually at intervals of 7-15 years). These are often triggered by increased infiltration of rainwater and, to a different extent, by leakage from the damaged water supply network. After the active movement stages, the slope is unloaded from the accumulated stresses and gradually falls in a state of intermediate stability.
- One general principle must be observed during the design of drainage facilities: all water (surface and groundwater) drained from the upper and lower sectors of the landslide area (through drainage, water catchments, deep shafts, etc.) must be led away from the landslides through a competent sewage system.
- It is necessary to construct three deep shafts in the sections with shallow groundwater – the "Boyana voivoda" Str., a "playground", and the site where the old hospital was located. The approach to the design and construction of these shafts should differ from the one used so far. The deep shafts must be combined with the constant drilling of an increasing number of short drainage rays inside it until a well-expressed reduction of the groundwater pressure around it is established by newly-constricted or existing piezometers. Further drilling of new short rays should be terminated. Long-length drilled rays from the shaft should be drilled at a much later stage, after the stabilization of the landslide processes and monitoring movement rates of no more than 0.10 mm/d.
- The construction of support structures must be carried out after reaching the reduction of the rate of terrain deformations due to the drainage facilities.
- In order to check the effectiveness of the power reinforcing structures, it is necessary to construct inclinometers for monitoring the deformations both on the ground surface and in depth.

References

„Геозащита Плевен" - Данни за отчетите на премествания на повърхностните геодезически земни репери, изградени в района на източната част на град Оряхово – архив „Геозащита Плевен", 2016 год. ("Geozashtita Pleven" – Danni za otchetite na premestvaniya na povarhnostnite geodezicheski zemni reperi, izgradeni v rayona na iztochnata chast na grad Oryahovo – arhiv "Geozashtita Pleven", 2016.)

КНИИБКС "Водоканолпроект", Укрепване свлачища в гр. Оряхово", работен проект – архив Водоканалпроект, 1989 г. (KNIIBKS "Vodokanalproekt", Ukrepvane svlachishta v grad Oryahovo, raboten proekt – arhiv Vodokanalproekt, 1989.)

Кузманов, К. и др. ИГП на свлачище с рег № 06.5402.02.23 (VRC 31.54020/02.23) на склона под водоем „Средна зона" от водоснабдителната мрежа на гр. Оряхово - Геофонд на «Геотехника АБС» ООД. 2014. (Kuzmanov, K. i dr. IGP na svlachishte s reg No. 06.5402.02.23 (VRC 31.54020/02.23) na sklona pod vodoem "Sredna zona" ot vodosnabditelnata mrezha na grad Oryahovo – *Geofond na* "Geotehnika ABC" OOD. 2014.)

Стойнев, С. и др. *Доклад за извършени инженерногеоложки и хидрогеоложки проучвания за укрепване на свлачище в кв. Изток, град Оряхово* – Геофонд на «Геотехника АБС» ООД. 2006. (Stoynev, S. i dr. *Doklad za izvursheni inzhenernogeolozhki i hidrogeolozhki prouchvaniya za ukrepvane na svlachishte v kv. Iztok, grad Oryahovo – Geofond na* "Geotehnika ABC" OOD. 2006.)

Стойнев, С. и др. Укрепване на свлачище в кв. „Изток", гр. Оряхово – II етап - Геофонд на «Геотехника АБС» ООД. 2017 (Stoynev, S. i dr. Ukrepvane na svlachishte v kv. "Iztok", grad Oryahovo – II etap – *Geofond na* "Geotehnika ABC" OOD. 2017.)

The article is reviewed by Prof. Stefan Dimovski, DSc. and Prof. Dr. Radoslav Varbanov.